



# $\eta^5$ -Oxocyclohexadienyl ruthenium complexes for base-free catalytic transformations

Raphaël Verron

## ► To cite this version:

Raphaël Verron.  $\eta^5$ -Oxocyclohexadienyl ruthenium complexes for base-free catalytic transformations. Organic chemistry. Université Rennes 1, 2022. English. NNT : 2022REN1S029 . tel-03867114

**HAL Id: tel-03867114**

**<https://theses.hal.science/tel-03867114>**

Submitted on 23 Nov 2022

**HAL** is a multi-disciplinary open access archive for the deposit and dissemination of scientific research documents, whether they are published or not. The documents may come from teaching and research institutions in France or abroad, or from public or private research centers.

L'archive ouverte pluridisciplinaire **HAL**, est destinée au dépôt et à la diffusion de documents scientifiques de niveau recherche, publiés ou non, émanant des établissements d'enseignement et de recherche français ou étrangers, des laboratoires publics ou privés.

# THESE DE DOCTORAT DE

L'UNIVERSITE DE RENNES 1

ECOLE DOCTORALE N° 596

*Matière, Molécules, Matériaux*

*Spécialité : Chimie Moléculaire et Macromoléculaire*

Par

**Raphaël VERRON**

$\eta^5$ -Oxocyclohexadienyl ruthenium complexes for base-free catalytic transformations

**Thèse présentée et soutenue à Rennes, le 25 Mars 2022**

**Unité de recherche : UMR 6226, Institut des Sciences Chimiques de Rennes**

**Thèse N° :**

## **Rapporteurs avant soutenance :**

Thibault Cantat  
Francine Agbossou-Niedercorn

Directeur de recherche CEA, Saclay  
Directrice de recherche CNRS, ENSCL, Lille

## **Composition du Jury :**

Président : Francine Agbossou-Niedercorn  
Examineurs : Walter Leitner  
Alain Igau  
Thibault Cantat  
Francine Agbossou-Niedercorn  
Dir. de thèse : Cédric Fischmeister

Directrice de recherche CNRS, ENSCL, Lille  
Professor, MPI für Chemische Energie Konversion (Mülheim)  
Directeur de recherche CNRS, LCC Toulouse  
Directeur de recherche CEA, Saclay  
Directrice de recherche CNRS, ENSCL, Lille  
Ingénieur de recherche CNRS, ISCR, Rennes







I would like to thank the ANR CatEngy (ANR-18-CE07-0006-01) for the financial support.





# Acknowledgement

In this part, I would like to thank all the person that could make this PhD work possible at the Institut des Sciences Chimiques de Rennes, Organometallics Materials and Catalysis research team, in the Organometallic and Sustainable catalysis group.

I would like to give a special thanks to Cédric Fischmeister, my PhD supervisor, for giving me the opportunity to make a PhD, the discussions we had, the support, the guidance and his optimism.

I would like to thank the member of the jury, Thibault Cantat, Francine Agbossou-Niedercorn, Walter Leitner, Alain Igau that gave me the honor to judge my work.

I would like to thank Bertrand Carboni and Jean-Luc Renaud that take part of the mid-thesis jury.

I would like to thank the other members of the ANR-projet CatEngy especially Alain Igau and Emmanuel Puig in Toulouse for the discussions and the progression of the project.

I would like to thank my lab mates throughout these 3 years, Liwei, Marie, Jonathan, Alexandre and all the PhD student, post-doc and master students I have met. A special thanks to Hana, that worked with me during her master internship.

I would like to thank my former master supervisors in Strasbourg, Valérie Benneteau and Thierry Achard that helped me to serenely envision a PhD.

I would like to thanks my friends for their support and their friendship. I have a special thought to my master team in Strasbourg, Elodie, Thibault, Morgane. I also have a special thought to my friend from the Orchestre d'Harmonie du Sud de l'Ernée in Andouillé for their support and for allowing me to escape from my PhD work.

Finally, I would like to thanks my family. Especially, I would like to deeply thank my parents Laurence and Philippe that supported me during all my scholarship no matter what, no matter the place. I am grateful for their support that gave me the opportunity to study up to a PhD. I would like to thanks my brother Corentin and my sister Alice for their support. I would like to thank my partner, Louisanne, for her indefectible support during those 3 years and more.

To conclude, I would like to thank those that I could not cited and all the person that contribute directly or indirectly to the realization of this PhD.

Thank you all.



## List of the abbreviations

UN: United Nation  
Gtoe: Giga ton oil equivalent  
GHG: GreenHouse Gas  
IPCC: Intergovernmental Panel on Climate Change  
PEM: Proton Exchange Membrane  
Cod: Cyclooctadiene  
CPME: Cyclopentyl methyl ether  
MLC : Metal Ligand Cooperation  
TEA : Triethylamine  
FA : Formic Acid  
*i*PrOH or *i*-PrOH: *iso*-Propanol  
DMSO : Dimethyl Sulfoxide  
ACN : Acetonitrile  
GVL :  $\gamma$ -Valerolactone  
Tol : Toluene  
THF : Tetrahydrofuran  
DCM : Dicloromethane  
C<sub>4+</sub>: Carbon chain of 4 or higher  
r.t: room temperature  
EtOH: Ethanol  
BuOH: n-Butanol  
2-EthylBuOH: 2-ethylbutanol  
HexOH: n-Hexanol  
2-ethylHexOH: 2-ethylhexanol  
OctOH: n-Octanol  
LOHC: Liquid Organic Hydrogen Carrier  
TEAO: Triethanolamine  
Dppe: Bis(Diphenylphosphino)ethane  
Dppp: Bis(Diphenylphosphino)propane  
Dppb: Bis(diphenylphosphino)butane



# Content

<b>CHAPTER I: GENERAL INTRODUCTION .....</b>	<b>13</b>
1. <i>World energy overview</i> .....	15
1.1. Context.....	15
2. <i>Global Energy consumption</i> .....	15
2.1. General presentation.....	15
2.2. Fossil resources.....	17
3. <i>Consequences</i> .....	18
3.1. Greenhouse gas effect .....	18
3.2. Climate change .....	21
4. <i>Energetical transition</i> .....	21
4.1. General presentation.....	21
4.2. Tackle CO <sub>2</sub> emission.....	21
4.3. Oil depletion .....	23
4.4. New energy sources.....	23
4.5. New fuels .....	24
4.5.1. Biofuels .....	24
4.5.2. Electricity .....	25
4.5.2.1. Battery .....	25
4.5.2.2. Proton Exchange Membrane Fuel cells.....	25
4.6. CO <sub>2</sub> Capture and Valorization .....	26
4.6.1. CO <sub>2</sub> Capture and Storage.....	26
4.6.2. Valorization.....	27
5. <i>Positioning of the Project</i> .....	27
5.1. Context.....	27
5.2. Objectives .....	30
6. <i>References:</i> .....	31
<b>CHAPTER II: BASE-FREE HYDROGENATION AND TRANSFER HYDROGENATION .....</b>	<b>35</b>
PART 1: GENERAL INTRODUCTION .....	35
1. <i>Homogeneous Hydrogenation</i> .....	37
1.1. Background.....	37
1.2. Use.....	37
1.2.1. H <sub>2</sub> .....	37
1.2.2. Transfer Hydrogenation ( <i>i</i> -PrOH, FA).....	38
1.3. Make the reaction greener .....	38
2. <i>Homogeneous Base-free Hydrogenation</i> .....	38
2.1. H <sub>2</sub> as donor .....	38
2.2. <i>i</i> -PrOH as donor.....	42
2.3. Formic acid as donor.....	49
3. <i>Conclusion</i> .....	51
4. <i>References:</i> .....	52
PART 2: CATALYTIC APPLICATION OF H <sup>5</sup> -OXOCYCLOHEXADIENYL RUTHENIUM COMPLEXES IN BASE-FREE HYDROGENATION AND TRANSFER HYDROGENATION.....	55
1. <i>Introduction</i> .....	57
2. <i>Base-free hydrogenation with H<sub>2</sub></i> .....	57
2.1. Preliminary tests .....	57
2.2. Study of the hydrogen pressure and temperature .....	58
2.3. Catalyst loading optimization .....	59
2.4. Optimization of the reaction time .....	59
2.5. Optimized condition .....	60
2.6. Scope .....	60
2.7. Conclusion on the base-free hydrogenation.....	63
3. <i>Base-free transfer Hydrogenation</i> .....	64
3.1. <i>Iso</i> -Propanol .....	64
3.1.1. Solvent and temperature optimization .....	64
3.2. Formic Acid .....	66
3.2.1. Preliminary tests.....	66

3.2.1.	Optimization of formic acid amount .....	68
3.2.2.	Concentration effect.....	69
3.2.3.	Time and catalytic amount .....	69
3.2.4.	Optimized conditions.....	70
3.2.5.	Scope .....	70
3.2.6.	Conclusion on base-free transfer hydrogenation with FA.....	74
3.3.	Mechanism proposal .....	74
4.	<i>Conclusion and perspectives</i> .....	77
5.	<i>References:</i> .....	78
6.	<i>Experimental part</i> .....	79
6.1.	General considerations .....	79
6.2.	Complex 1 synthesis .....	79
6.3.	Base-free hydrogenation with H <sub>2</sub> in <i>iso</i> -propanol .....	82
6.3.1.	General procedure.....	82
6.3.2.	Substrate analysis .....	82
6.4.	Base-free transfer hydrogenation with <i>i</i> PrOH .....	90
6.4.1.	General procedure.....	90
6.5.	Base-free transfer hydrogenation with FA.....	91
6.5.1.	General procedure.....	91
6.5.2.	Substrate analysis .....	91
<b>CHAPTER III: THE GUERBET REACTION.....</b>		<b>99</b>
PART 1: STATE OF THE ART .....		99
1.	<i>Introduction</i> .....	101
1.1.	Alcohol as an energy source .....	101
1.1.1.	Ethanol.....	101
1.1.2.	The Guerbet reaction .....	101
1.1.3.	From ethanol to n-butanol via the Guerbet reaction .....	102
2.	<i>State of the art of the Guerbet reaction on ethanol</i> .....	103
2.1.	Homogeneous Catalysis .....	103
2.2.	Heterogeneous catalysis .....	108
3.	<i>Conclusion</i> .....	109
4.	<i>References:</i> .....	110
PART 2: CATALYTIC APPLICATION OF H <sup>5</sup> -OXOCYCLOHEXADIENYL RUTHENIUM COMPLEX IN THE GUERBET REACTION .....		113
1.	<i>The Guerbet reaction with ethanol</i> .....	115
1.1.	Analytical set-up .....	116
1.2.	Results and discussion .....	118
1.2.1.	Temperature optimization .....	118
1.2.2.	Reaction scale.....	119
1.2.3.	Catalyst loading .....	119
1.2.4.	Base loading.....	120
1.2.5.	Preliminary test with complex 29.....	121
2.	<i>Conclusion</i> .....	122
3.	<i>References:</i> .....	123
4.	<i>Experimental Part</i> .....	124
4.1.	General information .....	124
4.2.	Reaction procedure .....	124
4.3.	Analytical procedure .....	124
4.4.	Reaction procedure attempts.....	126
<b>CHAPTER IV: THE HYDROGEN STORAGE .....</b>		<b>129</b>
PART 1: STATE OF THE ART .....		129
1.	<i>Introduction</i> .....	131
2.	<i>Hydrogen as an energy source</i> .....	131
2.1.	Liquid Organic Hydrogen Carrier.....	132
2.1.1.	Formic Acid as a LOHC .....	132
3.	<i>State of the art</i> .....	133
3.1.	Hydrogen storage by homogeneous catalysis (Hydrogenation of CO <sub>2</sub> in Formic Acid) .....	133
3.1.1.	With base.....	134
3.1.2.	Base free .....	136
3.2.	Hydrogen release in homogeneous catalysis (Dehydrogenation of Formic acid to H <sub>2</sub> ) .....	138

3.2.1.	Dehydrogenation of Formic Acid under basic conditions.....	139
3.2.2.	Base-free dehydrogenation of formic acid.....	144
3.3.	Reversible hydrogenation of Carbon dioxide.....	150
4.	<i>General conclusion</i> .....	155
5.	<i>References:</i> .....	156
PART 2:	CATALYTIC APPLICATION OF H <sup>5</sup> -OXOCYCLOHEXADIENYL RUTHENIUM COMPLEX IN THE HYDROGEN STORAGE .....	161
1.	<i>Introduction</i> .....	163
2.	<i>CO<sub>2</sub> hydrogenation / Hydrogen storage results and discussion</i> .....	163
2.1.	Preliminary results.....	163
2.2.	Solvent .....	165
2.3.	Pressure .....	165
2.4.	Temperature .....	166
2.5.	Reaction time.....	167
2.6.	CO <sub>2</sub> hydrogenation under basic condition .....	168
2.7.	Conclusion.....	168
3.	<i>Formic acid dehydrogenation / Hydrogen release results and discussion</i> .....	169
3.1.	Preliminary tests .....	169
3.2.	Effect of the concentration on the FA dehydrogenation .....	171
3.3.	CO detection .....	172
3.4.	Pressure generation.....	172
3.5.	Continuous addition of FA .....	173
3.6.	Latent behavior of the catalytic system.....	173
4.	<i>Storage and release cycle</i> .....	174
4.1.	Application .....	174
5.	<i>Mechanism proposal</i> .....	176
5.1.	Formic acid dehydrogenation .....	176
5.2.	CO <sub>2</sub> hydrogenation into formic acid .....	177
6.	<i>Conclusion</i> .....	178
7.	<i>References:</i> .....	179
8.	<i>Experimental part</i> .....	180
8.1.	General information .....	180
8.2.	CO <sub>2</sub> hydrogenation.....	180
8.2.1.	Reaction procedure .....	180
8.2.2.	Analytical procedure.....	180
8.3.	FA dehydrogenation .....	182
8.3.1.	General reaction procedure .....	182
8.3.2.	Analytical Procedure.....	183
8.4.	Cycle.....	183
CHAPTER V:	CONCLUSION AND PERSPECTIVES .....	185
1.	<i>Conclusion and perspectives</i> .....	187



# Chapter I: General Introduction



# 1. World energy overview

## 1.1. Context

Energy is crucial in our lives and you are probably reading this manuscript either on a computer that needs electricity or on paper that needs energy to be produced. We do not realize that we are surrounded by energy demands. Indeed, almost every step of our daily life requires direct or indirect energy sources. Without it, no more products in the shops, no more manufactured products, no more gasoline in the car, no more trains, no more internet etc. This extreme dependence to energy is a big challenge in the aim to satisfy the growing needs of humanity.

The use of energy has always played a role in the evolution of humanity. It began with the mastery of fire.<sup>[1,2]</sup> More recently, the industrial revolution in the XVIII century, based on the use of oil and coal, has deeply changed the society.<sup>[3]</sup> Currently, fossil resources still defines the energy model we are living in. Of course, new energy sources have been developed but the hegemony of fossil fuels is very strong and the global energy production still lies on it (Figure I-1-1).<sup>[4]</sup>

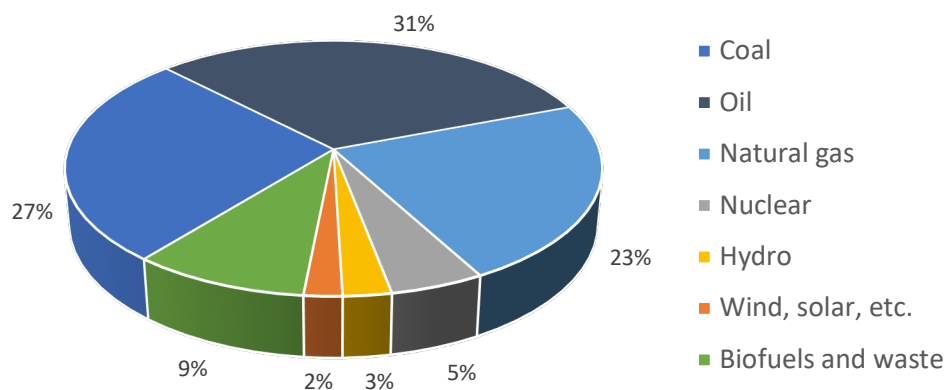


Figure I - 1 - 1: Total world energy supply by source in 2018.

## 2. Global Energy consumption

### 2.1. General presentation

As the global population is increasing, the energetic demand is also increasing all around the world. In 1971 the world consumption was about 5,5 Gtoe (Giga ton oil equivalent) and it increased to hit 14,3 Gtoe in 2018. A huge growth concerns the developing countries and especially China which has become the biggest consumer of energy in the world ahead Europe and the USA (Figure I-1-2).

According to probabilistic projection from the UN, the population should increase up to 11 billions by the end of the century compared to 7,8 billion today,<sup>[5]</sup> which means that the energy demand will continue to increase.

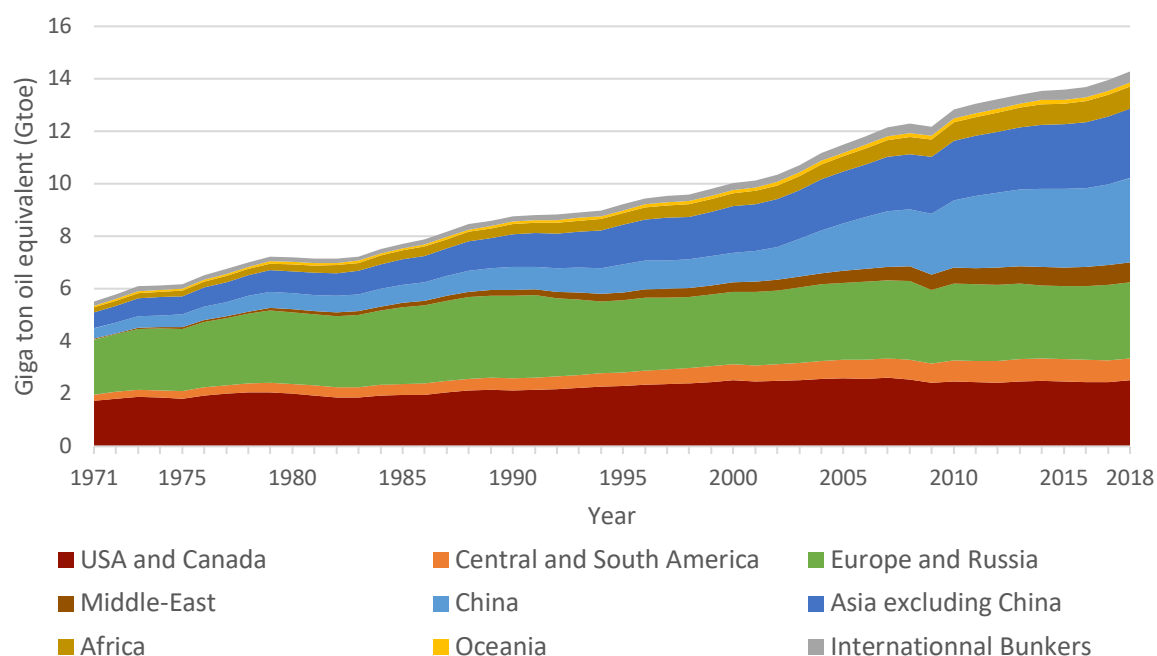


Figure I - 1 - 2: Global consumption of primary energy per year.

All the economic fields are concerned by the increase of the energetic demand because it is linked to the demographic expansion. More and more people mean more and more workers and consumers. The industry and the transport account for the largest share of energy consumption with 29% each in 2018 (Figure I-1-3).

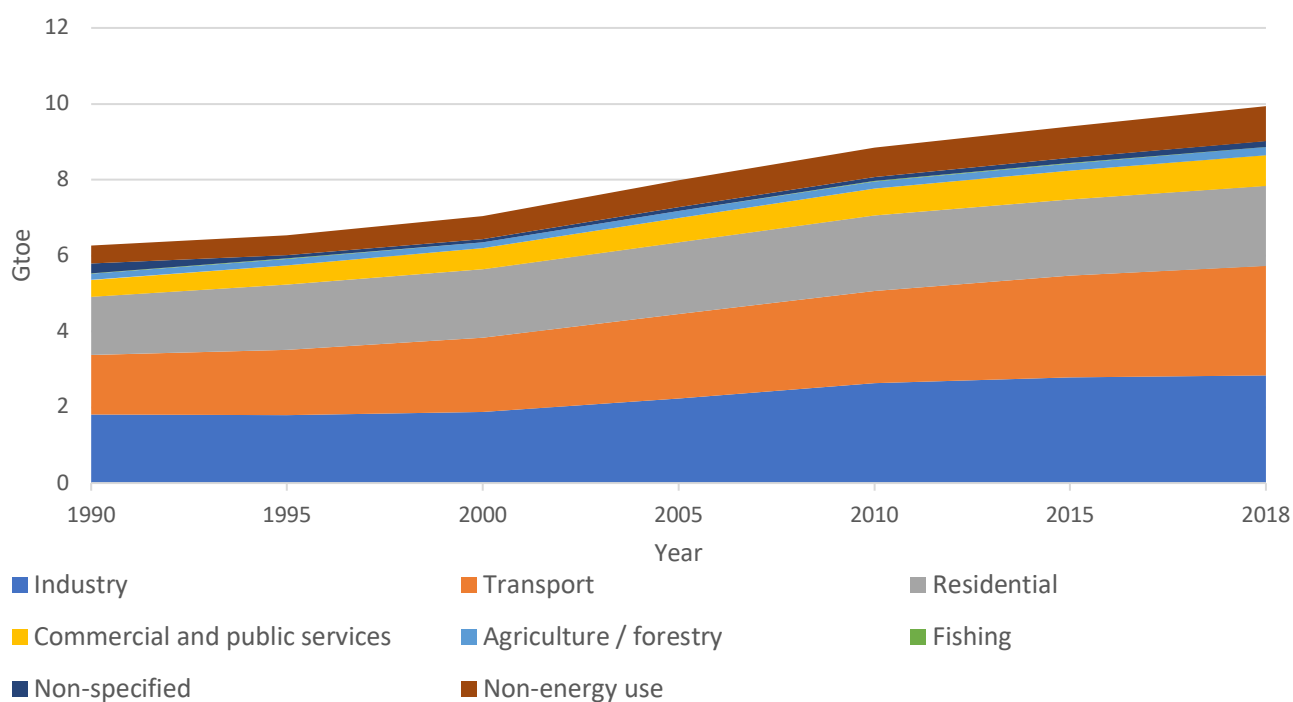


Figure I - 1 - 3: Total final consumption by sector in the world.

In France, the energy consumption increased gradually over the past decades but since 2005 it has been maintained and slowly decreased to reach 248 MToe in 2019 (Figure I-1-4).

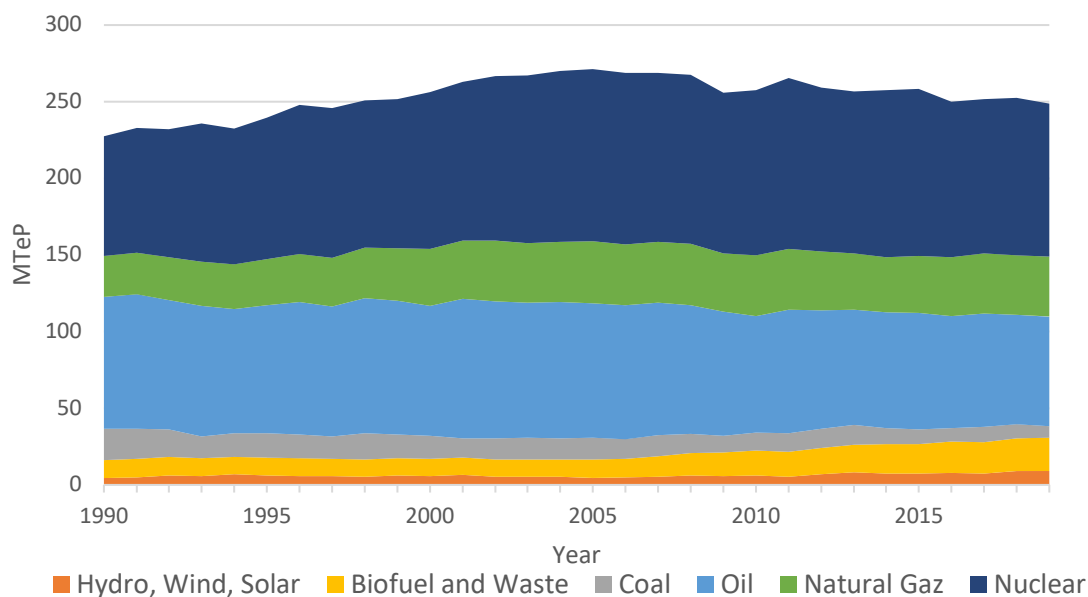


Figure I - 1 - 4: French primary energy consumption per year.

## 2.2. Fossil resources

As depicted in figure I-1-1, the world energy production relies on fossil fuels (coal, gas and oil). They are used from electricity production to transport and others. Coal is mainly used in industry and gas is used in industrial and residential sector. The transport sector is particularly dependent on oil. For example, in France in 2019, 91% of the transport energetic mix came from fossil fuels (Figure I-1-5).

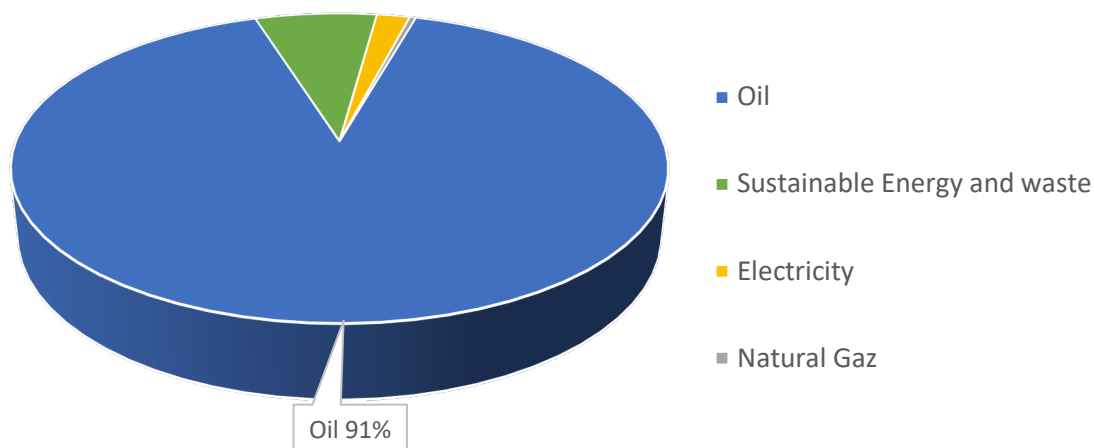


Figure I - 1 - 5: Repartition of fuels used in France in 2019.

The oil production has known a continuously increased since the 70's only slowed down by oil crisis (Figure I-1-6). More and more oil is required to satisfy the demand of the growing population either as an energy supplier or as raw material for industry (plastic, pharmaceutical, etc). This contributes to the oil dependance we are living in.

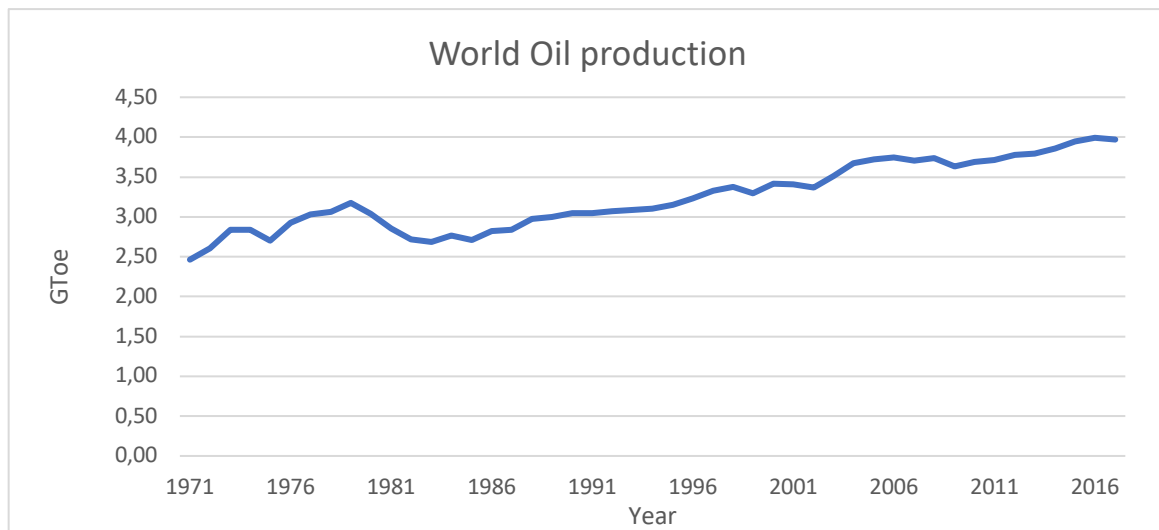


Figure I - 1 - 6: Worldwide oil production.

## 3. Consequences

### 3.1. Greenhouse gas effect

The use of fossil fuel results in the massive emission of GreenHouse Gas (GHG) especially CO<sub>2</sub>. Since the industrial era, anthropological activities produced a lot of CO<sub>2</sub> that continuously increased to reach more than 33 000 Mt of CO<sub>2</sub> in 2019 (Figure I-1-7).<sup>[6]</sup>

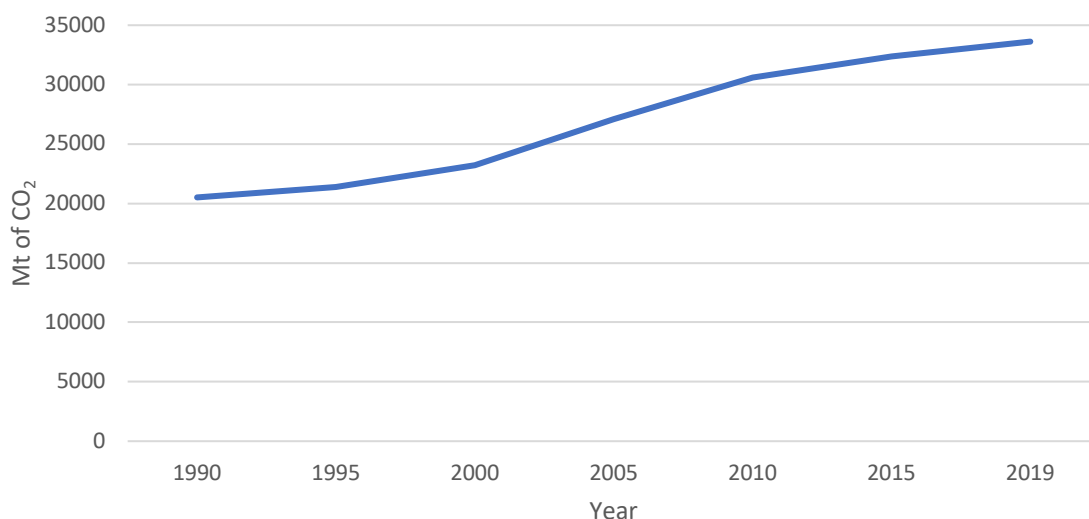


Figure I - 1 - 7: Evolution of the CO<sub>2</sub> emissions in the world.

Looking at CO<sub>2</sub> emissions by sectors of activity, transport is the one that causes 24% of CO<sub>2</sub> production in the world just behind electricity production (Figure I-1-8). On the opposite, in France, transport with 43% is the highest CO<sub>2</sub> producer ahead electricity production which is essentially produced by nuclear power plants (Figure I-1-9).

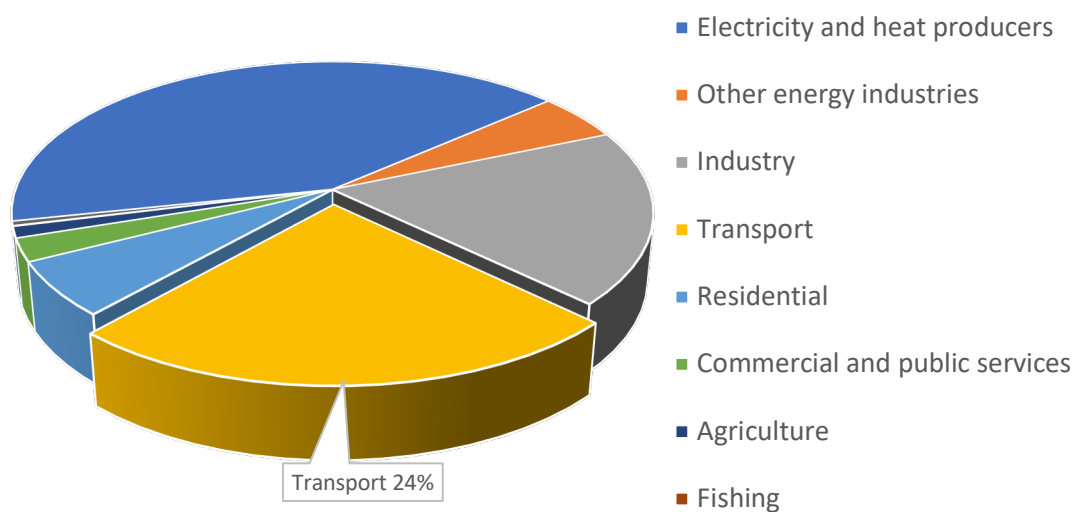


Figure I - 1 - 8: CO<sub>2</sub> emissions by sector in the world.

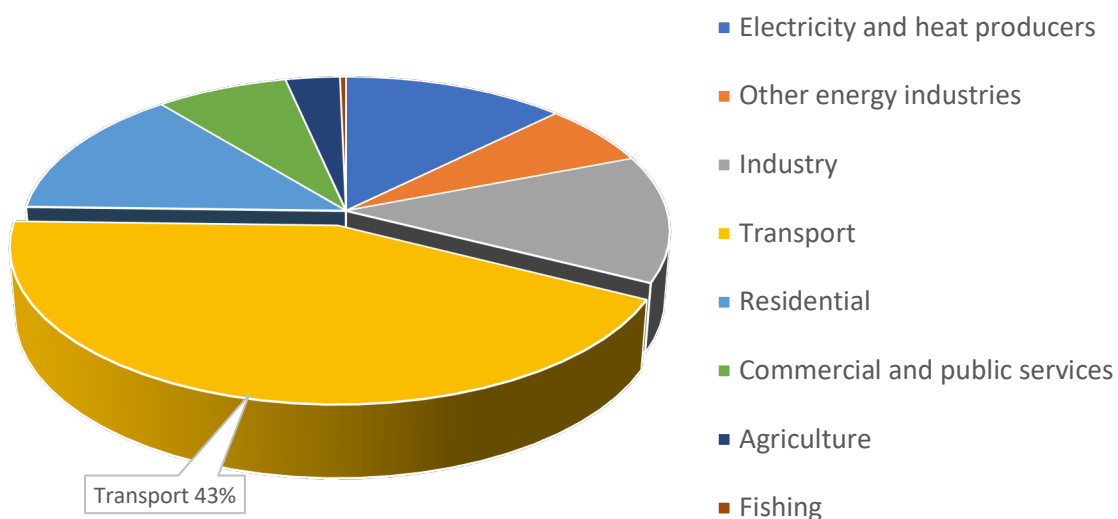


Figure I - 1 - 9: CO<sub>2</sub> emissions by sector in France in 2019.

As it cannot be fully absorbed by the earth's carbon sinks (oceans, forests, ...), this over production of CO<sub>2</sub> goes up into the atmosphere. Hence, the concentration of CO<sub>2</sub> that is increasing in the atmosphere exacerbates the greenhouse gas effect naturally present.

Thanks to the atmosphere, the greenhouse effect is a natural phenomenon which allows us to live on earth by maintaining an average temperature of 15 °C instead of -19 °C. However, by producing more greenhouse gas, more sun radiations are imprisoned and the overall temperature on earth will increase and deregulate the climate (Figure I-1-10).<sup>[7]</sup>

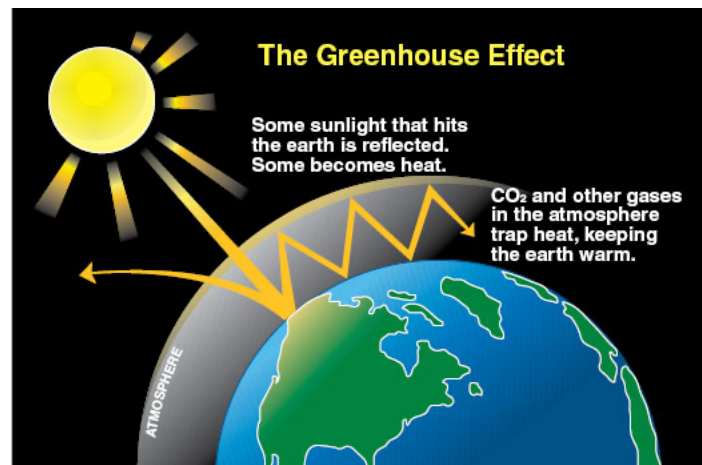


Figure I - 1 - 10: The Greenhouse effect.

One of the oldest CO<sub>2</sub> recording station in Mauna Loa, Hawaiï, USA, clearly measure an increased in the rate of CO<sub>2</sub> in the air since the beginning of the measurements in 1960. From 315 ppm in 1960, it now stands at 416 ppm in 2021 (Figure I-1-11).<sup>[8]</sup> Furthermore, a high level of CO<sub>2</sub> could have an impact on health in addition to its impact on the climate.<sup>[9]</sup>

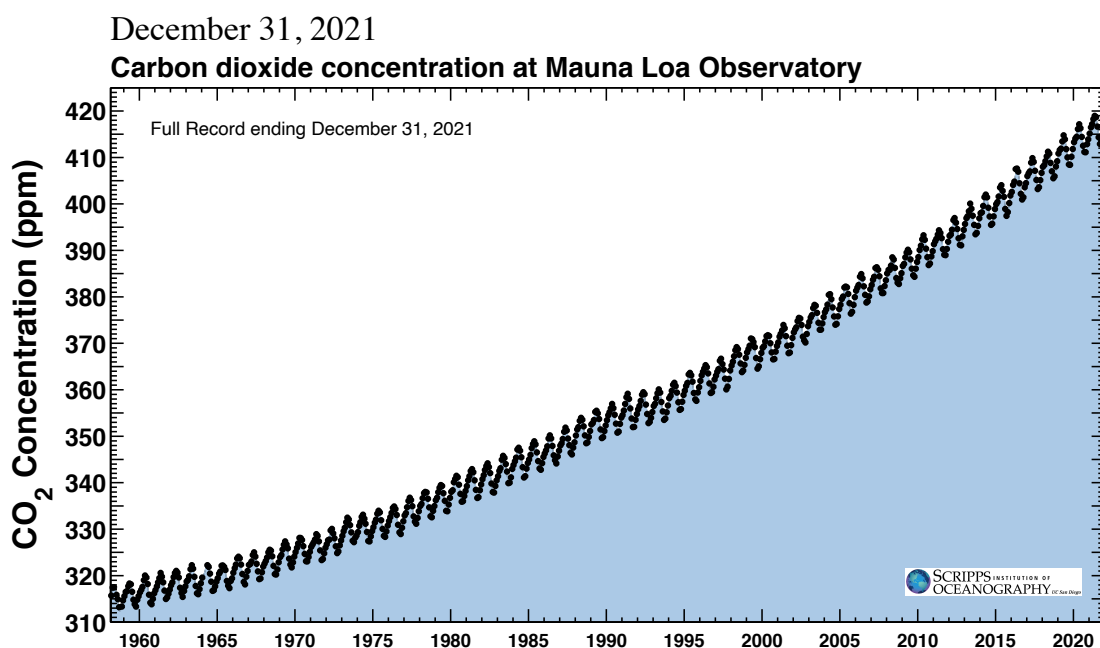


Figure I - 1 - 11: Evolution of carbon dioxide in air.

## 3.2. Climate change

Climate change is the consequence of the over-expression of the greenhouse effect due to an over-production of greenhouse gas by anthropological activities. The direct consequence is the augmentation of the temperature on earth. Then, this phenomenon brought to the melting ice, the increase of sea levels, more frequent extreme climate events (droughts, floods, storms, ...), loss of biodiversity, etc.

The main risk of the global increased of temperature is that it could lead to a chain reaction with no turning point. Therefore, it is crucial to face this danger, to collaborate and try to find solution at every level to preserve earth and humanity.<sup>[10]</sup>

## 4. Energetical transition

### 4.1. General presentation

Climate change is real but it took time to be properly considered as a threat for the global wellbeing by the scientific community and the population. In 1979 the first summit on climate was organized by the UN in Geneva. Because they wanted to know more, the Intergovernmental Panel on Climate Change (IPCC) was created in 1988 “to provide policymakers with regular scientific assessments on the current state of knowledge about climate change”. IPCC aims to give better understanding on climate change, analyze social and economic impact and also provide strategies to face issues.<sup>[11]</sup>

The creation of this panel and the reports it produced led to the hold of UN-supervised summits on climate change to take action. In 1997, the Kyoto Treaty was signed to reduce the greenhouse gas emission especially CO<sub>2</sub>.<sup>[12]</sup> It was the first summit where countries from all around the world set-up objectives to prevent climate change. Now regularly, countries gathered to target some objectives such as the limitation of the global temperature at maximum +2 °C compare to pre-industrial era with the Paris Agreement in 2016 with the COP21.<sup>[13]</sup> In 2021, the COP26 took place in Glasgow and lead to the Glasgow Climate pact.<sup>[14]</sup> The main decision taken during this summit was to progressively reduce the use of fossil resources.

### 4.2. Tackle CO<sub>2</sub> emission

CO<sub>2</sub> emissions play a key role in climate change as they are considered to be the major greenhouse gas contributors. Therefore, they need to be reduced if we want to address the global warming issue. A way to do that is to reduce the fossil fuel dependency as they are responsible for the major part of CO<sub>2</sub> emissions (Figure I-1-12). Another way is to change the way of life and be more concerned about the production of CO<sub>2</sub> emission. A solution that could really make the difference consists in finding and using alternative energy sources generating less or no CO<sub>2</sub>.

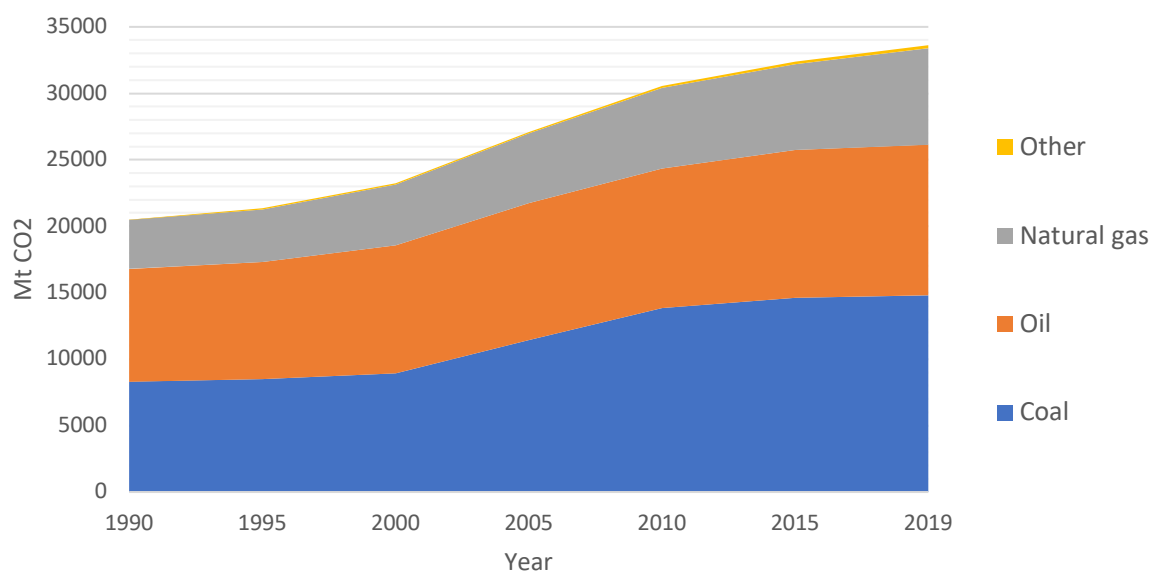


Figure I - 1 - 12: CO<sub>2</sub> emissions by source.

In some countries, like in France or generally Europe, we can already observed a small decrease of the CO<sub>2</sub> emissions (Figure I-1-13).<sup>[15]</sup> This is a good sign but efforts need to be amplified and followed globally.

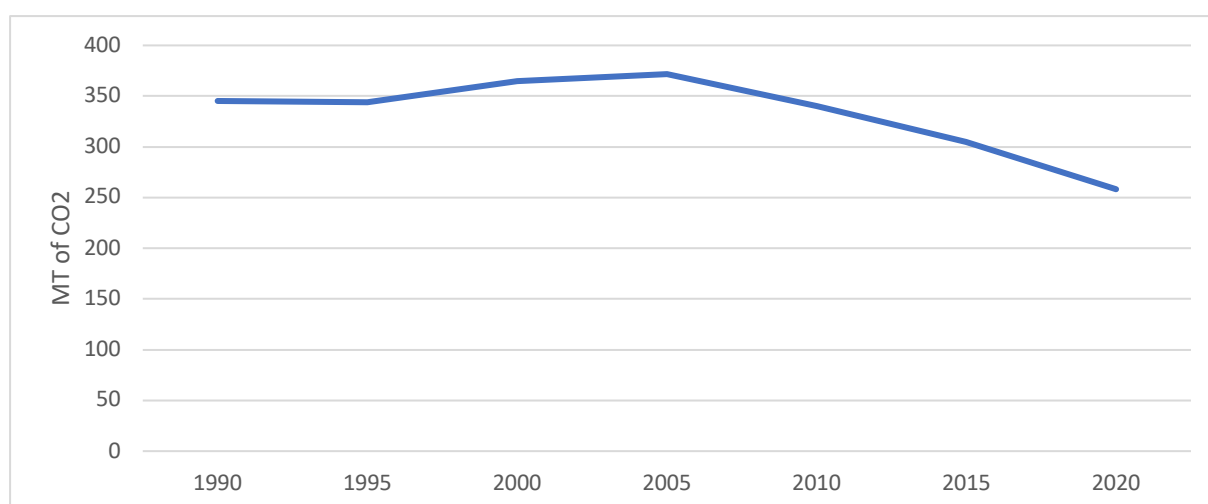


Figure I - 1 - 13: CO<sub>2</sub> emissions in France.

### 4.3. Oil depletion

Beside the environmental concerns, signs of oil depletion become stronger and stronger every year.<sup>[16]</sup> Oil fields are more and more difficult to find and/or exploit, they are sometimes located in politically unstable area, the consumption and the production are close to an equilibrium, the price is increasing, etc. Those observations indicate that the oil era seems near to its maximum. The oil production will decrease sooner or later but the energy demand will remain the same. Therefore, the need for new energy sources is required.

### 4.4. New energy sources

To overcome this energy crisis, carbon-free energy sources must replace fossil fuels in all areas of our daily lives.

Electricity seems in good position to replace this dependance to fossil fuel. Indeed, a lot of the energy we use is electricity, we just have to think about light, computers, Smartphone, industrial production line, etc. Electricity is used in a lot of sectors from industry to residential and commercial services. However, nowadays a lot of electricity is produced from coal (Figure I-1-14).<sup>[17]</sup> Sustainable electricity production is increasing with the use of solar, wind or hydro power. Nuclear power is a controversial carbon free electricity provider that suffers from the production of hazardous wastes which have to be stored for a very long time.

Regarding transport, the system is based on thermal engine. Thus, fuel with a lower carbon footprint must be employed or new power unit engines based on electricity have to be democratized.

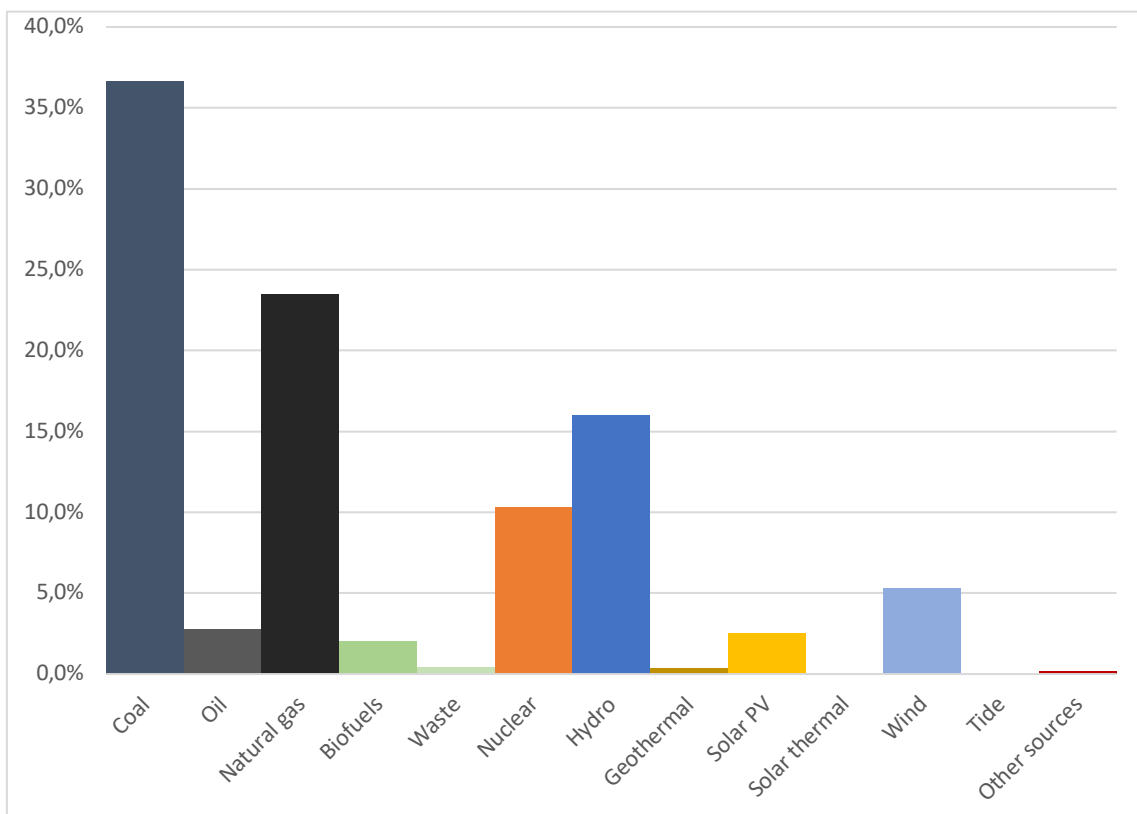


Figure I - 1 - 14: Worldwide electricity production by sources in 2019.

## 4.5. New fuels

Since transport represents a large share of CO<sub>2</sub> emissions (Figure I-1-8 and I-1-9), it is important to find alternative in this field, particularly. By reducing fossil fuel in transport, we could strongly reduce GHG emissions. Nowadays we have two main options consisting in replacing fossil fuels by biofuels or electricity.

### 4.5.1. Biofuels

Biofuels are fuels produced from biomass resources that can also be used in combustion engines. They can be either based on lipidic biomass (fats and oils) for diesel engine (biodiesel) or alcohol such as ethanol or butanol for gasoline substitute. This technology has been developed for years and can be sorted into four generations.<sup>[18]</sup>

First of all, the 1<sup>st</sup> generation was based on edible biomass such as corn, sugar cane, etc. This production based on edible crops competes with the production of food. Knowing that 720 to 811 million people face hunger<sup>[19]</sup> it rises some ethical and moral thought.

Therefore, a second generation was developed based on non-edible biomass like lignocellulosic biomass or by-products/wastes from agriculture industry.

The third generation was based on algae and micro-organism that do not compete on arable land or potable water as they can be cultivated in seawater.

The fourth generation is currently under research and development and rely on the optimization of the third generation by modifying the algae or enhance the process.

Whatever the biofuel considered, its synthesis and use should be efficient and present a positive CO<sub>2</sub> balance. This means that very efficient and low energy consuming chemical processes should be implemented for production using as much as possible decarbonated energy.

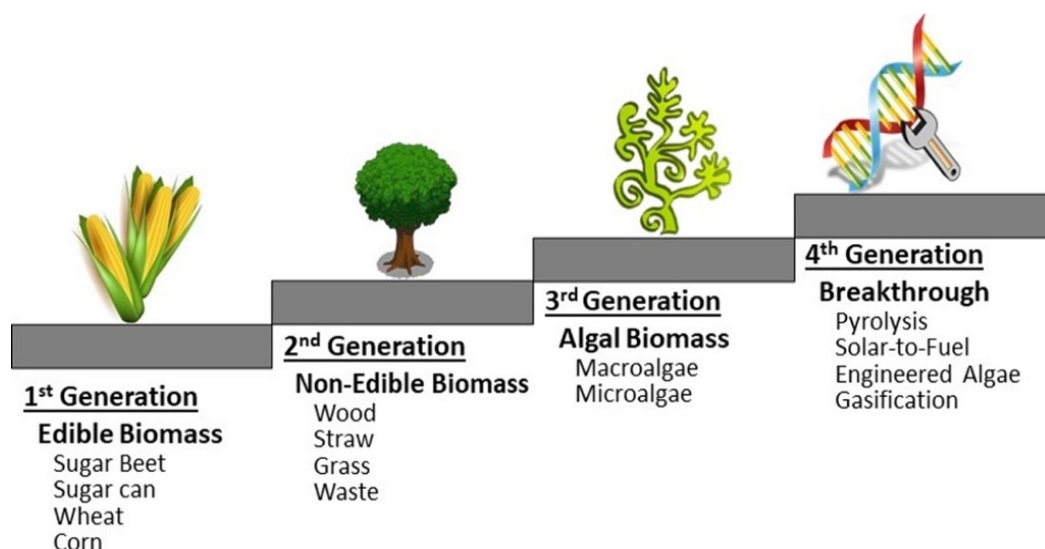


Figure I - 1 - 15: Presentation of the different generation of biofuels.

## 4.5.2. Electricity

Electricity could be the new source of power for road transport however, this alternative faces two major challenges. The first one is the way it is produced. Indeed, a lot of electricity is made in power plant using coal (Figure I-1-14). Therefore, the way electricity is produced needs to be more sustainable. The other challenge covers the storage of this energy. Because it is an electronic flux, it cannot be simply stored and it requires battery with specific component to avoid loss. If small scale batteries are available, larger storage capacity are not possible and electricity has to be consumed as soon as it is produced.

### 4.5.2.1. Battery

A way to use electricity for transportation is to store it in batteries after production. Currently it is the most used alternative because battery is a widely used apparatus. The performances and the storage capacity have been greatly improved in the past decades thanks to new technologies such as Li-ion batteries. The inventors of this technology were awarded by the Chemistry Nobel prize in 2019.<sup>[20]</sup> Electric cars are considerably increasing but there are several hurdles to overcome such as charging speed or building a distribution network. For now, it allows to have short to mid-range electric vehicles that can replace fossil fuel-powered vehicles.

### 4.5.2.2. Proton Exchange Membrane Fuel cells

If we can store electricity in vehicle, we can also think about producing it on board. The principle of fuel cell is to convert a chemical source (hydrogen, methanol, ...) into electricity via an electrochemical reaction using a cathode and an anode.<sup>[21]</sup>

One of the most developed fuel for fuel cells is hydrogen. Hydrogen is very interesting as it can be produced in a sustainable way by water splitting using green electricity produced from sunlight, wind, etc. However, Hydrogen from fossil resources is still more economically viable and largely employed.<sup>[22]</sup> Dealing with this technology, the hydrogen storage and transportation as well as a distribution network are the limitation for its democratization. It still needs research and development to be used at a large scale.

As depicted in Figure I-1-16, in a hydrogen fuel cells, hydrogen is oxidized at the anode to give on one hand electron that generates an electric current and on the other hand proton. The protons migrate through a polymer electrolyte exchange membrane to the cathode where they combine with oxygen rejecting water as the single process product.

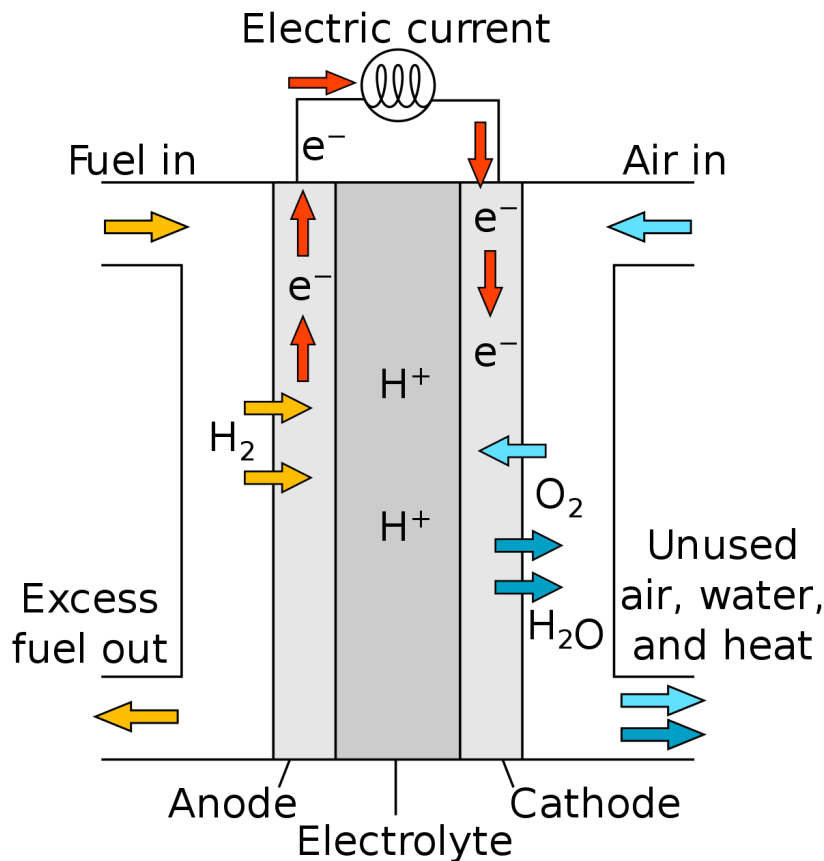


Figure I - 1 - 16: PEM Fuel cells.

## 4.6. CO<sub>2</sub> Capture and Valorization

Beside the reduction of CO<sub>2</sub> emissions, another way of thinking, as a lot of CO<sub>2</sub> is produced, is to use it as a feedstock for the production of chemicals or for hydrogen storage as it will be discussed and presented later. Therefore, CO<sub>2</sub> capture and storage or re-use are domains of growing interest.

### 4.6.1. CO<sub>2</sub> Capture and Storage

Storage of CO<sub>2</sub> from big GHG producers can be employed. The CO<sub>2</sub> is captured straight from the factory, purified, concentrated and sent to the storage place. Former oil fields can be used as there are already pipelines available and they have impermeable walls due to oil residues. Saline aquifer also allowed to store CO<sub>2</sub>. Pioneer works have been realized in 1996 in Norway. This methodology is not well developed and side effect especially on a long-term are unknown.<sup>[23]</sup>

Recently, the company Air liquid and its startup company CRYOCAP<sup>TM</sup> developed the cryogenic capture of CO<sub>2</sub> from a H<sub>2</sub> plant.<sup>[24]</sup> Then, they extended this process to numerous plants that produce CO<sub>2</sub> such as steel plant or heating plant.

In Iceland, they proceed to the CO<sub>2</sub> capture and its storage through mineral carbonation thanks to abundant geothermal activity.<sup>[25,26]</sup>

## 4.6.2. Valorization

Beside the captured and storage options, CO<sub>2</sub> could also be used in other processes to be valorized.<sup>[27]</sup> First of all, CO<sub>2</sub> can be useful in some industries. It is already used in oil industry in Enhance Oil Recovery<sup>[28]</sup>, to get more oil from the fields. Supercritical CO<sub>2</sub> extractions is used in food industry to extract caffeine from tea or coffee for example.<sup>[29]</sup> Finally, it is also used in fizzy drinks or beer.

Some biological valorization is possible with algae that can be feed with CO<sub>2</sub> to proliferate. By this way organic matter such as lipid or sugar is produced from it via photosynthesis and can be used as precursor for biofuel.<sup>[30]</sup>

CO<sub>2</sub> can also be used as a building block for value added chemical which represent another way of CO<sub>2</sub> storage, albeit in small scale. There is a big challenge to use CO<sub>2</sub> as a C1 building blocks and a lot of research are conducted on that topic.<sup>[31,32]</sup> Some molecules such as urea<sup>[33]</sup> which is widely used as a fertilizer can be produced from CO<sub>2</sub>.

A very interesting topic is the valorization of CO<sub>2</sub> for energetical value-added molecules. For example, hydrogenation of CO<sub>2</sub> into formic acid and alcohols<sup>[34]</sup> represent a challenging and promising possibility for the storage of hydrogen. Hydrogen is considered and foreseen as one of the energy vectors for the near future. However, as depicted hereafter, hydrogen suffers from several drawbacks. Hydrogenation of CO<sub>2</sub> into formic acid for hydrogen storage is one of the important topics to overcome some of these drawbacks and constitutes one of the research projects conducted during this PhD.

## 5. Positioning of the Project

### 5.1. Context

The ANR project CatEngy aims at implementing original homogeneous ruthenium catalysts in the domain of sustainable energy sources. This project gathered two teams with complementary skills in organometallic synthesis and homogeneous catalysis. The teams of Dr. Alain Igau in the Laboratoire de Chimie de Coordination (Toulouse) and Dr. Cédric Fischmeister at the Institute des Sciences Chimiques de Rennes collaborated for the implementation of ruthenium catalysts in the fields of hydrogen storage through the hydrogenation of CO<sub>2</sub> into formic acid and the upgrade of ethanol through the Guerbet reaction. The team in Rennes has a long experience in homogeneous catalysis for the valorization of biomass<sup>[35-37]</sup> and more recently, research have been oriented toward sustainable hydrogen storage with LOHC.<sup>[38]</sup>

The intensive use of fossil resources (oil, coal, etc) with the depletion of it and the environmental issues it causes make the research of alternative and sustainable energy source of a great interest. In recent years, this research field has been attracting intense research from academia and industry. Alcohol and Hydrogen represent energy carriers with a high potential to replace oil.<sup>[34,39]</sup> As an example of research project for a more sustainable future for energy, Leitner reported, very recently, an innovative process combining biomass fermentation with a chemo-catalytic CO<sub>2</sub> hydrogenation.<sup>[40]</sup> Hence while producing bio-ethanol, a part of the waste CO<sub>2</sub> was converted into the value added molecule formic acid.

Alcohol, especially ethanol, is already used either blended with gasoline in standard vehicle or pure in flex fuel vehicle. However, ethanol has two main drawbacks. First, it has a

low energy density (around 60%) compared to conventional fuel. Then, its hydrophilicity may damage the engine. Therefore, the upgrade of easily produced ethanol to higher alcohol with the Guerbet reaction represent an interesting way to overcome the downside of ethanol. Butanol represents a chemical of choice and will be targeted in this thesis work. This topic will be discussed in more detail in Chapter III.

Hydrogen represents the second alternative to gasoline as it has a highly energetic property. Whereas, due to its gaseous form and high flammability, it suffers from safety, transportation and storage issues. Therefore, the big challenge associated with hydrogen is the storage under safe and easy-to-handle conditions. Among the hydrogen storage possibilities, chemical storage is a topic of intense research. In this field, formic acid (FA) received a strong interest in recent years. FA has the advantage to be a safe, easy to handle, easy to store liquid that can release hydrogen (and CO<sub>2</sub>) by dehydrogenation. Hence, a virtuous cycle of energy storage based on FA/CO<sub>2</sub> can be envisaged. In a first step the hydrogenation of CO<sub>2</sub> to produce FA represent the energy storage. Then, in a second step, the dehydrogenation of FA into H<sub>2</sub> (and CO<sub>2</sub>) represent the energy release. This topic will be discussed in more detail in Chapter IV.

To achieve the reaction focused in this thesis work, we decided to use homogeneous catalysis as it is a useful tool to make efficient and selective transformations. Organometallic complexes are an important part in homogeneous catalysis as they can be finely tuned thanks to the ligand.

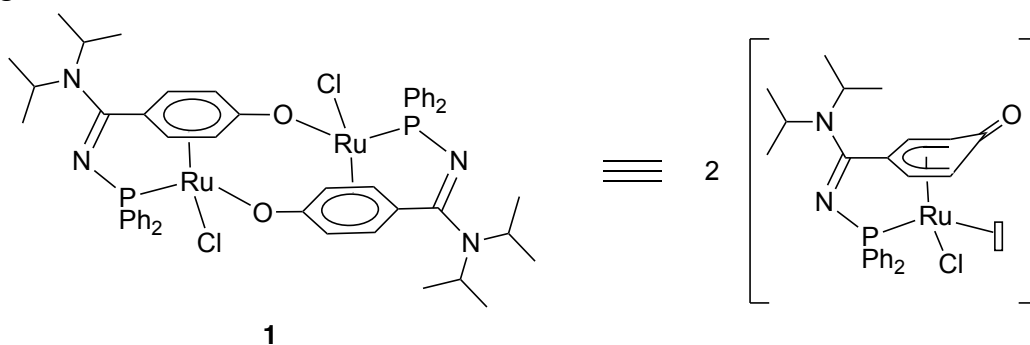


Figure I - 1 - 17: Complex isolated by Igau.

The complexes employed in the thesis belongs to the family of  $\eta^5$ -Oxocyclohexadienyl ruthenium complexes. The team of Alain Igau isolated and characterize a tethered  $\eta^5$ -oxocyclohexadienyl complex isolated as a bimetallic species (Figure I-1-17).<sup>[41,42]</sup> The complex design enables possible modifications of the backbone necessary to finely tune its properties (Figure I-1-19). This complex shows the characteristics of a bifunctional catalyst since it features a basic carbonyl moiety and an acidic metal center. It could therefore promote catalytic transformations through metal-ligand cooperation.<sup>[43]</sup> As such, this complex can be compared to the well-known Shvo catalyst (Figure I-1-18).<sup>[44]</sup> Preliminary catalytic experiment

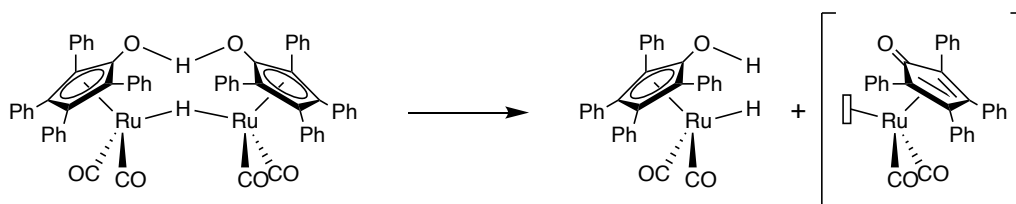


Figure I - 1 - 18: Shvo catalyst.

with this tethered  $\eta^5$ -oxocyclohexadienyl complex **1** have been done. The complex was involved in a base free isomerization of allylic-alcohol providing a selective and quantitative formation of ketone in a short period of time.

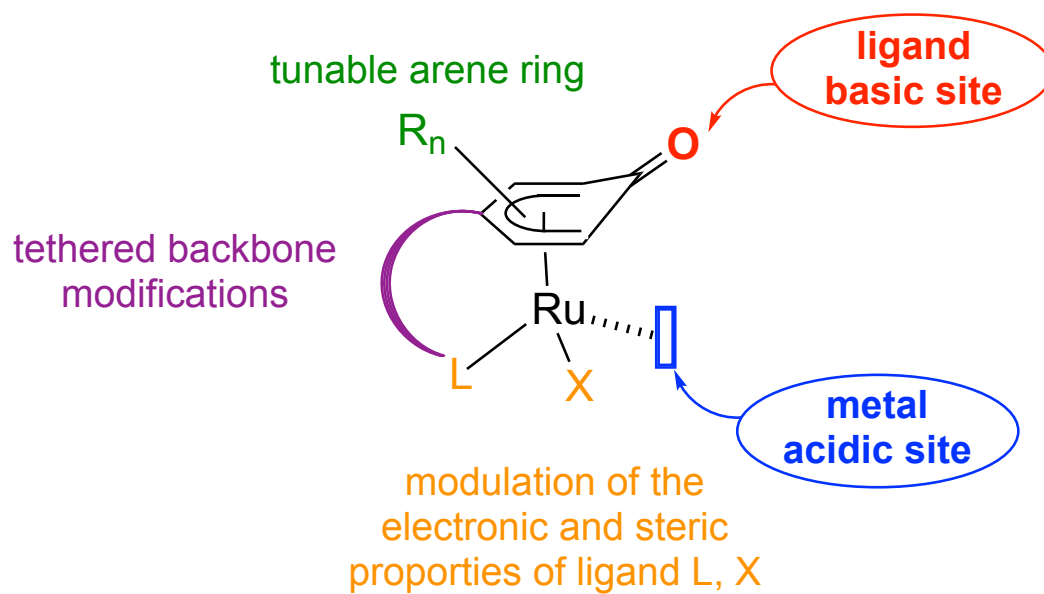
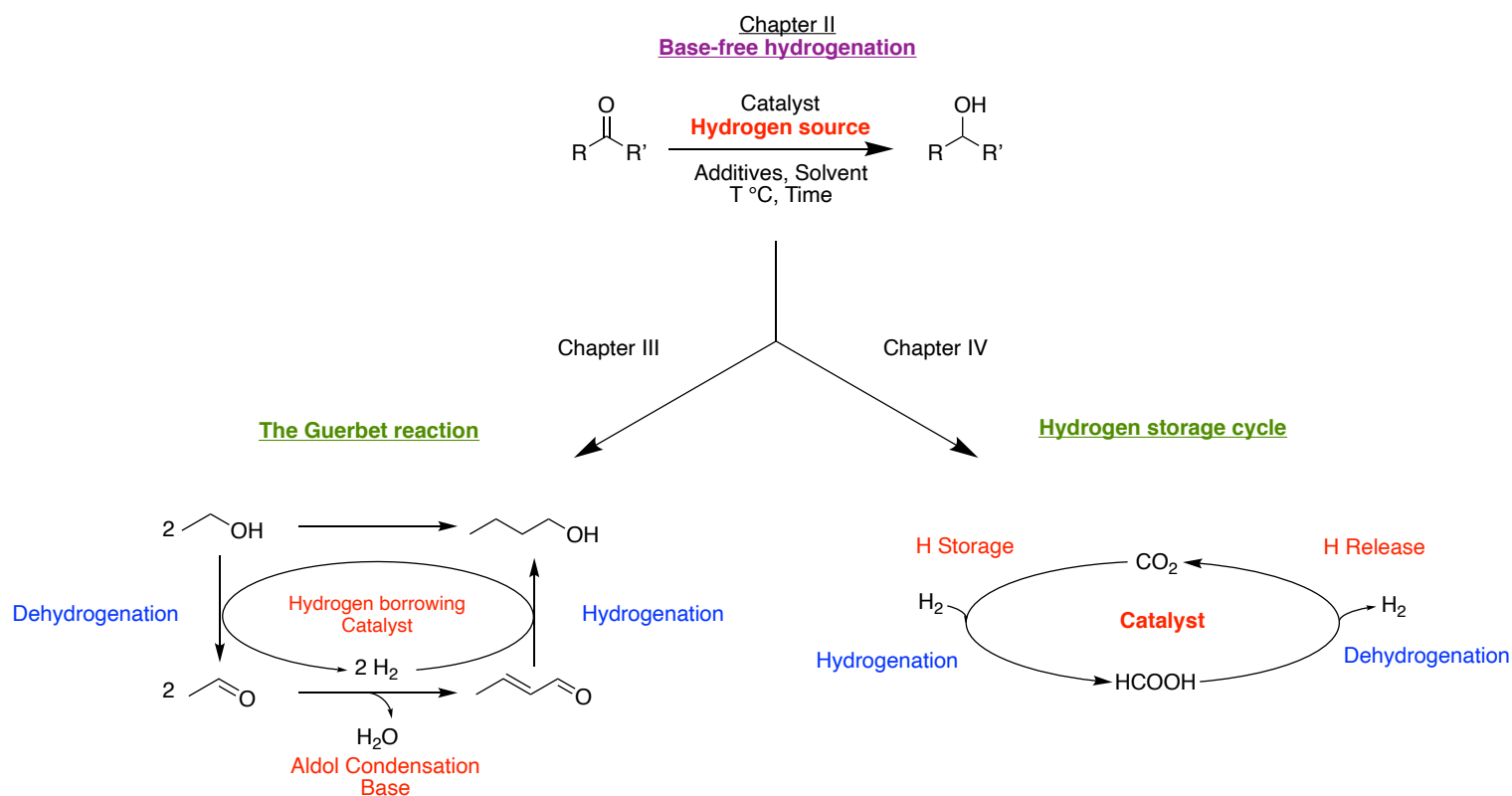


Figure I - 1 - 19 : Formal bifunctional properties of half-sandwich  $\eta^5$ -oxocyclohexadienyl Ruthenium complexes.

## 5.2. Objectives

First of all, in order to evaluate the bifunctional properties of complex **1** in reduction processes, its activity has been tested in the base-free hydrogenation and the base-free transfer hydrogenation of ketones. Those tests will contribute to feed the knowledge on the piano-stool complexes activity and serve as a proof of concept before implementation in more challenging catalytic applications (Chapter II).

In a second part, those tethered  $\eta^5$ -oxocyclohexadienyl complexes will be tested in more challenging reactions in the domain of sustainable energy involving hydrogenation and dehydrogenation process. The first reaction investigated will be the Guerbet reaction that aims to upgrade ethanol to n-butanol via a hydrogen borrowing mechanism (Chapter III). The second reaction explored will be the hydrogen storage associated with CO<sub>2</sub> hydrogenation to Formic Acid and the release of H<sub>2</sub> by dehydrogenation of formic acid (Chapter IV). These two reactions will be investigated as unitary steps but also in a full storage/release cycle.



Scheme I - 1 - 1: Scheme of the reactions studied in the thesis.

## 6. References:

- [1] K. S. Brown, C. W. Marean, A. I. R. Herries, Z. Jacobs, C. Tribolo, D. Braun, D. L. Roberts, M. C. Meyer, J. Bernatchez, *Science* **2009**, 325, 859–862.
- [2] W. Roebroeks, P. Villa, *Proc. Natl. Acad. Sci.* **2011**, 108, 5209–5214.
- [3] P. N. Stearns, *The Industrial Revolution in World History*, Routledge, New York, **2021**.
- [4] “IEA-Energy supply,” can be found under <https://www.iea.org/data-and-statistics/data-browser?country=WORLD&fuel=Energy%20supply&indicator=TPESbySource>, **2018**.
- [5] “UN-population projection,” can be found under <https://population.un.org/wpp/Graphs/Probabilistic/POP/TOT/900>, **2019**.
- [6] “Total CO<sub>2</sub> emission,” can be found under [https://www.iea.org/data-and-statistics/data-browser/?country=WORLD&fuel=CO<sub>2</sub>%20emissions&indicator=TotCO<sub>2</sub>](https://www.iea.org/data-and-statistics/data-browser/?country=WORLD&fuel=CO2%20emissions&indicator=TotCO2), **2022**.
- [7] M. Collins, R. Knutti, et al, *IPCC AR5* **2013**, 1029–1136.
- [8] R. Keeling, “Atmospheric Monthly In Situ CO<sub>2</sub> Data - Mauna Loa Observatory, Hawaii (Archive 2021-09-07). In Scripps CO<sub>2</sub> Program Data. UC San Diego Library Digital Collections,” can be found under <https://keelingcurve.ucsd.edu>, **2021**.
- [9] T. A. Jacobson, J. S. Kler, M. T. Hernke, R. K. Braun, K. C. Meyer, W. E. Funk, *Nat. Sustain.* **2019**, 2, 691–701.
- [10] W. Steffen, J. Rockström, K. Richardson, T. M. Lenton, C. Folke, D. Liverman, C. P. Summerhayes, A. D. Barnosky, S. E. Cornell, M. Crucifix, J. F. Donges, I. Fetzer, S. J. Lade, M. Scheffer, R. Winkelmann, H. J. Schellnhuber, *Proc. Natl. Acad. Sci.* **2018**, 115, 8252–8259.
- [11] “IPCC - Home Page,” can be found under <https://www.ipcc.ch/about/>
- [12] “UNFCCC - What is Kyoto protocol?,” can be found under [https://unfccc.int/kyoto\\_protocol](https://unfccc.int/kyoto_protocol),
- [13] “UNFCCC - Paris Agreement,” can be found under <https://unfccc.int/process-and-meetings/the-paris-agreement/the-paris-agreement>,
- [14] UNFCCC, **2021**.
- [15] “IEA - Total CO<sub>2</sub> emission in France and Europe,” can be found under [https://www.iea.org/data-and-statistics/data-browser/?country=FRANCE&fuel=CO<sub>2</sub>%20emissions&indicator=TotCO<sub>2</sub>](https://www.iea.org/data-and-statistics/data-browser/?country=FRANCE&fuel=CO2%20emissions&indicator=TotCO2), **2021**.
- [16] S. Sorrell, J. Speirs, R. Bentley, A. Brandt, R. Miller, *Energy Policy* **2010**, 38, 5290–5295.
- [17] “IEA-Electricity by source,” can be found under <https://www.iea.org/data-and-statistics/data-browser/?country=WORLD&fuel=Electricity%20and%20heat&indicator=ElecGenByFuel>, **2019**.
- [18] H. A. Alalwan, A. H. Alminshid, H. A. S. Aljaafari, *Renew. Energy Focus* **2019**, 28, 127–139.
- [19] “UN - FAO,” can be found under <https://www.fao.org/state-of-food-security-nutrition/fr/>
- [20] O. Ramström, “Nobel - Chemistry 2019 - Background,” can be found under <https://www.nobelprize.org/uploads/2019/10/advanced-chemistryprize2019.pdf>, **2019**.
- [21] R. P. O’Hayre, S.-W. Cha, W. G. Colella, F. B. Prinz, *Fuel Cell Fundamentals*, John Wiley & Sons Inc, Hoboken, New Jersey, **2016**.
- [22] M. Kayfeci, A. Keçebaş, M. Bayat, in *Sol. Hydrog. Prod.*, Elsevier, **2019**, pp. 45–83.
- [23] R. Farret, *INERIS, Captage et Stockage Géologique Du CO<sub>2</sub>: Retour d’expérience et Perspectives.*, **2017**.

- [24] D. Pichot, L. Granados, T. Morel, A. Schuller, R. Dubettier, F. Lockwood, *Energy Procedia* **2017**, *114*, 2682–2689.
- [25] “Carbfix,” can be found under <https://www.carbfix.com/how-it-works>.
- [26] S. Ó. Snæbjörnsdóttir, B. Sigfússon, C. Marieni, D. Goldberg, S. R. Gislason, E. H. Oelkers, *Nat. Rev. Earth Environ.* **2020**, *1*, 90–102.
- [27] L. Dumergues, *Les filières de valorisation du CO<sub>2</sub>*, **2014**.
- [28] M. Blunt, F. F. John, M. O. J. Franklin, *Energ. Convers. Manage.* **1993**, *34*, 1197–1204.
- [29] M. Raventós, S. Duarte, R. Alarcón, *Food Sci. Technol. Int.* **2002**, *8*, 269–284.
- [30] D. Moreira, J. C. M. Pires, *Bioresour. Technol.* **2016**, *215*, 371–379.
- [31] P. G. Jessop, T. Ikariya, R. Noyori, *Chem. Rev.* **1995**, *95*, 259–272.
- [32] K. Huang, C.-L. Sun, Z.-J. Shi, *Chem. Soc. Rev.* **2011**, *40*, 2435–2452.
- [33] F. Shi, Y. Deng, T. SiMa, J. Peng, Y. Gu, B. Qiao, *Angew. Chem. Int. Ed.* **2003**, *42*, 3257–3260.
- [34] K. Sordakis, C. Tang, L. K. Vogt, H. Junge, P. J. Dyson, M. Beller, G. Laurenczy, *Chem. Rev.* **2018**, *118*, 372–433.
- [35] H. Bilel, N. Hamdi, C. Fischmeister, C. Bruneau, *ChemCatChem* **2020**, *12*, 5000–5021.
- [36] L. Sarmiento Fernandes, D. Mandelli, W. A. Carvalho, C. Fischmeister, C. Bruneau, *Catal. Commun.* **2020**, *135*, 105893.
- [37] G. M. Vieira, A. V. Granato, E. V. Gusevskaya, E. N. dos Santos, P. H. Dixneuf, C. Fischmeister, C. Bruneau, *Appl. Catal. Gen.* **2020**, *598*, 117583.
- [38] S. Wang, H. Huang, T. Roisnel, C. Bruneau, C. Fischmeister, *ChemSusChem* **2019**, *12*, 179–184.
- [39] H. Aitchison, R. L. Wingad, D. F. Wass, *ACS Catal.* **2016**, *6*, 7125–7132.
- [40] N. Guntermann, H. G. Mengers, G. Franciò, L. M. Blank, W. Leitner, *Green Chem.* **2021**, *23*, 9860–9864.
- [41] M. Kechaou-Perrot, L. Vendier, S. Bastin, J.-M. Sotiropoulos, K. Miqueu, L. Menéndez-Rodríguez, P. Crochet, V. Cadierno, A. Igau, *Organometallics* **2014**, *33*, 6294–6297.
- [42] A. Igau, *Coord. Chem. Rev.* **2017**, *344*, 299–322.
- [43] J. R. Khusnutdinova, D. Milstein, *Angew. Chem. Int. Ed.* **2015**, *54*, 12236–12273.
- [44] Y. Blum, D. Czarkie, Y. Rahamim, Y. Shvo, *Organometallics* **1985**, *4*, 1459–1461.





# Chapter II: Base-free Hydrogenation and transfer hydrogenation

## Part 1: General Introduction



# 1. Homogeneous Hydrogenation

## 1.1. Background

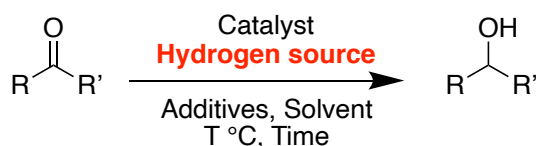
Hydrogenation is a widely used reducing reaction which became an important process in catalysis in both academia and industry. It can convert a broad scope of chemical function with good selectivity and conversion and the methodology is well-established. Indeed, the process was initiated in the late 1890 by Paul Sabatier who was awarded by the Nobel prize in 1912<sup>[1]</sup> for the hydrogenation of organic compound by heterogeneous metallic catalysts.<sup>[2]</sup> Since the 60's there was a growing development of homogeneous catalyst and so of homogeneous hydrogenation. The work of Wilkinson (Nobel laureate in 1973) and the catalyst developed for the homogeneous hydrogenation of olefins was an achievement in this field.<sup>[3]</sup> Since then, homogeneous hydrogenation had a big impact on the development of organic synthesis. The application of hydrogenation is quite important in industry especially in the field of pharmaceuticals.<sup>[4]</sup>

Currently, reduction processes including catalytic hydrogenations are at the heart of the transition from fossil feedstocks to bio-based materials. Indeed, while fossil raw materials are at a low oxidation state and thus require oxidation chemical processes for their functionalization, raw materials arising from biomass are highly oxidized and functionalized and therefore need to be reduced.<sup>[5,6]</sup> Hence, homogeneous hydrogenation has still an important role to play in the new challenges of chemistry.

## 1.2. Use

Carbonyl compounds and especially pro-chiral ketones are substrates of choice to reduce. They can lead to chiral carbon center which is of a big interest in fine chemistry, provided that stereoselective reductions are implemented.

Reduction of ketone can be accomplished with a variety of noble and non-noble transition metals using different sources of hydrogen. It can be hydrogen gas (H<sub>2</sub>) or hydrogen donors such as isopropanol or formic acid (Figure II-1-1).



*Scheme II - 1 - 1: General equation of ketone hydrogenation.*

### 1.2.1. H<sub>2</sub>

H<sub>2</sub> is the main source of hydrogen to perform ketone reduction. It is a well-established process that has been acknowledged by the Nobel prize of R. Noyori in 2001 (shared with W. Knowles and B. Sharpless).<sup>[7,8]</sup> Before that, one of the first homogeneous catalytic system able to hydrogenate ketone was made by Shvo with a dimeric Ruthenium catalyst.<sup>[9]</sup> Using H<sub>2</sub> has the advantage to be a full atom economy process but also a potentially hazardous process. As it will be presented later, most of the hydrogenation processes require a basic additive to activate the catalyst.

### 1.2.2. Transfer Hydrogenation (*i*-PrOH, FA)

Beside hydrogenation, transfer hydrogenation has known a growing attention over the past 20 years. Transfer hydrogenation relies on the use of small organic molecule as hydrogen donor. According to Astruc, we are currently in “the golden age” of transfer hydrogenation.<sup>[10]</sup> This process avoids to deal with hazardous and pressurized gas but it is not fully atom economic as coproducts are generated. Compared to H<sub>2</sub>, the literature data fluctuate depending on the hydrogen source used. For example, *iso*-propanol has been extensively used compared to formic acid. Like hydrogenation process, most of the transfer hydrogenation required basic additive to activate the starting complex for catalysis. A major breakthrough was made by Noyori with a high enantioselectivity for the hydrogenation of ketone with a FA/Et<sub>3</sub>N mixture as a hydrogen source.<sup>[11]</sup>

### 1.3. Make the reaction greener

Hydrogenation of ketones as it is a widely used process has attracted a lot of attention to looking for improvements in terms of activity, stereoselectivity and mild reaction conditions. One of the improvements that could be done concern the reduction of wastes produced. As presented here, the majority of the catalytic systems required a basic additive that generates waste. It also limits the scope of functional groups in the substrate. Of course, protection and deprotection strategies may be useful and implemented but those strategies are no longer desired dealing with sustainable chemistry. Therefore, base-free catalytic processes have been developed with, for example, the use of bifunctional catalysts.

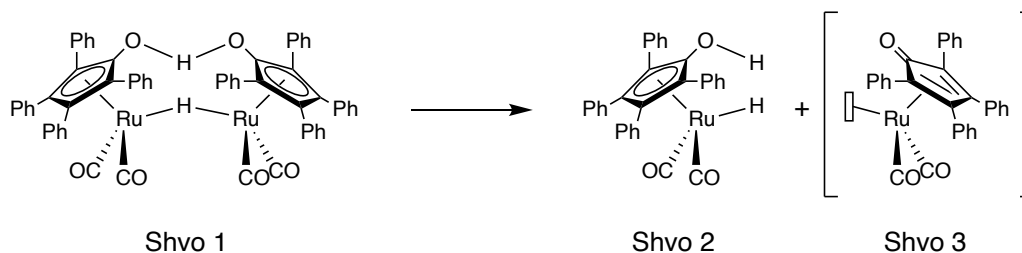
Bifunctional catalyst is a class of catalyst having at least 2 functional groups that allows new reactivity. The metal ligand cooperation (MLC) is present in this group of catalyst to introduce new properties of the catalytic system via the ligand. MLC implies that the ligand is no longer a witness of the catalytic reaction occurring on the metal center but it plays a role and can also be chemically modified to perform the transformation.<sup>[12]</sup> For example, the catalyst **1** studied in this PhD project exhibit a basic function on the ligand associated with an acidic function on the metal center.

A selection of prominent base-free ketone hydrogenation and transfer hydrogenation examples is presented below.

## 2. Homogeneous Base-free Hydrogenation

### 2.1. H<sub>2</sub> as donor

The pioneer work was made by Shvo in 1985 with a dimeric catalyst (Scheme II-1-2).<sup>[9]</sup> In fact, the Shvo complex is a precatalyst that dissociate into a hydride species (Shvo 2) and a “naked” species (Shvo 3) but there is still discussion in the scientific community about the structure of Shvo 3.<sup>[13]</sup> Shvo 2 is the catalyst responsible of the hydrogenation and it is converted into Shvo 3 that can activate H<sub>2</sub> to form Shvo 2. Hence, Shvo catalyst was able to hydrogenate ketones, aldehydes, alkynes and alkenes under 34,5 bar of H<sub>2</sub> at 145 °C.



Scheme II - 1 - 2: Shvo's Catalyst.

In 2002, Noyori continued the exploration of asymmetric hydrogenation reaction and a base-free system was used.<sup>[14]</sup> A chiral ruthenium borohydride catalyst (Figure II-1-1) was employed to hydrogenate acetophenone in *i*-PrOH using 0,025 mol% of catalyst with 8 bar of H<sub>2</sub> giving a yield of 100% and an enantiomeric excess (ee) of 99%. The reaction could be applied to several ketones (substituted acetophenone, alkyl ketone) with yield around 99% and ee above 97%.

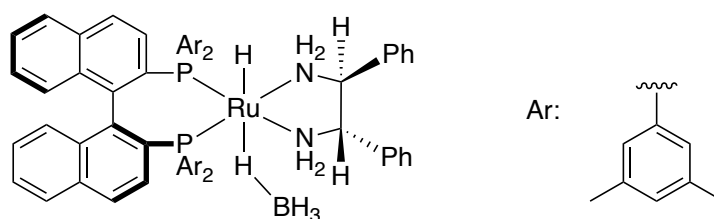
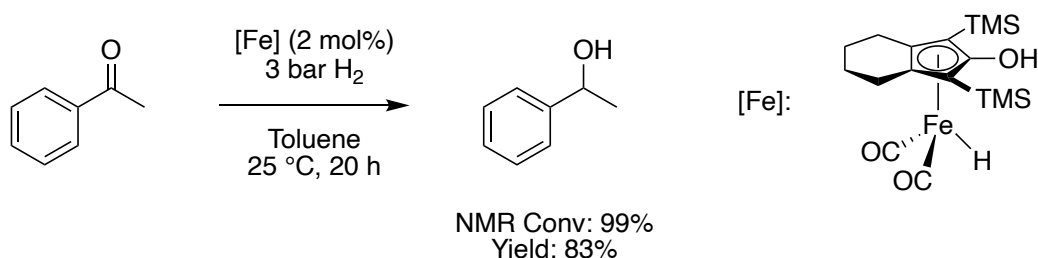


Figure II - 1 - 1: Catalyst used by Noyori.

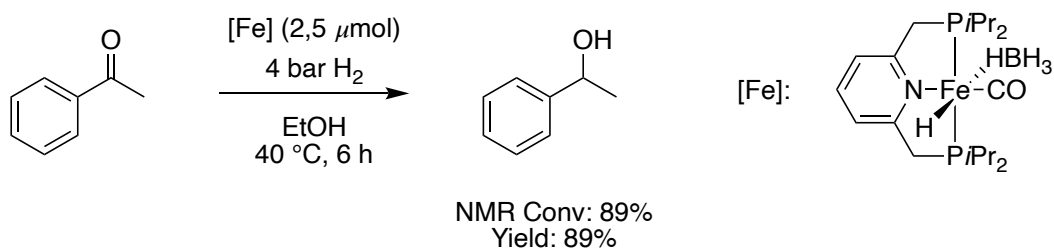
Several non-precious metals have also been implemented in base-free hydrogenation processes. In 2007, Casey used a Knölker iron catalyst and applied it in base free hydrogenation of ketones.<sup>[15]</sup> The experimental conditions were very mild with only 3 bar of gas at room temperature with a catalyst loading of 2 mol% (Scheme II-1-3). Those conditions could be applied to a scope of ketone. The mechanism proposed is based on Shvo catalyst with a hydrogenated species and a naked one with a vacant site on the metal center and a carbonyl on the ligand.



Scheme II - 1 - 3: Hydrogenation by Casey.

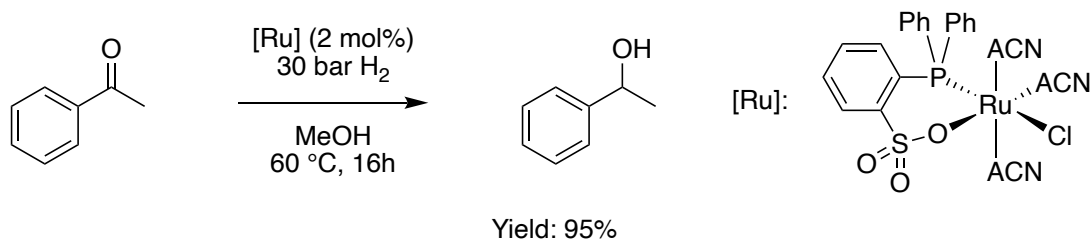
Milstein in 2012, used an iron borohydride pincer catalyst to realize the reaction under mild and base-free conditions.<sup>[16]</sup> The reaction was conducted under 4 bar of H<sub>2</sub> at 40 °C in ethanol and the yield on the test substrate (acetophenone) was 89% (Scheme II-1-4). Then, the reaction was tested with several substituted acetophenone derivatives. Different

mechanism proposals were discussed but they all started from an activation of the catalyst to a hydride iron complex with a dearomatized pyridine moiety.



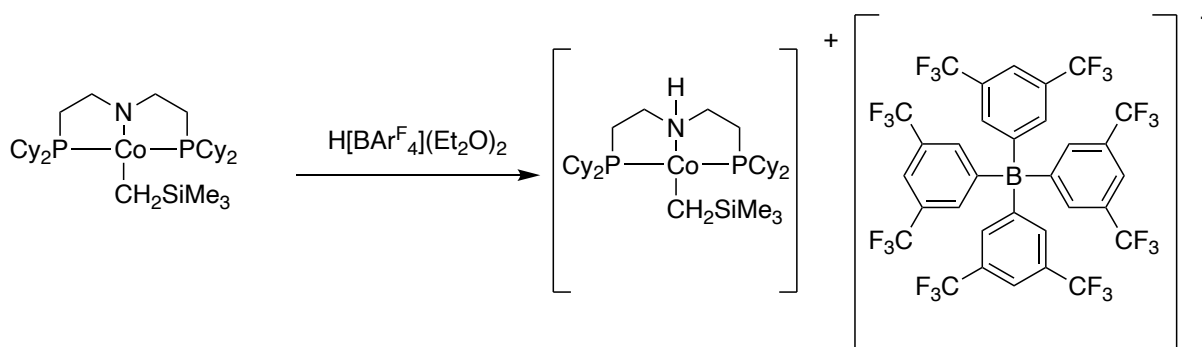
*Scheme II - 1 - 4: Hydrogenation made by Milstein with an iron pincer catalyst.*

In 2013, Bruneau and Achard reported the base-free hydrogenation of acetophenone with a ruthenium phosphine-sulfonate catalyst.<sup>[17]</sup> The yield obtained on acetophenone was about 95% with 30 bar of H<sub>2</sub> at 60 °C for 16 h (Scheme II-1-5). A scope was applied on ketones with an acetophenone backbone and very good yields were obtained.



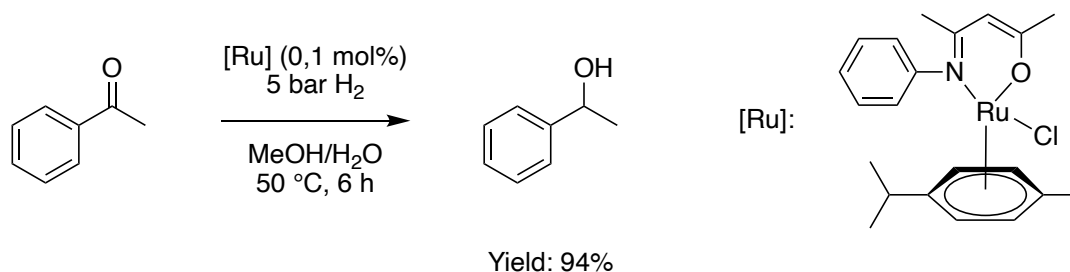
*Scheme II - 1 - 5: Hydrogenation by Bruneau.*

Beside iron, in the non-noble metal series, cobalt was also used in base-free hydrogenation reactions. Hanson published a series of articles dealing with cobalt tridentate (PNP) catalysts and pre-catalysts (Scheme II-1-6) to perform the base free hydrogenation of ketones but also alkenes and imines.<sup>[18,19]</sup> The test reaction with acetophenone under 1 bar of H<sub>2</sub> with 2 mol% of catalyst in THF at 25 °C for 24 h gave a NMR conversion of 98% and a yield of 89%. The cobalt precatalyst used was associated with the acid H[B(3,5-(CF<sub>3</sub>)<sub>2</sub>C<sub>6</sub>H<sub>3</sub>)<sub>4</sub>](Et<sub>2</sub>O)<sub>2</sub> to give the active species in situ. The mechanism was not elucidated but a metal ligand cooperation was evidenced as a methyl group on the nitrogen of the ligand inhibited the catalytic activity.



*Scheme II - 1 - 6: Cobalt catalyst used by Hanson.*

Recently in 2019, Deng published on a ruthenium bidentate catalyst to perform the base-free hydrogenation of acetophenone as a model substrate.<sup>[20]</sup> The reaction was conducted in a MeOH/H<sub>2</sub>O mixture at 50 °C under 5 bar of H<sub>2</sub> (Scheme II-1-7) and could be applied to ketones and aldehydes. The mechanism proposed did not involve a MLC but an oxonium intermediate.



*Scheme II - 1 - 7: Hydrogenation by Deng.*

The same year, Xing used an Iridium bipyridine catalyst (Figure II-1-2) to perform the reaction under base-free conditions.<sup>[21]</sup> The results were excellent with the model substrate acetophenone with yield of 96-98% using 0,5 mol% of catalyst and tert-amyl alcohol as a solvent at 30 °C under only one bar of gas for 12 h. The reaction conditions could be applied to a broad scope of ketones with yields above 90%. The mechanism proposed involved a MLC and started with the formation of a hydride species with a hydroxy function under H<sub>2</sub> pressure. Then, a concerted transfer of the hydride and the proton to the ketone occurred.

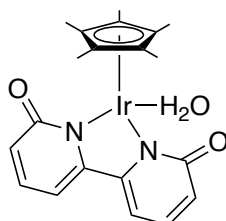


*Figure II - 1 - 2: Catalyst used by Xing in 2019.*

The same group of Xing reported the use of another Iridium bipyridine catalyst (Figure II-1-3) able to make the reaction under base-free condition and in water.<sup>[22]</sup> Using similar condition of the previous work with a catalyst loading of 1 mol% under 1 bar of gas at 30 °C for 12 h and water as solvent, a yield of 95% was obtained. The catalyst could also be applied to aldehydes and unsaturated aldehydes.

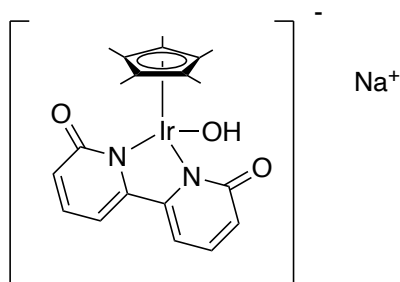
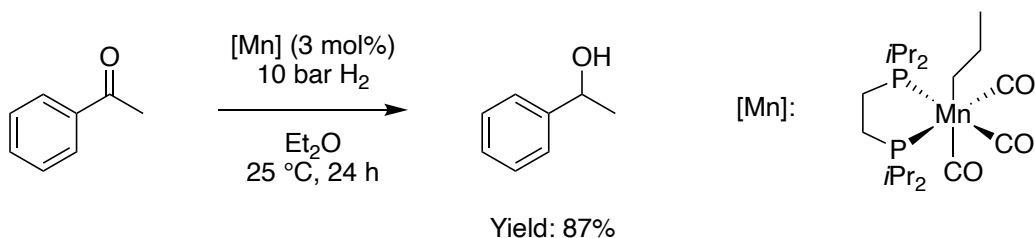


*Figure II - 1 - 3: Catalyst used by Xing.*

Very recently in 2021, Kirchner worked on manganese bidentate catalyst to perform the base-free hydrogenation reaction of ketones.<sup>[23]</sup> A yield of 87% was obtained in Et<sub>2</sub>O, at 25 °C under 10 bar of H<sub>2</sub> for 24 h (Scheme II-1-8). A broad scope of ketones was tested with success. The mechanism proposed is based on an inner sphere mechanism with no MLC. It relies on the formation of a hydride species after the alkyl moiety of the complex underwent a CO insertion with release of butanal thanks to the presence of H<sub>2</sub>.



Scheme II - 1 - 8: Hydrogenation made by Kirchner.

## 2.2. *i*-PrOH as donor

*Iso*-Propanol is the most widely used molecule as a hydrogen donor. The base-free transfer hydrogenation with *i*PrOH started with the pioneer work of Yamagishi<sup>[24]</sup> and Noyori<sup>[25]</sup> in 1997. Yamagishi used a ruthenium dihydride catalyst [RuH<sub>2</sub>(PPh<sub>3</sub>)<sub>4</sub>] (0,5 mol%) that was efficient in base-free transfer hydrogenation of acetophenone as model substrate in *i*PrOH at 85 °C leading to a yield of 93%. No scope was applied nevertheless, the reaction conditions could be applied with success to imine. Noyori with a diamine ruthenium catalyst (Figure II-1-4) observed the reduction of acetophenone without base with no further details.

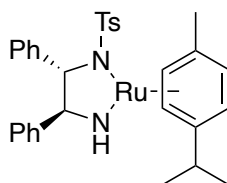
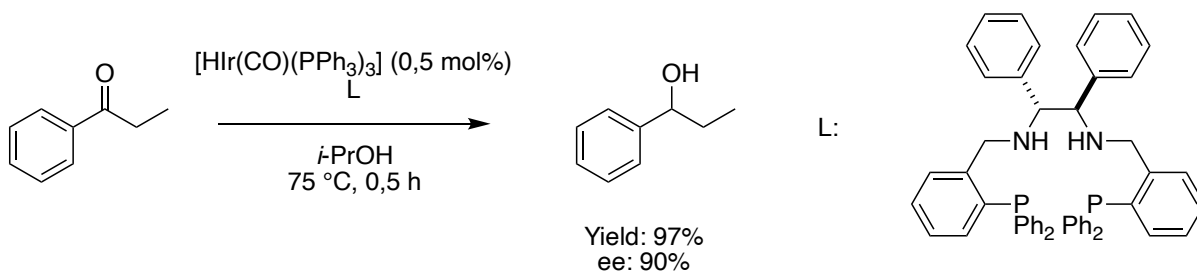


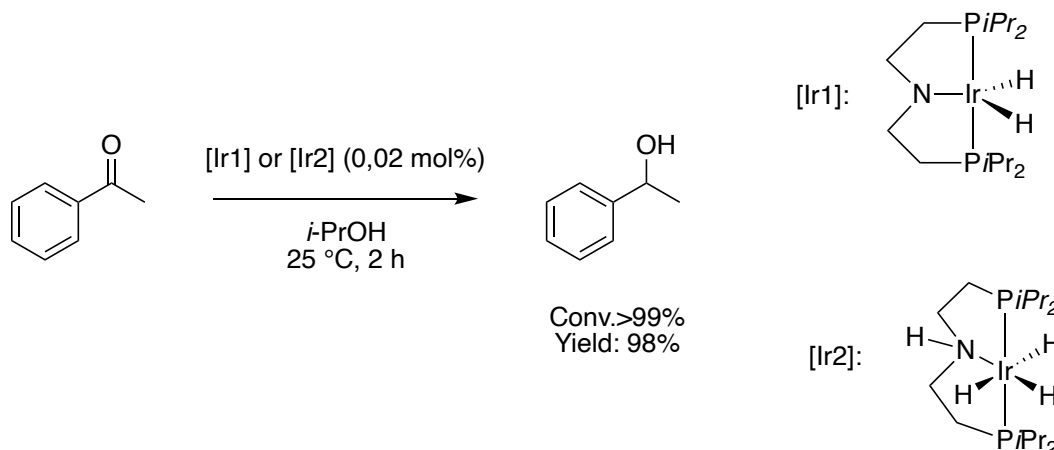
Figure II - 1 - 4: Pioneer catalyst for base-free transfer hydrogenation with *i*-PrOH by Noyori.

In 2005, Gao associated an iridium complex with a PNNP ligand to generate a catalytic system in situ able to perform the base-free transfer hydrogenation.<sup>[26]</sup> A yield of 97% was obtained in *i*PrOH at 75 °C after 30 min (Scheme II-1-9). A small scope was applied with several ketones.



Scheme II - 1 - 9: Base-free transfer hydrogenation with *i*PrOH by Gao.

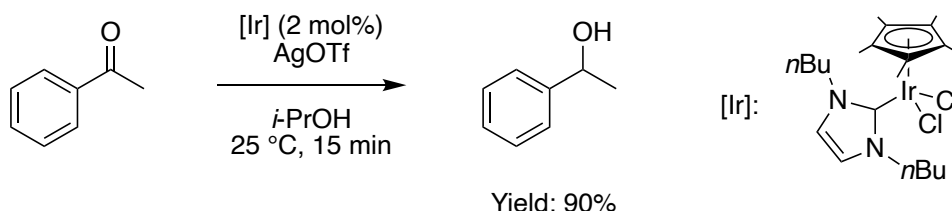
One year later in 2006, Abdur-Rashid was interested in the formation of iridium hydride complexes for base-free transfer hydrogenation with *i*PrOH.<sup>[27]</sup> The excellent yield of 98% was obtained with acetophenone and *i*PrOH at 25 °C for 2 h (Scheme II-1-10). The reaction conditions were adapted for other ketones and an imine. A bifunctional mechanism was proposed involving the amido- [Ir1] and amino- [Ir2] species.



Scheme II - 1 - 10: Base-free transfer hydrogenation with *i*PrOH by Abdur-Rashid.

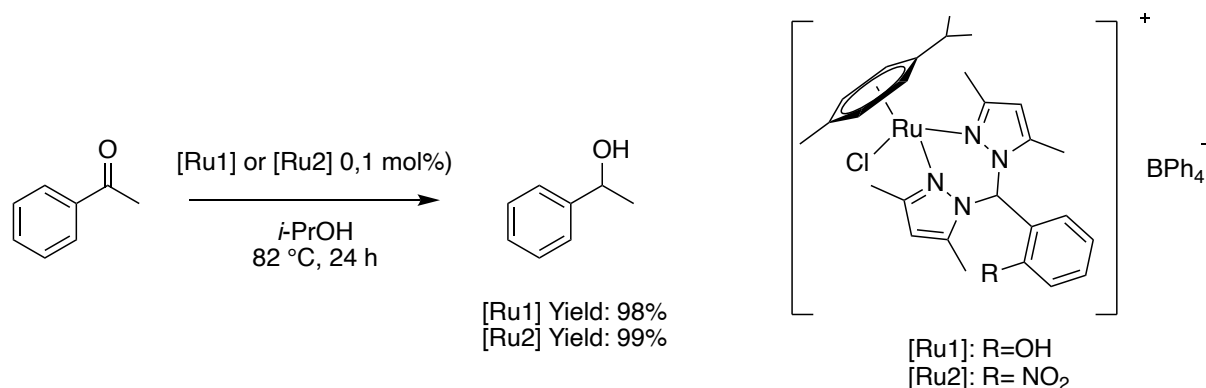
As presented in the precedent paragraph, Casey published in 2007 results obtained in hydrogenation with an iron catalyst. In this article, the use of *i*PrOH as donor was also briefly reported leading to a yield of 87% for the reduction of acetophenone.<sup>[15]</sup>

In 2008 Peris tested an iridium-NHC catalyst for the base-free transfer hydrogenation.<sup>[28]</sup> The iridium precatalyst [Cp\*IrCl<sub>2</sub>NHC] was associated with AgOTf in *i*PrOH was efficient at room temperature to perform the reduction of acetophenone giving a yield of 90% (Scheme II-1-11). The reaction could be applied to other functional groups such as aldehydes and imines with excellent yields (>90%). No direct evidence for a mechanism was mentioned but a mechanism without MLC and the formation of a dihydride intermediate was proposed.



Scheme II - 1 - 11: Base-free transfer hydrogenation by Peris.

Manzano in 2009 and in 2013 used arene-ruthenium catalysts bearing bipyrazole backbone ligands to perform the base-free hydrogenation of ketones and aldehydes.<sup>[29,30]</sup> The best catalytic system found leading to a yield above 98% is presented in the Scheme II-1-12. A small scope of ketone was tested. In the mechanism proposed by the group, the ligand plays the role of a base that leads to the decoordination of one nitrogen of the ligand and the formation of a hydride species. Then, the liberation of HCl occurred and the ligand can re-coordinate. Hence, the active species is a hydride bidentate ligand.



Scheme II - 1 - 12: Base-free transfer hydrogenation by Manzano.

In 2012, the research made by Berke was based on rhenium catalysts (Figure II-1-5).<sup>[31]</sup> A yield of 97% within a short time (10 min) but high temperature (120 °C) with 0,5 mol% of catalyst was obtained for the reduction of acetophenone in *i*PrOH. Then, several ketones and imines were tested with good yields. The mechanism proposed is based on the Shvo catalyst with a hydrogenated species able to hydrogenate the ketone. Then the “naked” species by reacting with *i*PrOH generate the starting hydrogenated catalyst.

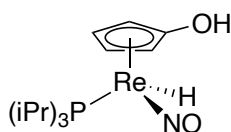
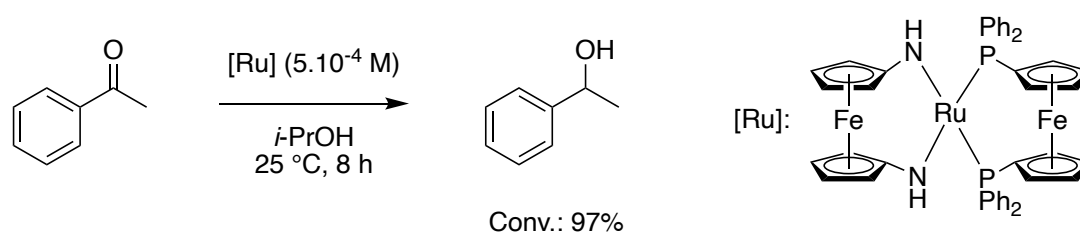


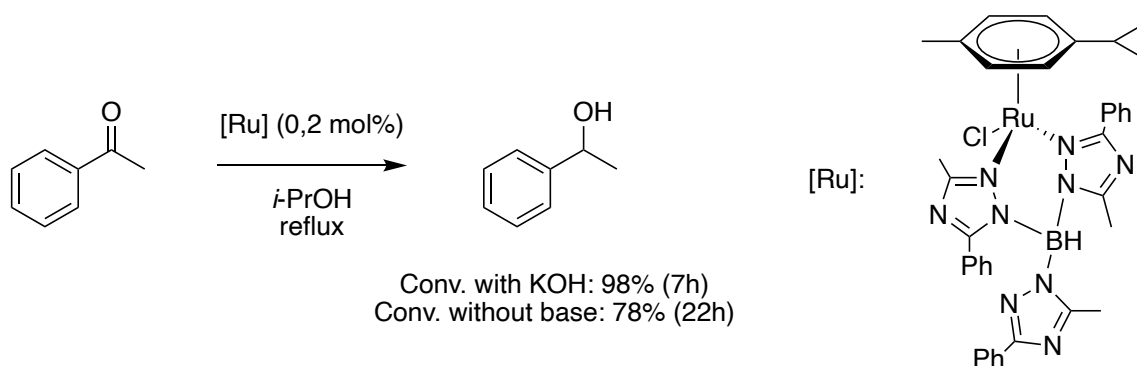
Figure II - 1 - 5: Catalyst developed by Berke.

Diaconescu in 2012 used ferrocenediamide ruthenium catalyst and performed the hydrogenation of several ketones to the corresponding alcohols.<sup>[32]</sup> On the model substrate acetophenone a conversion of 98% was obtained within 8 h at room temperature in *i*PrOH. The mechanism is supposed to act as a Noyori type ligand with, in a first step, the formation of a hydride intermediate and the protonation of the nitrogen moiety thanks to the H donor. Then, the hydrogenation of the carbonyl function can take place.



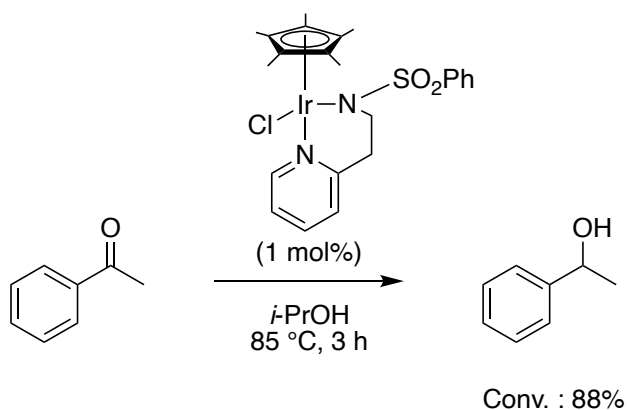
*Scheme II - 1 - 13: Base-free transfer hydrogenation with *i*PrOH by Diaconescu.*

Papish in 2013, compared the activity of ruthenium catalyst with tris(triazolyl)borate ligand in acetophenone transfer hydrogenation with and without base.<sup>[33]</sup> The catalyst used were active under both conditions but catalytic activity was much more higher with base compared to base-free system (Scheme II-1-14). In the base free system, it is suggested that the ligand plays the role of a base to form a hydride ruthenium species and a partially decoordinated ligand. Then, the hydrogenation of the substrate can take place in a concerted mechanism. This study did not consider the possible reduction promoted by the base only as reported by Manzano.<sup>[34]</sup>



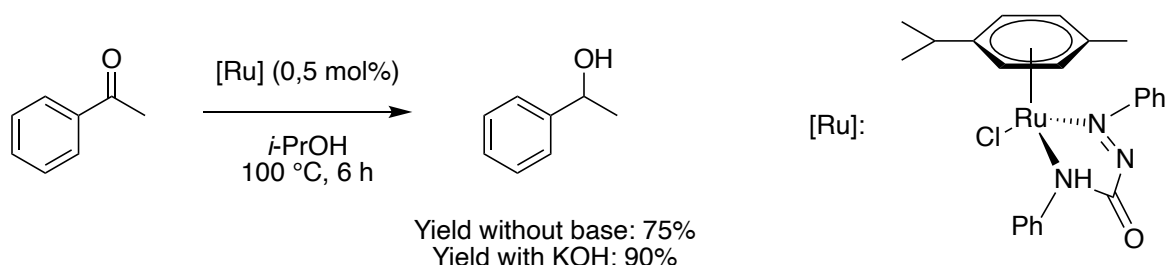
*Scheme II - 1 - 14: Base-free transfer hydrogenation with *i*PrOH by Papish.*

In 2016, O'Connor used an iridium pyridinesulfonamide catalyst to obtain a conversion of 88% at 85 °C for 3 h in *i*PrOH (Scheme II-1-15).<sup>[35]</sup> A broad scope of ketones was applied with good results. Mechanism investigation was not studied in this publication but we could speculate on the participation of the amido-ligand as a base.



*Scheme II - 1 - 15: Base-free transfer hydrogenation with *i*PrOH by O'Connor.*

Still in 2016, Sarkar used a half sandwich complex with an azocarboxamide ligand.<sup>[36]</sup> The catalytic system was used with and without base for comparison (Scheme II-1-15). The yield obtained at 100 °C for 6 h without base was 75% compared to 90 % with base. Aldehydes were also tested with a yield up to 95 % obtained within 19 h. An outer sphere mechanism is suggested with a MLC.



*Scheme II - 1 - 16: Base-free transfer hydrogenation with *i*PrOH by Sarkar.*

The next year, the use of an iridium catalyst (Figure II-1-6) was briefly reported by Albrecht. The catalyst (0,01 mmol) reduced acetophenone with *i*PrOH under reflux with a yield of 99% after 24 h.<sup>[37]</sup> The system also worked well with aldehydes. Mechanistic investigation was not deeply performed. The group suggested the formation of an Ir-H species via the coordination of the *i*PrOH and its potentially ligand-assisted dehydrogenation.

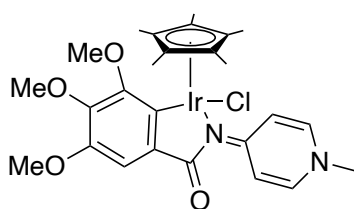


*Figure II - 1 - 6: Catalyst used by Albrecht.*

The same year, Mezzetti used a macrocyclic iron hydride catalyst (Figure II-1-7) in base-free transfer hydrogenation of ketones.<sup>[38]</sup> On the model substrate acetophenone, a yield of 92% was reached with 0,1 mol% of catalyst in *i*PrOH at 50 °C in 1 h. No mechanistic insight is given in this publication.

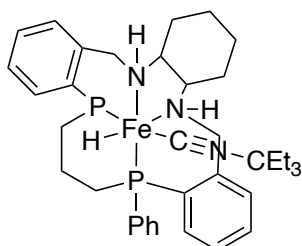
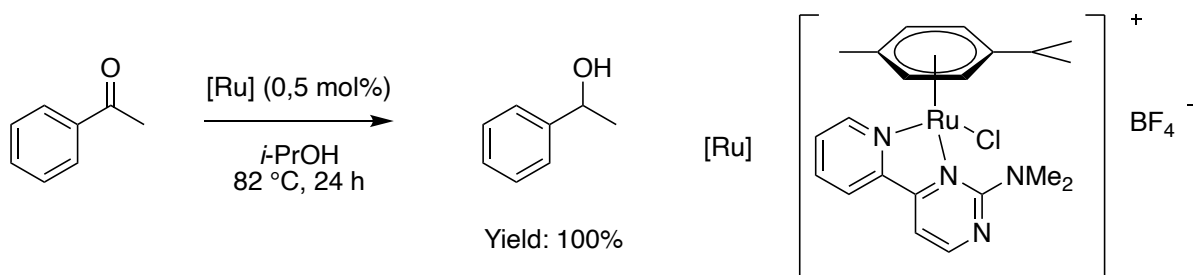


Figure II - 1 - 7: Iron catalyst used by Mezzetti.

Thiel the same year used ruthenium catalysts holding a backbone ligands composed of an arene and a pyridine-pyrimidine.<sup>[39]</sup> Among the catalyst tested, the yield obtained varied from 0 to 100%. The best catalyst is presented below with 0,5 mol% of catalyst loading at 82 °C after 24 h (Scheme II-1-17). Several ketones were tested with very good yields. DFT calculation were performed and they believed that a roll-over cyclometallation process occurred and a hydride intermediate was formed as a starting point for the hydrogen transfer.



Scheme II - 1 - 17: Base-free transfer hydrogenation with *i*PrOH by Thiel.

In 2018, Singh obtained very good results with various iridium catalysts (Figure II-1-8) with a chalcogenated Schiff-base anthracene ligand.<sup>[40]</sup> The conditions of 0,5 mol% catalyst loading at 80 °C for 4 h in *i*PrOH could be applied to the model substrate acetophenone but also to other ketones. Later, Palladium and Rhodium metallic center were tested instead of Iridium with very good results too.<sup>[41]</sup>

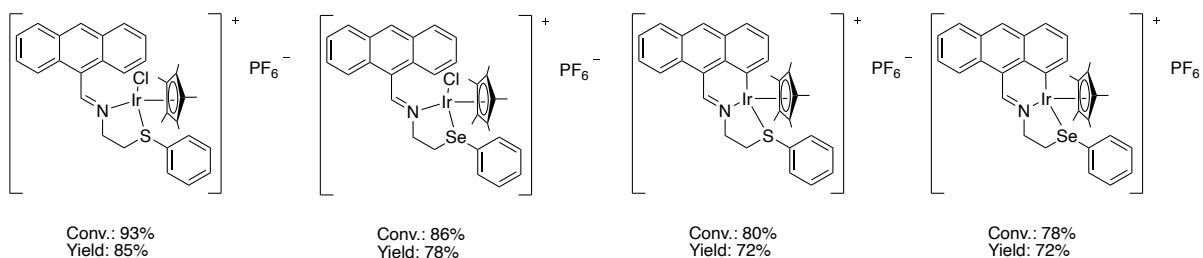


Figure II - 1 - 8: Catalysts used by Singh.

The commercially available Ru-MACHO catalyst (Figure II-1-9) was used by de Vries in 2018 to perform the base-free transfer hydrogenation with *i*PrOH under reflux with 0,1 mol% of catalyst.<sup>[42]</sup> Excellent yields were obtained with acetophenone (99%) and a broad range of ketones. Based on DFT computation and experimental results, an outer-sphere mechanism with a metal-ligand cooperation was presumed based on the amino/amido equilibrium.

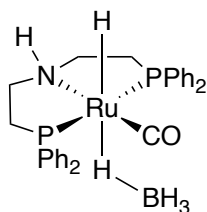


Figure II - 1 - 9: Ru-MACHO used by de Vries.

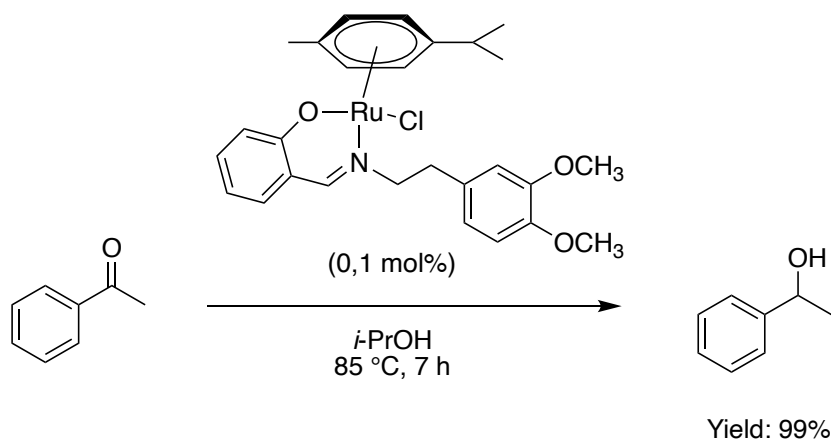
An original example of a nickel complex bearing NHC-Amidate ligand (Figure II-1-10) was reported by Kalman in the base-free transfer hydrogenation with *i*PrOH on acetophenone at 100 °C with modest results (17%) even with an extended reaction time of 40 h (31%) and 5 mol% of catalyst. The mechanism proposal is based on a MLC with the hydrogenation of the amido group.



R: *i*Pr

Figure II - 1 - 10: Catalyst used by Kalman.

In 2019, Kumara employed a half-sandwich ruthenium complex with a Schiff-base ligand, similar to those reported earlier by Deng, as a catalyst for base-free transfer hydrogenation of ketones.<sup>[43]</sup> The catalytic system was efficient on a broad range of ketones. For example, on the model substrate acetophenone, a yield of 99% was achieved in refluxing *i*PrOH within 7 h (Scheme II-1-18). No mechanistic details were provided in this publication.



Scheme II - 1 - 18: Base-free transfer hydrogenation made by Kumara.

Recently, in 2020, a Cp\*-iridium complex with a triazenide ligand (Figure II-1-11) was used by Parra-Hake.<sup>[44]</sup> The system was used on acetophenone at 90 °C with 2 mol% of catalyst and long reaction time of 39 h to give a yield of 93%. Several ketones could be tested with good yields. Based on experimental tests, a MLC is envisaged for the mechanism with the formation of a hydride species and a cationic complex with a nitrogen acting like a base.

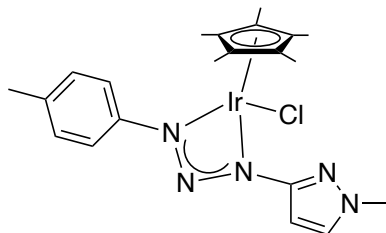


Figure II - 1 - 11: Catalyst used by Parra-Hake.

This literature survey of the base-free transfer hydrogenation of ketones with *i*PrOH as hydrogen source clearly demonstrate that this field has been extensively developed. A variety of catalyst based on noble and non-noble transition metals has been used and several examples provided excellent yields under mild conditions.

## 2.3. Formic acid as donor

Besides *i*PrOH as a hydrogen source, formic acid can also be employed for the same purpose. Formic acid has been very often used under basic conditions for the catalytic reduction of ketones. For instance, it was used by Noyori in an azeotropic mixture of FA/TEA for asymmetric hydrogenation.<sup>[11]</sup> Inversely, the base-free transfer hydrogenation with FA is far less developed.

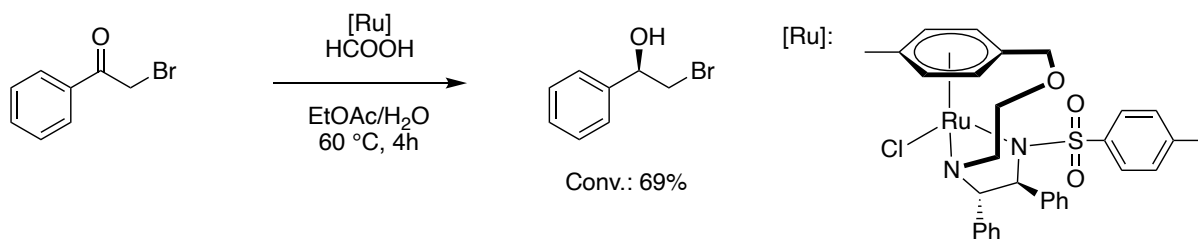
It seems that the early works on base-free transfer hydrogenation of ketone with FA as hydrogen source was published by Watanabe in the 80's.<sup>[45,46]</sup> A Ruthenium catalyst [RuCl<sub>2</sub>(PPh<sub>3</sub>)<sub>3</sub>] was employed with formic acid without solvent and stirred at 125 °C for 3h. With the model substrate acetophenone, a yield of alcohol of 84% was obtained. Furthermore, the reaction could be applied to other ketones and also to aldehydes. However, esters were formed with aldehydes due to the reaction between the alcohol formed and the FA.

Ten years later, in 1993, Gordon reported the base-free transfer hydrogenation of benzaldehyde under microwave using [RuHCl(CO)(PPh<sub>3</sub>)<sub>3</sub>] as catalyst.<sup>[47]</sup> This reaction led essentially to esters instead of the corresponding alcohols.

In 1996, Shvo's catalyst was evaluated for the transfer hydrogenation of ketones to alcohols without base but some esterification took place. Small amount of water and sodium formate were added to produce only the corresponding alcohol.<sup>[48]</sup>

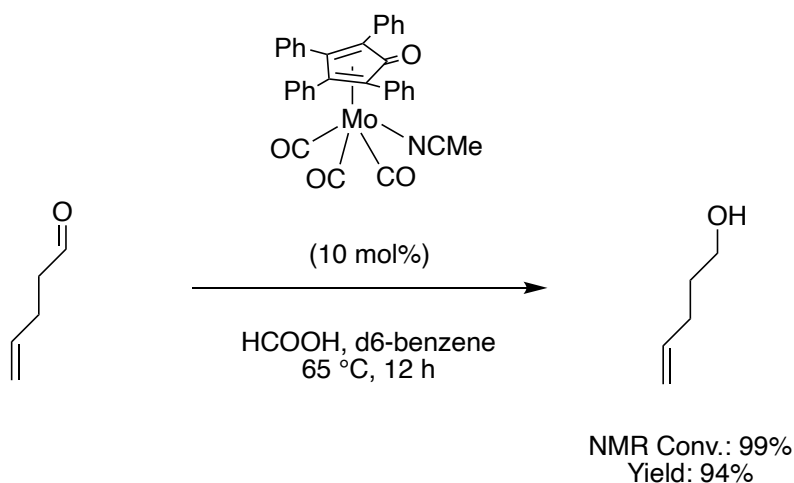
It is only recently that we could find more easily reports on base-free transfer hydrogenation with FA. Most of the time the publications are dedicated to the process with base and briefly reported without base.

In 2018, Kayaki and Ikariya briefly reported the base-free transfer hydrogenation of a ketone with FA using a ruthenium catalyst.<sup>[49]</sup> A good conversion of 69% was obtained in a mix of EtOAc/H<sub>2</sub>O as solvent at 60 °C for 4h using 0,1 mol% of catalyst (Scheme II-1-19).



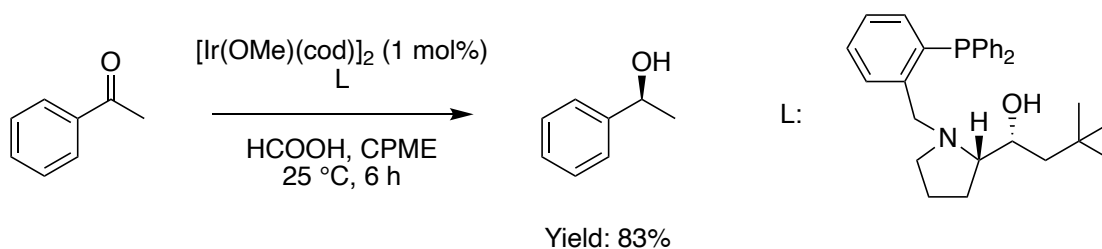
Scheme II - 1 - 19: Base-free transfer hydrogenation with FA by Kayaki and Ikariya.

In 2018, Waymouth used a “Shvo like” molybdenum catalyst to perform the base-free transfer hydrogenation of ketones with *i*PrOH and FA.<sup>[50]</sup> The FA was only used with one substrates for an ease of separation of the volatile products (Scheme II-1-21). The unsaturated aldehyde was tested with FA in benzene at 65 °C for 12 h using 10 mol% of catalyst.



Scheme II - 1 - 20: Base-free transfer hydrogenation with FA made by Waymouth.

Finally, in 2020, Sawamura briefly reported an iridium precursor associated with a prolinol-phosphine ligand to perform the base-free transfer hydrogenation with FA.<sup>[51]</sup> A yield of 83% was obtained on the model substrate acetophenone (Scheme II-1-21).



Scheme II - 1 - 21: Base-free transfer hydrogenation with FA by Sawamura.

### 3. Conclusion

The literature on the reduction of ketone behaves like a bottle neck. The data are abundant dealing with hydrogenation under basic conditions and a bit less with the base-free hydrogenation. Then, moving to transfer hydrogenation, *i*PrOH has also been widely used with bases but when we focused on the base-free reaction, the number of publications decreased significantly. Finally, the phenomenon is exacerbated with FA. FA is almost systematically associated with a base and the number of publications dealing with base-free transfer hydrogenation with FA as the hydrogen source are rare. To the best of my knowledge, except the pioneer work of Watanabe<sup>[45,46]</sup>, no publications focused on this field. Base-free process was always diluted within a publication using base. Whatever the hydrogen donor, most base-free reduction of ketones were achieved with bifunctional catalyst displaying Metal Ligand Cooperation. In this context, the complex synthesized by our partners in Toulouse seems appropriate to be tested in base-free hydrogenation of ketones. The suspected bifunctional properties could be tested and evaluated in this simple reaction and could feed a field with a lack of documentation.

## 4. References:

- [1] “The Nobel Prize in Chemistry 1912,” can be found under <https://www.nobelprize.org/prizes/chemistry/1912/sabatier/lecture/>, **2021**.
- [2] P. Sabatier, *Ind. Eng. Chem.* **1926**, *18*, 4.
- [3] J. A. Osborn, F. H. Jardine, J. F. Young, G. Wilkinson, *J. Chem. Soc. A* **1966**, 1711–1732.
- [4] C. S. G. Seo, R. H. Morris, *Organometallics* **2019**, *38*, 47–65.
- [5] P. J. Deuss, K. Barta, J. G. de Vries, *Catal. Sci. Technol.* **2014**, *4*, 1174–1196.
- [6] K. Barta, P. C. Ford, *Acc. Chem. Res.* **2014**, *47*, 1503–1512.
- [7] R. Noyori, T. Ohkuma, *Angew. Chem. Int. Ed.* **2001**, *34*.
- [8] R. Noyori, *Asymmetric Catalysis* **2002**, 15.
- [9] Y. Blum, D. Czarkie, Y. Rahamim, Y. Shvo, *Organometallics* **1985**, *4*, 1459–1461.
- [10] D. Wang, D. Astruc, *Chem. Rev.* **2015**, *115*, 6621–6686.
- [11] A. Fujii, S. Hashiguchi, N. Uematsu, T. Ikariya, R. Noyori, *J. Am. Chem. Soc.* **1996**, *118*, 2521–2522.
- [12] J. R. Khusnutdinova, D. Milstein, *Angew. Chem. Int. Ed.* **2015**, *54*, 12236–12273.
- [13] D. G. Gusev, D. M. Spasyuk, *ACS Catal.* **2018**, *8*, 6851–6861.
- [14] T. Ohkuma, M. Koizumi, K. Muñiz, G. Hilt, C. Kabuto, R. Noyori, *J. Am. Chem. Soc.* **2002**, *124*, 6508–6509.
- [15] C. P. Casey, H. Guan, *J. Am. Chem. Soc.* **2007**, *129*, 5816–5817.
- [16] R. Langer, M. A. Iron, L. Konstantinovski, Y. Diskin-Posner, G. Leitun, Y. Ben-David, D. Milstein, *Chem. Eur. J.* **2012**, *18*, 7196–7209.
- [17] F. Jiang, K. Yuan, M. Achard, C. Bruneau, *Chem. Eur. J.* **2013**, *19*, 10343–10352.
- [18] G. Zhang, B. L. Scott, S. K. Hanson, *Angew. Chem. Int. Ed.* **2012**, *51*, 12102–12106.
- [19] G. Zhang, K. V. Vasudevan, B. L. Scott, S. K. Hanson, *J. Am. Chem. Soc.* **2013**, *14*.
- [20] Z.-J. Yao, J.-W. Zhu, N. Lin, X.-C. Qiao, W. Deng, *Dalton Trans.* **2019**, *48*, 7158–7166.
- [21] R. Wang, J. Qi, Y. Yue, Z. Lian, H. Xiao, S. Zhuo, L. Xing, *Tetrahedron* **2019**, *75*, 130463.
- [22] R. Wang, Y. Yue, J. Qi, S. Liu, A. Song, S. Zhuo, L.-B. Xing, *J. Catal.* **2021**, *399*, 1–7.
- [23] S. Weber, J. Brünig, L. F. Veiros, K. Kirchner, *Organometallics* **2021**, *40*, 1388–1394.
- [24] E. Mizushima, M. Yamaguchi, T. Yamagishi, *Chem. Lett.* **1997**, *26*, 237–238.
- [25] K.-J. Haack, S. Hashiguchi, A. Fujii, T. Ikariya, R. Noyori, *Angew. Chem. Int. Ed. Engl.* **1997**, *36*, 285–288.
- [26] Z.-R. Dong, Y.-Y. Li, J.-S. Chen, B.-Z. Li, Y. Xing, J.-X. Gao, *Org. Lett.* **2005**, *7*, 1043–1045.
- [27] Z. E. Clarke, P. T. Maragh, T. P. Dasgupta, D. G. Gusev, A. J. Lough, K. Abdur-Rashid, *Organometallics* **2006**, *25*, 4113–4117.
- [28] R. Corberán, E. Peris, *Organometallics* **2008**, *27*, 1954–1958.
- [29] M. C. Carrión, F. Sepúlveda, F. A. Jalón, B. R. Manzano, A. M. Rodríguez, *Organometallics* **2009**, *28*, 3822–3833.
- [30] M. C. Carrión, F. Sepúlveda, F. A. Jalón, B. R. Manzano, A. M. Rodríguez, *Eur. J. Inorg. Chem.* **2013**, *2013*, 217–227.
- [31] A. Landwehr, B. Duddle, T. Fox, O. Blacque, H. Berke, *Chem. Eur. J.* **2012**, *18*, 5701–5714.
- [32] A. G. Elliott, A. G. Green, P. L. Diaconescu, **2012**, *41*, 7852.
- [33] M. Kumar, J. DePasquale, N. J. White, M. Zeller, E. T. Papish, *Organometallics* **2013**, *32*, 2135–2144.
- [34] M. C. Carrión, F. A. Jalón, B. R. Manzano, A. M. Rodríguez, F. Sepúlveda, M. Maestro, *Eur. J. Inorg. Chem.* **2007**, *2007*, 3961–3973.
- [35] A. Ruff, C. Kirby, B. C. Chan, A. R. O’Connor, *Organometallics* **2016**, *35*, 327–335.

- [36] M. G. Sommer, S. Marinova, M. J. Krafft, D. Urankar, D. Schweinfurth, M. Bubrin, J. Košmrlj, B. Sarkar, *Organometallics* **2016**, *35*, 2840–2849.
- [37] M. Navarro, C. A. Smith, M. Albrecht, *Inorg. Chem.* **2017**, *56*, 11688–11701.
- [38] L. D. Luca, A. Mezzetti, *Angew. Chem. Int. Ed.* **2017**, 11949–11953.
- [39] C. Kerner, J. Lang, M. Gaffga, F. S. Menges, Y. Sun, G. Niedner-Schatteburg, W. R. Thiel, *ChemPlusChem* **2017**, *82*, 212–224.
- [40] P. Dubey, S. Gupta, A. K. Singh, *Dalton Trans.* **2018**, *47*, 3764–3774.
- [41] P. Dubey, S. Gupta, A. K. Singh, *Organometallics* **2019**, *38*, 944–961.
- [42] R. A. Farrar-Tobar, Z. Wei, H. Jiao, S. Hinze, J. G. de Vries, *Chem. Eur. J.* **2018**, *24*, 2725–2734.
- [43] C. E. Satheesh, P. N. Sathish Kumar, P. R. Kumara, R. Karvembu, A. Hosamani, M. Nethaji, *Appl. Organometal. Chem.* **2019**, *33*, DOI 10.1002/aoc.5111.
- [44] L. J. Medrano-Castillo, M. Á. Collazo-Flores, J. P. Camarena-Díaz, E. Correa-Ayala, D. Chávez, D. B. Grotjahn, A. L. Rheingold, V. Miranda-Soto, M. Parra-Hake, *Inorg. Chim. Acta* **2020**, *507*, 119551.
- [45] Y. Watanabe, T. Ota, Y. Tsuji, *Chem. Lett.* **1980**, 1595.
- [46] Y. Watanabe, T. Ohta, Y. Tsuji, *B. Chem. Soc. Jpn* **1982**, *55*, 2441–2444.
- [47] E. M. Gordon, D. C. Gaba, K. A. Jebber, D. M. Zacharias, *Organometallics* **1993**, *12*, 5020–5022.
- [48] N. Menashe, E. Salant, Y. Shvo, *J. Org. Chem.* **1996**, *514*, 97–102.
- [49] Y. Yuki, T. Touge, H. Nara, K. Matsumura, M. Fujiwhara, Y. Kayaki, T. Ikariya, *Adv. Synth. Catal.* **2018**, *360*, 568–574.
- [50] W. Wu, T. Seki, K. L. Walker, R. M. Waymouth, *Organometallics* **2018**, *37*, 1428–1431.
- [51] H. Murayama, Y. Heike, K. Higashida, Y. Shimizu, N. Yodsin, Y. Wongnongwa, S. Jungsuttiwong, S. Mori, M. Sawamura, *Adv. Synth. Catal.* **2020**, *362*, 1–8.



Part 2: Catalytic application of  $\eta^5$ -  
Oxocyclohexadienyl Ruthenium  
complexes in base-free hydrogenation  
and transfer hydrogenation



## 1. Introduction

As a reminder, the catalyst (Figure II-2-1) used was developed and prepared by the team of Alain Igau at the LCC in Toulouse. The suspected bifunctional properties of the complex will be tested in base-free catalytic tests as a proof of concept. Therefore, the base-free hydrogenation and the base-free transfer hydrogenation of ketones have been selected. Those tests will contribute to feed the knowledge on the piano-stool complexes and could extend the catalytic application.

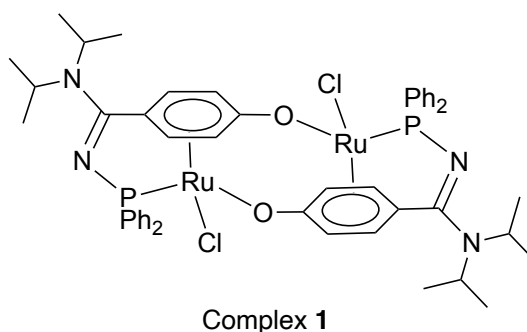
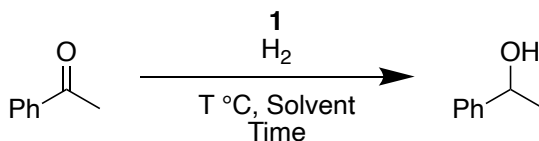


Figure II - 2 - 1: Complex used in the catalytic tests.

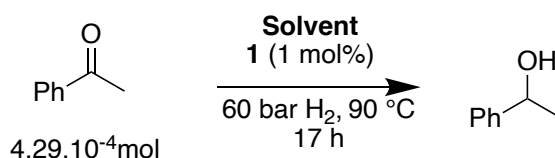
## 2. Base-free hydrogenation with H<sub>2</sub>

The catalytic activity of **1** was evaluated with the base-free hydrogenation of acetophenone as a benchmark substrate (Scheme II-2-1). The reactions were conducted in GC vials (1,5 mL) inserted in 22 mL high pressure reactors.



Scheme II - 2 - 1: Model hydrogenation reaction used.

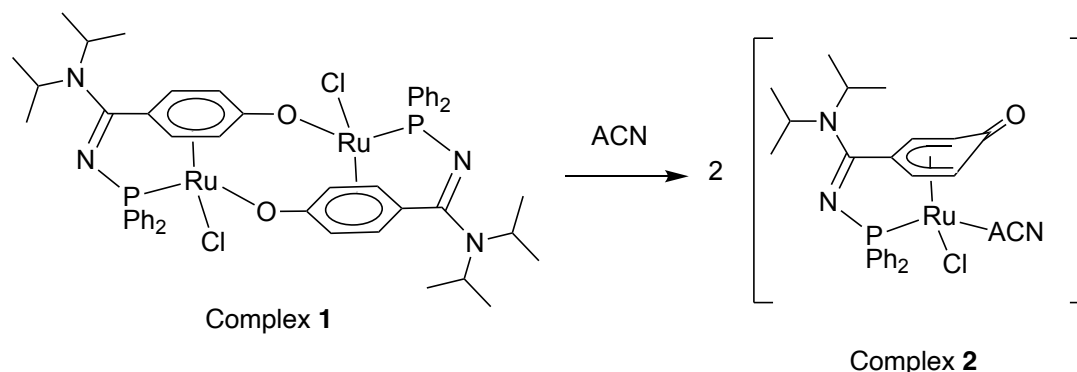
### 2.1. Preliminary tests



Scheme II - 2 - 2: Preliminary test with various solvent.

The preliminary tests were conducted with 1 mol% of **1** (2 mol% of ruthenium) at 90 °C for 17 h under 60 bar of H<sub>2</sub> using 0,5 mL of solvent (Scheme II-2-2). Several solvents including coordinating solvents were evaluated. Indeed, it was shown that acetonitrile promoted the evolution of the bimetallic complex **1** into a monometallic complex **2** (Scheme II-2-3).<sup>[1]</sup> Thus, dimethyl sulfoxide (DMSO), tetrahydrofuran (THF) and acetonitrile (ACN) were included in this

study.  $\gamma$ -valerolactone (GVL) was also considered as a biosourced and green solvent.<sup>[2]</sup> *Isopropanol* (*i*PrOH) was evaluated as a protic solvent also able to participate in the transformation as hydrogen donor. Finally, toluene (Tol) was also considered as an aromatic solvent. Among the solvent tested, summarized in table II-2-1, GVL, ACN and *i*PrOH led to the best NMR conversions above 95%. However, due to a boiling point close to the substrates that could be a problem during purification, GVL was discarded and further optimization conducted with ACN and *i*PrOH.



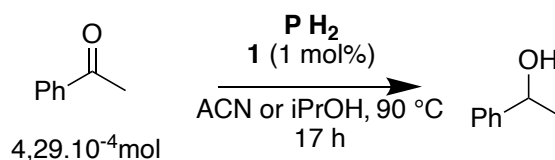
Scheme II - 2 - 3: Formation of the monometallic complex **2** from complex **1** in ACN reported by A. Igau.

Table II - 2 - 1: Solvent tested at 90 °C<sup>a</sup>

Solvent	DMSO	THF	Tol	GVL	ACN	<i>i</i> PrOH
Conversion <sup>b</sup>	32	51	59	95	99 <sup>c</sup>	99 <sup>c</sup>

<sup>a</sup> Acetophenone (0,429 mmol, 50  $\mu$ L), **1** (1 mol%, 4,6 mg), Solvent (0,5 mL), 60 bar H<sub>2</sub> 90 °C, 17h. <sup>b</sup>Determined by <sup>1</sup>H NMR. <sup>c</sup>No acetophenone detected by <sup>1</sup>H NMR.

## 2.2. Study of the hydrogen pressure and temperature



Scheme II - 2 - 4: Optimization of the pressure.

With the best solvents identified, the influence of the hydrogen pressure was investigated looking for the lowest pressure (Scheme II-2-4). Different pressures were tested (Table II-2-2) and we could demonstrate that the pressure could be reduced drastically. Indeed, the conversion was unchanged upon lowering the pressure from 60 to 30 bar (Table II-2-2, entry 1 to 4) and a slight decrease was only observed in *i*PrOH with a pressure of 10 bar (Table II-2-2, entry 6). Decreasing further the pressure to 5 bar led to a pronounced lowering of the conversion in *i*PrOH (Table II-2-2, Entry 10) but still an interesting conversion of 82% in ACN (Table II-2-3, entry 9).

The influence of the temperature was also investigated at a pressure of 10 bar. Lowering the temperature to 75 °C (Table II-2-2, entry 7 and 8) led to a deterioration of the conversion

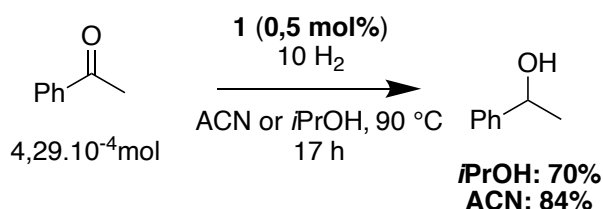
to 67% in ACN and 36% in *i*PrOH. Therefore, the temperature of 90 °C was selected as the reaction temperature for further optimizations.

Table II - 2 - 2: Pressure optimization<sup>a</sup>

Entry	Pressure (bar)	Solvent	Conversion
1	60	ACN	99%
2		<i>i</i> -PrOH	99%
3	30	ACN	99%
4		<i>i</i> -PrOH	99%
5	10	ACN	99%
6		<i>i</i> -PrOH	91%
7		ACN	67% <sup>b</sup>
8		<i>i</i> -PrOH	36% <sup>b</sup>
9	5	ACN	82%
10		<i>i</i> -PrOH	54%

<sup>a</sup> Acetophenone (0,429 mmol, 50  $\mu$ L), **1** (1 mol%, 4,6 mg), Solvent (0,5 mL), desired bar of H<sub>2</sub> 90 °C, 17 h. <sup>b</sup>75 °C

## 2.3. Catalyst loading optimization



Scheme II - 2 - 5: Hydrogenation with 0,5 mol% of catalyst.

Reducing the catalyst amount to 0,5 mol% (1 mol% Ru) was attempted and resulted in a drop of the conversion to 70% in *i*PrOH and 84% in ACN (Scheme II-2-5). As demonstrated in the next paragraph, an extended reaction time would likely lead to higher conversions, but this option was not considered here.

## 2.4. Optimization of the reaction time

Having the best solvent, pressure, temperature and catalyst loading parameters in hand the reaction time was investigated (Table II-2-3). By reducing the reaction time from 17h to 6 h (Table II-2-3, entry 3 and 4) resulted in a drop of the conversion to 62% and 64% in ACN and *i*PrOH. On the contrary, by extending the reaction time to 24 h in *i*PrOH (Table II-2-3, entry 6), the conversion could be improved from 91% to 99%. It also demonstrated the good catalyst stability and lifetime.

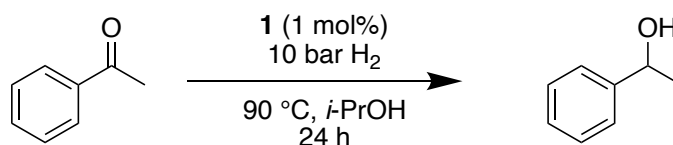
Table II - 2 - 3: Time optimization<sup>a</sup>

Entry	Time (h)	Solvent	Conversion
1	17	ACN	99%
2		<i>i</i> -PrOH	91%
3	6	ACN	64%
4		<i>i</i> -PrOH	62%
5	24	<i>i</i> -PrOH	99%

<sup>a</sup> Acetophenone (0,429 mmol, 50  $\mu$ L), **1** (1 mol%, 4,6 mg), Solvent (0,5 mL), 10 bar H<sub>2</sub> 90 °C, desired time.

## 2.5. Optimized condition

The optimization phase revealed that the best results were obtained in ACN at 90 °C with 10 bar of H<sub>2</sub> within 17 h (99% conversion). The performances of the catalyst in *i*PrOH were also very good albeit slightly lower than in ACN. However, on a green and sustainable chemistry point of view, we decided to employ *i*PrOH with an extended time of 24h as the reference condition (Scheme II-2-6). Indeed, *i*PrOH is less toxic than ACN and also cheaper.



Scheme II - 2 - 6: Best condition for base-free hydrogenation with Dimer 1.

In this first phase of the work, we managed to perform and optimize hydrogenation of the model substrate acetophenone. Most importantly, it was demonstrated that the catalyst is active under base-free hydrogenation hence confirming that the initial bifunctional property hypothesized is operating.

## 2.6. Scope

Following the completion of the reaction condition optimization on the base-free hydrogenation of the model substrate acetophenone, the scope of application with other substrates was investigated. The steric hindrance and the electronic properties of the substrate were tested. Its application to other functional groups was also explored.

First, the steric hindrance was evaluated with hindered aromatic cycles. A small decrease in conversion (91%) was observed with the ortho-tolyl reagent (Table II-2-4, entry 3). However, when increased steric hindrance was introduced with a trimethylated cycle, the conversion dropped drastically to 16% (Table II-2-4, entry 4). The reaction was not sensitive to the steric hindrance at the meta-position since using a naphthalene-moiety (Table II-2-4, entry 5) only a small decrease in the conversion (94%) was observed.

The steric hindrance on the aliphatic part of the model substrate was also investigated. The reaction was found to be sensitive to sterically-hindered substrate as the introduction of either an isopropyl- (Table II-2-4, entry 6) or a cyclohexyl- (Table II-2-4, entry 7) substituent led to an important drop of the conversion around 30 %. The diphenyl substrate gave a moderate conversion of 46% (Table II-2-4, entry 8). Although the reaction was found sensitive

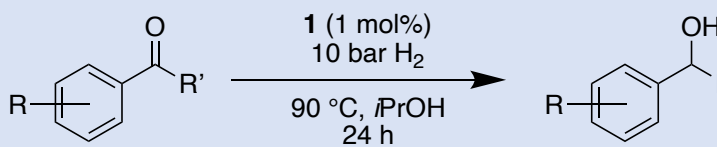
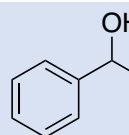
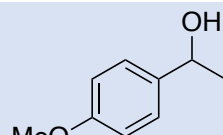
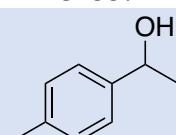
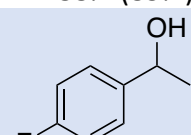
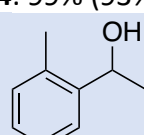
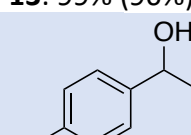
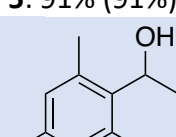
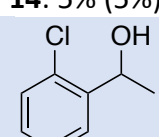
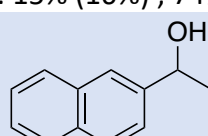
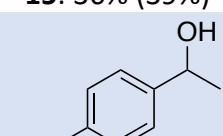
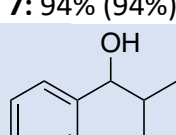
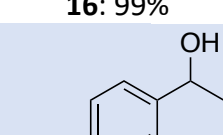
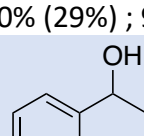
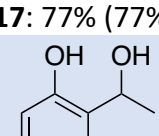
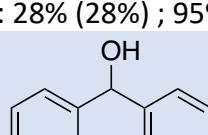
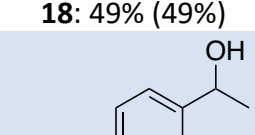
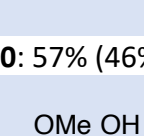
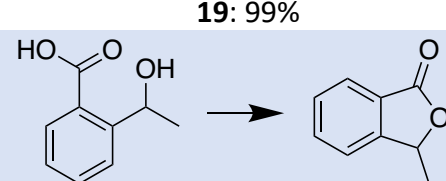
to the steric hindrance of the substrate, excellent conversions could be obtained upon extended reaction time, thanks to the stability of the catalyst.

Then, some functional groups on the acetophenone motif were tested to evaluate the influence of their electronic properties. Thus, substrates with electron-donating groups at the para-position such as methyl- and methoxy- group were tested and both led to high conversions of 93 and 85 %, respectively (Table II-2-4, entry 2 and 10). There was no difference compared to the model substrate when an ortho-methoxy substituent was used (Table II-2-4, entry 9).

In addition, some electron-withdrawing groups were also tested. Two strong electron-withdrawing group were tested in para position. The trifluoromethyl group provided a full conversion (Table II-2-4, entry 14). On the opposite, the nitro group implemented in para position gave a small decrease of the conversion to 77% (Table II-2-4, entry 15). Halogenated acetophenone derivatives were evaluated and delivered an excellent conversion (99%) with the *para*-fluoro derivative (Table II-2-4, entry 10). On the contrary and surprisingly, the bromo derivatives in para position gave a very poor conversion of 5% (Table II-2-4, entry 11). In some way, a deactivation of the catalyst may occur with the bromo derivatives. The *ortho*-chloro derivative also provided a poor conversion of 39% (Table II-2-4, entry 13).

Finally, using a base-free system we were interested about substrates bearing base-sensitive functional groups that are not evaluated in studies dealing with ketone reduction under basic conditions. Therefore, 2-(1-hydroxyethyl)phenol was tested giving a moderate conversion of 49% (Table II-2-4, entry 16) likely due to the steric hindrance of the hydroxy group. A more sensitive compound, with a carboxylic acid function at the para position, was tested. This functional group was tolerated as the reaction proceeded with an excellent conversion of 99% (Table II-2-4, entry 17). Attempts to run the reaction with a carboxylic functional group at the ortho position led to an intramolecular esterification and the formation of a benzofuran derivative (Table II-2-4, entry 18). This reaction has been already reported by Noyori<sup>[3]</sup> for example.

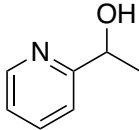
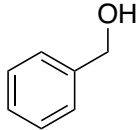
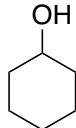
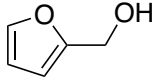
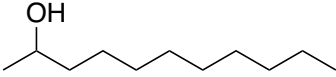
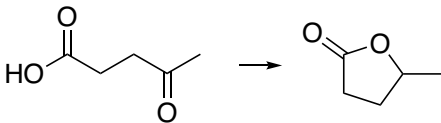
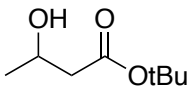
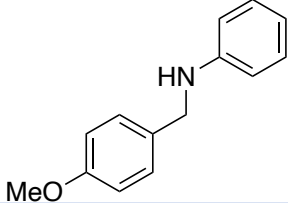
Table II - 2 - 4: Acetophenone derivatives scope in the base-free hydrogenation<sup>a</sup>

			
Entry	Product <sup>b</sup>	Entry	Product <sup>b</sup>
1	 <b>3: 99%</b>	10	 <b>12: 88% (85%)</b>
2	 <b>4: 99% (93%)</b>	11	 <b>13: 99% (96%)</b>
3	 <b>5: 91% (91%)</b>	12	 <b>14: 5% (5%)</b>
4	 <b>6: 15% (16%) ; 74%<sup>c</sup></b>	13	 <b>15: 36% (39%)</b>
5	 <b>7: 94% (94%)</b>	14	 <b>16: 99%</b>
6	 <b>8: 30% (29%) ; 94%<sup>c</sup></b>	15	 <b>17: 77% (77%)</b>
7	 <b>9: 28% (28%) ; 95%<sup>c</sup></b>	16	 <b>18: 49% (49%)</b>
8	 <b>10: 57% (46%)</b>	17	 <b>19: 99%</b>
9	 <b>11: 99% (99%)</b>	18	 <b>20: 61%</b>

<sup>a</sup> Substrate (0,429 mmol), **1** (1 mol%, 4,6 mg), *i*PrOH (0,5 mL), 10 bar H<sub>2</sub> 90 °C, 24h. <sup>b</sup> NMR Conversion (crude) and NMR Conversion dried (solvent evaporated in parentheses <sup>c</sup> 65h

Besides acetophenone-related substrates, other types of substrates including heteroaromatic substrates, aliphatic ketones, keto-ester, aldehydes, iminine and the renewable levulinic acid were submitted to the base-free hydrogenation. Results are summarized in Table II-2-5. A good conversion of 69% was obtained with a 1-(pyridin-2-yl)ethan-1-one (Table II-2-5, entry 1). Both cyclohexanone and undecan-2-one were converted into the corresponding alcohols (Table II-2-5, entry 2 and 3) with excellent results (99%) as well as a beta-keto ester (Table II-2-5, entry 7). In the same manner, both benzaldehyde (Table II-2-5, entry 5) and furfural (Table II-2-5, entry 6) were fully converted. Levulinic acid, an important bio-sourced chemical platform<sup>[4]</sup> led to a cyclisation to form the  $\gamma$ -valerolactone with an excellent conversion (Table II-2-5, entry 7). The imine function could also be reduced thanks to this process in a very good yield of 83% (Table II-2-5, entry 8).

Table II - 2 - 5: Substrate scope in the base-free hydrogenation<sup>a</sup>

Entry	Product <sup>b</sup>	Entry	Product <sup>b</sup>
1		5	
	21: 67% (69%)		25: 99% (99%)
2		6	
	22: 99%		26: 99%
3		7	
	23: 99% (99%)		27: 99%
4		8	
	24: 99%		28: 99% 83% <sup>c</sup>

<sup>a</sup> Substrate (0,429 mmol), **1** (1 mol%, 4,6 mg), *i*PrOH (0,5 mL), 10 bar H<sub>2</sub> 90 °C, 24h <sup>b</sup> NMR Conversion (crude) and NMR Conversion dried (solvent evaporated in parentheses) <sup>c</sup> yield

## 2.7. Conclusion on the base-free hydrogenation

As demonstrated in this study, catalyst **1** is active in the base-free hydrogenation of a broad scope of ketones and other functional groups as well. Its activity is comparable to other kind of ruthenium catalyst developed in the laboratory by Bruneau having the advantage to use less H<sub>2</sub> but a higher temperature.<sup>[5]</sup>

The reaction conditions could be applied to a broad scope of substituted acetophenone derivatives including base-sensitive ones bearing an acidic hydroxy- or an acidic carboxyl-function. We were also able to perform the hydrogenation of other functional groups such as aldehydes and imine in excellent conversion.

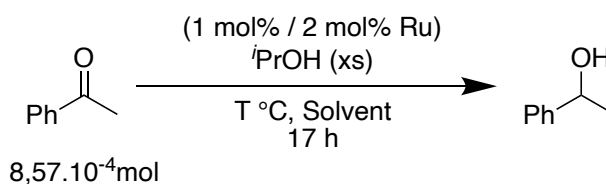
These results demonstrate that the catalyst is active in base-free hydrogenation. This catalytic activity confirms the bifunctional properties we suspected as a working hypothesis. Based on these results, we have extended the use of the catalyst to other kind of reactions such as transfer hydrogenation, as presented hereafter, and also to other domains related to energy that will be presented in the forthcoming chapters.

### 3. Base-free transfer Hydrogenation

Following the studies on the reduction of ketones using dihydrogen, the base-free transfer hydrogenation was investigated using either *i*PrOH or FA as a hydrogen donors.

#### 3.1. *Iso*-Propanol

Base-free transfer hydrogenation with *i*PrOH was conducted in labmade heavy-wall Schlenk tubes. Acetophenone was still used as the test substrate with 1 mol% of **1** in pure *i*PrOH or in solvent mixtures containing 0,5 mL solvent/0,5mL *i*PrOH (Scheme II-2-7).



*Scheme II - 2 - 7: Model reaction for base free transfer hydrogenation with iPrOH*

##### 3.1.1. Solvent and temperature optimization

Having previously observed that the hydrogenation reaction was operating at 75 °C and 90 °C, we explored and extended temperature range for the transfer hydrogenation reaction (Table II-2-6). The first temperature tested was 50 °C with four different solvents (ACN/*i*PrOH, THF/*i*PrOH, DCM/*i*PrOH and pure *i*PrOH). Unfortunately, there was no results at this temperature (Table II-2-6, entry 1 to 4). The temperature was increased to 75 °C and the reaction run with ACN/*i*PrOH, THF/*i*PrOH and *i*PrOH. DCM was discarded for safety reason due to its low boiling point. At 75 °C, the catalyst began to show activity but only traces of product were detected in ACN/*i*PrOH (Table II-2-6, entry 6) and 11% conversion in THF/*i*PrOH (Table II-2-6, entry 5). In *i*PrOH the conversion was about 13% and could be increased to 33% with a longer reaction time of 66 h (Table II-2-6, entry 7).

At 90 °C, DMSO/*i*PrOH and GVL/*i*PrOH were tested in addition to ACN/*i*PrOH and *i*PrOH. In ACN/*i*PrOH there was only traces but by a preactivation of **1** in ACN for 1h15 the conversion was 16% (Table II-2-6, entry 10). This preactivation was implemented to form the monomeric species **2** which is suspected to be the active species. The reaction in DMSO/*i*PrOH gave only 10% conversion (Table II-2-6, entry 8). The best conversion was obtained in *i*PrOH with 33% conversion (Table II-2-6, entry 11) just prior GVL that was found a suitable solvent as the conversion in GVL /*i*PrOH allowed reaching 36% conversion (Table II-2-6, entry 9)

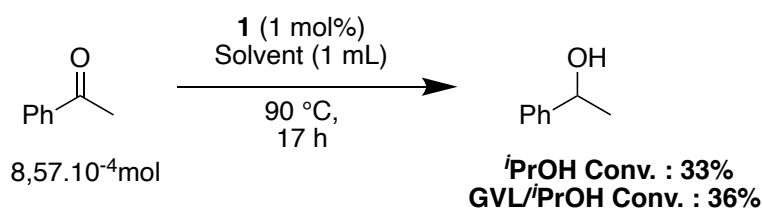
Table II - 2 - 6: Solvent and temperature optimization<sup>a</sup>

Entry	Temperature (°C)	Solvent	Conversion
1	50	DCM/ <i>i</i> -PrOH	Traces
2		THF/ <i>i</i> -PrOH	0%
3		ACN/ <i>i</i> -PrOH	0%
4		<i>i</i> -PrOH	Traces
5	75	THF/ <i>i</i> -PrOH	11%
6		ACN/ <i>i</i> -PrOH	Traces
7		<i>i</i> -PrOH	13% ; 33% <sup>b</sup>
8	90	DMSO/ <i>i</i> -PrOH	10%
9		GVL/ <i>i</i> -PrOH	36%
10		ACN/ <i>i</i> -PrOH	Traces ; 16% <sup>c</sup>
11		<i>i</i> -PrOH	33%

<sup>a</sup> Acetophenone (0,857 mmol, 100  $\mu$ L), **1** (1 mol%, 9,3 mg), *i*-PrOH (0,5 mL), solvent (0,5 mL), T °C, 17h <sup>b</sup> 66h ; <sup>c</sup> 1h15 activation in ACN at r.t

It is important to consider that since *i*PrOH is active in transfer hydrogenation, the results obtained previously on hydrogenation with *i*PrOH as solvent can be partially attributed to transfer hydrogen although to a small extent.

Having obtained modest results in this preliminary study (Scheme II-2-8), no further optimization and scope were studied. However, the activity under base-free condition is once again a proof of the bifunctional character of the catalyst.



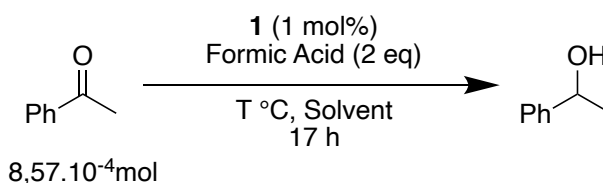
Scheme II - 2 - 8: Optimized conditions for base-free transfer hydrogenation with *i*PrOH.

## 3.2. Formic Acid

After the base-free transfer hydrogenation with *i*PrOH, the use of formic acid as hydrogen donor in a base-free process was considered. As described in the state of the art, such process has been rarely studied and reported.

### 3.2.1. Preliminary tests

First, based on the work in *i*PrOH, different solvents were tested at 50, 75 and 90 °C in a set of preliminary tests. Those preliminary reactions summarized in table II-2-7 were conducted with 1 mol% of **1** using 2 equivalents of FA as hydrogen donor in 1 mL of solvent for 17 h in a heavy-wall Schlenk tube (Scheme II-2-9).



*Scheme II - 2 - 9: Model reaction of the preliminary tests for base-free transfer hydrogenation with FA.*

At 50 °C, among the solvent tested (ACN, DCM, Pure FA, THF, Tol, H<sub>2</sub>O, *i*PrOH) only the reaction in THF (Table II-2-7, entry 4), water (Table II-2-7, entry 6) and *i*PrOH (Table II-2-7, entry 7) showed some conversion of 14%, 15%, 6% respectively.

When the temperature was increased to 75 °C some improvement of the conversion from 15% to 23% was observed in THF (Table II-2-7, entry 10). The reaction in toluene also provided a modest conversion (26%) of acetophenone (Table II-2-7, entry 11). On the contrary, an important growth was observed in *i*PrOH (Table II-2-7, entry 13) with 48% conversion and in water (Table II-2-7, entry 12) with 50% conversion. A mixture of *i*PrOH and H<sub>2</sub>O did not show any improvement (Table II-2-7, entry 14).

In order to compare the performance of **1** with the Shvo catalyst, the latter was engaged in the transfer hydrogenation of acetophenone at 75 °C under strictly identical conditions. A conversion of 51% was obtained hence demonstrating that the very first generation of  $\eta^5$ -oxocyclohexadienyl ruthenium complexes display similar performance as this reference catalyst.

Once again, the best conversions were obtained at 90 °C. In ACN with a preactivation of **1** at room temperature (Table II-2-7, entry 15), the conversion was still very low (10%). The conversion in toluene (Table II-2-7, entry 18) remained unchanged (23% vs 26 at 75 °C). The conversion using THF slightly increased to 35% (Table II-2-7, entry 17). DMSO that has not been tested at 50 and 75 °C gave a conversion of 40% (Table II-2-7, entry 16). The results in water (Table II-2-7, entry 19) were very good (up to 86% conversion) but the repeatability was an issue due to the moderate solubility of the catalyst in water. The best conversion was achieved using *i*PrOH (Table II-2-7, entry 20) with a conversion around 60% in several runs. Despite its problematic elimination or separation from the reaction products, GVL, was tested and led to a conversion of 63% (Table II-2-7, entry 21).

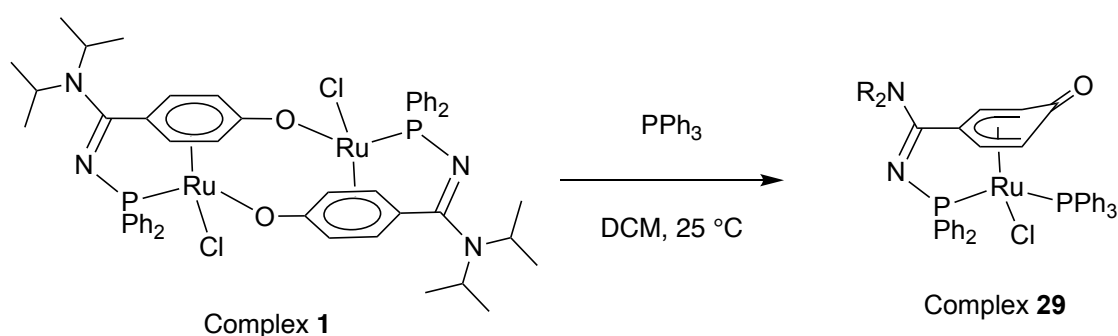
Hence, *i*PrOH and GVL were the solvent selected for further optimizations. *i*PrOH has the advantage to have a low boiling point (82 °C) for an ease of separation compared to GVL (205 °C). For these reasons, *i*PrOH was the solvent used for the reaction scope.

Table II - 2 - 7: Preliminary test on temperature and solvents for base-free transfer hydrogenation with FA<sup>a</sup>

Entry	Temperature (°C)	Solvent	Conversion
1	50	ACN	0%
2		DCM	Traces
3		Pure FA	0%
4		THF	15%
5		Tol	Traces
6		H <sub>2</sub> O	14%
7		<i>i</i> -PrOH	6%
8	75	ACN	0%
9		Pure FA	0%
10		THF	23%
11		Tol	26%
12		H <sub>2</sub> O	50%
13		<i>i</i> -PrOH	48%
14		0,5 <i>i</i> -PrOH / 0,5 H <sub>2</sub> O	18%
15	90	ACN	10% <sup>b</sup>
16		DMSO	40%
17		THF	35%
18		Tol	23%
19		H <sub>2</sub> O	72-86%
20		<i>i</i> -PrOH	57%
21		GVL	63%
22		0,8 <i>i</i> -PrOH / 0,2 H <sub>2</sub> O	35%

<sup>a</sup> Acetophenone (0,857 mmol, 100 μL), **1** (1 mol%, 9,3 mg), Formic Acid (2 equivalent, 1,71 mmol), solvent (1 mL), T °C, 17h<sup>b</sup> 1h15 activation in ACN at r.t

During the preliminary test, a monomeric species derived from complex **1** provided by our partner was also tested (Scheme II-2-10). Overall, the conversion obtained are quite similar to the ones obtained with **1** but with a lower amount of ruthenium species as it is not a dimer.



Scheme II - 2 - 10: Formation of complex **29** from complex **1**.

The use of **29** in THF (Table II-2-8, entry 3 and 7) showed a slight improvement compared to the use of **1** with a conversion of 35% and 38% at 75 and 90 °C, respectively. The same behavior was observed in toluene (Table II-2-8, entry 4 and 8). Surprisingly, we noticed a decrease in the activity in *i*PrOH (Table II-2-8, entry 6 and 10) from 75 °C to 90 °C but also compared to the use of **1**. Once again, the best conversions were obtained in water (Table II-2-8, entry 5 and 9) but there was again a problem of solubility.

Overall, it seems that the activity of the complex **29** decreased as the temperature increased. This is an indication of lower thermal stability of **29** as compared to **1**.

Table II - 2 - 8: Preliminary test on temperature and solvents for base-free transfer hydrogenation with FA using **29**<sup>a</sup>

Entry	Temperature (°C)	Solvent	Conversion
1	75	ACN	0%
2		Pure FA	0%
3		THF	35%
4		Tol	36%
5		H <sub>2</sub> O	88%
6		<i>i</i> -PrOH	37%
7	90	THF	38%
8		Tol	26%
9		H <sub>2</sub> O	77%
10		<i>i</i> -PrOH	34%

<sup>a</sup> Acetophenone (0,857 mmol, 100 μL), **29** (1 mol%, 6,9 mg), Formic Acid (2 equivalent, 1,71 mmol), solvent (1 mL), T °C, 17h

### 3.2.1. Optimization of formic acid amount

Having the appropriate solvents and temperature parameters in hands, the first parameters we explored was the amount of hydrogen donor i.e., FA to further increase the conversion of acetophenone (Table II-2-8).

In *i*PrOH, increasing the amount of formic acid to 5 equiv. (Table II-2-8, entry 2) did not translate in a large improvement since a conversion of 65% was obtained when 57% conversion was reached using 2 equiv. of FA (Table II-2-8, entry 1). However, we noticed an improvement of the conversion in GVL using 5 equivalents of FA (Table II-2-8, entry 4). Indeed, the conversion of acetophenone increased from 63% to 88%.

Using FA as a hydrogen source led to the release of CO<sub>2</sub> hence an increase of pressure in a closed reactor. Furthermore, the potential activity of the catalyst in FA dehydrogenation (demonstrated later in chapter IV) could also contribute to the pressure increase. All together, these potential safety issue prompted us to monitor the pressure generated by the reaction in a high-pressure reactor. With 5 equivalents of FA in GVL at 90 °C (Table II-2-8, entry 5), the pressure reached 10 bar and the conversion decreased to 74%. We measured that up to 20 bar of pressure was generated using 10 equivalents of FA leading to a conversion of 81% (Table II-2-8, entry 6). It should be noted that results in high pressure reactors and closed Schleck tubes could not be directly compared due to the different setup and the particular mechanism in GVL that will be commented later. However, due to these observations further experiments were conducted in ACE® pressure tubes supporting up to 10 bar that are more convenient than high pressure reactors.

Table II - 2 - 9: Effect on the FA amount on the base-free transfer hydrogenation of acetophenone<sup>a</sup>

Entry	Solvent	FA equivalence	Conversion
1	<i>i</i> -PrOH	2	57%
2		5	65%
3	GVL	2	63%
4		5	88%
5		5 <sup>b</sup>	74%
6		10 <sup>c</sup>	81%

<sup>a</sup> Acetophenone (0,857 mmol, 100  $\mu$ L), **1** (1 mol%, 9,3 mg), Formic Acid, solvent (1 mL), 90 °C, 17h. <sup>b</sup> Pressure monitoring in a 22 mL high pressure reactor: 10 bar; <sup>c</sup> Pressure monitoring in a 22 mL high pressure reactor : 20 bar.

### 3.2.2. Concentration effect

We next investigated if the concentration of acetophenone could have an influence on the reaction outcome. Thus, using the conditions established previously, the concentration was doubled by decreasing the solvent volume (Table II-2-9). By doing this, the conversion in *i*PrOH and GVL increased to 56% and 95%, respectively. Further increase of the concentration was not considered for practical and safety reasons.

Table II - 2 - 10: Effect on the concentration on the base-free transfer hydrogenation of acetophenone<sup>a</sup>

Solvent	Concentration (mol.L <sup>-1</sup> )	Conversion
<i>i</i> -PrOH	0,857	47%
	1,714	56%
GVL	0,857	83%
	1,714	85-95%

<sup>a</sup> Acetophenone (0,857 mmol, 100  $\mu$ L), **1** (1 mol%, 9,3 mg), Formic Acid (5 eq, 4,3 mmol), solvent, 90 °C, 17h, Ace tube.

### 3.2.3. Time and catalytic amount

Having reached very high conversions in GVL, further optimizations were conducted in *i*PrOH, by varying the reaction time and catalyst loading (Table II-2-11). As previously depicted with transfer hydrogenation in *i*PrOH, the conversion increased as the reaction time was longer. Hence, using a longer reaction time the conversion was increased to 80% in 36 h and 94% in 66 h. Maintaining a reasonable reaction time was achieved using a higher catalyst loading. Thus, using 1,5 mol% of **1**, a very high conversion (> 90%) could be obtained in 24 h.

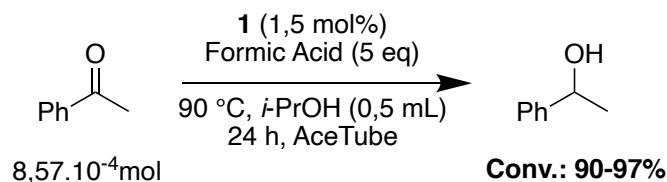
Table II - 2 - 11: Effect on the time on the base-free transfer hydrogenation of acetophenone<sup>a</sup>

Entry	Time (h)	Conversion
1	17	56%
2	36	80%
3	66	94% <sup>b</sup>
4	24	90-97% <sup>c</sup>

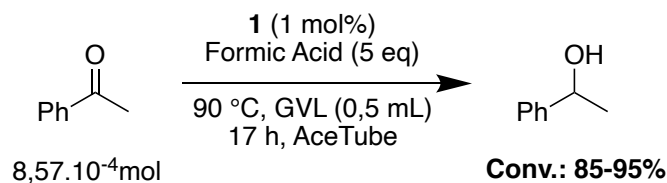
<sup>a</sup> Acetophenone (0,857 mmol, 100  $\mu$ L), **1** (1 mol%, 9,3 mg), Formic Acid (5 eq, 4,3 mmol), *i*PrOH (0,5 mL), 90 °C, 17h, Ace tube. <sup>b</sup> 1 mL *i*PrOH; <sup>c</sup> 1,5 mol% catalyst

### 3.2.4. Optimized conditions

Two solvents (*i*PrOH and GVL) have been selected to lead to optimized reaction conditions for the base-free transfer hydrogenation of acetophenone with FA. During this optimization study it was demonstrated that better performances were achieved using GVL as solvent. Similarly high performances could be obtained in both solvents, but the reaction performed in *i*PrOH required a higher catalyst loading and a longer reaction time (Scheme II-2-11 and 12). The reaction condition with *i*PrOH was selected to proceed to a scope study due to an easier workup procedure.



Scheme II - 2 - 12: Best condition in base-free transfer hydrogenation with FA in *i*PrOH.



Scheme II - 2 - 11: Best condition of base-free transfer hydrogenation with FA in GVL.

### 3.2.5. Scope

*i*PrOH has the advantage to have a low boiling point (82 °C) as compared to GVL (205 °C). In the context of our studies dealing with compounds with boiling points ranging around 200 °C, the use of *i*PrOH was considered for the development of the reaction scope.

Having the best conditions in hand, a large scope of substrates previously studied for the hydrogenation reaction has been tested.

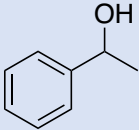
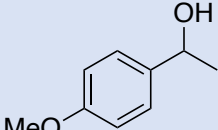
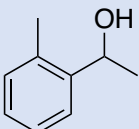
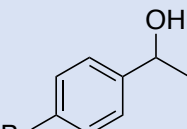
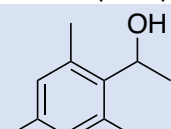
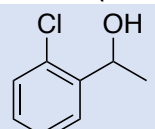
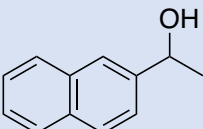
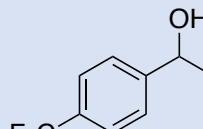
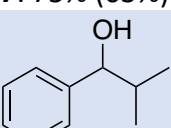
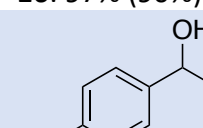
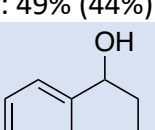
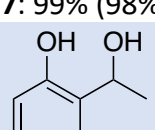
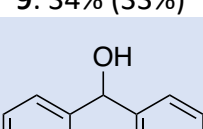
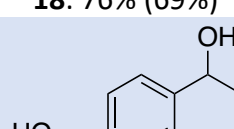
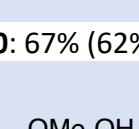
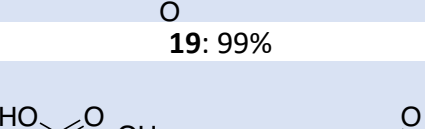
First, the steric hindrance of the aryl part of the substrate was evaluated. As previously observed, one methyl group in ortho-position did not inhibit the reaction to a large extent since the conversion was good with 65% (Table II-2-12, entry 2). On the contrary the conversion dropped to 15% when the mesityl-fragment was introduced (Table II-2-12, entry 3). The bulkier naphthalene-moiety also led to a good conversion of 75% (Table II-2-12, entry 4). As also observed with the hydrogenation reaction, increasing the steric hindrance on the aliphatic part of the substrate with an *iso*-propyl (Table II-2-12, entry 5) or a cyclohexyl substituent (Table II-2-12, entry 6) reduced the conversion to 49% and 34%, respectively. The diphenyl substrate presented a good conversion of 67%.

The electronic influence of the substituents started with the electron-donating group. A methoxy group was implemented in the ortho position, with a good conversion of 75% (Table II-2-12, entry 8) but a moderate one of 52% in para (Table II-2-12, entry 9).

Halogenated electron-withdrawing groups (Table II-2-12, entry 10, 11, 12) had no influence on the conversion. This is a major difference with the hydrogenation conditions where these reagents were poorly or not converted. The nitro substituent in para position provided an excellent conversion of 99% (Table II-2-12, entry 13).

Base sensitive phenol and carboxylic acid substituents were tested as there are not usually tested in this kind of scope. The acetophenone with a hydroxyl-substituent in the ortho-position provided a good conversion of 76% (Table II-2-12, entry 14), that was higher than the one obtained upon hydrogenation (49%). The 4-acetylbenzoic acid provided an excellent conversion (Table II-2-12, entry 15). As previously observed, the acid substituent in ortho of the ketone group lead to a cyclisation and provide a benzofuran based molecule in 21% conversion.

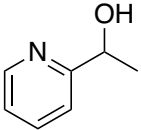
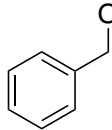
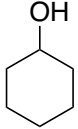
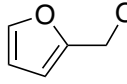
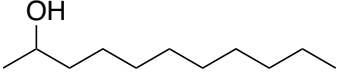
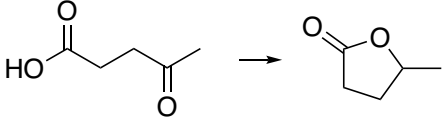
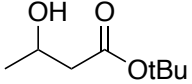
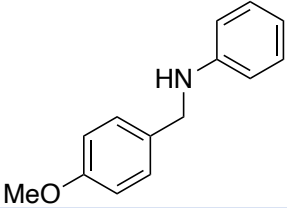
Table II - 2 - 12: Acetophenone based substrate scope in the base-free transfer hydrogenation with FA<sup>a</sup>

$  \begin{array}{c}  \text{R}-\text{C}_6\text{H}_4-\text{C}(=\text{O})\text{R}' \\  \xrightarrow[\text{90 } ^\circ\text{C, } i\text{-PrOH (0,5 mL), 24 h, AceTube}]{\text{1 (1,5 mol\%), Formic Acid (5 eq)}} \\  \text{R}-\text{C}_6\text{H}_4-\text{CH}(\text{OH})\text{R}'  \end{array}  $			
Entry	Product <sup>b</sup>	Entry	Product <sup>b</sup>
1	 <b>3: 90-97%</b>	9	 <b>12: 52% (45%)</b>
2	 <b>5: 65% (61%)</b>	10	 <b>14: 95% (89%)</b>
3	 <b>6: 15% (14%)</b>	11	 <b>15: 98% (97%)</b>
4	 <b>7: 75% (63%)</b>	12	 <b>16: 97% (90%)</b>
5	 <b>8: 49% (44%)</b>	13	 <b>17: 99% (98%)</b>
6	 <b>9: 34% (33%)</b>	14	 <b>18: 76% (69%)</b>
7	 <b>10: 67% (62%)</b>	15	 <b>19: 99%</b>
8	 <b>11: 75% (52%)</b>	16	 <b>20: 21%</b>

<sup>a</sup> Acetophenone (0,857 mmol, 100  $\mu$ L), **1** (1 mol%, 9,3 mg), Formic Acid (5 eq, 4,3 mmol), *i*PrOH (0,5 mL), 90  $^\circ$ C, 24h, Ace tube. <sup>b</sup> NMR conversion and yield in parenthesis

After the study of the stereoelectronic substitution of the model substrate acetophenone, the reaction was applied to various substrates and functional groups summarized in Table II-2-13. A very good conversion (86%) was obtained with 1-(pyridin-2-yl)ethan-1-one (Table II-2-12, entry 1). Excellent conversions were obtained with aliphatic ketones such as cyclohexanone and undecan-2-one (Table II-2-13, entry 2 and 3) and also with a  $\beta$ -keto ester (Table II-2-12, entry 4). The reaction condition suits with the use of aldehyde with a 99% conversion using benzaldehyde (Table II-2-12, entry 5) or furfural (Table II-2-12, entry 6). The cyclisation of levulinic acid into GVL occurred in an excellent 99% conversion. The conditions could also be applied to imine reduction (Table II-2-12, entry 8) but in a moderate conversion of 50%.

Table II - 2 - 13: Substrate scope in the base-free transfer hydrogenation with FA<sup>a</sup>

Entry	Substrate <sup>b</sup>	Entry	Substrate <sup>b</sup>
1		5	
	21: 86% (63%)		25: 99% (94%)
2		6	
	22: 99% (91%)		26: 99% (99%)
3		7	
	23: 99% (92%)		27: 99% (85%)
4		8	
	24: 99% (85%)		28: 50%

<sup>a</sup> Acetophenone (0,857 mmol, 100  $\mu$ L), **1** (1 mol%, 9,3 mg), Formic Acid (5 eq, 4,3 mmol), *i*PrOH (0,5 mL), 90 °C, 24h, Ace tube.<sup>b</sup> NMR Conversion and yield in parenthesis

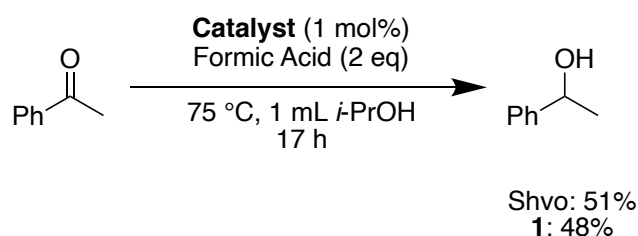
The base-free transfer hydrogenation with FA could be applied to acetophenone as the model substrate and to a broad range of ketone derivatives with various stereoelectronic properties. The steric hindrance was the effect that influenced the most the conversion. To be noted, using base-free condition, we were able to use base sensitive substrates with good conversion.

### 3.2.6. Conclusion on base-free transfer hydrogenation with FA

The rarely reported base-free transfer hydrogenation with FA was possible in excellent conversions using *i*PrOH or GVL as solvents. Its application was possible on a broad scope of acetophenone derivatives including base sensitive ones. The process was also applied to different substrates and functional group such as aldehydes and imines.

An interesting point was the choice of *i*PrOH as a solvent as it can also perform transfer hydrogenation. However, as seen in 3.1, the conversion in *i*PrOH was limited to 33% but with the addition of FA, it could be largely improved (>90%). It would be interesting to have a deeper understanding on the role of each component. FA may have a role of an initiator or doping molecule. There is still work to do to clearly understand the mechanism of this reaction.

The base-free transfer hydrogenation with FA was run with the Shvo catalyst and the results compared to the reaction catalyzed by **1** (Scheme II-2-13) giving similar results.



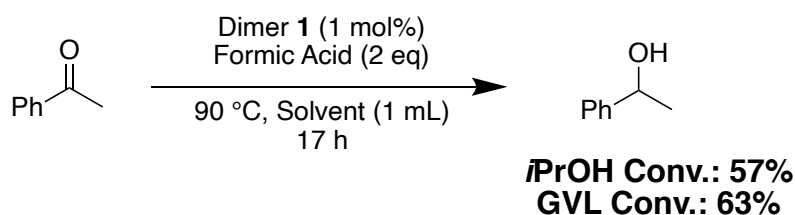
Scheme II - 2 - 13: Shvo and complex **1** comparison in base-free transfer hydrogenation with FA.

### 3.3. Mechanism proposal

During this study on the base-free hydrogenation and transfer hydrogenation with FA, several observations were made providing some important information on the potential mechanisms involved in the different processes. Adding some studies on the reactivity of **1** carried out in the group of Alain Igau also contributed to envision potential mechanism.

First of all, we noticed that very different results were obtained with aryl halides depending on the process implemented either hydrogenation or transfer hydrogenation with FA. This is a hint for different reaction mechanisms or different organometallic species present in the reaction media.

Then, during the studies on transfer hydrogenation with formic acid, some contrary observations were made. Indeed, very different results were obtained depending on the



Scheme II - 2 - 14: Base-free transfer hydrogenation with FA in a closed system.

solvent (*i*PrOH or GVL) and the reaction setup. When the reactions were performed in a closed Schlenk tube with 1 mol% of **1** and 2 equivalents of FA for 17 h, similar results were obtained in both solvents (Scheme II-2-14). Interestingly, when the same reactions were performed in an open system with and without an argon flow, the results were unchanged in *i*PrOH whereas the conversion dropped significantly in GVL from 63% to 20-21% (Figure II-2-2).

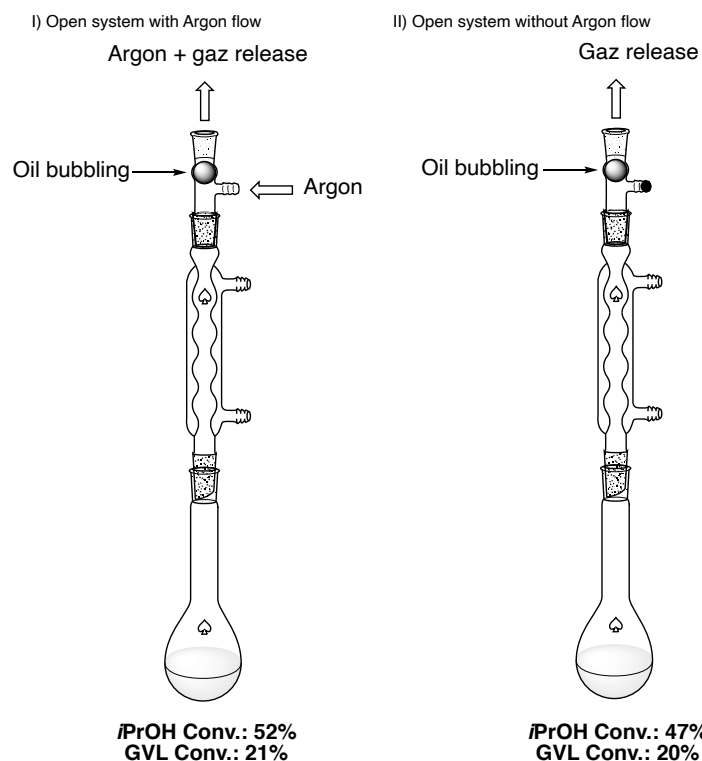


Figure II - 2 - 2: Open system used in base-free transfer hydrogenation with FA.

These observations demonstrate that different mechanisms are involved in these solvents. Using *i*PrOH, a classical hydrogen transfer mechanism is likely involved whereas, in GVL the dehydrogenation of FA in CO<sub>2</sub> and H<sub>2</sub> happened prior to the hydrogenation of ketone. In a closed reactor, the reversibility of the dehydrogenation reaction allowed the reduction of ketone to proceed but it is not the case in an open reactor.

Based on these observations, a hypothetical mechanism (Scheme II-2-15) inspired by the Shvo catalyst mechanism is proposed.<sup>[6]</sup>

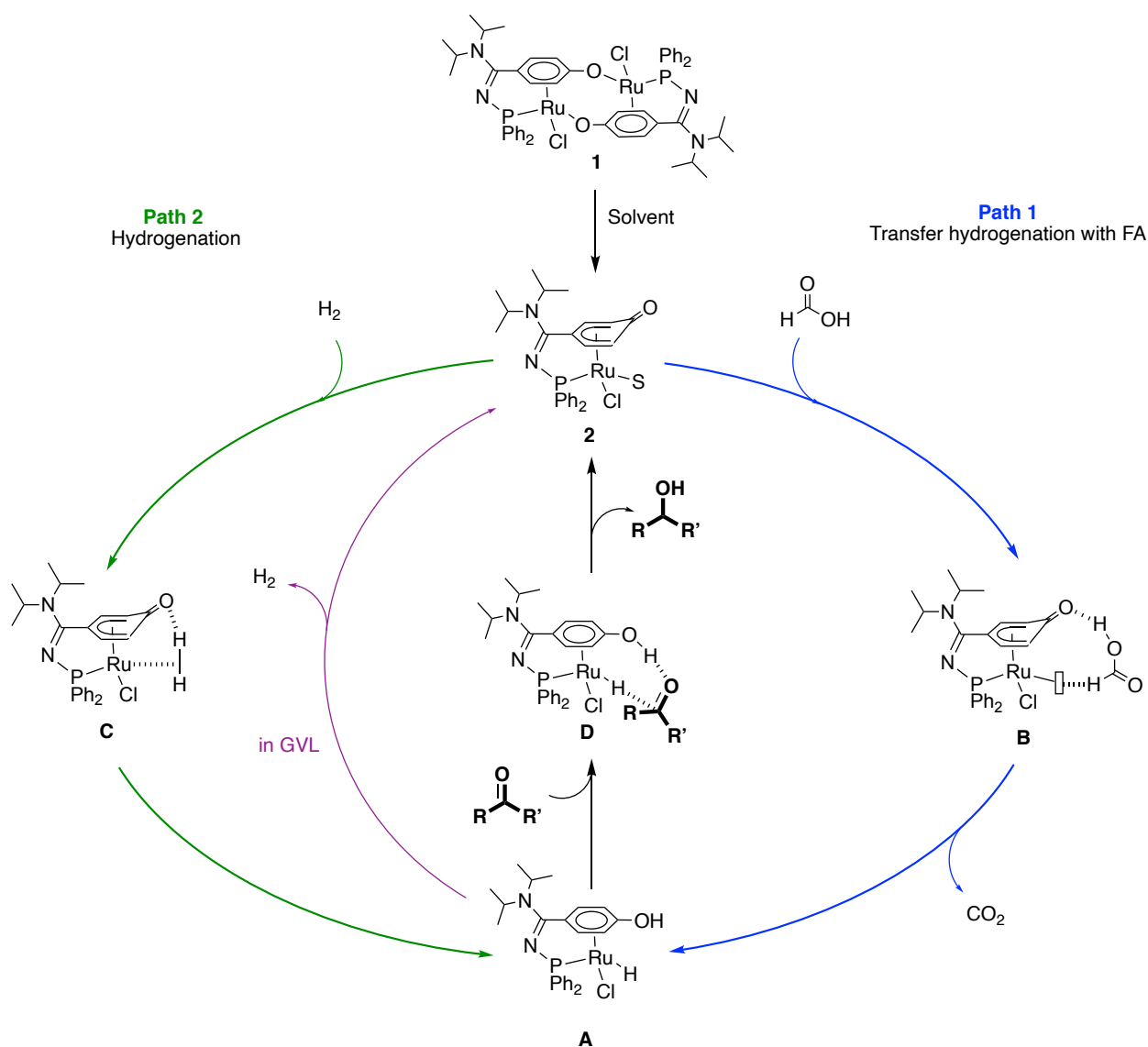
In the first step of the transfer hydrogenation, formic acid is dehydrogenated hence transferring hydrogen to the catalyst. This process would involve ligand cooperation via the basic-character of the oxo-dienyl ligand leading to species **A**. It is important to mention that

during this project, the group of A. Igau was able to detect and characterize the species **2** by  $^1\text{H}$  NMR in an NMR tube loaded with **1** in DCM or ACN and pressurized with 3 bar of  $\text{H}_2$ .

This species **A** would then transfer hydrogen to the carbonyl functional group, possibly via a concerted outer-sphere mechanism (species **D**) as proposed by Bäckvall<sup>[7]</sup> and Ujaque<sup>[8]</sup> for the Shvo catalyst leading to the alcohol products and concomitantly regenerating **2**. Alternatively, species **A** may release hydrogen, a process likely operating in GVL at a higher rate than transfer to the organic substrate. It is reasonably conceivable that species **A** could be stabilized through hydrogen bonding in *i*PrOH hence explaining the observation described above.

The hydrogenation pathway would involve the preliminary coordination of dihydrogen as a  $\eta^2$ -dihydride complex. Here again the basic character of the oxo-dienyl ligand would act as a base and deprotonate the coordinated dihydrogen leading to **A**. It must be mentioned here that the protonation of  $\eta^5$ -oxocyclohexadienyl transition metal complexes to their phenol derivatives is a well-known and reported process.<sup>[9]</sup>

Of course, these mechanisms are hypothetical and would need further experimental and theoretical investigations to be validated, amended or rebutted.



Scheme II - 2 - 15: Mechanism proposal for base free hydrogenation and transfer hydrogenation.

## 4. Conclusion and perspectives

This chapter was dedicated to the activity of complex **1** in base free hydrogenation and transfer hydrogenation with the objective to demonstrate the bifunctional nature of this catalyst. Very good results were obtained with H<sub>2</sub> where a scope of substrates has been made showing the broad application of the reaction. Concerning the transfer hydrogenation, *i*PrOH as a hydrogen donor was not successful leading to moderate results. On the contrary, the use of FA provided very good results in an area where it has been rarely reported. Whatever the process used (hydrogenation or transfer hydrogenation), the use of base-free conditions made possible the conversion of base-sensitive substrates that are not used in literature data using basic conditions.

This work clearly demonstrated the catalytic activity of  $\eta^5$ -oxocyclohexadienyl ruthenium complex **1** in base-free process. This is a proof of concept of the bifunctional character of this catalyst operating by metal-ligand cooperation albeit further studies, in particular theoretical investigations, will be necessary to fully confirm this characteristic. Last but not least, the stereoselective version of this reaction will necessarily have to be developed. This will involve the design and synthesis of new versions of this catalyst.

Having demonstrated the catalytic activity of **1**, this catalyst was further evaluated in the domain of energy with two different approaches dealing with hydrogen storage and biofuels. The next chapters will deal with the hydrogen storage and release in the CO<sub>2</sub>/formic acid cycle and alcohol upgrading by the Guerbet reaction.

## 5. References:

- [1] E. Puig, R. Verron, M. Kechaou-Perrot, L. Vendier, H. Gornitzka, K. Miqueu, J.-M. Sotiropoulos, C. Fischmeister, P. Sutra, A. Igau, **2022**, *submitted*.
- [2] Z. Zhang, *ChemSusChem* **2016**, 9, 156–171.
- [3] Masato. Kitamura, Takeshi. Ohkuma, Shinichi. Inoue, Noboru. Sayo, Hidenori. Kumobayashi, Susumu. Akutagawa, Tetsuo. Ohta, Hidemasa. Takaya, Ryoji. Noyori, *J. Am. Chem. Soc.* **1988**, 110, 629–631.
- [4] F. D. Pileidis, M.-M. Titirici, *ChemSusChem* **2016**, 9, 562–582.
- [5] F. Jiang, K. Yuan, M. Achard, C. Bruneau, *Chem. - Eur. J.* **2013**, 19, 10343–10352.
- [6] N. Menashe, E. Salant, Y. Shvo, *J. Organomet. Chem.* **1996**, 514, 97–102.
- [7] J. B. Johnson, J.-E. Bäckvall, *J. Org. Chem.* **2003**, 68, 7681–7684.
- [8] A. Comas-Vives, G. Ujaque, A. Lledós, *Organometallics* **2007**, 26, 4135–4144.
- [9] A. Igau, *Coord. Chem. Rev.* **2017**, 344, 299–322.
- [10] M. Kechaou-Perrot, L. Vendier, S. Bastin, J.-M. Sotiropoulos, K. Miqueu, L. Menéndez-Rodríguez, P. Crochet, V. Cadierno, A. Igau, *Organometallics* **2014**, 33, 6294–6297.

## 6. Experimental part

### 6.1. General considerations

All reactions were carried out with dried glassware.

The different commercial reagents used were purchased from Acros, Alfa Aesar or Sigma Aldrich. They were purified by Kugelrohr distillation system prior to use.

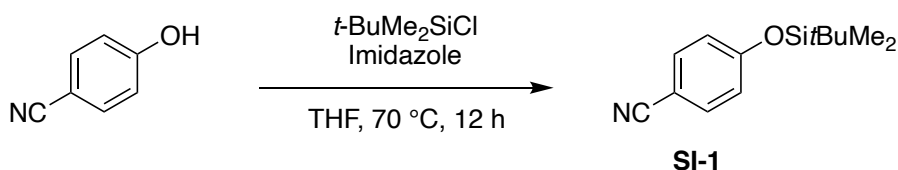
Column chromatography was performed on Acros Organics Ultrapure silica gel (mesh size 40-60 $\mu$ m, 60Å).

NMR spectra were recorded at 300 °K on a Bruker AV III 400 MHz spectrometer fitted with a BBFO probe.

### 6.2. Complex 1 synthesis

Although complex **1** was essentially provided by the group of Alain Igau, this complex was also prepared in Rennes. Complex **1** was synthesis following the procedure taken from the publication of Alain Igau and all the NMR data were consistent with the reported data.<sup>[10]</sup> Solvents used for the synthesis of catalyst were obtained from a MB SPS-800 MBRAUN purification system.

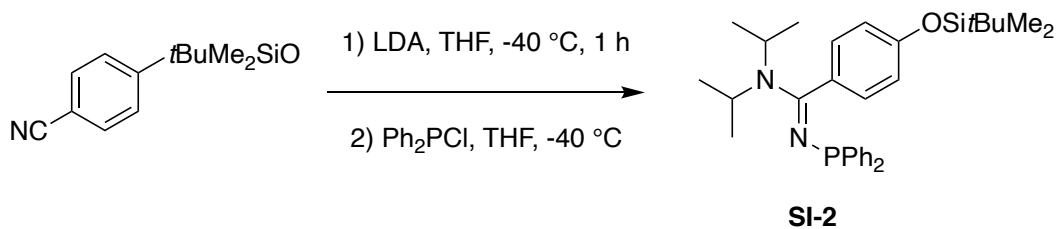
#### 1) Synthesis of **SI-1**; Protection of 4-cyanophenol



4-cyanophenol (1 g; 8.395 mmol), *t*-butyldimethylchlorosilane *t*-BuMe<sub>2</sub>SiCl (1.51 g; 10.074 mmol; 1.2 eq), and imidazole (1.4575 g; 20.9875 mmol; 2.5 eq) were added to a Schlenk tube in air. Three vacuum/argon cycles were performed in the Schlenk. After that, 25 mL of distilled and degassed THF were added to the Schlenk under argon conducting to a cloudy white solution. The reaction was stirred and refluxed overnight at 70 °C. After returning to room temperature, the solvent was evaporated. 5 ml of saturated NH<sub>4</sub>Cl solution was added, to the white residue and the solution was extracted thrice with ethyl acetate. The organic phase was dried on Na<sub>2</sub>SO<sub>4</sub>. Finally, the obtained oil was purified by column chromatography using a mixture of heptane and ethyl acetate: 95/5. After drying under vacuum, the product was isolated in the form of a white powder (1.0735 g, 55% yield, molar mass = 233.38 g/mol).

<sup>1</sup>H NMR (400 MHz, CDCl<sub>3</sub>)  $\delta$  7.54 (d, *J* = 9.0 Hz, 2H), 6.89 (d, *J* = 6.9 Hz, 2H), 0.98 (s, 9H), 0.23 (s, 6H).

## 2) Synthesis of phosphino ligand **SI-2**

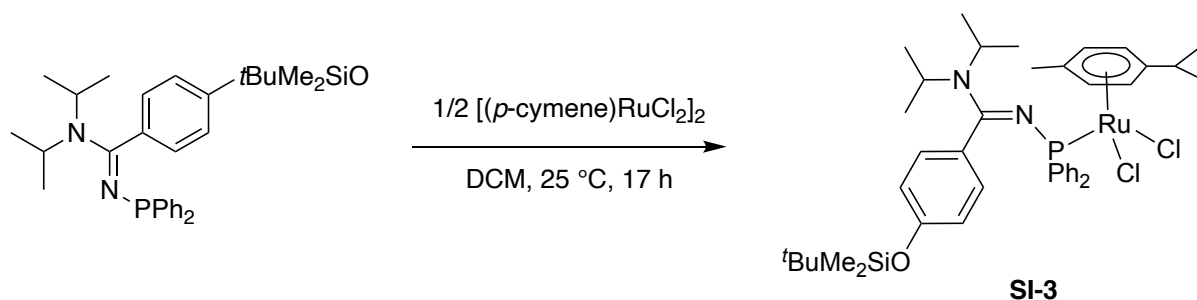


Into a dry Schlenk tube, the protected phenol **SI-1** (0.5 g, 2.14 mmol) was added, and three vacuum-argon cycles were performed. 8 ml of distilled THF were added into the Schlenk, after degassing with argon, to dissolve the protected compound. The Schlenk tube was refrigerated in an ACN/N<sub>2</sub> bath at – 40 °C. LDA (1.4 ml, 0.275 g, 2.785 mmol) was added dropwise under argon. The solution turned yellow and was stirred for 1 hour at – 40 °C.

After 1 h, chlorodiphenylphosphine Ph<sub>2</sub>PCl (0.385 ml, 0.472 g, 2.14 mmol) was added to the Schlenk under argon and the solution was stirred at – 40 °C for another hour. Then, when the solution returned to ambient temperature, the solvent was evaporated under vacuum. An orange oil was obtained. 24 ml of dry pentane were added leading to a white insoluble suspension of LiCl that was observed. The solution was filtered under argon by using a double filter cannula (filter paper and frit). The precipitate was washed again by 20 ml of pentane and filtered. Finally, the filtrate was evaporated. A yellow, air-and-water sensitive oil was obtained (1.0152 g, 92%).

The obtained product is very sensitive to oxidation, and thus it is directly dissolved in dried and degassed DCM and directly engaged to further obtain the linear complex.

## 3) Synthesis of the linear complex **SI-3**



The dimer complex [(*p*-cymene)RuCl<sub>2</sub>]<sub>2</sub> (0.598 g, 0.9785 mmol, 0.5 eq) was weighed in a dried Schlenk tube; three vacuum-argon processes were performed. DCM (10 ml) was added, after degassing, under argon.

10 ml of DCM were also added under argon to the just synthesized phosphino-ligand **SI-2**, present in a separate Schlenk tube. Then, this solution was cannulated under argon to the solution of the dimer. The reaction was stirred overnight at 30 °C.

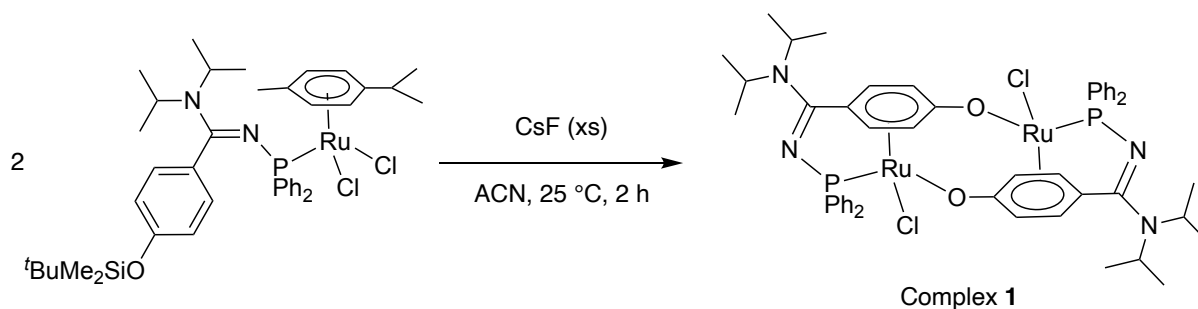
After that, DCM was evaporated under vacuum. Diethyl ether (15 ml) was added, and the solution was stirred for 15 min. The red solution troubled, and an orange precipitate formed. Using a cannula, the solution was filtered, and the obtained precipitate was washed twice with

diethyl ether (10 ml each) and dried under vacuum. The linear product was isolated in the form of an orange powder (1.16 g, 824.94 g/mol, 72%).

**$^1\text{H}$  NMR** (400 MHz,  $\text{CD}_2\text{Cl}_2$ )  $\delta$  7.70 – 7.59 (m, 4H), 7.19 – 7.06 (m, 6H), 6.72 (d,  $J$  = 8.4 Hz, 2H), 6.28 (d,  $J$  = 8.2 Hz, 2H), 5.24 – 5.22 (m, 4H), 3.46 – 3.40 (m, 1H), 2.72 (hept,  $J$  = 6.9 Hz, 1H), 1.84 (s, 6H), 1.65 (s, 3H), 1.07 (d,  $J$  = 6.9 Hz, 6H), 1.01 (d,  $J$  = 6.9 Hz, 6H), 0.96 (s, 9H), 0.19 (s, 6H).

**$^{31}\text{P}$  NMR** (162 MHz,  $\text{CD}_2\text{Cl}_2$ )  $\delta$  44.71 (s, broad).

#### 4) Synthesis of the complex **1**



In the glovebox, CsF (1.28 g, 8.46 mmol, 6 eq) was weighed using a Teflon spatula in a Schlenk tube. Then, the produced linear complex (1.16 g, 1.41 mmol, 1 equiv.) was added to the Schlenk tube under argon. After three vacuum-argon cycles, distilled MeCN (40 ml) was added to the Schlenk while continuously stirring at 25 °C for two hours. The solvent was evaporated under reduced pressure. On the obtained orange residue, 10 ml of DCM were added and filtered by a double-filtered cannula (filter paper and P3 frit glassware). This operation was repeated twice to rinse the Schlenk.

The orange filtrate obtained was then concentrated under vacuum to 2 ml. To make the product precipitate, 10 ml of  $\text{Et}_2\text{O}$  was added and let to stir for 5 min. A strong orange precipitate was observed. After decantation, this precipitate was filtered-off by a cannula. After drying the filter, we obtained 500 mg (65%) of **1** in the form of orange powder.

**$^1\text{H}$  NMR** (400 MHz,  $\text{CDCl}_3$ )  $\delta$  8.12 – 8.01 (m, 2H), 7.48 – 7.37 (m, 4H), 7.31 – 7.22 (m, 4H), 6.91 (dd,  $J$  = 5.3 Hz, 1H), 5.64 (dd,  $J$  = 5.3 Hz, 1H), 5.13 (dd,  $J$  = 5.3 Hz, 1H), 4.86 (dd,  $J$  = 5.3, 1.3 Hz, 1H), 4.24 (hept,  $J$  = 6.5 Hz, 1H), 3.80 (hept,  $J$  = 6.5 Hz, 1H), 1.65 (d,  $J$  = 11 Hz, 3H), 1.64 (d,  $J$  = 6.5 Hz, 3H), 1.22 (d,  $J$  = 2.7 Hz, 3H), 1.16 (d,  $J$  = 6.5 Hz, 3H).

**$^{31}\text{P}$  NMR** (162 MHz,  $\text{CDCl}_3$ )  $\delta$  75.95.

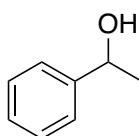
## 6.3. Base-free hydrogenation with H<sub>2</sub> in *iso*-propanol

### 6.3.1. General procedure

Within the Glovebox, a GC vial was loaded with the catalyst (1 mol%,  $4,29 \cdot 10^{-6}$  mol, 4,6 mg). The catalyst was dissolved in dried *i*-PrOH (0,5 mL). Then, substrate ( $4,29 \cdot 10^{-4}$  mol) was added. Finally, the GC vial was put into the high-pressure reactor which was charged with 10 bar of H<sub>2</sub>. The reaction was stirred (600 rpm) at 90 °C for 24 h.

### 6.3.2. Substrate analysis

#### Synthesis of 1-phenylethanol 3

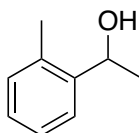


**NMR Conversion:** 99%

**<sup>1</sup>H NMR** (400 MHz, CDCl<sub>3</sub>) δ 7.46 – 7.32 (m, 4H), 7.28 (m, 1H), 4.88 (q, *J* = 6.5, 1.5 Hz, 1H), 1.49 (d, *J* = 6.4 Hz, 3H).

**<sup>13</sup>C NMR** (101 MHz, CDCl<sub>3</sub>) δ 145.8, 128.5, 127.5, 125.4, 70.40, 25.2.

#### Synthesis of 1-(*o*-tolyl)-ethanol 5



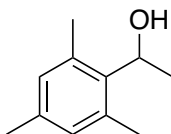
**NMR Conversion:** 91%

**Dried NMR conversion:** 91%

**<sup>1</sup>H NMR** (400 MHz, CDCl<sub>3</sub>) δ 7.61 – 7.46 (m, 1H), 7.34 – 7.25 (m, 1H), 7.24 – 7.13 (m, 2H), 5.16 (q, *J* = 6.4 Hz, 1H), 2.39 (s, 3H), 1.51 (d, *J* = 6.4 Hz, 3H).

**<sup>13</sup>C NMR** (101 MHz, CDCl<sub>3</sub>) δ 143.9, 134.2, 130.4, 127.2, 126.4, 124.5, 66.8, 23.9, 18.9.

#### Synthesis of 1-mesitylethanol 6



**NMR Conversion:** 15%

**Dried NMR conversion:** 16%

For 65h:

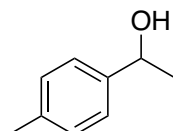
**NMR Conversion:** 78%

**Dried NMR conversion:** 74%

**$^1\text{H}$  NMR** (400 MHz,  $\text{CDCl}_3$ )  $\delta$  6.84 (s, 2H), 5.36 (q,  $J$  = 6.8 Hz, 1H), 2.43 (s, 6H), 2.27 (s, 3H), 1.53 (d,  $J$  = 6.8 Hz, 3H).

**$^{13}\text{C}$  NMR** (101 MHz,  $\text{CDCl}_3$ )  $\delta$  137.7, 136.4, 135.7, 130.2, 67.5, 21.6, 20.7, 20.5.

#### Synthesis of 1-(*p*-tolyl)ethanol 4

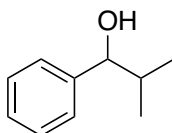


**NMR Conversion:** 99%

**Dried NMR conversion:** 93%

**$^1\text{H}$  NMR** (400 MHz,  $\text{CDCl}_3$ )  $\delta$  7.32 – 7.22 (m, 2H), 7.20 – 7.12 (m, 2H), 4.87 (q,  $J$  = 6.5 Hz, 1H), 2.35 (s, 3H), 1.49 (d,  $J$  = 6.5 Hz, 3H).

#### Synthesis of 2-methyl-1-phenylpropanol 8



**NMR Conversion:** 30%

**Dried NMR conversion:** 29%

For 65h:

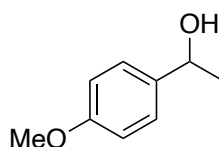
**NMR Conversion:** 94%

**Dried NMR conversion:** 93%

**$^1\text{H}$  NMR** (400 MHz,  $\text{CDCl}_3$ )  $\delta$  7.41 – 7.17 (m, 5H), 4.35 (d,  $J$  = 6.9 Hz, 1H), 2.04 – 1.88 (o,  $J$  = 6.7 Hz, 1H), 1.01 (d,  $J$  = 6.6 Hz, 3H), 0.80 (d,  $J$  = 6.8 Hz, 3H).

**$^{13}\text{C}$  NMR** (101 MHz,  $\text{CDCl}_3$ )  $\delta$  143.7, 128.2, 127.4, 126.6, 80.1, 35.3, 19.0, 18.3.

#### Synthesis of 1-(4-methoxyphenyl)-ethanol 12



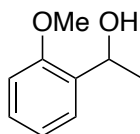
**NMR Conversion:** 88%

**Dried NMR conversion:** 85%

**$^1\text{H}$  NMR** (400 MHz,  $\text{CDCl}_3$ )  $\delta$  7.28 (d,  $J$  = 8.7 Hz, 1H), 6.87 (d,  $J$  = 8.7 Hz, 1H), 4.83 (q,  $J$  = 6.4 Hz, 1H), 3.79 (s, 3H), 1.46 (d,  $J$  = 6.5 Hz, 3H).

**$^{13}\text{C}$  NMR** (101 MHz,  $\text{CDCl}_3$ )  $\delta$  159.0, 138.1, 126.7, 113.9, 69.9, 55.3, 25.0.

### Synthesis of 1-(2-methoxyphenyl)ethanol 11



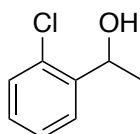
**NMR Conversion:** 99%

**Dried NMR conversion:** 99%

**<sup>1</sup>H NMR** (400 MHz, CDCl<sub>3</sub>) δ 7.35 (dd, *J* = 7.6, 1.8 Hz, 1H), 7.25 (td, *J* = 7.8, 1.8 Hz, 1H), 6.97 (t, *J* = 7.5 Hz, 1H), 6.88 (d, *J* = 8.2 Hz, 1H), 5.10 (q, *J* = 6.5 Hz, 1H), 3.86 (s, 3H), 1.51 (d, *J* = 6.5 Hz, 3H).

**<sup>13</sup>C NMR** (101 MHz, CDCl<sub>3</sub>) δ 156.6, 133.5, 128.3, 126.1, 120.8, 110.5, 66.5, 55.3, 22.9.

### Synthesis of 1-(2-chlorophenyl)ethanol 15



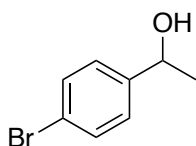
**NMR Conversion:** 36%

**Dried NMR conversion:** 39%

**<sup>1</sup>H NMR** (400 MHz, CDCl<sub>3</sub>) δ 7.57 (dd, *J* = 7.7, 1.7 Hz, 1H), 7.40 – 7.27 (m, 2H), 7.18 (td, *J* = 7.6, 1.7 Hz, 1H), 5.26 (q, *J* = 6.4 Hz, 1H), 1.46 (dd, *J* = 6.4, 1.9 Hz, 3H).

**<sup>13</sup>C NMR** (101 MHz, CDCl<sub>3</sub>) δ 143.1, 131.6, 129.4, 128.4, 127.2, 126.4, 66.9, 23.5.

### Synthesis of 1-(4-bromophenyl)-ethanol 14



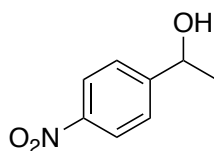
**NMR Conversion:** 5%

**Dried NMR conversion:** 5%

**<sup>1</sup>H NMR** (400 MHz, CDCl<sub>3</sub>) δ 7.46 (dd, *J* = 8.5, 2.0 Hz, 2H), 7.23 (dd, *J* = 8.7, 2.4 Hz, 2H), 4.85 (q, *J* = 6.4 Hz, 1H), 1.46 (d, *J* = 6.7, 2.4 Hz, 3H).

**<sup>13</sup>C NMR** (101 MHz, CDCl<sub>3</sub>) δ 144.8, 131.6, 127.2, 121.2, 69.8, 25.2.

### Synthesis of 1-(4-nitrophenyl)-ethanol 17



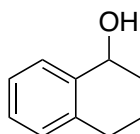
**NMR Conversion:** 77%

**Dried NMR conversion:** 77%

**<sup>1</sup>H NMR** (400 MHz, CDCl<sub>3</sub>) δ 8.14 – 8.03 (m, 2H), 7.57 – 7.40 (m, 2H), 4.95 (q, *J* = 6.5 Hz, 1H), 1.45 (d, *J* = 6.5 Hz, 3H).

**<sup>13</sup>C NMR** (101 MHz, CDCl<sub>3</sub>) δ 153.4, 147.0, 126.2, 123.7, 69.3, 25.3.

### Synthesis of 1,2,3,4-tetrahydronaphthalen-1-ol 9



**NMR Conversion:** 28%

**Dried NMR conversion:** 28%

For 65h:

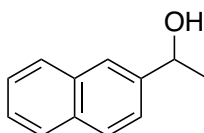
**NMR Conversion:** 95%

**Dried NMR conversion:** 95%

**<sup>1</sup>H NMR** (400 MHz, CDCl<sub>3</sub>) δ 7.55 – 7.37 (m, 1H), 7.28 – 7.16 (m, 2H), 7.14 – 7.04 (m, 1H), 4.77 (t, *J* = 4.6 Hz, 1H), 2.96 – 2.56 (m, 2H), 2.07 – 1.85 (m, 3H), 1.85 – 1.66 (m, 1H).

**<sup>13</sup>C NMR** (101 MHz, CDCl<sub>3</sub>) δ 138.8, 137.1, 129.0, 128.7, 127.6, 126.2, 68.2, 32.3, 29.3, 18.8.

### Synthesis of 1-(naphthalen-2-yl)ethanol 7



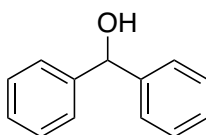
**NMR Conversion:** 94%

**Dried NMR conversion:** 94%

**<sup>1</sup>H NMR** (400 MHz, CDCl<sub>3</sub>) δ 7.90 – 7.76 (m, 4H), 7.55 – 7.42 (m, 3H), 5.06 (q, *J* = 6.5 Hz, 1H), 1.58 (d, *J* = 6.5 Hz, 3H).

**<sup>13</sup>C NMR** (101 MHz, CDCl<sub>3</sub>) δ 143.3, 133.5, 133.0, 128.4, 128.0, 127.8, 126.3, 125.9, 124.0, 123.9, 70.6, 25.2.

### Synthesis of Benzophenol 10



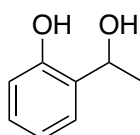
**NMR Conversion:** 57%

**Dried NMR conversion:** 46%

**<sup>1</sup>H NMR** (400 MHz, CDCl<sub>3</sub>) δ 7.47 – 7.23 (m, 10H), 5.81 (s, 1H).

**<sup>13</sup>C NMR** (101 MHz, CDCl<sub>3</sub>) δ 143.9, 128.5, 127.6, 126.6, 76.3.

### Synthesis of 2-(1-hydroxyethyl)phenol 18



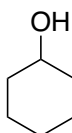
**NMR Conversion:** 49%

**Dried NMR conversion:** 49%

**<sup>1</sup>H NMR** (400 MHz, CDCl<sub>3</sub>) δ 7.17 (td, *J* = 7.7, 1.8 Hz, 1H), 6.99 (dd, *J* = 7.6, 1.7 Hz, 1H), 6.91 – 6.71 (m, 2H), 5.07 (q, *J* = 6.6 Hz, 1H), 1.59 (d, *J* = 6.6, 0.9 Hz, 3H).

**<sup>13</sup>C NMR** (101 MHz, CDCl<sub>3</sub>) δ 155.5, 129.0, 126.5, 119.9, 117.2, 71.7, 23.5.

### Synthesis of Cyclohexanol 22

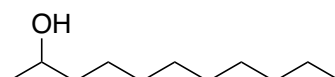


**NMR Conversion:** 99%

**<sup>1</sup>H NMR** (400 MHz, CDCl<sub>3</sub>) δ 3.65 – 3.51 (m, 1H), 1.94 – 1.83 (m, 2H), 1.79 – 1.65 (m, 2H), 1.58 – 1.47 (m, 1H), 1.33 – 1.19 (m, 4H), 1.20 – 1.10 (m, 1H).

**<sup>13</sup>C NMR** (101 MHz, CDCl<sub>3</sub>) δ 70.3, 35.6, 25.5, 24.1.

### Synthesis of undecane-2-ol 23



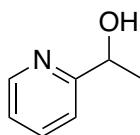
**NMR Conversion:** 99%

**Dried NMR conversion:** 99%

**<sup>1</sup>H NMR** (400 MHz, CDCl<sub>3</sub>) δ 3.78 (h, *J* = 6.2 Hz, 1H), 1.52 – 1.35 (m, 2H), 1.35 – 1.21 (m, 14H), 1.18 (d, *J* = 6.2 Hz, 3H), 0.88 (t, *J* = 6.7 Hz, 3H).

**<sup>13</sup>C NMR** (101 MHz, CDCl<sub>3</sub>) δ 68.1, 39.4, 31.9, 29.7, 29.6, 29.6, 29.3, 25.8, 23.4, 22.7, 14.1.

### Synthesis of 1-(pyridin-2-yl)ethanol 21



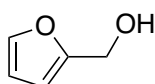
**NMR Conversion:** 67%

**Dried NMR conversion:** 69%

**<sup>1</sup>H NMR** (400 MHz, CDCl<sub>3</sub>) δ 8.50 (d, *J* = 4.9 Hz, 1H), 7.66 (td, *J* = 7.7, 1.8 Hz, 1H), 7.28 (d, *J* = 7.9 Hz, 1H), 7.17 (dd, *J* = 7.5, 4.8, 1.1 Hz, 1H), 4.87 (q, *J* = 6.5 Hz, 1H), 1.48 (d, *J* = 6.5 Hz, 3H).

**<sup>13</sup>C NMR** (101 MHz, CDCl<sub>3</sub>) δ 163.2, 148.1, 136.8, 122.2, 119.8, 69.0, 24.2.

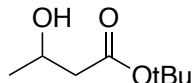
### Synthesis of furan-2-yl-methanol 26



**NMR Conversion:** 99%

**<sup>1</sup>H NMR** (400 MHz, CDCl<sub>3</sub>) δ 7.36 (dd, *J* = 1.8, 0.9 Hz, 1H), 6.30 (dd, *J* = 3.2, 1.8 Hz, 1H), 6.27 – 6.22 (m, 1H), 4.56 (s, 2H).

### Synthesis of *tert*-butyl 3hydroxybutanoate 24

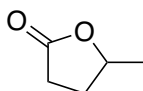


**NMR Conversion:** 99%

**<sup>1</sup>H NMR** (400 MHz, CDCl<sub>3</sub>) δ 4.27 – 4.07 (m, 1H), 2.40 – 2.31 (m, 2H), 1.46 (s, 9H), 1.19 (d, *J* = 6.6 Hz, 3H).

**<sup>13</sup>C NMR** (101 MHz, CDCl<sub>3</sub>) δ 172.5, 81.3, 64.4, 43.8, 28.1, 22.3.

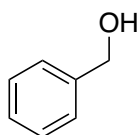
### Synthesis of γ-valerolactone 27



**NMR Conversion:** 99%

**<sup>1</sup>H NMR** (400 MHz, CDCl<sub>3</sub>) δ 4.71 – 4.56 (m, 1H), 2.67 – 2.49 (m, 2H), 2.48 – 2.27 (m, 1H), 1.86 – 1.66 (m, 1H), 1.41 (d, *J* = 6.2 Hz, 3H).

### Synthesis of benzyl alcohol 25



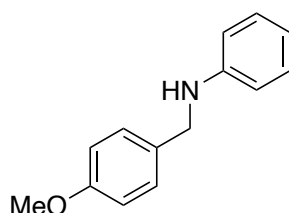
**NMR Conversion:** 99%

**Dried NMR conversion:** 99%

**<sup>1</sup>H NMR** (400 MHz, CDCl<sub>3</sub>) δ 7.42 – 7.27 (m, 5H), 4.62 (s, 2H).

**<sup>13</sup>C NMR** (101 MHz, CDCl<sub>3</sub>) δ 140.9, 128.5, 127.6, 127.0.

### Synthesis of N-(methoxybenzyl)-aniline 28

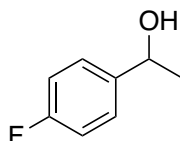


**NMR Conversion:** 99%

**<sup>1</sup>H NMR** (400 MHz, CDCl<sub>3</sub>) δ 7.41 – 7.33 (m, 2H), 7.30 – 7.18 (m, 2H), 7.02 – 6.93 (m, 2H), 6.85 – 6.76 (m, 1H), 6.74 – 6.66 (m, 2H), 4.32 (s, 2H), 4.01 (s, 1H), 3.87 (d, *J* = 1.4 Hz, 3H).

**<sup>13</sup>C NMR** (101 MHz, CDCl<sub>3</sub>) δ 158.9, 148.3, 131.5, 129.3, 128.9, 117.6, 114.1, 112.9, 55.4, 47.9.

### Synthesis of 1-(4-fluorophenyl)ethanol 13

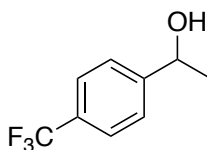


**NMR Conversion:** 99%

**Dried NMR conversion:** 96%

**<sup>1</sup>H NMR** (400 MHz, CDCl<sub>3</sub>) δ 7.39 – 7.30 (m, 2H), 7.07 – 6.98 (m, 2H), 4.89 (q, *J* = 6.4 Hz, 1H), 1.48 (d, *J* = 6.5 Hz, 3H).

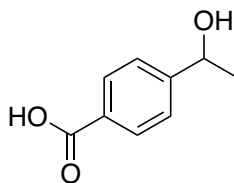
### Synthesis of 1-(4-trifluoromethyl-phenyl)-ethanol 16



**NMR Conversion:** 99%

**<sup>1</sup>H NMR** (400 MHz, CDCl<sub>3</sub>) δ 7.61 (d, *J* = 8.1 Hz, 2H), 7.49 (d, *J* = 8.1 Hz, 2H), 4.97 (q, *J* = 6.5 Hz, 1H), 1.51 (d, *J* = 6.5 Hz, 3H).

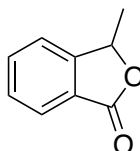
### Synthesis of 4-(1-hydroxyethyl)benzoic acid 19



**NMR Conversion:** 99%

**<sup>1</sup>H NMR** (400 MHz, CDCl<sub>3</sub>) δ 8.08 (d, *J* = 8.3 Hz, 2H), 7.47 (d, *J* = 8.3 Hz, 2H), 4.98 (q, *J* = 6.5 Hz, 1H), 1.52 (d, *J* = 6.5 Hz, 3H).

### Synthesis of 3-methylisobenzofuran-1-one 20



**NMR Conversion dried:** 61%

**<sup>1</sup>H NMR** (400 MHz, CDCl<sub>3</sub>) δ 7.95 – 7.84 (m, 1H), 7.72 – 7.63 (m, 1H), 7.57 – 7.48 (m, 1H), 7.47 – 7.40 (m, 1H), 5.56 (q, *J* = 6.7 Hz, 1H), 1.63 (d, *J* = 6.7 Hz, 3H).

**<sup>13</sup>C NMR** (101 MHz, CDCl<sub>3</sub>) δ 170.5, 151.2, 134.1, 129.1, 125.8, 125.7, 121.6, 77.7, 20.4.

## 6.4. Base-free transfer hydrogenation with *i*PrOH

### 6.4.1. General procedure

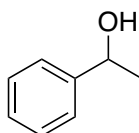
In a dried Schlenk tube, the catalyst **1** was loaded (1 mol%,  $8,57 \cdot 10^{-6}$  mol, 9,3 mg) and an Argon/Vacuum process was applied. The catalyst was dissolved in the solvent (0,5 mL) and *i*-PrOH (0,5 mL). Finally, the distilled acetophenone ( $8,57 \cdot 10^{-4}$  mol, 100  $\mu$ L) was added. The reaction was heated at 90 °C for 17 h.

## 6.5. Base-free transfer hydrogenation with FA

### 6.5.1. General procedure

In a dried Ace® Pressure Tube, the catalyst **1** was loaded (1,5 mol%) and a vacuum/Argon process applied. Degassed *iso*-propanol (0,5 mL) and the substrate ( $8,54 \cdot 10^{-4}$  mol) were added under a flow of argon. Then, the formic acid (5 equivalents) was added. Finally, the tube was closed and placed in an oil bath at 90 °C for 24 h.

### 6.5.2. Substrate analysis



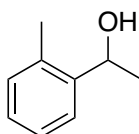
#### Synthesis of 1-phenylethanol **3**

**NMR Conversion:** 90-97%

**<sup>1</sup>H NMR** (400 MHz, CDCl<sub>3</sub>) δ 7.46 – 7.32 (m, 4H), 7.28 (dt, *J* = 7.1, 3.0 Hz, 1H), 4.88 (q, *J* = 6.5, 1.5 Hz, 1H), 1.49 (d, *J* = 6.4 Hz, 3H).

**<sup>13</sup>C NMR** (101 MHz, CDCl<sub>3</sub>) δ 145.8, 128.5, 127.5, 125.4, 70.4, 25.2.

#### Synthesis of 1-(*o*-tolyl)-ethanol **5**



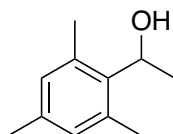
**NMR Conversion:** 65%

**Yield:** 61%

**<sup>1</sup>H NMR** (400 MHz, CDCl<sub>3</sub>) δ 7.61 – 7.46 (m, 1H), 7.34 – 7.25 (m, 1H), 7.24 – 7.13 (m, 2H), 5.16 (q, *J* = 6.4 Hz, 1H), 2.39 (s, 3H), 1.51 (d, *J* = 6.4 Hz, 3H).

**<sup>13</sup>C NMR** (101 MHz, CDCl<sub>3</sub>) δ 143.9, 134.3, 130.4, 127.2, 126.4, 124.5, 66.8, 23.9, 18.9.

#### Synthesis of 1-mesitylethanol **6**



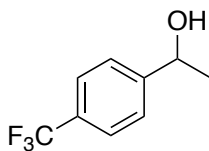
**NMR Conversion:** 15%

**Yield:** 14%

**<sup>1</sup>H NMR** (400 MHz, CDCl<sub>3</sub>) δ 6.84 (s, 2H), 5.36 (q, *J* = 6.8 Hz, 1H), 2.43 (s, 6H), 2.27 (s, 3H), 1.53 (d, *J* = 6.8 Hz, 3H).

**<sup>13</sup>C NMR** (101 MHz, CDCl<sub>3</sub>) δ 137.7, 136.4, 135.7, 130.2, 67.5, 21.6, 20.7, 20.5.

### Synthesis of 1-(4-trifluoromethyl-phenyl)-ethanol 16

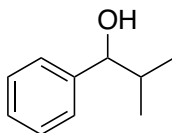


**NMR Conversion:** 97%

**Yield:** 90%

**<sup>1</sup>H NMR** (400 MHz, CDCl<sub>3</sub>) δ 7.61 (d, *J* = 8.1 Hz, 2H), 7.49 (d, *J* = 8.1 Hz, 2H), 4.97 (q, *J* = 6.5 Hz, 1H), 1.51 (d, *J* = 6.5 Hz, 3H).

### Synthesis of 2-methyl-1-phenylpropanol 8



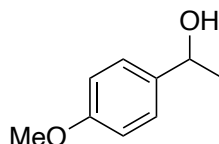
**NMR Conversion:** 49%

**Yield:** 44%

**<sup>1</sup>H NMR** (400 MHz, CDCl<sub>3</sub>) δ 7.41 – 7.17 (m, 5H), 4.35 (d, *J* = 6.9 Hz, 1H), 2.04 – 1.88 (o, *J* = 6.7 Hz, 1H), 1.01 (d, *J* = 6.6 Hz, 3H), 0.80 (d, *J* = 6.8 Hz, 3H).

**<sup>13</sup>C NMR** (101 MHz, CDCl<sub>3</sub>) δ 143.7, 128.2, 127.4, 126.6, 80.1, 35.3, 19.0, 18.3.

### Synthesis of 1-(4-methoxyphenyl)-ethanol 12



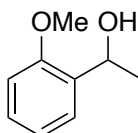
**NMR Conversion:** 52%

**Yield:** 45%

**<sup>1</sup>H NMR** (400 MHz, CDCl<sub>3</sub>) δ 7.28 (d, *J* = 8.7 Hz, 1H), 6.87 (d, *J* = 8.7 Hz, 1H), 4.83 (q, *J* = 6.4 Hz, 1H), 3.79 (s, 3H), 1.46 (d, *J* = 6.5 Hz, 3H).

**<sup>13</sup>C NMR** (101 MHz, CDCl<sub>3</sub>) δ 159.0, 138.1, 126.7, 113.9, 69.9, 55.3, 25.0.

### Synthesis of 1-(2-methoxyphenyl)ethanol 11



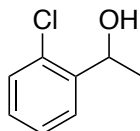
**NMR Conversion:** 75%

**Yield:** 52%

**<sup>1</sup>H NMR** (400 MHz, CDCl<sub>3</sub>) δ 7.35 (dd, *J* = 7.6, 1.8 Hz, 1H), 7.25 (td, *J* = 7.8, 1.8 Hz, 1H), 6.97 (t, *J* = 7.5 Hz, 1H), 6.88 (d, *J* = 8.2 Hz, 1H), 5.10 (q, *J* = 6.5 Hz, 1H), 3.86 (s, 3H), 1.51 (d, *J* = 6.5 Hz, 3H).

**<sup>13</sup>C NMR** (101 MHz, CDCl<sub>3</sub>) δ 156.6, 133.5, 128.3, 126.1, 120.8, 110.5, 66.5, 55.3, 22.9.

### Synthesis of 1-(2-chlorophenyl)ethanol 15



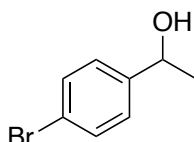
**NMR Conversion:** 98%

**Yield:** 97%

**<sup>1</sup>H NMR** (400 MHz, CDCl<sub>3</sub>) δ 7.57 (dd, *J* = 7.7, 1.7 Hz, 1H), 7.40 – 7.27 (m, 2H), 7.18 (td, *J* = 7.6, 1.7 Hz, 1H), 5.26 (q, *J* = 6.4 Hz, 1H), 1.46 (dd, *J* = 6.4, 1.9 Hz, 3H).

**<sup>13</sup>C NMR** (101 MHz, CDCl<sub>3</sub>) δ 143.1, 131.6, 129.4, 128.4, 127.2, 126.4, 66.9, 23.5.

### Synthesis of 1-(4-bromophenyl)-ethanol 14



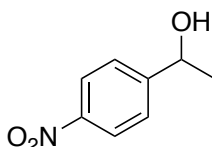
**NMR Conversion:** 95%

**Yield:** 89%

**<sup>1</sup>H NMR** (400 MHz, CDCl<sub>3</sub>) δ 7.46 (dd, *J* = 8.5, 2.0 Hz, 2H), 7.23 (dd, *J* = 8.7, 2.4 Hz, 2H), 4.85 (q, *J* = 6.4 Hz, 1H), 1.46 (d, *J* = 6.7, 2.4 Hz, 3H).

**<sup>13</sup>C NMR** (101 MHz, CDCl<sub>3</sub>) δ 144.8, 131.6, 127.2, 121.2, 69.8, 25.2.

### Synthesis of 1-(4-nitrophenyl)-ethanol 17



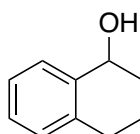
**NMR Conversion:** 99%

**Yield:** 98%

**<sup>1</sup>H NMR** (400 MHz, CDCl<sub>3</sub>) δ 8.14 – 8.03 (m, 2H), 7.57 – 7.40 (m, 2H), 4.95 (q, *J* = 6.5 Hz, 1H), 1.45 (d, *J* = 6.5 Hz, 3H).

**<sup>13</sup>C NMR** (101 MHz, CDCl<sub>3</sub>) δ 153.4, 147.0, 126.2, 123.7, 69.3, 25.3.

### Synthesis of 1,2,3,4-tetrahydronaphthalen-1-ol 9



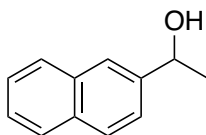
**NMR Conversion:** 34%

**Yield:** 33%

**<sup>1</sup>H NMR** (400 MHz, CDCl<sub>3</sub>) δ 7.55 – 7.37 (m, 1H), 7.28 – 7.16 (m, 2H), 7.14 – 7.04 (m, 1H), 4.77 (t, *J* = 4.6 Hz, 1H), 2.96 – 2.56 (m, 2H), 2.07 – 1.85 (m, 3H), 1.85 – 1.66 (m, 1H).

**<sup>13</sup>C NMR** (101 MHz, CDCl<sub>3</sub>) δ 138.8, 137.1, 129.0, 128.7, 127.6, 126.2, 68.2, 32.3, 29.3, 18.8.

### Synthesis of 1-(naphthalen-2-yl)ethanol 7



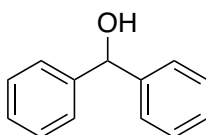
**NMR Conversion:** 75%

**Yield:** 63%

**<sup>1</sup>H NMR** (400 MHz, CDCl<sub>3</sub>) δ 7.90 – 7.76 (m, 4H), 7.55 – 7.42 (m, 3H), 5.06 (q, *J* = 6.5 Hz, 1H), 1.58 (d, *J* = 6.5 Hz, 3H).

**<sup>13</sup>C NMR** (101 MHz, CDCl<sub>3</sub>) δ 143.3, 133.5, 133.0, 128.4, 128.1, 127.8, 126.3, 125.9, 124.0, 123.9, 70.6, 25.2.

### Synthesis of Benzophenol 10



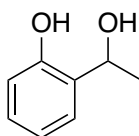
**NMR Conversion:** 67%

**Yield:** 62%

**<sup>1</sup>H NMR** (400 MHz, CDCl<sub>3</sub>) δ 7.47 – 7.23 (m, 10H), 5.81 (s, 1H).

**<sup>13</sup>C NMR** (101 MHz, CDCl<sub>3</sub>) δ 143.9, 128.5, 127.6, 126.6, 76.3.

### Synthesis of 2-(1-hydroxyethyl)phenol 18



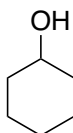
**NMR Conversion:** 76%

**Yield:** 69%

**<sup>1</sup>H NMR** (400 MHz, CDCl<sub>3</sub>) δ 7.17 (td, *J* = 7.7, 1.8 Hz, 1H), 6.99 (dd, *J* = 7.6, 1.7 Hz, 1H), 6.91 – 6.71 (m, 2H), 5.07 (q, *J* = 6.6 Hz, 1H), 1.59 (d, *J* = 6.6, 0.9 Hz, 3H).

**<sup>13</sup>C NMR** (101 MHz, CDCl<sub>3</sub>) δ 155.5, 129.0, 126.5, 119.9, 117.2, 71.7, 23.5.

### Synthesis of Cyclohexanol 22



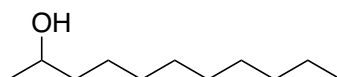
**NMR Conversion:** 99%

**Yield:** 91%

**<sup>1</sup>H NMR** (400 MHz, CDCl<sub>3</sub>) δ 3.65 – 3.51 (m, 1H), 1.94 – 1.83 (m, 2H), 1.79 – 1.65 (m, 2H), 1.58 – 1.47 (m, 1H), 1.33 – 1.19 (m, 4H), 1.20 – 1.10 (m, 1H).

**<sup>13</sup>C NMR** (101 MHz, CDCl<sub>3</sub>) δ 70.3, 35.5, 25.5, 24.1.

### Synthesis of undecane-2-ol 23



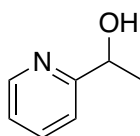
**NMR Conversion:** 99%

**Yield:** 92%

**<sup>1</sup>H NMR** (400 MHz, CDCl<sub>3</sub>) δ 3.78 (h, *J* = 6.2 Hz, 1H), 1.52 – 1.35 (m, 2H), 1.35 – 1.21 (m, 14H), 1.18 (d, *J* = 6.2 Hz, 3H), 0.88 (t, *J* = 6.7 Hz, 3H).

**<sup>13</sup>C NMR** (101 MHz, CDCl<sub>3</sub>) δ 68.1, 39.4, 31.9, 29.7, 29.6, 29.6, 29.3, 25.8, 23.4, 22.7, 14.1.

### Synthesis of 1-(pyridin-2-yl)ethanol 21



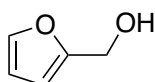
**NMR Conversion:** 86%

**Yield:** 63%

**<sup>1</sup>H NMR** (400 MHz, CDCl<sub>3</sub>) δ 8.50 (d, *J* = 4.9 Hz, 1H), 7.66 (td, *J* = 7.7, 1.8 Hz, 1H), 7.28 (d, *J* = 7.9 Hz, 1H), 7.17 (dd, *J* = 7.5, 4.8, 1.1 Hz, 1H), 4.87 (q, *J* = 6.5 Hz, 1H), 1.48 (d, *J* = 6.5 Hz, 3H).

**<sup>13</sup>C NMR** (101 MHz, CDCl<sub>3</sub>) δ 163.2, 148.1, 136.8, 122.2, 119.8, 69.0, 24.2.

### Synthesis of furan-2-ylmethanol 26

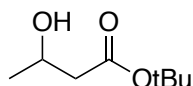


**NMR Conversion:** 99%

**Yield:** 99%

**<sup>1</sup>H NMR** (400 MHz, CDCl<sub>3</sub>) δ 7.36 (dd, *J* = 1.9, 0.9 Hz, 1H), 6.30 (dd, *J* = 3.2, 1.9 Hz, 1H), 6.27 – 6.22 (m, 1H), 4.56 (s, 2H).

### Synthesis of *tert*-butyl 3hydroxybutanoate 24



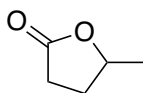
**NMR Conversion:** 99%

**Yield:** 85%

**<sup>1</sup>H NMR** (400 MHz, CDCl<sub>3</sub>) δ 4.27 – 4.07 (m, 1H), 2.40 – 2.31 (m, 2H), 1.46 (s, 9H), 1.19 (d, *J* = 6.6 Hz, 3H).

**<sup>13</sup>C NMR** (101 MHz, CDCl<sub>3</sub>) δ 172.5, 81.3, 64.4, 43.8, 28.1, 22.3.

### Synthesis of $\gamma$ -valerolactone 27

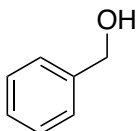


**NMR Conversion:** 99%

**Yield:** 85%

**$^1\text{H}$  NMR** (400 MHz,  $\text{CDCl}_3$ )  $\delta$  4.71 – 4.56 (m, 1H), 2.67 – 2.49 (m, 2H), 2.48 – 2.27 (m, 1H), 1.86 – 1.66 (m, 1H), 1.41 (d,  $J$  = 6.2 Hz, 3H).

### Synthesis of benzyl alcohol 25



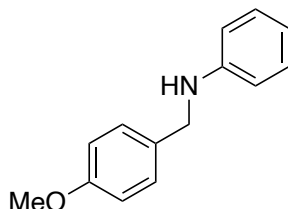
**NMR Conversion:** 99%

**Yield:** 94%

**$^1\text{H}$  NMR** (400 MHz,  $\text{CDCl}_3$ )  $\delta$  7.42 – 7.27 (m, 5H), 4.62 (s, 2H).

**$^{13}\text{C}$  NMR** (101 MHz,  $\text{CDCl}_3$ )  $\delta$  140.9, 128.5, 127.6, 127.0.

### Synthesis of N-(methoxybenzyl)-aniline 28

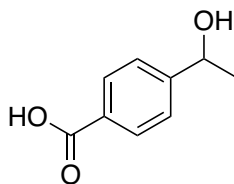


**NMR Conversion:** 50%

**$^1\text{H}$  NMR** (400 MHz,  $\text{CDCl}_3$ )  $\delta$  7.41 – 7.33 (m, 2H), 7.30 – 7.18 (m, 2H), 7.02 – 6.93 (m, 2H), 6.85 – 6.76 (m, 1H), 6.74 – 6.66 (m, 2H), 4.32 (s, 2H), 4.01 (s, 1H), 3.87 (d,  $J$  = 1.4 Hz, 3H).

**$^{13}\text{C}$  NMR** (101 MHz,  $\text{CDCl}_3$ )  $\delta$  158.9, 148.3, 131.5, 129.3, 128.9, 117.6, 114.1, 112.9, 55.3, 47.8.

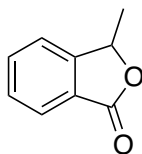
### Synthesis of 4-(1-hydroxyethyl)benzoic acid 19



**NMR Conversion:** 99%

**$^1\text{H}$  NMR** (400 MHz,  $\text{CDCl}_3$ )  $\delta$  8.08 (d,  $J$  = 8.3 Hz, 2H), 7.47 (d,  $J$  = 8.3 Hz, 2H), 4.98 (q,  $J$  = 6.5 Hz, 1H), 1.52 (d,  $J$  = 6.5 Hz, 3H).

### Synthesis of 3-methylisobenzofuran-1-one **20**



**NMR Conversion dried:** 21%

**<sup>1</sup>H NMR** (400 MHz, CDCl<sub>3</sub>) δ 7.95 – 7.84 (m, 1H), 7.72 – 7.63 (m, 1H), 7.57 – 7.48 (m, 1H), 7.47 – 7.40 (m, 1H), 5.56 (q, *J* = 6.7 Hz, 1H), 1.63 (d, *J* = 6.7 Hz, 3H).

**<sup>13</sup>C NMR** (101 MHz, CDCl<sub>3</sub>) δ 170.5, 151.2, 134.1, 129.1, 125.8, 125.7, 121.6, 77.7, 20.4.



# Chapter III: The Guerbet reaction

## Part 1: State of the art



## 1. Introduction

As presented in the general introduction, this PhD targets the production of energy sources via homogeneous catalysis in a context of over-exploitation of fossil fuel that cause environmental damages. Following our researches to highlight the activity of  $\eta^5$ -oxocyclohexadienyl ruthenium complexes in hydrogenation reaction, we have investigated the potential of these catalysts for the production of alcohols in the domain of biofuels.

### 1.1. Alcohol as an energy source

#### 1.1.1. Ethanol

Alcohols and bio-alcohols are already used as fuels for combustion engine in transport. Indeed, alcohol, especially ethanol, is used as a fuel. Superethanol E85 containing up to 85% of ethanol can be used in flexfuel vehicles.<sup>[1]</sup> Bioethanol can also be blended in a small amount with conventional gasoline to be used in conventional vehicles.<sup>[2]</sup> For instance, SP95-E10 can contain up to 10% of ethanol.

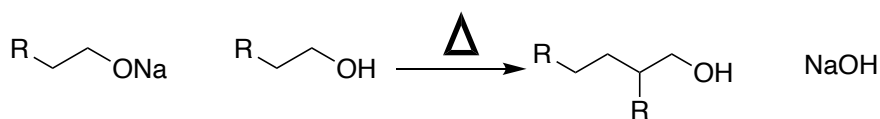
Ethanol can be produced by transforming sugars from crops into alcohol thanks to an alcoholic fermentation process.<sup>[3]</sup> By this way, bio-ethanol is produced in a sustainable manner ranked in 4 generations.<sup>[4]</sup> As mentioned in the general introduction, the 1<sup>st</sup> generation of bioethanol was based on edible biomass such as corn, wheat, sugar cane etc. Due to a competition with food production, a second generation of biofuel was developed. This 2<sup>nd</sup> generation of biofuel based on non-edible feedstock relies on lignocellulosic biomass or by-product/waste from agriculture industry. More recently, the 3<sup>rd</sup> generation of biofuel was developed aiming at not using arable lands or potable water for its production. Therefore, algae and micro-organism were used to produce biofuel.

Despite its interest, we notice some limitations to the use of bio-ethanol as an energetic source. First, the energy density of ethanol (20 MJ/L) is lower compared to gasoline (32 MJ/L). This results in an overconsumption of the flexfuel vehicles hence reducing the impact on CO<sub>2</sub> emission reduction. The other issue is that ethanol is hydrophilic and it is known that water in combustion engines may cause some damages.

To overcome those issues, ethanol, as a widely produced chemical, can be used as a starting material to lead to other fuels.<sup>[5]</sup> Hence upgrading of ethanol into higher alcohols is considered. By synthesizing higher alcohols, we would increase the energy density and reduce the hydrophilicity of the produced alcohols. As bio-ethanol is easily produced it would be great to use it as a starting material for upgrading. In this context, the Guerbet reaction, published in the late 19<sup>th</sup> century, has received renewed attention in recent years.

#### 1.1.2. The Guerbet reaction

The Guerbet reaction was named after the French chemist who discovered the upgrading of primary alcohol into higher ones (Scheme III-1-1). Originally higher alcohols were obtained from primary or secondary alcohol and their alkoxide derivatives.<sup>[6-8]</sup> The reaction conditions were quite harsh with temperature around 200 °C and stoichiometric amount of the reagents were used.



Scheme III - 1 - 1: Original Guerbet Reaction.

Currently the goal of researches in this domain concerns the upgrading of bio-ethanol into bio-butanol under mild conditions using catalysis in a renewed Guerbet reaction. n-Butanol is an alcohol that is gaining in interest as fuel alternative.<sup>[9]</sup> Therefore, researchers are investigating various ways to synthesize it especially via sustainable routes.<sup>[10,11]</sup> n-Butanol dismisses the problem of hydrophilicity known with ethanol. It also has an energy density (29 MJ/L) close to gasoline (32 MJ/L) which is better compared to ethanol (20 MJ/L) (Figure III-1-1). Those characteristics make n-butanol of great interest and a promising alternative to fossil fuels. Butanol gives the opportunity to be mixed in a higher amount with gasoline or used alone with higher performances compared to ethanol. Having the possibility to synthesize n-butanol from ethanol in a sustainable way is a topic of great interest requiring efficient catalysts.

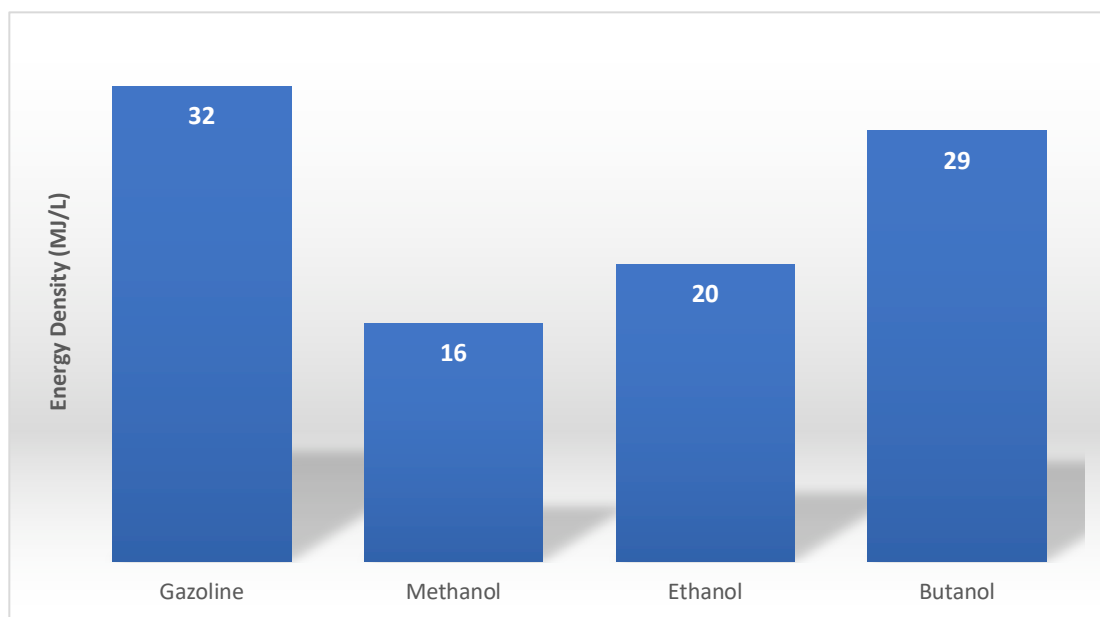
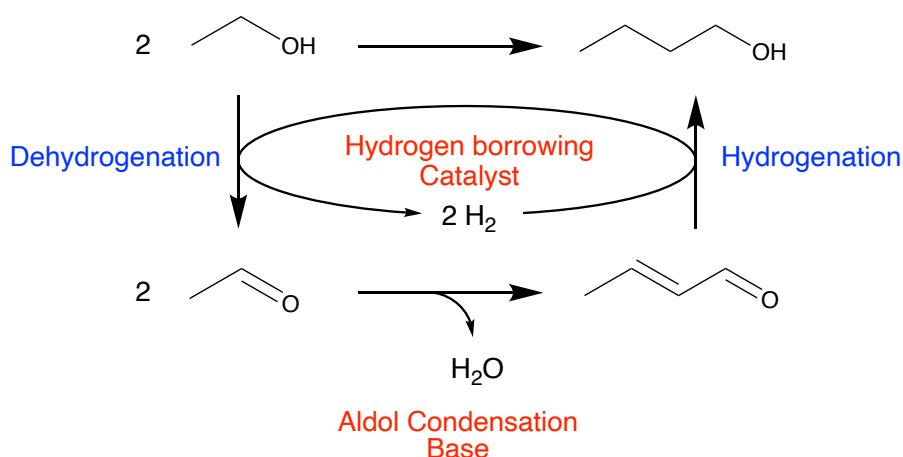


Figure III - 1 - 1: Energy density of gasoline and alcohols.

### 1.1.3. From ethanol to n-butanol via the Guerbet reaction

The catalytic upgrading of ethanol into n-butanol by the renewed Guerbet reaction implies three steps (Scheme III-1-2). In a first step, ethanol is dehydrogenated into acetaldehyde thanks to a catalyst. Then, in the presence of a base, the just formed acetaldehyde undergoes an aldol condensation leading to crotonaldehyde. Finally, the crotonaldehyde is hydrogenated with a catalyst to give n-butanol. Ideally, the catalyst used in this reaction is planned to work by a hydrogen borrowing process i.e., the same catalyst is used to proceed to the dehydrogenation and the hydrogenation steps.



*Scheme III - 1 - 2: The Guerbet reaction on ethanol.*

The targeted reaction may have some limitation. First of all, some selectivity issues may be encountered. Indeed, if the objective is to produce n-butanol from ethanol, the n-butanol synthesized could also undergo a Guerbet reaction leading to n-hexanol and isomers (Figure III-1-2). Therefore, the catalytic system has to be selective toward n-butanol to avoid having branched or higher alcohols than butanol. Nevertheless, although studies devoted to ethanol upgrading to n-butanol are looking for high selectivity, it is reasonable to envision that high selectivity is not mandatory for an engine fuel. The other limitation encountered in the Guerbet reaction is the conversion of ethanol which is rather low in most cases. As it will be presented hereafter in the state of the art, conversion and selectivity are the two essential parameters for the Guerbet reaction.

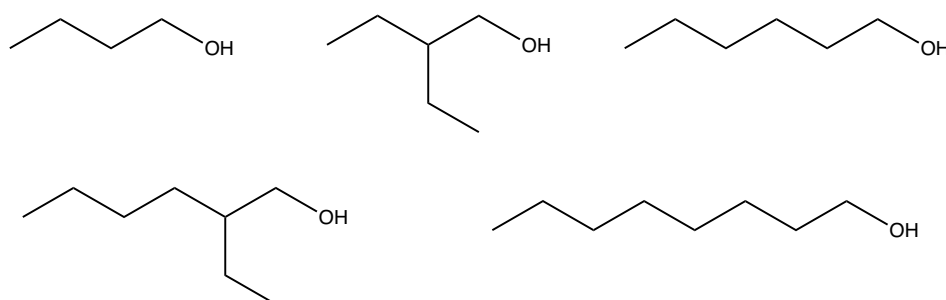


*Figure III - 1 - 2: Possible products of the Guerbet reaction.*

## 2. State of the art of the Guerbet reaction on ethanol

### 2.1. Homogeneous Catalysis

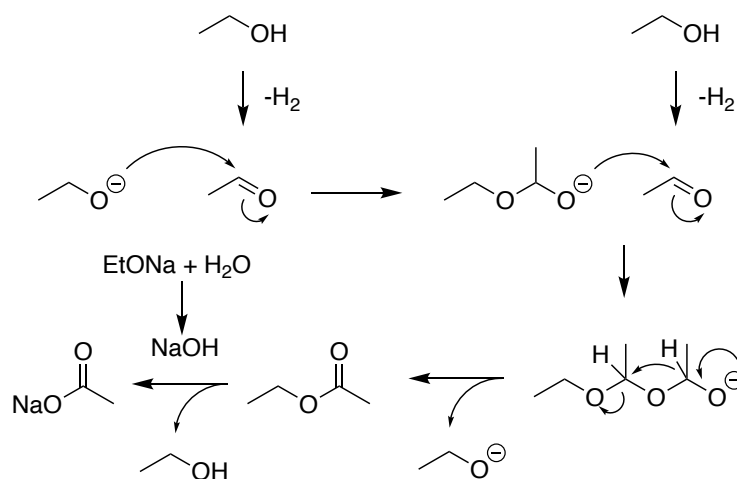
The pioneer work in homogeneous catalysis concerning the upgrade of alcohol using the Guerbet reaction was performed by Gregorio and coworkers in 1972. Within a short publication, the upgrade of n-butanol was studied using simple transition metal complexes with phosphine ligand and sodium butoxide.<sup>[12]</sup> The best results (yield: 90%) was obtained with a rhodium catalyst and sodium butoxide in boiling butanol. Looking at those results, a step back is necessary as no many details are provided.

In 2005, homogeneous catalyst based on iridium were studied by Fujita using secondary alcohols and C<sub>4+</sub> chain alcohol (C<sub>4+</sub>: carbon chain of 4 or higher) suggesting that the catalyst is involved in 2 steps, the dehydrogenation of alcohol to form an hydride species and then the hydrogenation of the unsaturated ketone.<sup>[14]</sup>

$2 \text{ CH}_3\text{CH}_2\text{OH} \xrightarrow[\text{EtONa (5 mol\%), rt (2 h), 120 }^\circ\text{C}]{\text{[Ir(acac)(cod)] (0,01 mol\%), dppp (0,01 mol\%), 1,7-octadiene (1 mol\%)}} \text{CH}_3\text{CH}_2\text{CH}_2\text{CH}_2\text{OH} + \text{longer alcohol}$   
**Conv: 41%**  
**Sel: 51%**

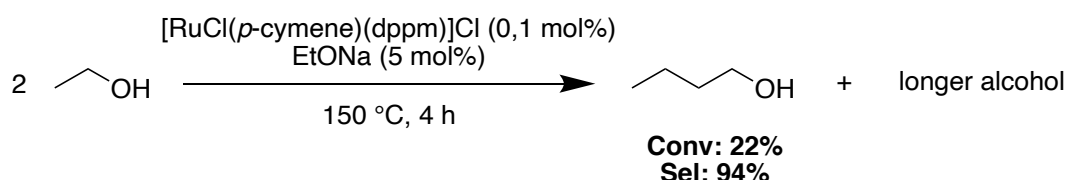
Ishii noticed the limitation of this reaction with the problem of selectivity that may arise. The Guerbet reaction worked with ethanol to produce n-butanol but it could further react to produce higher alcohols. Hence, the main Guerbet products are n-butanol with 2-ethyl-butanol, n-hexanol, 2-ethyl-hexanol, n-octanol (Figure III-1-2). This group also noticed that because of water generating NaOH via hydrolysis of NaOEt, side reactions could lead to sodium acetate via Cannizzaro and Tishchenko transformations (Scheme III-1-4 and III-1-5). Consequently, high conversion of EtOH does not necessarily mean high yield in Guerbet products. This issue is sometimes considered and discussed as missing EtOH.





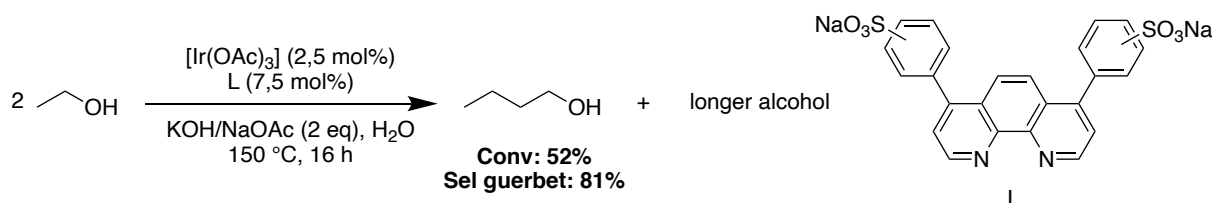
Scheme III - 1 - 5: Tishchenko pathway.

A few years later, Wass focused on the selectivity of the reaction working with ruthenium catalysts.<sup>[17]</sup> A selectivity up to 94% was obtained with the ruthenium catalyst  $[\text{RuCl}(\textit{p}\text{-cymene})(\text{dppm})]\text{Cl}$  ( $\text{dppm}$  = 1,2-bis(diphenylphosphino)methane) at 22% conversion with anhydrous EtOH (Scheme III-1-6). The best ratio between conversion (46%) and selectivity (85%) was achieved using a  $\textit{trans}$ - $[\text{RuCl}_2(\text{dppm})_2]$ . Wass suggested that the catalyst influence the aldol condensation to give the desired  $\text{C}_4$  product.



Scheme III - 1 - 6: Guerbet reaction reported by Wass.

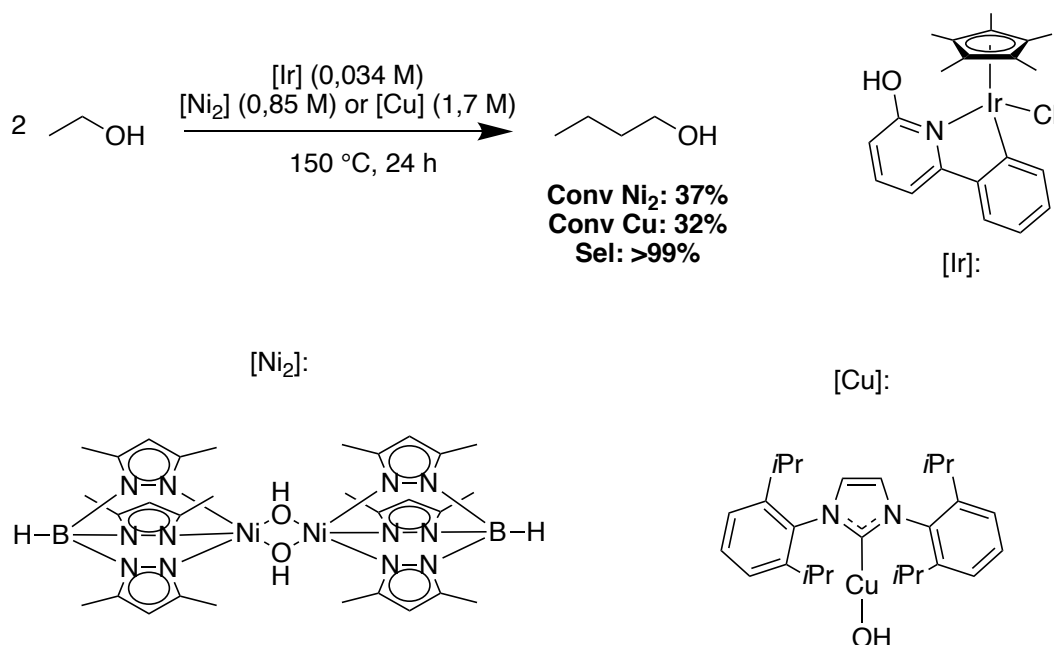
In 2014, Xu proceeded to the reaction in water with  $[\text{Ir}(\text{OAc})_3]$  and phenanthroline based ligands (Scheme III-1-7).<sup>[18]</sup> Overall, the conversion obtained was more than 40% (including missing ethanol) and a selectivity for Guerbet product ( $\text{C}_4$  and higher) more than 70%.



Scheme III - 1 - 7: Best conditions for the Guerbet reaction by Xu.

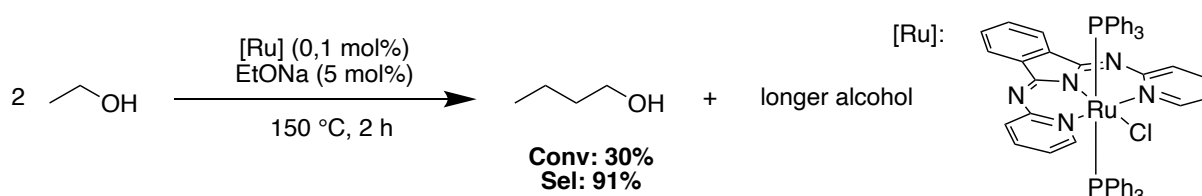
A major breakthrough was made by Jones in 2015 who reached 99% selectivity.<sup>[19]</sup> To achieve this performance, sterically hindered and basic nickel or copper transition metal complexes (Scheme III-1-8) developed by other groups<sup>[20,21]</sup> were used to perform the aldol condensation instead of the inorganic bases usually employed. It was demonstrated that aldol condensation of acetaldehyde promoted by those complexes was fully selective toward the

formation of crotonaldehyde. The catalyst used was an iridium catalyst already developed by the group of Fujita for the dehydrogenation of primary alcohol.<sup>[22]</sup> Jones performed the Guerbet reaction using the Iridium catalyst associated with those unusual bases and managed to obtain an excellent selectivity of 99% (Scheme III-1-8). However, this high selectivity was associated with a quite low conversion of 32%. The ethanol used in the reaction was anhydrous and stored on molecular sieves.



*Scheme III - 1 - 8: Guerbet reaction reported by Jones.*

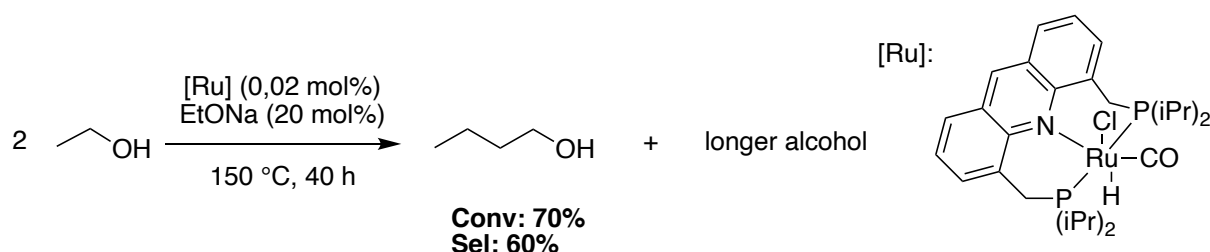
Szymczak applied a ruthenium catalyst developed in his laboratory and active in dehydrogenation and hydrogenation of alcohols and ketones<sup>[23]</sup> to the Guerbet reaction.<sup>[24]</sup> Absolute ethanol further dried over molecular sieves was used with a ruthenium pincer catalyst and sodium ethanoate to obtain 30% conversion with a selectivity to n-butanol of 91% (Scheme III-1-9). The best conversion of 53% was obtained upon addition of triphenylphosphine (0,4 mol%) but, the selectivity decreased to 78%.



*Scheme III - 1 - 9: Guerbet reaction reported by Szymczak.*

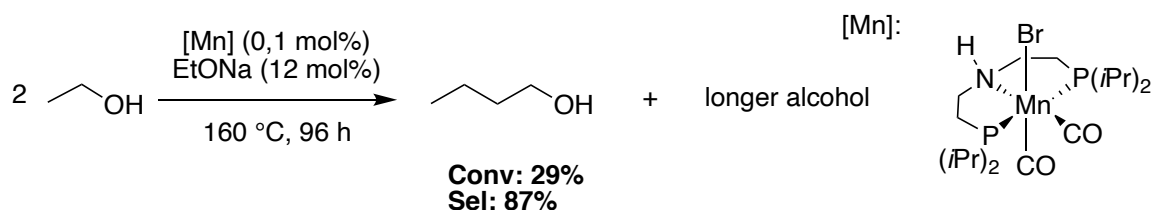
By trying different reaction conditions, Szymczak realized the duality between conversion and selectivity. Indeed, on one hand when the selectivity was improved, the conversion was decreased. On the other hand, when the conversion was improved, the selectivity was decreased. To conclude, Szymczak noticed that gasoline is a blend of hydrocarbons thus mixtures of n-butanol and higher alcohols can play a similar role.

Milstein also used a pincer ruthenium catalyst to obtain 70% conversion and a selectivity about 60% for n-butanol under optimized condition requiring a large amount of base (20 mol%)(Scheme III-1-10).<sup>[25]</sup> Very good results were also obtained under milder conditions using the same catalyst with 4 mol% of EtONa at 110 °C for 16 h with a conversion of 62% and a selectivity toward n-butanol of 68%. Even with a good balance between selectivity and conversion, the conflict between those parameters was again evidenced. Milstein tried to tackle the undesired production of NaOAc via Cannizzaro or Tischchenko pathway to improve the results. Hence, the reaction was run with molecular sieves or desiccant such as Na<sub>2</sub>SO<sub>4</sub> to trap water but this strategy did not lead to any improvement. The grade of the EtOH used was not mentioned.



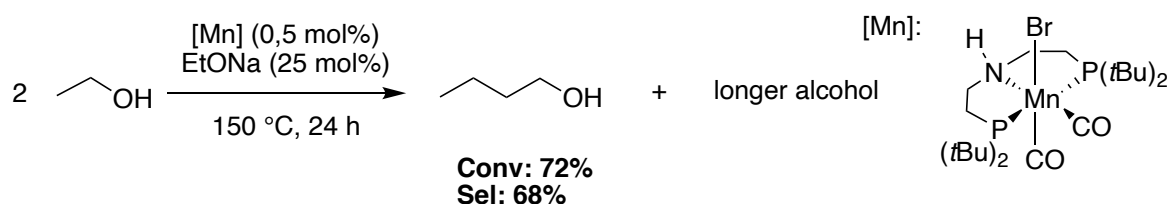
Scheme III - 1 - 10: Guerbet reaction reported by Milstein.

Non-noble metals have also been studied in the Guerbet reaction. In 2017, Liu and coworkers used a manganese pincer catalyst.<sup>[26]</sup> A maximum conversion of 29 % with a selectivity of 87% was achieved but the temperature was high and the reaction was run for a very long time in addition to a high amount of base used (scheme III-1-11). The EtOH was dried over Mg/I<sub>2</sub> prior to use in this study.



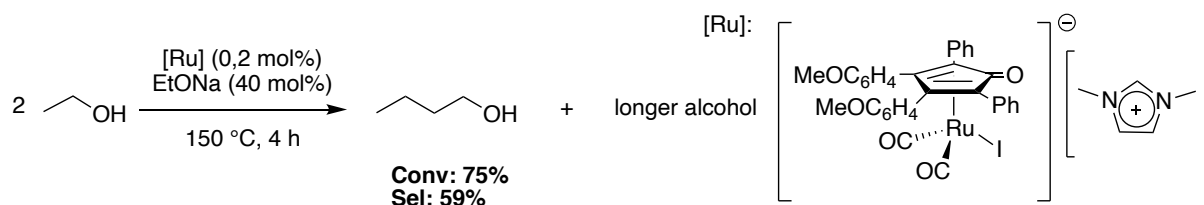
Scheme III - 1 - 11: Guerbet reaction by Liu with a Manganese catalyst.

The next year, Jones worked with a similar manganese catalyst featuring a different pincer ligand. This catalyst displayed better performances with a conversion of 72% and a selectivity of 68% with a large amount of base (scheme III-1-12).<sup>[26]</sup> Reactions were conducted with anhydrous ethanol that was distilled over Mg and stored over 3 Å molecular sieves.



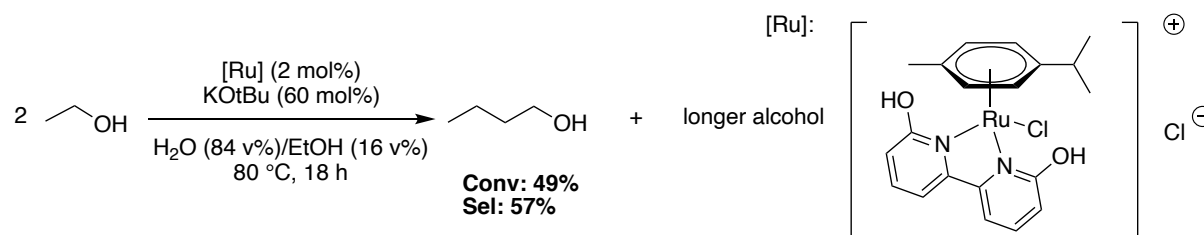
Scheme III - 1 - 12: Guerbet reaction reported by Jones.

Recently the group of Cavani, envisaged to apply the Guerbet reaction directly on ethanol arising from waste of wine industry.<sup>[27]</sup> The ruthenium catalyst used was based on Shvo catalyst and achieved a 75% conversion with a selectivity of 59% and a carbon loss of 21% (Scheme III-1-13). However, once again, a large amount of base was used. It should be noted that this study showed that water did not have a detrimental effect on the outcome of the reaction, contrary to what previous studies had suggested. Indeed, similar results were obtained with various grades of EtOH using a base loading of 20 mol%



Scheme III - 1 - 13: Guerbet reaction with wine waste industry by Cavani.

Very recently, Jones also performed the Guerbet reaction in a mixture of ethanol and water that is similar to fermentation brew.<sup>[28]</sup> This reaction carried out with a ruthenium catalyst in a water/ethanol mixture led to a 49% conversion with 57% of selectivity (Scheme III-1-14). Of note, this reaction was performed under mild condition of temperature (80 °C) compared to the vast majority of other reports where the temperature is in general around 150 °C. Unlike the reported procedures earlier, a high catalyst amount (2 mol%) and a very high base loading (60 mol%) was used.



Scheme III - 1 - 14: The Guerbet reaction made by Jones with a ruthenium catalyst.

## 2.2. Heterogeneous catalysis

Although this thesis is concerned with homogeneous catalysis, it is important to briefly mention the state of the art in heterogeneous catalysis.<sup>[29,30]</sup> A number of metal-oxides system have been used and specially MgO that seems to be considered as a reference. A conversion up to 60% was reported for the Guerbet reaction of methanol with primary alcohol.<sup>[31]</sup> An improvement was achieved with the use of mixed metal oxides such as MgAlO. Recently, Wang obtained a conversion up to 48% and a selectivity up to 93% with a NiSn/MgAlO catalyst at 250 °C.<sup>[32]</sup>

Hydroxyapatite  $\text{Ca}_5(\text{PO}_4)_3\text{OH}$  has also been reported. Tuning the composition had an influence on both the conversion and the selectivity. Once again, the temperature used were very high (400 °C) and the conversion quite low (23% conversion with 70% selectivity).<sup>[33]</sup>

Metal-oxide coupled with supported metals have been investigated to enhance the reactivity and try to reduce the temperature. For example, by using Ni-MgAlO for the transformation of EtOH, Zheng obtained a conversion of 18% and a selectivity towards n-butanol of 55% at a temperature of 250 °C.<sup>[34]</sup>

Metal-impregnated zeolites have been reported in the 90's by Yang. For example, a rubidium impregnated zeolite X (Rb-LiX) at 420 °C produced n-butanol from ethanol.<sup>[35]</sup>

Overall, heterogeneous processes are struggled with low conversion and/or selectivity associated with very harsh condition despite the advantage of catalyst stability and ease of separation.

### 3. Conclusion

The Guerbet reaction has attracted a lot of interest over the past years. It was shown through the state-of-the-art presentation that is difficult to get both a high conversion and a high selectivity. The duality between those two parameters can be illustrated by the work of Jones who managed to reach almost a full selectivity for n-butanol but the conversion was low.<sup>[19]</sup> Overall, considering homogeneous catalysis the selectivity ranges from 50% to 99% while the conversion ranges from 22% to 75%. It must be mentioned that the Guerbet reaction requires high temperatures and very basic reaction media which are likely to induce fast decomposition of organometallic complexes. It is also worth mentioning that the conversion results are not always directly comparable as they are not always calculated in the same manner. Indeed, as mentioned earlier in the introduction, side reactions (Tischchenko or Canizarro) may consume EtOH to produce ethyl acetate or sodium acetate. This is sometimes taken into consideration as "missing EtOH" but sometimes it is ignored or not mentioned. Regarding the selectivity, most studies search for high selectivity but for fuel application, having a mixture of isomers may not be a problem. Therefore, it may be worth focusing on the conversion to Guerbet products rather than on a high selectivity toward n-butanol. Another issue is the formation of by-products produced due to the release of water during the reaction. In conclusion, progress could be made toward the transformation of ethanol into Guerbet products under milder conditions of temperature to achieve a higher conversion.

## 4. References:

- [1] L. C. de Freitas, S. Kaneko, *Energy Econ.* **2011**, *33*, 1146–1154.
- [2] “Carburant et combustibles autorisés en France,” can be found under <https://www.ecologie.gouv.fr/carburants-et-combustibles-autorises-en-france>, **2021**.
- [3] M. Gavahian, P. E. S. Munekata, I. Eş, J. M. Lorenzo, A. Mousavi Khaneghah, F. J. Barba, *Green Chem.* **2019**, *21*, 1171–1185.
- [4] H. A. Alalwan, A. H. Alminshid, H. A. S. Aljaafari, *Renew. Energy Focus* **2019**, *28*, 127–139.
- [5] N. M. Eagan, M. D. Kumbhalkar, J. S. Buchanan, J. A. Dumesic, G. W. Huber, *Nat. Rev. Chem.* **2019**, *3*, 223–249.
- [6] M. Guerbet, *C. R. Acad. Sci. Paris* **1899**, *128*, 1002–1004.
- [7] M. Guerbet, *C. R. Acad. Sci. Paris* **1901**, 300–302.
- [8] M. Guerbet, *C. R. Acad. Sci. Paris* **1909**, *149*, 129–132.
- [9] W. R. da S. Trindade, R. G. dos Santos, *Renew. Sustain. Energy Rev.* **2017**, *69*, 642–651.
- [10] P. H. Pfromm, V. Amanor-Boadu, R. Nelson, P. Vadlani, R. Madl, *Biomass Bioenergy* **2010**, *34*, 515–524.
- [11] S. Atsumi, A. F. Cann, M. R. Connor, C. R. Shen, K. M. Smith, M. P. Brynildsen, K. J. Y. Chou, T. Hanai, J. C. Liao, *Metab. Eng.* **2008**, *10*, 305–311.
- [12] G. Gregorio, G. F. Pregaglia, R. Ugo, *J. Organomet. Chem.* **1972**, *37*, 385–387.
- [13] P. L. Burk, *J. Mol. Catal.* **1985**, *33*, 15–21.
- [14] K. Fujita, C. Asai, T. Yamaguchi, F. Hanasaka, R. Yamaguchi, *Org. Lett.* **2005**, *7*, 4017–4019.
- [15] K. Koda, T. Matsu-ura, Y. Obora, Y. Ishii, *Chem. Lett.* **2009**, *38*, 838–839.
- [16] T. Matsu-ura, S. Sakaguchi, Y. Obora, Y. Ishii, *J. Org. Chem.* **2006**, *71*, 8306–8308.
- [17] G. R. M. Dowson, M. F. Haddow, J. Lee, R. L. Wingad, D. F. Wass, *Angew. Chem. Int. Ed.* **2013**, *52*, 9005–9008.
- [18] G. Xu, T. Lammens, Q. Liu, X. Wang, L. Dong, A. Caiazzo, N. Ashraf, J. Guan, X. Mu, *Green Chem* **2014**, *16*, 3971–3977.
- [19] S. Chakraborty, P. E. Piszal, C. E. Hayes, R. T. Baker, W. D. Jones, *J. Am. Chem. Soc.* **2015**, *137*, 14264–14267.
- [20] G. C. Fortman, A. M. Z. Slawin, S. P. Nolan, *Organometallics* **2010**, *29*, 3966–3972.
- [21] S. Hikichi, M. Yoshizawa, Y. Sasakura, H. Komatsuzaki, Y. Moro-oka, M. Akita, *Chem. - Eur. J.* **2001**, *7*, 5011–5028.
- [22] K. Fujita, T. Yoshida, Y. Imori, R. Yamaguchi, *Org. Lett.* **2011**, *13*, 2278–2281.
- [23] K.-N. T. Tseng, J. W. Kampf, N. K. Szymczak, *ACS Catal.* **2015**, *5*, 5468–5485.
- [24] K.-N. T. Tseng, S. Lin, J. W. Kampf, N. K. Szymczak, *Chem. Commun.* **2016**, *52*, 2901–2904.
- [25] Y. Xie, Y. Ben-David, L. J. W. Shimon, D. Milstein, *J. Am. Chem. Soc.* **2016**, *138*, 9077–9080.
- [26] N. V. Kulkarni, W. W. Brennessel, W. D. Jones, *ACS Catal.* **2018**, *8*, 997–1002.
- [27] R. Mazzoni, C. Cesari, V. Zanotti, C. Lucarelli, T. Tabanelli, F. Puzzo, F. Passarini, E. Neri, G. Marani, R. Prati, F. Viganò, A. Conversano, F. Cavani, *ACS Sustain. Chem. Eng.* **2019**, *7*, 224–237.
- [28] T. A. DiBenedetto, W. D. Jones, *Organometallics* **2021**, *40*, 1884–1888.
- [29] H. Aitchison, R. L. Wingad, D. F. Wass, *ACS Catal.* **2016**, *6*, 7125–7132.
- [30] J. T. Kozlowski, R. J. Davis, *ACS Catal.* **2013**, *3*, 1588–1600.

- [31] W. Ueda, T. Kuwabara, T. Ohshida, Y. Morikawa, *J. Chem. Soc. Chem. Commun.* **1990**, 1558.
- [32] X. Wu, X. Cai, Q. Zhang, P. Bi, Q. Meng, Y. Pi, T. Wang, *ACS Sustain. Chem. Eng.* **2021**, 9, 11269–11279.
- [33] T. Tsuchida, S. Sakuma, T. Takeguchi, W. Ueda, *Ind. Eng. Chem. Res.* **2006**, 45, 8634–8642.
- [34] J. Pang, M. Zheng, L. He, L. Li, X. Pan, A. Wang, X. Wang, T. Zhang, *J. Catal.* **2016**, 344, 184–193.
- [35] C. Yang, Z. Y. Meng, *J. Catal.* **1993**, 142, 37–44.



## Part 2: Catalytic application of $\eta^5$ - Oxocyclohexadienyl Ruthenium complex in the Guerbet reaction



## 1. The Guerbet reaction with ethanol

The Guerbet reaction, used in the alternative fuel research field, was investigated with the  $\eta^5$ -Oxocyclohexadienyl ruthenium complex **1** (Figure III-2-1). Having demonstrated its capability to promote hydrogenation reactions of ketones, complex **1** was investigated in the upgrading of ethanol into butanol and higher alcohols (Scheme III-2-1). This reaction implies a hydrogen borrowing process that could be fulfilled by the bifunctional properties of the catalyst demonstrated earlier in the manuscript. In this reaction, a base is required to perform the aldol condensation.

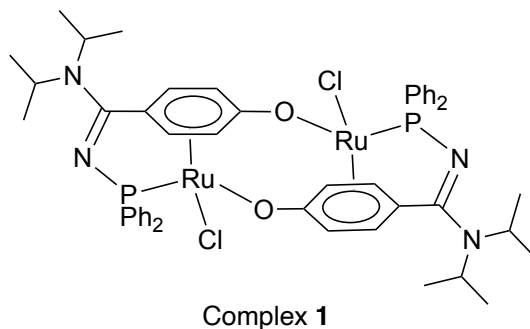
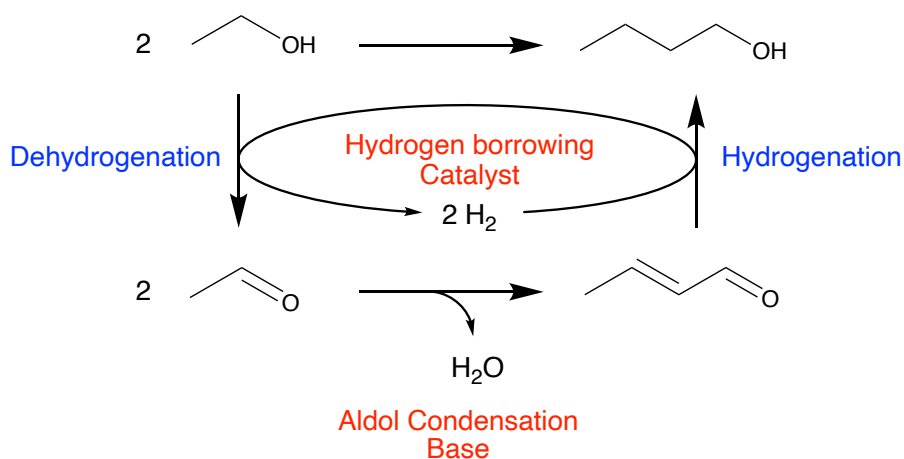


Figure III - 2 - 1: Catalyst used in the Guerbet reaction study.

The literature data presented in the previous part highlighted that it is difficult to get both a high conversion of ethanol and a high selectivity toward n-butanol. It was also demonstrated that water could be detrimental to the reaction by neutralizing the strong base. Hence, high amounts of base were used to ensure good performances. All these parameters were closely examined in the following study.



Scheme III - 2 - 1: The Guerbet reaction with ethanol.

## 1.1. Analytical set-up

The products produced by the Guerbet reaction are alcohols (ethanol, butanol and higher alcohols) and undesired by-product (AcOEt, AcONa). We have used gas chromatography for the analysis of the soluble components of the reaction mixture. There are potentially several products that can be formed (Figure III-2-2). They were all identified using authentic commercial compounds and calibrated using dioxane as an internal standard (Figure III-2-3).

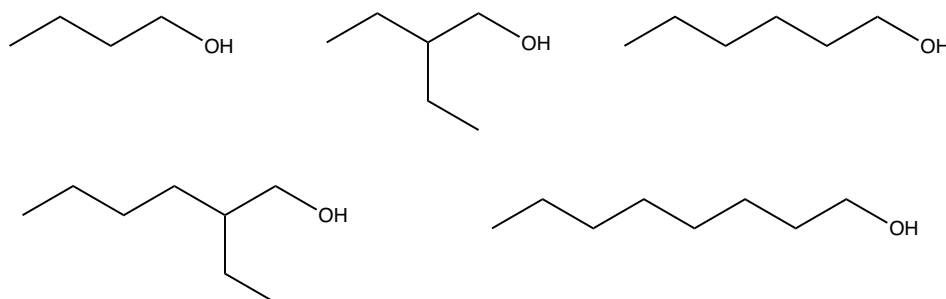


Figure III - 2 - 2: Plausible products of the guerbet reaction.

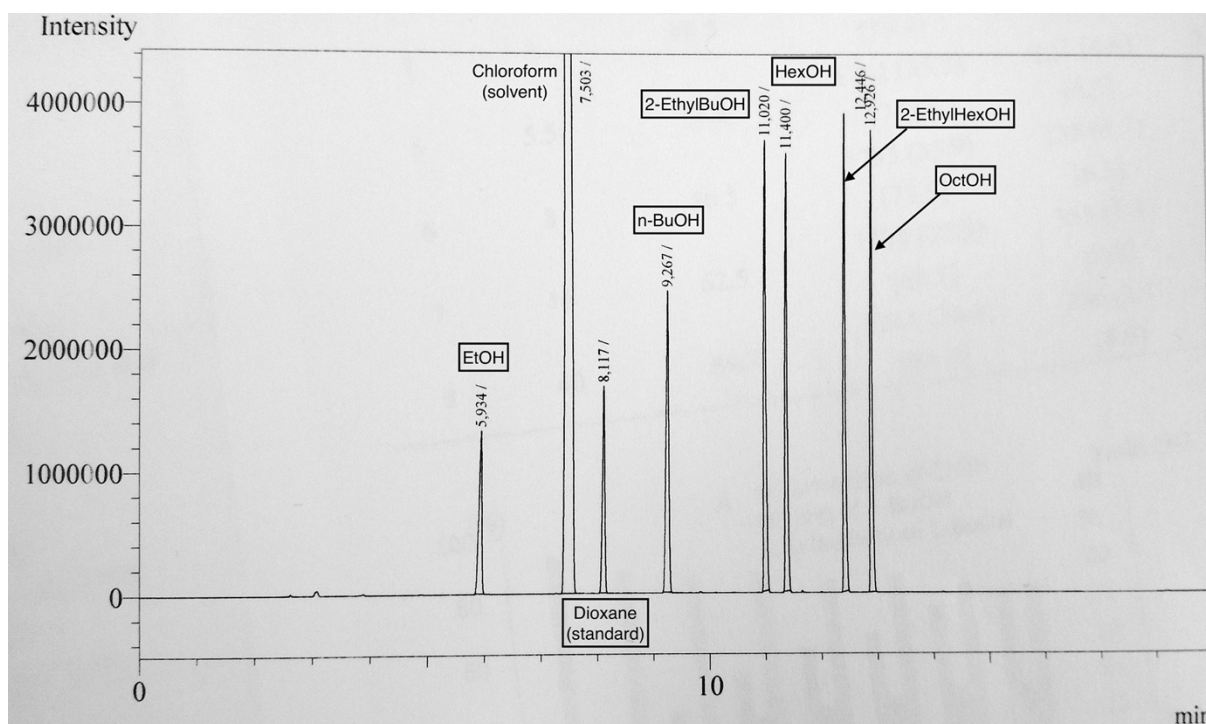
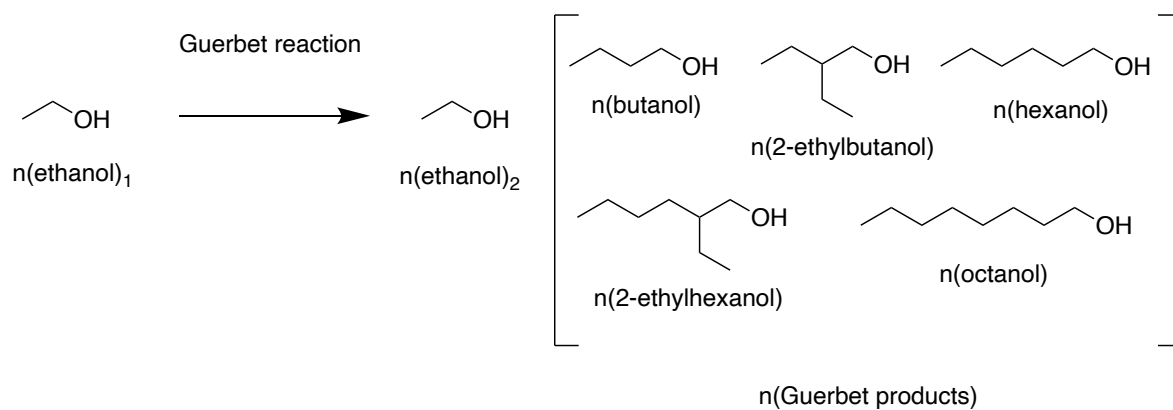


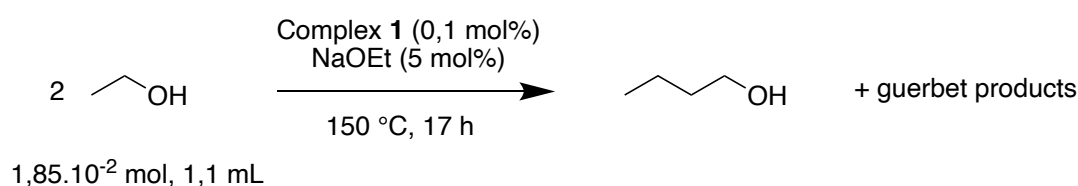
Figure III - 2 - 3: Chromatogram of the plausible Guerbet products.

Following calibration, the unreacted EtOH and every product could be quantified (Figure III-2-4) allowing the determination of the total conversion of EtOH and amount of EtOH used for the production of Guerbet products. Comparison of these two values was used to determine the amount of “missing ethanol” representing the transformation of ethanol into unknown product that were not quantified. This missing ethanol was not always considered in the results described earlier in the state-of-the-art part.



## 1.2. Results and discussion

Based on the literature data, the reactions were run in extra-dry ethanol (99,5%), used as received which served both as solvent and reactant. The temperature was set at 150 °C which is commonly used for this reaction. Sodium ethoxide (NaOEt) was used as a base as it provided the best results among the bases tested by the other groups. The catalytic loading used was 0,1 mol%. Initially, we performed our reactions in thick wall Schlenk tubes and later in Ace<sup>®</sup> tubes but this resulted in the degradation of the glassware material likely due to the presence of NaOEt at high temperature. An attempt to use Biotage microwave vials as reported by Szymczak<sup>[1]</sup> also failed as the tube did not resist the pressure. Finally, we implemented our experiments in Parr<sup>®</sup> high pressure steel reactors albeit their volume (22.5 mL) was not ideal for the scale of our reactions (1-1.5 mL).



*Scheme III - 2 - 2: Guerbet preliminary reaction.*

The preliminary reaction (Scheme III-2-2) performed with 5 mol% of NaOEt led to a modest conversion of 15% but a high selectivity toward n-butanol of 83% (Table III-2-1, entry 1). However, we were concerned about the missing ethanol due to the production of sodium acetate via a Tischenko or Cannizzaro pathway as reported by Ishii.<sup>[2]</sup>

A blank test was made without base with no success as no conversion occurred in this condition (Table III-2-1, entry 2).

*Table III - 2 - 1: Guerbet preliminary results*

Entry	Conversion	EtOH used in Guerbet	Missing EtOH	BuOH Select.
<b>1</b>	15%	7%	8%	83%
<b>2<sup>a</sup></b>	No conv	-	-	-
Conditions: EtOH (1,85.10 <sup>-2</sup> mol, 1,1 mL), <b>1</b> (0,1 mol%, 1,85.10 <sup>-5</sup> mol, 20 mg), NaOEt (5 mol%, 9,26. 10 <sup>-4</sup> mol, 63 mg), 150 °C, 17h. <sup>a</sup> base-free condition				

### 1.2.1. Temperature optimization

We have performed our initial test at 150 °C since most of the reported examples were implemented at this temperature. As explained earlier, one can question the stability of organometallic complexes at this temperature under basic conditions. For this reason, we decided to perform the reaction at lower temperatures. The very low and challenging temperature of 45 °C was attempted with no success as we obtained a conversion of 2% (Table III-2-2, Entry 1). Then, a temperature of 120 °C (Table III-2-1, Entry 2) was tested with a conversion of 16% equivalent to the run of 150 °C (Table III-2-1, Entry 3) and a selectivity of

91% for nBuOH. However, the part of “missing ethanol” was more important with 12%. As a result, further studies were performed at 150 °C.

Table III - 2 - 2 : Temperature optimization

Entry	Temp. (°C)	Conversion	EtOH used in Guerbet	Missing EtOH	nBuOH Select.
1	45	2%	1%	1%	100%
2	120	16%	4%	12%	91%
3	150	15%	7%	8%	83%

Conditions: EtOH ( $1,85 \cdot 10^{-2}$  mol, 1,1 mL), **1** (0,1 mol%,  $1,85 \cdot 10^{-5}$  mol, 20 mg), NaOEt (5 mol%,  $9,26 \cdot 10^{-4}$  mol, 63 mg), T °C, 17h.

### 1.2.2. Reaction scale

From a practical point of the view and due to the high volume of the reactor that may have an impact of the reaction, we decided to pay attention to this parameter. For this study and based on our feedback on practical aspects, the volume of EtOH was slightly increased from 1.1 to 1.5 mL. As depicted in Table III-2-3, the change in the volume used lead to an improvement of the conversion (20%) and the selectivity (91%) but also of the “missing ethanol”.

Table III - 2 - 3: Reaction scale

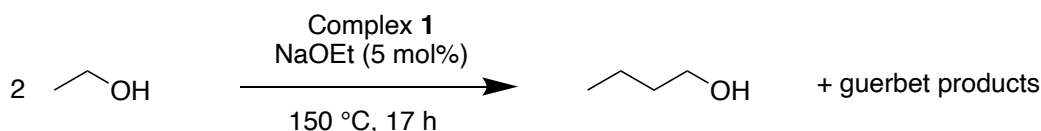
Entry	Vol. (mL)	Conversion	EtOH used in G	Missing EtOH	BuOH Select.
1	1,1	15%	7%	8%	83%
2	1,5	20%	8%	12%	91%

Conditions: EtOH ( $1,85 \cdot 10^{-2}$  mol, 1,1 mL or  $2,56 \cdot 10^{-2}$  mol, 1,5 mL), **1** (0,1 mol%), NaOEt (5 mol%,  $9,26 \cdot 10^{-4}$  mol, 63 mg), 150 °C, 17h.

### 1.2.3. Catalyst loading

The reduction of the catalyst loading to 0,05 mol% (Table III-2-4, entry 2) gave the same results as the run at 0,1 mol% (Table III-2-4, Entry 1) regarding conversion and selectivity. Further reduction of the catalyst loading to 0,025 mol% by using 3 mL instead of 1,5 mL (as EtOH is both the solvent and the reagent), led to the same conversion around 20% with a slight decrease in the selectivity (Table III-2-4, Entry 3). Interestingly, the part of “missing ethanol” reduced significantly to 5 %. For this reason, we used 3 mL with 0,05 mol% of catalyst (Table III-2-4, Entry 4) to see if we could decrease the “missing ethanol”. We obtained the same conversion and the same selectivity around 20 % and 90% with 0,05 mol% of catalyst using either 1,5 mL or 3 mL of solvent. However, the “missing ethanol” with 3 mL of EtOH was reduced to 8% compared to 12%. Those results indicate that the catalyst loading has not a strong influence on the EtOH conversion. It also shows the influence on the “missing ethanol” of the volume ratio between the reaction mixture and the reactor. Hence suggesting that part of the missing ethanol could be due to loss of ethanol in the reactor tubing and during depressurization.

Table III - 2 - 4: Catalyst loading study



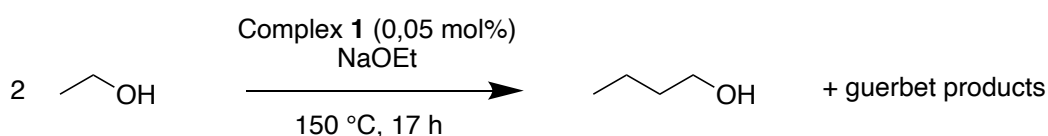
Entry	Cata (mol%)	Conversion	EtOH used in G	Missing EtOH	BuOH Select.
1	0,1	20%	8%	12%	91%
2	0,05	21%	9%	12%	90%
3	0,025 <sup>a</sup>	19%	14%	5%	85%
4	0,05 <sup>a</sup>	20%	12%	8%	91%

Conditions: EtOH ( $2,56 \cdot 10^{-2}$  mol, 1,5 mL), 1, NaOEt (5 mol%,  $1,28 \cdot 10^{-4}$  mol, 87 mg), 150 °C, 17h. <sup>a</sup> 3 mL of EtOH

### 1.2.4. Base loading

The base loading was evaluated since the first experiments were carried out with a low loading of 5 mol% (Table III-2-5, Entry 1). As demonstrated in the state-of-the-art presentation, it is proposed that water generated during the aldol condensation inhibits the reaction by consuming the base. Hence, higher base loadings led in general to higher conversions. When the base loading was increased to 15 mol% (Table III-2-5, Entry 2) the conversion increased to 40% but half of it was due to “missing EtOH”. Similarly, to observations made in the literature, this conversion improvement was accompanied by an erosion of the selectivity for nBuOH to 80%. Albeit modest, these results are encouraging with regards to the state of the art.

Table III - 2 - 5: Base loading study

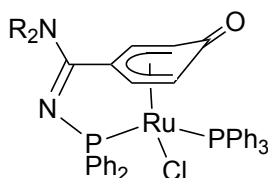


Entry	Base (mol%)	Conversion	EtOH used in G	Missing EtOH	BuOH Select.
1	5	21%	9%	12%	90%
2	15	40%	18%	22%	80%

Conditions: EtOH ( $2,56 \cdot 10^{-2}$  mol, 1,5 mL), 1 (0,05 mol%,  $1,28 \cdot 10^{-5}$  mol), NaOEt (5 mol%,  $1,28 \cdot 10^{-3}$  mol, 87 mg or 15 mol%,  $3,84 \cdot 10^{-3}$  mol, 261 mg), 150 °C, 17h.

### 1.2.5. Preliminary test with complex 29

Just like with base-free hydrogenation, complex **29** (Figure III-2-5) was briefly tested in the Guerbet reaction. These tests could be the basis for further exploration in the new subject of Guerbet reaction developed in the laboratory.

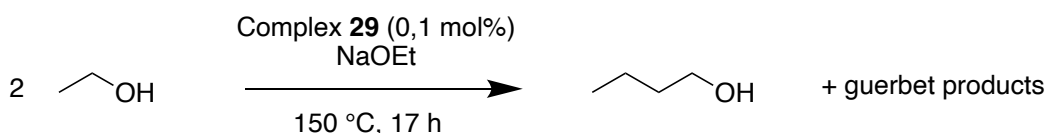


Complex **29**

Figure III - 2 - 5: Complex 29 used in the Guerbet reaction.

The methodology employed with complex **29** was the same as used with complex **1**. Two different amounts of base were used and could be compared to the results obtained with complex **1** in Table III-2-5 in the previous paragraph. Indeed, as complex **29** is a monomeric species, 0,1 mol% was used while 0,05 mol% of complex **1** was used. The results summarized in table III-2-6 showed no improvement in the conversion but a slight decrease in the selectivity toward nBuOH.

Table III - 2 - 6: Preliminary tests with complex **29**



Entry	Base (mol%)	Conversion	EtOH used in G	Missing EtOH	BuOH Select.
<b>1</b>	5	25%	9%	16%	81%
<b>2</b>	15	40%	19%	21%	75%

Conditions: EtOH ( $2,56 \cdot 10^{-2}$  mol, 1,5 mL), **29** (0,1 mol%,  $2,56 \cdot 10^{-5}$  mol), NaOEt (5 mol%,  $1,28 \cdot 10^{-3}$  mol, 87 mg or 15 mol%,  $3,84 \cdot 10^{-3}$  mol, 261 mg), 150 °C, 17h.

As the two complexes exhibit similar results, we hypothesized that the same active catalytic species could be involved. Those exploratory studies demonstrate that oxocyclohexadienyl ruthenium complexes are competent to promote the Guerbet reaction with good selectivity but moderate conversions.

## 2. Conclusion

During this study, it was demonstrated that complex **1** and **29** were active in the Guerbet reaction albeit with modest conversion. Using complex **1**, the maximum conversion (40%) was obtained with a 0,05 mol% catalyst loading and 15 mol% NaOEt. The selectivity for nBuOH was about 80% and the “missing ethanol” represented 22%. The best ratio between the conversion, the selectivity and “missing ethanol” was obtained with a catalyst loading of 0,05 mol% and 5 mol% of base in 3 mL of ethanol. The conversion was modest (20%) but the “missing ethanol” was only 8% with a selectivity for nBuOH 91%.

This new research field in the laboratory initiated by this study was confronted to the harsh reaction condition of the Guerbet reaction. Generally speaking, the high temperature required and the base used might create a hostile environment for the homogeneous catalyst. This reaction also suffers from side reaction leading to NaOAc that polluted the reaction mixture. It seems difficult to obtain better results in this field unless the robustness and the stability of the catalyst is developed and improved. Nevertheless, catalyst **1** displayed encouraging performances in a field where only a few organometallic complexes were found competent. In fact, complex **1** displays performance in the range of catalysts used in the early days by Ishii<sup>[2]</sup>, Xu<sup>[3]</sup> or Wass.<sup>[4]</sup> Further improvements could be reached with more robust catalyst of the same family. Another way for improvement concerns the aldol condensation step which is in turn responsible for the low selectivity and conversion. While selectivity is not a major concern for fuel application, conversion is a key feature to improve.

### 3. References:

- [1] K.-N. T. Tseng, S. Lin, J. W. Kampf, N. K. Szymczak, *Chem. Commun.* **2016**, 52, 2901–2904.
- [2] K. Koda, T. Matsu-ura, Y. Obora, Y. Ishii, *Chem. Lett.* **2009**, 38, 838–839.
- [3] G. Xu, T. Lammens, Q. Liu, X. Wang, L. Dong, A. Caiazzo, N. Ashraf, J. Guan, X. Mu, *Green Chem.* **2014**, 16, 3971–3977.
- [4] G. R. M. Dowson, M. F. Haddow, J. Lee, R. L. Wingad, D. F. Wass, *Angew. Chem. Int. Ed.* **2013**, 52, 9005–9008.

## 4. Experimental Part

### 4.1. General information

Extra-dry ethanol (99,5%) was used as received. The gas chromatography analysis were run on a Shimadzu GC 2014 apparatus fitted with a polar WAX-Optima column (30m x 0,25 mm x 0,25  $\mu$ m). T °C injection: 245 °C. Temperature program: (40 ° for 5min) - (T increase to 220 °C at a rate of 20°C/min) - (Hold 5 min at 220)

### 4.2. Reaction procedure

In a standard procedure, a Parr® high pressure reactor was loaded in a glovebox with the catalyst **1** (0,1 mol%,  $2,56 \cdot 10^{-5}$  mol, 27,6 mg), the base EtONa (5 mol%,  $1,28 \cdot 10^{-3}$  mol, 87,1 mg) and the EtOH ( $2,56 \cdot 10^{-2}$ , 1,5 mL). The reactor was removed from the glovebox and sealed. The reaction was heated at 150 °C for 17 h. At the end of the reaction, the reactor was allowed to cool down to r.t and gently open. 1,4-Dioxane (100  $\mu$ L,  $1,17 \cdot 10^{-3}$  mol) was added as an internal standard. The reaction mixture was filtered through a cotton plug and washed with chloroform.

### 4.3. Analytical procedure

A calibration of EtOH and the reaction products was made by measuring the response factor of each of the Guerbet products vs dioxane as internal standard with 5 different reference solutions. Then, using this calibration method and applying it to a crude reaction mixture, we could calculate the amount of remaining ethanol, the ethanol used for the production of Guerbet products, the conversion, the selectivity toward n-butanol and the missing EtOH.

$$K = \frac{A_{\text{standard}}}{A_{\text{sample}}} \times \frac{n_{\text{sample}}}{n_{\text{standard}}}$$

*K* : response factor for a given product

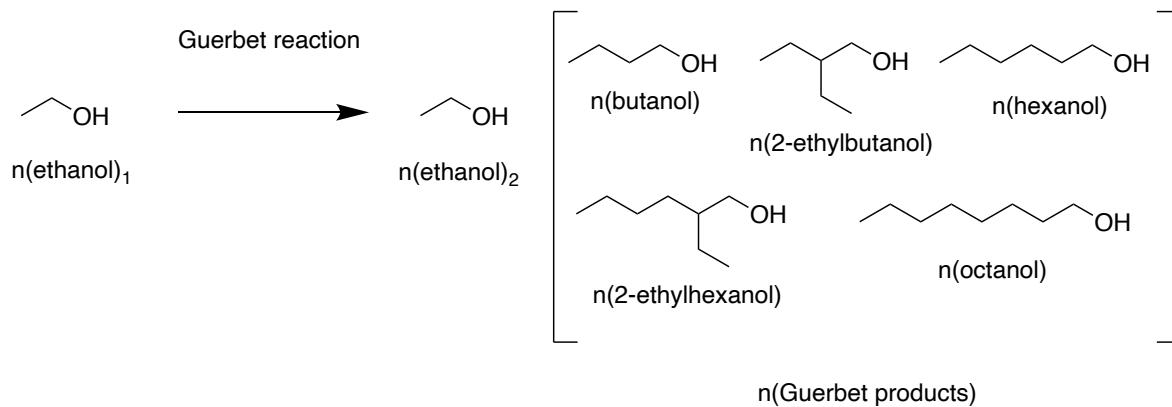
*A<sub>standard</sub>* : Area of the standard

*A<sub>sample</sub>* : Area of the sample

*n<sub>standard</sub>* : mole of the standard

*n<sub>sample</sub>* : mole of the sample

$$n_{\text{sample}} = K_{\text{sample}} \times \frac{A_{\text{sample}}}{A_{\text{standard}}} \times n_{\text{standard}}$$



#### 4.4. Reaction procedure attempts

- 1) Standard procedure in a heavy wall Schlenk tube.
- 2) Standard procedure in an Ace<sup>®</sup> tube.
- 3) Standard procedure in a Biotage microwave vial inserted into a reactor with sand used for heat transfer.
- 4) Standard procedure in a glasstube that was sealed by the glassblower. The tube was inserted into a reactor with sand used for heat transfer.
- 5) Standard procedure in a glass-cup inserted in a high-pressure reactor.
- 6) Standard procedure in a Teflon-cup inserted in a high-pressure reactor.





# Chapter IV: The Hydrogen Storage

## Part 1: State of the art



## 1. Introduction

As presented in the general introduction, this PhD targets the production of energy sources via homogeneous catalysis in a context of over-exploitation of fossil fuels that cause environmental damages. Following our researches on hydrogenation reaction and the Guerbet reaction, we have investigated the potential of  $\eta^5$ -oxocyclohexadienyl ruthenium catalysts in the hydrogen storage field.

## 2. Hydrogen as an energy source

Hydrogen has been used as an energy source for years by the space and military fields. Hydrogen was the fuel of the first space rocket and it is still employed in this field.<sup>[1]</sup> Some researcher like Bockris in 1972 try to spread the idea of a “Hydrogen Economy”.<sup>[2]</sup> It was a concept that relied on the hydrogen production and use instead of fossil fuels. The energy density of 120 MJ/Kg from dihydrogen is much higher than gasoline with 44 MJ/Kg.

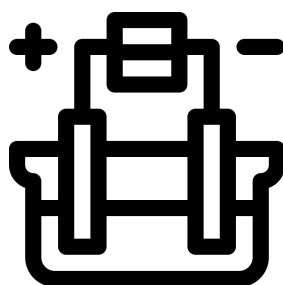


Figure IV - 1 - 1: Electrolysis of water.

Hydrogen can be produced in a sustainable way by the electrolysis of water leading to dioxygen and dihydrogen. However, it is not an energy source of the daily life due to some storage, transportation and production issues. Concerning the production of hydrogen, currently it is cheaper to produce it from hydrocarbons (called grey hydrogen) than water splitting.<sup>[3]</sup> Furthermore, the electricity required for the water electrolysis may come from non-sustainable source such as coal. Hence, there is still some research and development to be done to produce hydrogen in a complete sustainable way (called green hydrogen).

The second issue is about storage and transportation of hydrogen. Nowadays, hydrogen is stored either under pressure (up to 700 bar) or as a cryogenic liquid (-252 °C; 21 °K). Both storage methods require specific equipment and intensive energy processing. Those conditions are not suitable for the development and the democratization of hydrogen energy. Therefore, new routes have been developed for hydrogen storage. Beside the routes involving hydrogen physisorption on different support zeolite, MOF, polymers, Metal-Hydride, Nitrogen based compound, etc,<sup>[4–6]</sup> the concept of Liquid Organic Hydrogen Carrier (LOHC) emerged and gained in interest in the past decades.<sup>[5,7]</sup>

## 2.1. Liquid Organic Hydrogen Carrier

Liquid Organic Hydrogen Carriers (LOHC) are organic molecules with a high content of hydrogen ideally non or poorly hazardous and toxic that can be easily handle. These molecules act as a hydrogen reservoir that can release dihydrogen when needed by dehydrogenation.

LOHCs are an alternative that can overcome the issues of liquid and compressed hydrogen. Being a liquid material, the storage and transportation of LOHCs are easier and do not require specific equipment because they are compatible with the existing infrastructures. Several LOHCs have been investigated<sup>[8]</sup> starting with a toluene/methylcyclohexane system in the 80's.<sup>[9]</sup> Some molecules, such as methanol and formic acid (FA), have additional advantages as they can be produced from carbon dioxide and dihydrogen. By this way, H<sub>2</sub> can be stored and CO<sub>2</sub> recycled.<sup>[10]</sup> FA possesses a very good volumetric density, higher than H<sub>2</sub> under pressure and close to cryogenic H<sub>2</sub> (Figure IV-1-2), making it a good candidate as a liquid organic hydrogen carrier.

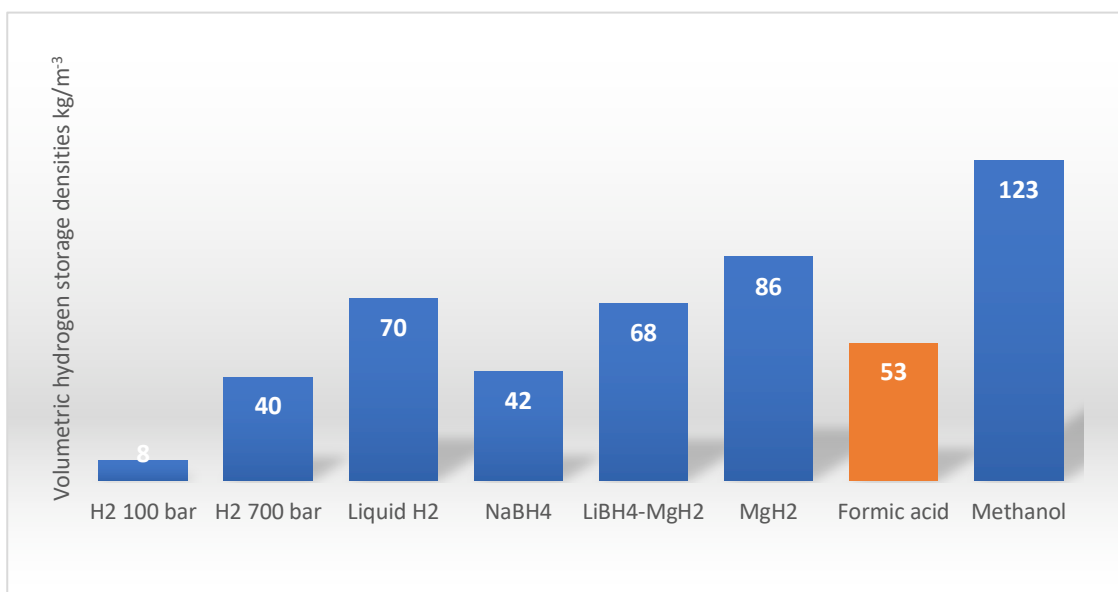
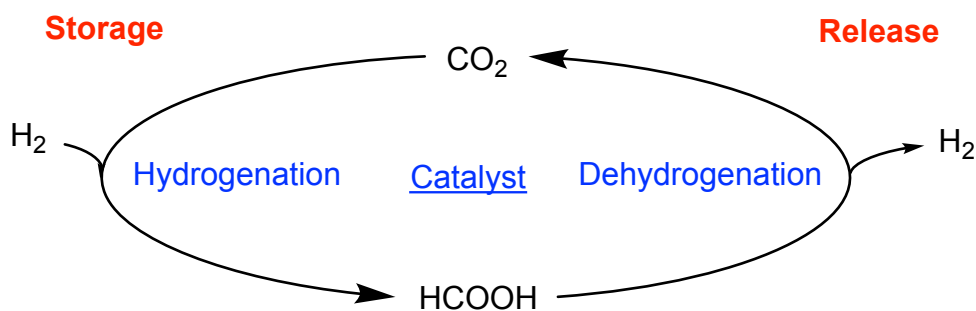


Figure IV - 1 - 2: Comparison of Hydrogen densities.

### 2.1.1. Formic Acid as a LOHC

Formic acid is a good alternative to use as an energetical vector<sup>[11]</sup> because it has a hydrogen density higher than compressed hydrogen. Currently FA is prepared essentially from



Scheme IV - 1 - 1: CO<sub>2</sub>/Formic Acid couple in hydrogen storage.

fossil resources, new routes for its sustainable preparation are investigated.<sup>[12]</sup> FA also has the ability to be produced by CO<sub>2</sub> hydrogenation. In this case, the storage and the release of hydrogen can occur in a CO<sub>2</sub> neutral process with a full atom economy (Scheme IV-1-1). Developing this technology has two positive consequences. First, it contributes to use FA as a LOHC to overcome the hydrogen storage and transportation issues. Thus, it will contribute to withdraw the fossil fuel dependence by improving the use of hydrogen. Then, it also contributes to recycle the CO<sub>2</sub> rejected by human activities.

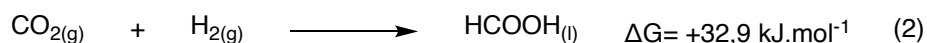
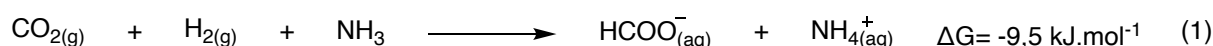
The idea of using Formic Acid as an energetic vector and LOHC (Scheme IV-1-1) was published independently at the same time by Beller<sup>[13]</sup> and Laurency.<sup>[14]</sup> They both generated H<sub>2</sub> from formic acid and use it in fuel cell technology.

Two reactions are involved in the CO<sub>2</sub>/FA couple hydrogen storage and release process. The first one is the storage of H<sub>2</sub> by hydrogenation of CO<sub>2</sub> into FA. The second one is the release of H<sub>2</sub> by dehydrogenation of FA. At the end, the ideal system should be able to promote both reactions. Having this knowledge in hand, the couple Carbon Dioxide/Formic Acid that attract a lot of research <sup>[10,15-17]</sup> will be targeted in this thesis.

### 3. State of the art

#### 3.1. Hydrogen storage by homogeneous catalysis (Hydrogenation of CO<sub>2</sub> in Formic Acid)

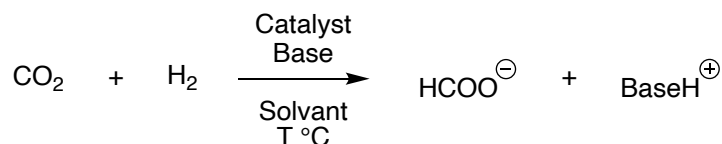
The pioneer work on the hydrogenation of CO<sub>2</sub> with homogenous catalysts was reported by Inoue in 1976.<sup>[18]</sup> Different catalysts based on Pd, Ni, Rh, Ru and Ir were used with triethylamine as a base. The use of base is predominant in this reaction because it forms the conjugated formate base. Thus, it makes the reaction thermodynamically feasible compared to the formation of FA without base (Scheme IV-1-2).<sup>[19]</sup>



*Scheme IV - 1 - 2: Gibbs free energy for CO<sub>2</sub> hydrogenation with base eq (1) and without eq (2).*

For this reason, there is much more literature dealing with the hydrogenation of CO<sub>2</sub> under basic conditions compared to base-free hydrogenation of CO<sub>2</sub>. Several recent reviews cover the extensive contribution in this domain<sup>[10,15,17]</sup> and we will hereafter provide some of the important contributions in CO<sub>2</sub> hydrogenation under basic-conditions. Base-free processes are more recent and will be more developed in this chapter.

### 3.1.1. With base



*Scheme IV - 1 - 3: Hydrogenation of CO<sub>2</sub> with base.*

After the pioneer work by Inoue in the 70's, a major breakthrough was made by Leitner in the 90's with a series of publication based on rhodium catalyst with high TON (TON>1000).<sup>[20–23]</sup> Triethylamine (TEA) was used as a base in these studies and the use of DMSO and water as a solvents provided the best results. For example, a TON up to 3439, was obtained with a rhodium catalyst (0,54.10<sup>-3</sup> mol.L<sup>-1</sup>) (Figure IV-1-3) in an aqueous mixture of H<sub>2</sub>O/HNMe<sub>2</sub> under 40 bar at 25 °C.

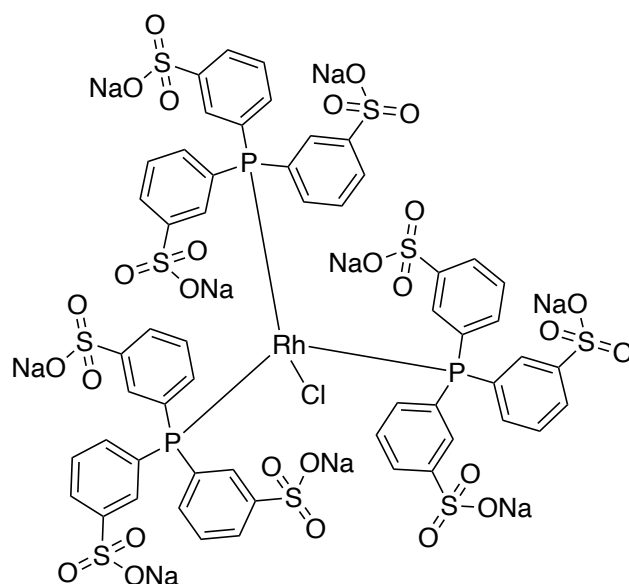


*Figure IV - 1 - 3: One of the catalysts used by Leitner.*

In 1995, Noyori provided the first review on CO<sub>2</sub> hydrogenation to formic acid/formate salt within a review dealing with the use of CO<sub>2</sub> as a C<sub>1</sub> building block for chemicals.<sup>[24]</sup> Noyori also ran the reaction in supercritical CO<sub>2</sub> and a TON of 7200 was obtained in an amine/water mix.<sup>[25]</sup> This high TON was made possible thanks to the solubilizing properties of the supercritical carbon dioxide.

In 2002, Jessop studied the effect of bases and additives (especially alcohol) with a [RuCl(OAc)(PMe<sub>3</sub>)<sub>4</sub>] catalyst. A TOF of 95 000 h<sup>-1</sup> was obtained in supercritical CO<sub>2</sub>/H<sub>2</sub> mixture (120/70 bar) using 0,6 μmol of catalyst with TEA and a small amount of pentafluorophenol at 50 °C. During the study, Jessop also noticed the beneficial effect of DMSO on the reaction.<sup>[26]</sup>

Later, in 2003, Jessop started to study the non-precious metals (Fe, Mo, Ni, Co, Cr, ...) in the hydrogenation of CO<sub>2</sub> with a combinatorial screening of homogeneous catalyst in DMSO under a total gas pressure of 100 bar (40 H<sub>2</sub>) at 50 °C for 8 h. The TON and TOF obtained ranged between 20/2,7 h<sup>-1</sup> and 117/16 h<sup>-1</sup>. A maximum TON of 4400 was obtained with [NiCl<sub>2</sub>(dcpe)] (5 μmol) in DMSO under 200 bar of gas for 216 h.<sup>[27]</sup>

During the 2000's several research have been conducted and in 2009, Nozaki peaked TON around 3 500 000 with an Iridium pincer catalyst.<sup>[28]</sup> The Iridium-hydride pincer catalyst used (Figure IV-1-4) was very efficient and the results are still among the best reached so far. The reaction was performed in a potassium hydroxide aqueous solution at 120 °C for 48 h under 50 bar of gas.

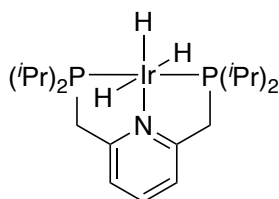
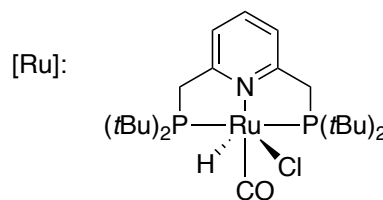
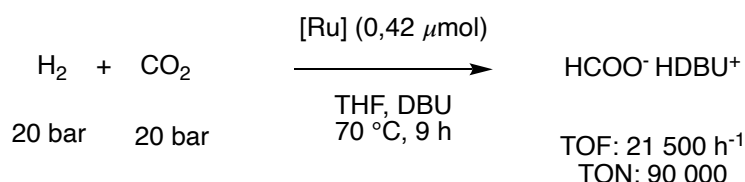


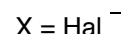
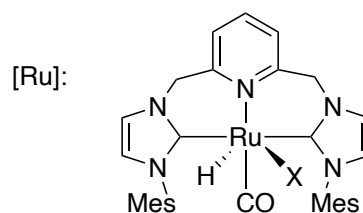
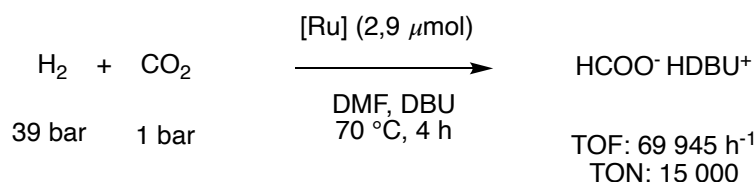
Figure IV - 1 - 4: Catalyst used by Nozaki.

During the last decade, several contributions and progress were achieved. We could in particular note the results reported by the group of Pidko with a work based on several ruthenium-pincer catalysts (Scheme IV-1-4) and mechanistic analysis.<sup>[29–31]</sup> Those catalysts displayed high TON and TOF under mild conditions of pressure and temperature. Pidko used a base to facilitate the reaction but also to activate the bifunctional catalyst used.

1)



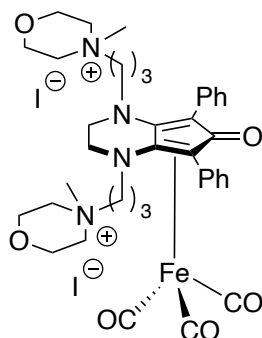
2)



Scheme IV - 1 - 4: CO<sub>2</sub> hydrogenation reported by Pidko.

As depicted here above, noble transition metals (Rh, Ir, Ru) have been almost exclusively used in the early researches. More recently, effort have been devoted to the utilisation of more abundant and lower cost transition metals. For example, in 2012, Beller and coworkers reported an Iron precursor [Fe(BF<sub>4</sub>)<sub>2</sub>·6H<sub>2</sub>O] associated with a tetradentate phosphorous ligand in MeOH/H<sub>2</sub>O at 100 °C under 60 bar of gas for 20 h leading to a TON of 1897.<sup>[32]</sup> Recently, in 2020, Renaud and coworkers proceed to the hydrogenation of CO<sub>2</sub> in

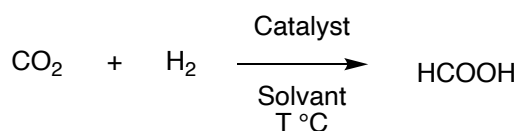
water with a bifunctional iron catalyst bearing ammonium moiety as solubilizing groups.<sup>[33]</sup> To run the reaction, the pre-catalyst (Figure IV-1-5) and the ligand Me<sub>3</sub>NO loadings were 0,001 mmol with triethanolamine (TEOA) as base under 20 bar of CO<sub>2</sub> and 60 bar of H<sub>2</sub> for 20 h at 100 °C. A TON up to 3343 was reached.



TON: 3 343

Figure IV - 1 - 5: Iron catalyst employed by Renaud.

### 3.1.2. Base free



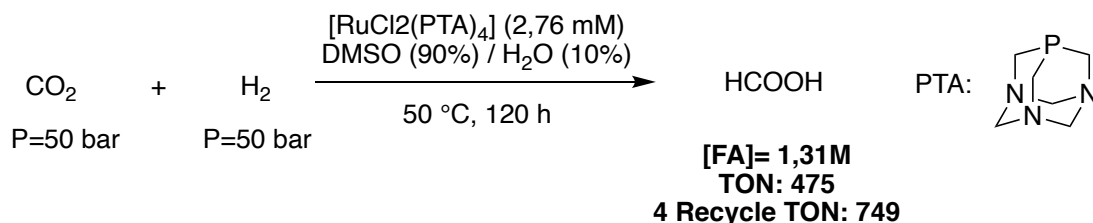
Scheme IV - 1 - 5: Hydrogenation of CO<sub>2</sub> without base.

Base free hydrogenation of carbon dioxide into Formic Acid is less developed because it is a more challenging transformation as it is not thermodynamically favored. Pioneer work have been accomplished in 1989 by Khan using a ruthenium catalyst in aqueous media under 34 bar of gases (H<sub>2</sub>/CO<sub>2</sub>) at 40 °C.<sup>[34]</sup> In this work the hydrogenation of CO<sub>2</sub> into formic acid was accompanied with the formation of formaldehyde and further decomposition into CO.

Then very few works have been published on base-free process in the 90's. We can find some example reported by Leitner with a rhodium catalyst under 40 bar<sup>[22]</sup>, Nicholas with a rhodium catalyst under 96 bar of gas<sup>[35]</sup> and Wong with a ruthenium catalyst under 80 bar of gas.<sup>[36]</sup> In all cases, very low TONs ranging from 6 to 64 were obtained.

Between 2000 and 2010, once again very few publications have been reported. The team of Ogo published some result still with low TON (35-55) with a ruthenium catalyst in water.<sup>[37,38]</sup>

It was during the last decade that the base free hydrogenation of CO<sub>2</sub> gained in interest and results were improved. In 2014, Laurenczy obtained a maximum TON of 475 that could be increased beyond 700 by recycling the catalyst.<sup>[39]</sup> A [RuCl<sub>2</sub>(PTA)<sub>4</sub>] catalyst was used in a DMSO/H<sub>2</sub>O mixture with a pressure of 100 bar and for an extended time of 120 h (Scheme IV-1-6). A hydride and dihydride species were observed by NMR under a pressure of 100 bar suggesting an inner sphere mechanism.



*Scheme IV - 1 - 6: Hydrogenation of Carbon dioxide by Laurenczy.*

In 2016, Leitner obtained a TON of 4200 that was a major breakthrough in a base free process with an AcriPhos Ruthenium catalyst (0,23 μmol) (Figure IV-1-6) in a 95% DMSO / 5% H<sub>2</sub>O media under high pressure (80 bar H<sub>2</sub>, 40 bar CO<sub>2</sub>) at 60 °C for 16 h.<sup>[40]</sup> As it was already noticed with previous work<sup>[20,22]</sup>, DMSO greatly improved the results of the reaction. The base free reaction is possible thanks to the stabilization of formic acid by DMSO through hydrogen bonding.

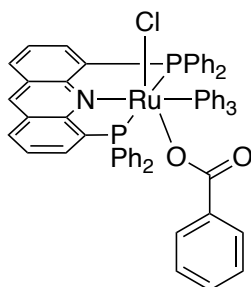
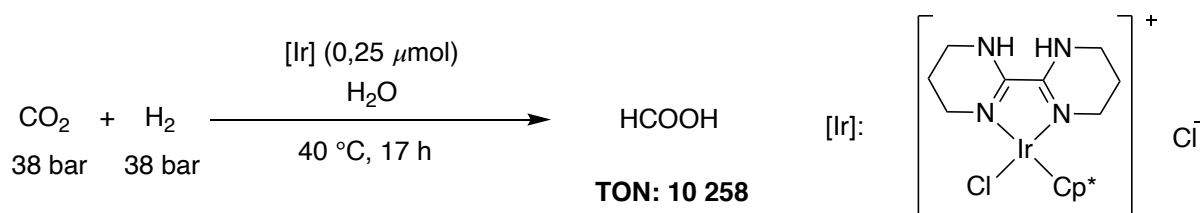


*Figure IV - 1 - 6: Catalyst used by Leitner.*

The same year, Li and co-workers performed their research with a diimine iridium catalyst.<sup>[41]</sup> Several diimine ligand were tested associated with an iridium precursor but it was a preformed catalyst that provided the best TON of 10 258 at a moderate temperature of 40 °C and pressure of 76 bar (Scheme IV-1-7). The mechanistic study run by the group did not show any implication of the ligand in the catalytic reaction.



*Scheme IV - 1 - 7: Hydrogenation reaction of Carbon dioxide by Li and co-workers.*

In Rennes, in 2017, Achard managed to obtain a TON of 355-370 with 6  $\mu\text{mol}$  of a ruthenium catalyst (Figure IV-1-7) in DMSO and 70 bar of gas for 72h. <sup>[42]</sup>

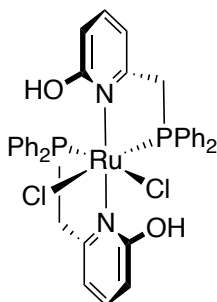


Figure IV - 1 - 7 : Catalyst used by Achard.

Very recently Han, adapted the  $[\text{RuCl}_2(\text{PTA})_4]$  catalyst in a continuous flow of formic acid production in water. <sup>[43]</sup> The reactor was split into two parts separated by a semi-permeable membrane with the reaction mixture and catalyst on one side and only water on the other side. The formic acid produced could pass through the membrane due to a difference in concentration and the flowing water hence shifting the equilibrium. Then, the flow of FA/ $\text{H}_2\text{O}$  went through an electrodialysis system to be concentrated and the residual mixture was returned to the reactor. Using this system, a TON of 35 000 was obtained in 10 days.

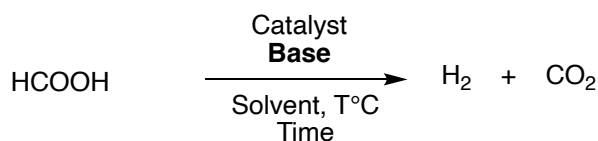
Finally, we can mention the use of ionic liquid for  $\text{CO}_2$  hydrogenation. Recently, in 2018 Dupont reported the hydrogenation of formic acid in ionic liquids. <sup>[44]</sup> Although no base was added, only ionic liquids made of anions with basic character led to the formation of formic acid. A TON of 3609 was achieved with the precursor  $[\text{Ru}_3(\text{CO})_{12}]$  under 40 bar of gas at 60 °C. The TON was increased up to 17 000 with a longer reaction time of 168 h.

### 3.2. Hydrogen release in homogeneous catalysis (Dehydrogenation of Formic acid to $\text{H}_2$ )

Pioneering work were reported by Coffey in 1967 using various metal transition-catalysts (Ru, Ir, Pt) in acidic media. <sup>[45]</sup> Then, studies about dehydrogenation of formic acid as the main subject were rare over decades because they were mostly associated with water-gas shift reaction and/or with low results. <sup>[35,46–51]</sup> We can cite the work of Puddephatt in the late 90's that focused on the decomposition of FA with a ruthenium catalyst  $[\text{Ru}_2(\mu\text{-CO})(\text{CO})_4(\mu\text{-dppm})_2]$  at 20 °C in acetone as solvent. Good results were obtained without base ( $\text{TOF}=500\text{h}^{-1}$ ) but those results were improved with a base. <sup>[52,53]</sup>

An expansion in the studies came after the concept of using formic acid as an energetic vector i.e., as a Liquid Organic Hydrogen Carrier (LOHC) to produce Hydrogen. This concept was independently published in 2008 by Beller <sup>[13]</sup> and Laurenczy. <sup>[14]</sup> Since then, the subject has gained in interest with researches dealing with noble or non-noble transition-metals and with base or base processes. <sup>[10,15,17]</sup>

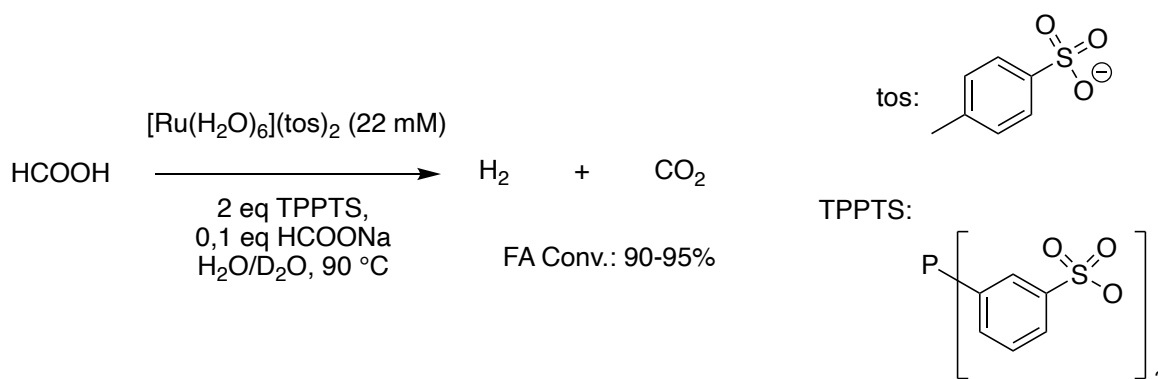
### 3.2.1. Dehydrogenation of Formic Acid under basic conditions



*Scheme IV - 1 - 8: Dehydrogenation of Formic Acid.*

First, it is important to have a look at the breakthrough work of Beller and Laurency in 2008 and the following years as they contributed a lot to that topic.

Laurency and coworkers published on a ruthenium catalyst in an aqueous media with sodium formate as an initiator that could convert all the formic acid into CO<sub>2</sub> and H<sub>2</sub> at 90 °C in less than 1 h (Scheme IV-1-9).<sup>[14]</sup>



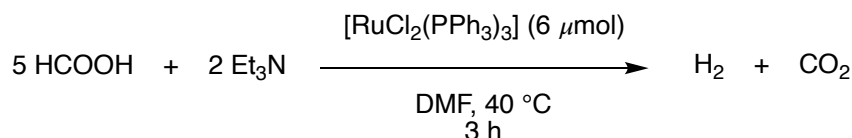
*Scheme IV - 1 - 9: Dehydrogenation of FA by Laurency.*

To apply this reaction on an energetical purpose, some parameters such as the gas generated, the pressure and the stability of the system over time have been evaluated. The gases detected were only CO<sub>2</sub> and H<sub>2</sub> without any trace of CO (below detection level). Generation of CO would be a downside because it can poison the fuel cell electrodes and so reduce its activity. For application in the energy field, it is important to generate a pressure of H<sub>2</sub> so it's mandatory to generate enough gas. Laurency measured a pressure of CO<sub>2</sub> and H<sub>2</sub> between 1 and 220 bar with no inhibition of the catalytic activity in a closed reactor. The stability and lifetime of the catalyst in solution was evaluated and the catalyst was still active over a year. The group applied with success a continuous addition of FA to the catalytic mixture. In this publication the group suggested this reaction as a step of a carbon dioxide cycle for a hydrogen storage system.

One year later the results obtained were developed and reinforced.<sup>[54]</sup> For example, a TON of 40 000 was calculated using the catalyst for 90 h over a month with a TOF of 670h<sup>-1</sup>. It was also noticed that the use of formate as an initiator was mandatory to ensure a short reaction time of 4 h vs 200 h in the absence of formate. Regarding the catalytic mechanism, an activation of the catalyst to form a hydride species was verified. Since then, Laurency regularly published on that subject. The group used various ligands to observed the stereo-electronic effects of the ligands on the reaction outcome.<sup>[55-57]</sup> They also evaluated other metallic center with the use of iridium and rhodium based catalyst with very good result

providing TOF above 1000 h<sup>-1</sup> and a full conversion of the FA.<sup>[58,59]</sup>

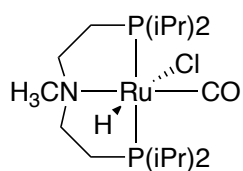
At the same period, Beller and coworkers, investigated the generation of hydrogen with a ruthenium complexes and a FA/Et<sub>3</sub>N mixture.<sup>[13]</sup> The preliminary tests were conducted with a neat 5FA/2Et<sub>3</sub>N mixture used in transfer hydrogenation<sup>[60]</sup> and a [RuCl<sub>2</sub>(*p*-cymene)]<sub>2</sub> catalyst at 40 °C during 6 h. Thanks to a pretreatment of [RuCl<sub>2</sub>(PPh<sub>3</sub>)<sub>3</sub>] in DMF, the results were improved and the maximum TOF (2688 h<sup>-1</sup>) obtained (Scheme IV-1-10) but a low



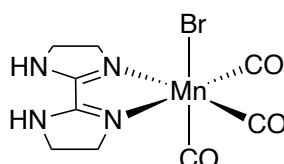
*Scheme IV - 1 - 10: Formic acid dehydrogenation by Beller.*

conversion of 8,9% was obtained. The reaction was connected to a H<sub>2</sub>/O<sub>2</sub> PEM fuel cell and was able to generate a maximum electric power of 47 mW. CO<sub>2</sub> and H<sub>2</sub> were the only gases detected during the experiments. Shortly after, the study was developed and parameters such as the ruthenium precursors and phosphine ligands tested.<sup>[61]</sup> Bis(Diphenylphosphino)ethane (Dppe) and Bis(Diphenylphosphino)propane (Dppp) bidentate ligand and also long chain amine base provided good catalyst activity. Nevertheless, the highest TOF (3630 h<sup>-1</sup>) was obtained with RuBr<sub>3</sub> associated with PPh<sub>3</sub> and TEA as base. No carbon monoxide was detected during the experiment which is mandatory if one want to apply this process to a power supply. The catalyst could be recycled at least once giving the same activity. Beller had the opportunity to create a set-up which used the hydrogen generated by the catalytic reaction to supply a fuel cell. The power generated decreased from 48 mW to 26 mW to remain constant for more than 42 h.

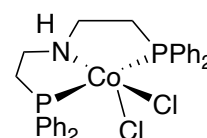
One year later, Beller, by using [RuCl<sub>2</sub>(benzene)]<sub>2</sub> with dppe as ligand, HexNMe<sub>2</sub> as a base and solvent at 40 °C, managed to reuse the system up to 10 times obtaining a TON of 60 000. The reaction could also be used continuously over 264h to achieve a TON of 260 000.<sup>[62]</sup> Bases and additives were further investigated in 2009.<sup>[63]</sup> Those researches guided Beller to set-up a mini plant generating continuously hydrogen from a FA/Amine mixture in 2013.<sup>[64]</sup> The same group investigated Ru pincer catalyst<sup>[65]</sup> as well as non-noble metal catalyst such as Fe<sup>[66,67]</sup>, Mn<sup>[68,69]</sup> or Co<sup>[70]</sup> (Figure IV-1-8).



TOF: 8981 h<sup>-1</sup>



TOF: 2161 h<sup>-1</sup>



TOF: 246 h<sup>-1</sup>

*Figure IV - 1 - 8: Recent work published by Beller.*

Wills in 2009, tested different metal-based catalyst and the best results were obtained with ruthenium catalysts. Three different ruthenium catalysts i.e. RuCl<sub>2</sub>(DMSO)<sub>4</sub>, anhydrous RuCl<sub>3</sub> and [Ru(NH<sub>3</sub>)<sub>6</sub>]Cl<sub>2</sub> exhibited similar activities with a maximum TOF of 17 400-18 000 using an azeotrope mixture of FA/Et<sub>3</sub>N at 120 °C. Extra FA could be added with no decrease in

the catalytic activity. The hydrogen generated could be used in a PEM fuel cell but no details were provided.

In 2013, Xiao tested a series of bifunctional cyclometallated-Iridium catalyst at 25 °C with a FA/Et<sub>3</sub>N mixture without solvent.<sup>[71]</sup> After ligand optimization (Figure IV-1-9) the initial

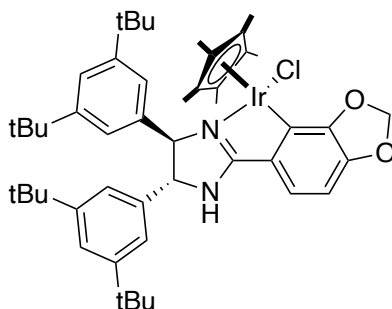
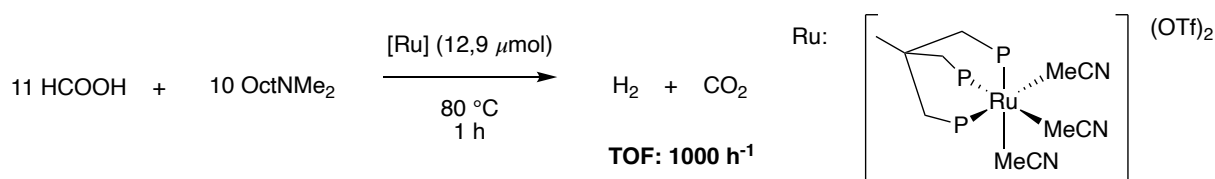


Figure IV - 1 - 9: Catalyst used by Xiao.

TOF obtained was 2570 h<sup>-1</sup>. The TOF was enhanced, by increasing the temperature to 40 °C, to an average of 3080-3340 h<sup>-1</sup>. To test the durability of the catalyst, the reaction was run over 2h with refill of FA and the TOF went up to 147 000 h<sup>-1</sup> for a short period of 10 seconds. A “long-range” MLC is envisaged for the mechanism with an important role of the N-H functionality.

The same year, Gonsalvi performed the dehydrogenation of FA with tripodal P-ligands with a FA/OctNMe<sub>2</sub> mixture at 80 °C.<sup>[72]</sup> Using the [Ru(k<sup>3</sup>-Triphos)(MeCN)<sub>3</sub>](OTf)<sub>2</sub>, a maximum TOF of 1000 h<sup>-1</sup> was achieved (Scheme IV-1-11). The reaction could be recycled with a gradual decrease of the TOF after the first cycle to 377 h<sup>-1</sup> at the 8<sup>th</sup> cycle but the conversion was still complete.



Scheme IV - 1 - 11: Formic Acid dehydrogenation reported by Gonsalvi.

One year later, the same group worked in an aqueous media with RuCl<sub>3</sub> catalyst precursor and a variety of aryl/alkyl sulfonated phosphine ligand to dehydrogenate a 9HCOOH/1HCOONa mixture at 90 °C.<sup>[73]</sup> The best TOF (1668 and 1776 h<sup>-1</sup>) was obtained with MTBS, P(biph)<sub>3</sub>TS and PhP(bisbiph)DS ligand (Figure IV-1-10). Once again it was possible to recycle the system and no CO was detected.

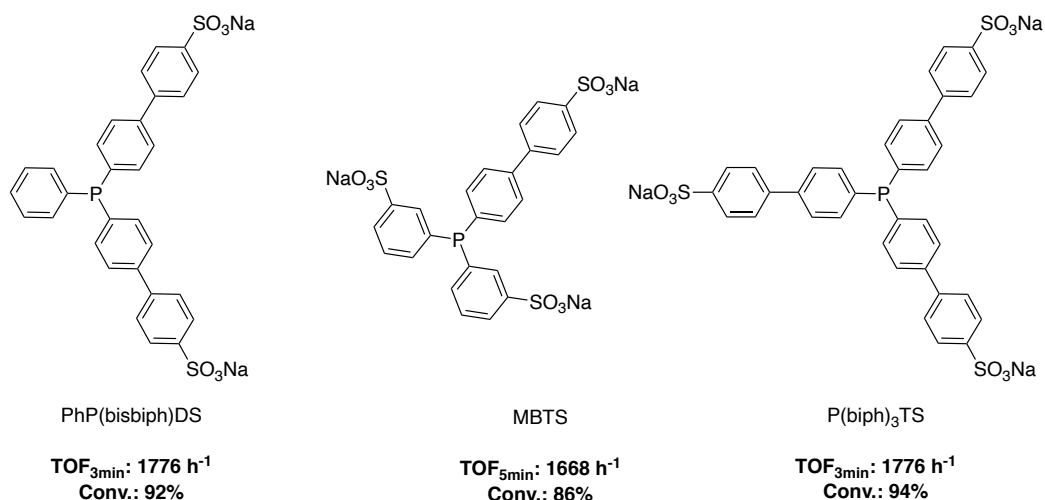


Figure IV - 1 - 10: Ligand used by Gonsalvi.

The same group further explored this field with a Ru precursor and tetraphosphine ligand.<sup>[74]</sup> A TOF up to 5579 h<sup>-1</sup> could be obtained with a FA/ N,N-Dimethyloctylamine at 80 °C.

After the use of non-noble metal for FA dehydrogenation by Beller,<sup>[66,67]</sup> Milstein and coworkers used an iron pincer catalyst to perform the reaction in 2013.<sup>[75]</sup> Initially, the objective was to perform the reaction without base but it was a failure. As a consequence, the reaction was made with a hydride iron PNP pincer catalyst (Figure IV-1-11) in the presence of 0,5 equivalent of TEA at 40 °C. TOFs between 520 and 653 h<sup>-1</sup> were obtained with THF, 1,4-dioxane and DMF as solvent. The best result (TOF: 836 h<sup>-1</sup>) was obtained using 1 equiv. of TEA and reducing the catalyst loading to 0,05 mol%.

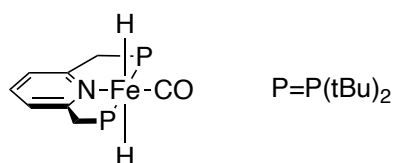
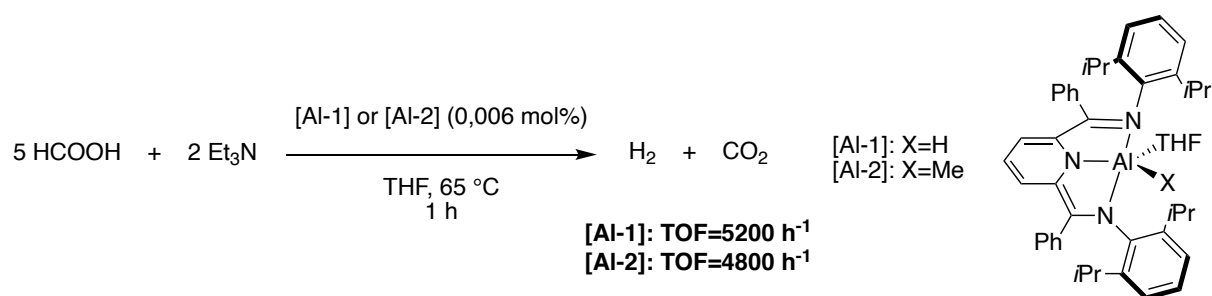


Figure IV - 1 - 11: Pincer Iron catalyst used by Milstein.

In 2014, Berben developed a pincer catalysts based on aluminium in refluxing THF and a FA/Et<sub>3</sub>N mixture with a TOF of 5200 h<sup>-1</sup> (Scheme IV-1-11).<sup>[76]</sup> The team envisage to obtained a protonated catalyst and the aromatization of the pyridine backbone with the coordination of two formate in a first step. Then, a β-hydride abstraction occurred leading to an Al-hydride intermediate which quickly release H<sub>2</sub> upon protonation by more FA.



Scheme IV - 1 - 12: Formic Acid dehydrogenation by Berben.

The same year, a study was made by Zacheria with Copper catalysts such as [Cu(OAc)<sub>2</sub>], [Cu(acac)<sub>2</sub>], [Cu(OOCH)<sub>2</sub>], [CuCl<sub>2</sub>], associated with different bulky amine base.<sup>[77]</sup> It was only a preliminary study with low results having a TOF ranging from 0,08 to 0,98 associated with a maximum conversion of 20%. A strong dependence to the amine used was noticed because the more basic and bulkier ones provided the best results.

In 2014, the group of Schneider studied the influence of Lewis acids (LA) with iron pincer catalysts (Figure IV-1-13) on the dehydrogenation of FA.<sup>[78]</sup> The aim of replacing a basic additive with a Lewis-acid was to enhance the efficiency of the reaction by reducing the amount of ligand used and/or the catalyst loading. Thanks to the use of LiBF<sub>4</sub> the dehydrogenation took place without base at a very low catalytic loading (0,0001 mol%) in

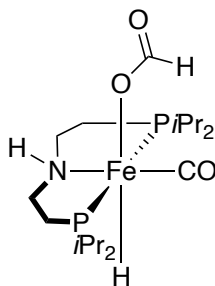


Figure IV - 1 - 12: Iron pincer used with LA by Schneider.

dioxane at 80 °C providing a TOF of 196 728 h<sup>-1</sup>. The LA co-catalyst aims to assist the decarboxylation of the iron formate intermediate.

Joó, in 2016, obtained one of the highest TOF (298 000h<sup>-1</sup>) with the dehydrogenation of a HCOOH/HCOONa mixture by an Iridium catalyst (9,9.10<sup>-6</sup> mol) (Figure IV-1-13) in an aqueous solution at 100 °C.<sup>[79]</sup> The batch can be re-used with fresh FA with a full conversion at least 5 times.

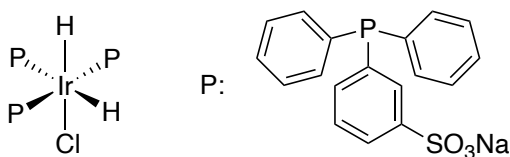
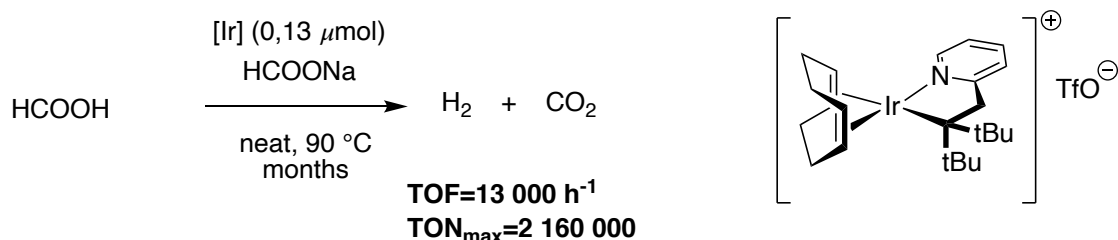


Figure IV - 1 - 13: Iridium catalyst used by Joó

The same year, Williams published one of the rare example on the dehydrogenation of neat formic acid with an Iridium cationic catalyst.<sup>[80]</sup> The system performed under neat condition at 90 °C and similar results were obtained with different base. This system had the advantage to be reused and yielded a TON of 2 160 000 and a maximum TOF of 13 000 h<sup>-1</sup> over a period of 4 months with 40 cycles (Scheme IV-1-13). During the mechanistic study, the group realized that the complex dimerized and then form a formate-bridged species.



*Scheme IV - 1 - 13: Dehydrogenation of Formic acid over 4 months by Williams*

Besides catalyst based on transition-metals center, in 2015, Cantat and coworkers reported the first metal-free catalyst able to dehydrogenate FA. Using boron based catalyst in deuterated-acetonitrile at 130 °C, a full conversion with a TON of 20 could be obtained with a FA/TEA mixture in 8 h.<sup>[81]</sup> The reaction could be run for a longer period of time showing a good stability. The catalyst dissociates in to an active formyloxyborane intermediate and the boron center can act as a lewis acid to proceed to the decarboxylation of the formate present.

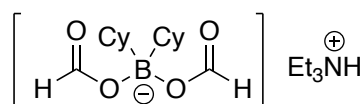
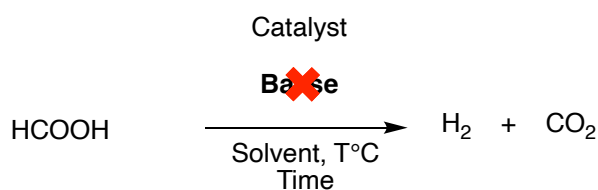


*Figure IV - 1 - 14: Organocatalyst used by Cantat.*

Dehydrogenation of formic acid with base (either formate or amine) is a field with intensive research since it has been proven that FA can be used as a hydrogen source. Beside the use of base to perform the dehydrogenation of FA, a strong interest has been growing recently concerning base-free dehydrogenation processes.

### 3.2.2. Base-free dehydrogenation of formic acid



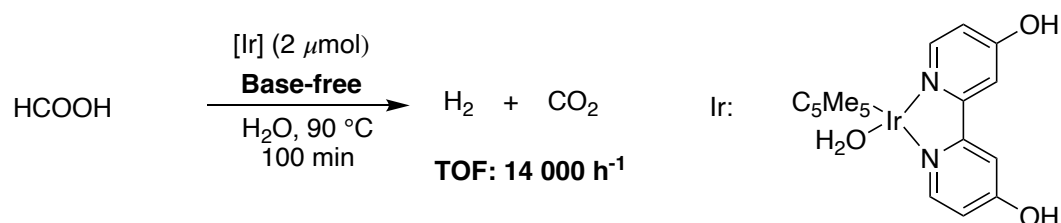
*Scheme IV - 1 - 14: Base-free Dehydrogenation reaction.*

We have notice, in the previous part, that the use of basic media promotes, accelerates and give better performances for the dehydrogenation of formic acid. However, the use of base or basic additives presents several drawbacks for the implementation of formic acid as a LOHC. Indeed, besides the economic and environmental cost implied by the use of a base,

those bases may require the application of a purification step between the production of hydrogen and its use in a fuel cell. Furthermore, the use of amine could have a negative impact on the fuel cell. In addition, the use of additives lowers the hydrogen content of the FA mixture. For all these reasons, base free FA dehydrogenation gained in interest in the recent years.

As mentioned earlier the base-free dehydrogenation started with the pioneer work of Coffey in 1967 where numerous catalyst (Pt, Ru, Ir) were employed in acetic acid with no additional additives.<sup>[45]</sup> In the late 90's, Puddephatt mentioned the decomposition of FA in acetone with a binuclear ruthenium catalyst in acetone (TOF: 500 h<sup>-1</sup>). In addition, improved performance in the presence of TEA was mentioned.<sup>[52,53]</sup>

The first publication focused on base-free dehydrogenation of FA was reported by Himeda in 2009. An iridium catalyst was used with a pH-responsive bipyridine ligand in an aqueous formic acid solution at 90 °C without any other additives (scheme IV-1-15).<sup>[82]</sup> A TOF of 14 000 h<sup>-1</sup> was obtained with almost a complete consumption of formic acid. The mixture could be refilled 5 times without degradation of the activity. No MLC is proposed for this mechanism. The first step is the formation of a formate complex as an intermediate to a hydride species via the elimination of CO<sub>2</sub>. Ir-H reacted with H<sup>+</sup> to produce H<sub>2</sub> and the catalyst was regenerated



*Scheme IV - 1 - 15: Base-free dehydrogenation of FA by Himeda.*

Prosenc and coworkers in 2010 used a platinum catalyst [PtH(PP<sub>3</sub>)]PF<sub>6</sub> (PP<sub>3</sub>: tris[(2-diphenylphosphino)ethyl]phosphine [P(CH<sub>2</sub>CH<sub>2</sub>PPh<sub>2</sub>)<sub>3</sub>]) in DCM at 35 °C (Figure IV-1-15). The initial FA concentration was reduced by half after 17 h with no further details.<sup>[83]</sup>

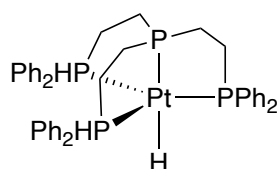
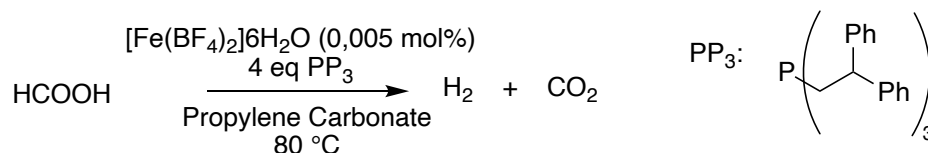


*Figure IV - 1 - 15: Catalyst used by Prosenc.*

In 2011, Laurenczy and Beller, described a non-noble transition-metal catalyst associated with a base free system.<sup>[67]</sup> Based either on iron precursors and phosphorus ligands or presynthesized iron-hydride catalysts in propylene carbonate as solvent, the best result (TOF= 9425 h<sup>-1</sup>) was obtained with Fe(BF<sub>4</sub>)<sub>6</sub>H<sub>2</sub>O and 4 equivalents of the tetradentate ligand tris[(2-diphenylphosphino)ethyl]phosphine [P(CH<sub>2</sub>CH<sub>2</sub>PPh<sub>2</sub>)<sub>3</sub>] at 80 °C (Scheme IV-1-16). To control the long-term stability, the reaction was run for 16 h before deactivation occurred. This work was further developed later in 2014 with CO measurement and scope for example.

[84] Two hypothesis are proposed for the mechanism using this catalyst. Nevertheless, both agreed on the formation of a hydride iron species  $[\text{HFePP}_3]$ . In a first proposal, formic acid coordinate in a chelating mode via the release of  $\text{H}_2$ . A  $\beta$ -elimination take place with the release of  $\text{CO}_2$  to reform the hydride catalyst. The second proposal consist of the coordination of the formate to the metal center. Then, the formation of  $\text{H}_2$  via the release of  $\text{CO}_2$  and the addition of  $\text{H}^+$  and finally, the release of  $\text{H}_2$  and the regeneration of the hydride species.



*Scheme IV - 1 - 16: FA dehydrogenation reported by Beller and Laurenczy.*

In 2013, Reek and coworkers, reported an Iridium-bisMETAMORPhos catalyst.<sup>[85]</sup> The ligand was chosen on purpose to act as a Brønsted base to provide a bifunctional catalyst (Figure IV-1-17) that could be used in base free reaction. The way of thinking was good since the base-free dehydrogenation of FA occurred with 0,005 mmol of catalyst in toluene at  $85^\circ\text{C}$  with a TOF of  $3092 \text{ h}^{-1}$ . The stability of the catalyst was proven as it could be left in the open air for a week without any deactivation. The batch could also be reused without deactivation.

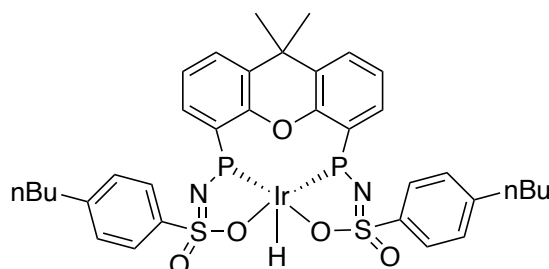
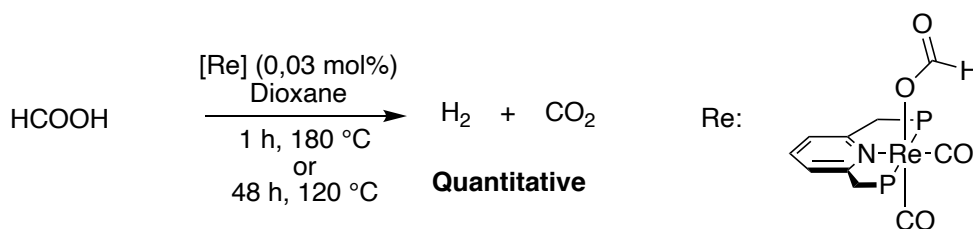


*Figure IV - 1 - 16: Catalyst used by Reek.*

Milstein briefly reported in 2014 the quantitative dehydrogenation of FA with a rhenium pincer complex with no need of a base thanks to a MLC (Scheme IV-1-16).<sup>[86]</sup>



*Scheme IV - 1 - 17: Dehydrogenation of Formic acid by the Rhenium catalyst developed by Milstein.*

Later on, Ikariya and Kayaki used a bifunctional [Cp\*Ir] catalyst (Figure IV-1-17) featuring Noyori-type diamino ligands and obtained a TOF of 4990 h<sup>-1</sup> (TON 1910) in a DME/H<sub>2</sub>O mixture at 35 °C for 1h.<sup>[87]</sup> The reaction could be run on a longer time to provide a maximum TON of 6780. Once the hydrido complex was isolated the performance was increased with a TOF of 6090 h<sup>-1</sup> (TON 2340) under the same conditions.

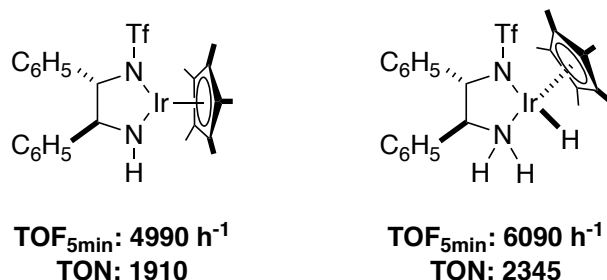


Figure IV - 1 - 17: Catalyst used by Ikariya.

In 2017, Kayaki studied the thermal stability of the catalyst developed earlier.<sup>[88]</sup> Due to a cyclometallation of the phenyl substituent of the diamino ligand backbone, the catalytic activity of the species was limited. The new catalyst synthesized (Figure IV-1-18) exhibited an increased stability that allows to run the reaction for a longer period and also to prevent the deactivation at higher temperature. For example, instead of running the reaction at 35 °C, it could be run at 60 °C to consumed 97% of the FA in 80 min instead of 98% in 5h the previous one.

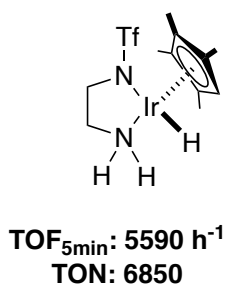
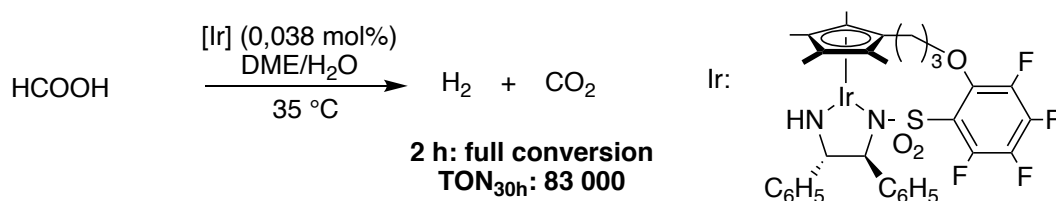


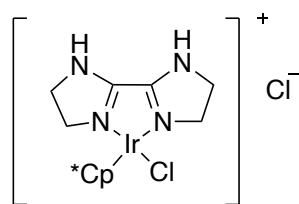
Figure IV - 1 - 18: Optimised catalyst by Kayaki.

In 2021 a tethered-iridium catalyst was developed by the same group to perform the FA dehydrogenation in DME/H<sub>2</sub>O (Scheme IV-1-17).<sup>[89]</sup> A full conversion was obtained and the catalyst was stable enough to run the reaction over 30 h with extra addition of FA.



Scheme IV - 1 - 18: Dehydrogenation of Formic Acid by tethered Iridium catalyst of Kayaki.

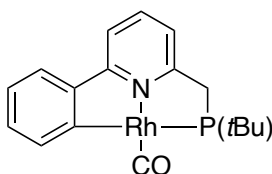
Li and coworker achieved unprecedented results with an iridium diimine catalyst (Figure IV-1-19).<sup>[90]</sup> With 1  $\mu\text{mol}$  of catalyst in an aqueous media at 90 °C the FA dehydrogenation was made in 10 min and a TOF of 487 000  $\text{h}^{-1}$  obtained with a conversion of 94%. The catalyst was active for 37 cycles with only a slight decrease in reactivity.



**Conv.: 94%**  
**TOF: 487 500  $\text{h}^{-1}$**

Figure IV - 1 - 19: Diimine Iridium catalyst used by Li.

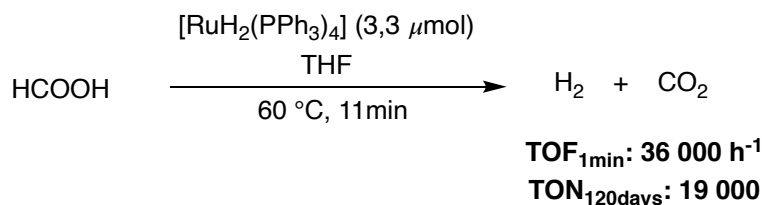
In 2016, Vlucht and coworker, used the dehydrogenation of FA as a proof of concept for a bifunctional rhodium catalyst (Figure IV-1-20).<sup>[91]</sup> A TOF of 169  $\text{h}^{-1}$  was obtained in dioxane at 75°C. The reaction did not produce any CO and can be recycled up to 8 times with a total TON of 1024. Using this catalyst, the reversible cyclometallation was investigated as the key element of the catalytic activity



**TOF: 169  $\text{h}^{-1}$**

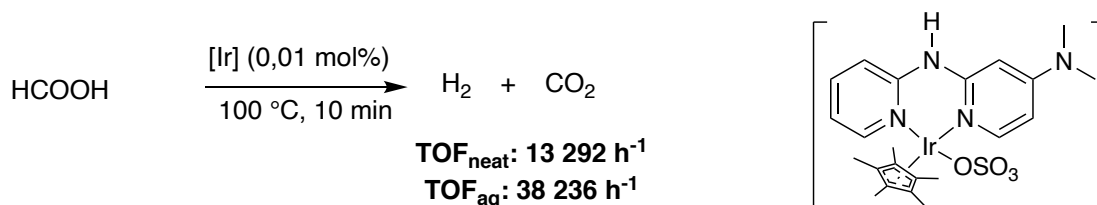
Figure IV - 1 - 20: Rhodium catalyst used by Vlucht.

In 2018, Beller used a rather simple ruthenium dihydride catalyst  $[\text{H}_2\text{Ru}(\text{PPh}_3)_4]$  that was active at 60 °C in THF providing a TOF of 36 000  $\text{h}^{-1}$  and a full conversion reached after 11 min (Scheme IV-1-18). A very good stability was proven as the reaction was loaded with 10 times the amount of FA and left running for 120 days providing a TON of 19 000 and a conversion about 95%.<sup>[92]</sup>



Scheme IV - 1 - 19: Dehydrogenation of Formic Acid made by Beller with a Ruthenium Hydride catalyst.

In 2019, Fischmeister and coworkers proceeded to the dehydrogenation of neat formic acid with an iridium dipyriddyamine catalyst at 100 °C (Scheme IV-1-19).<sup>[93]</sup> The TOF obtained was about 13 292 h<sup>-1</sup>. The reaction was also performed in aqueous media with a higher TOF of 38 236 h<sup>-1</sup>. The catalyst demonstrated a good stability with a latent behaviour i.e the reaction mixture could be prepared in advance, stored in a fridge for 2 and 10 days. The dehydrogenation was initiated later upon heating delivering TOFs about 4600 h<sup>-1</sup>. The result was only slightly lower compared to the reference reaction. No CO was detected in the gas flow generated during the dehydrogenation. The presence of the N-H bridge was found mandatory for the catalyst efficiency suggesting that H-bonding were involved in the reaction mechanism.



Scheme IV - 1 - 20: Formic acid dehydrogenation made by Fischmeister.

Recently the first cobalt catalyst (Figure IV-1-21) active in base-free dehydrogenation of FA was reported by Cantat. The PCP-hydride catalyst displayed a good activity with a TOF of 67 min<sup>-1</sup> at 80°C in Dioxane.<sup>[94]</sup> In this complex, the ligand participate in the catalytic activity as a hydrogen-bond donor. Indeed, a formate-complex intermediate is formed via the release of H<sub>2</sub> and it was stabilized thanks to the ligand prior the release of CO<sub>2</sub>.

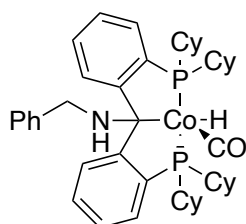


Figure IV - 1 - 21: Cobal catalyst used by Cantat.

Very recently, Milstein with a ruthenium-pincer catalyst (Figure IV-1-22) managed to obtain a TOF of 3067 h<sup>-1</sup> and to run the reaction in neat FA over a month to achieve a TON of 1 701 150.<sup>[95]</sup> The system could work in a closed system to reach up to 100 bar. It could also be set-up with a continuous addition of FA over 19 days to consumed a total of 1,2 L of FA with a decreasing flow rate. A plausible mechanism discussed in the publication consist of

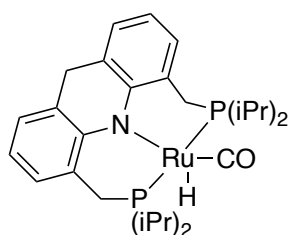


Figure IV - 1 - 22: Pincer Ruthenium catalyst used by Milstein in 2021.

the coordination of the FA in a first step. Then, dihydrogen is released and the formate act as a chelate ligand. Finally, CO<sub>2</sub> was released and the hydride complex reformed.

### 3.3. Reversible hydrogenation of Carbon dioxide

We have discussed above about the catalysts acting either as hydrogenation of CO<sub>2</sub> to Formic acid for the hydrogen storage or the dehydrogenation of formic acid for the release of H<sub>2</sub>. Having a catalyst able to perform the two reactions would be of a great interest specially on an energetical point of view. Indeed, the same system, depending on the reaction conditions, could either proceed to hydrogen storage or release. During this literature research, two possible cycles have been identified. The first system consists of identical reaction condition for the hydrogenation and the dehydrogenation except the pressure and the temperature (Figure IV-1-23 1)). The second system has different reaction conditions for the hydrogenation and the dehydrogenation with the addition of an additive or a change of solvent for example that imply a purification step (Figure IV-1-23 2)).

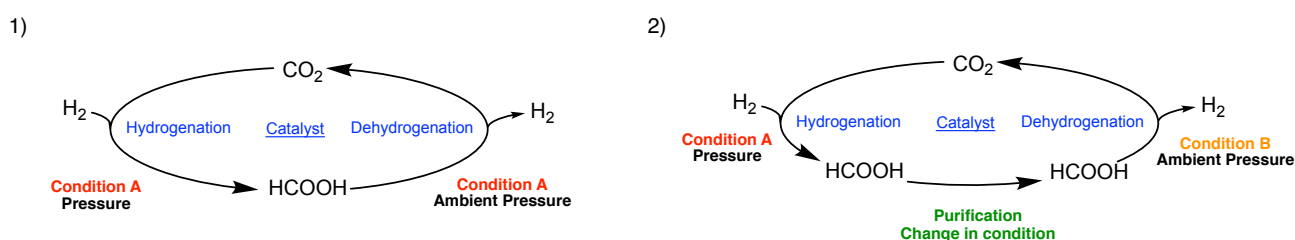


Figure IV - 1 - 23: Two different ways to make the reversible hydrogenation of Carbon Dioxide.

In an early work, Leitner realized the interest to have a catalyst able to make both reactions in the field of Hydrogen storage. Within a study on CO<sub>2</sub> hydrogenation, the decomposition of the FA/TEA mixture was observed after the gas pressure was released.<sup>[22]</sup> Hence the possibility for a catalyst to promote the two reactions of hydrogen storage and release was demonstrated.

A few years later, in 2000, by Puddephatt using a binuclear ruthenium catalyst (Figure IV-1-24) performed the reaction in both ways under different reaction conditions.<sup>[53]</sup> The hydrogenation of CO<sub>2</sub> to FA occurred with TEA in acetone reaching a total pressure of 70 bar. The TON obtained was about 2160 or 170 without base. On the opposite the dehydrogenation occurred in acetone without base with a TOF of 500 h<sup>-1</sup>.

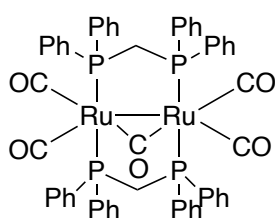
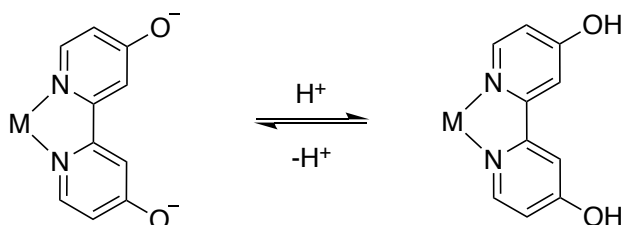


Figure IV - 1 - 24: Catalyst used by Puddephatt.

Following previous work on CO<sub>2</sub> conversion<sup>[96]</sup>, Himeda investigated the possibility to perform the reverse reaction.<sup>[97]</sup> Himeda employed ruthenium and rhodium catalyst with a pH-responsive dihydroxy-bipyridine ligand. Thus, CO<sub>2</sub> was treated with aqueous KOH to form potassium bicarbonate before the hydrogenation of the bicarbonate to formate took place. Then, the dehydrogenation happened with a FA/Formate mixture in an acidic media. Himeda observed a pH dependence of the system because the decomposition of FA was very poor with a pH above 4. Therefore, depending on the pH and so the catalyst structure, the system could be active either on hydrogenation or dehydrogenation (Scheme IV-1-20). Nevertheless, the two experiments were not tested one after the other.



*Scheme IV - 1 - 21: pH responsive catalyst by Himeda.*

Other groups worked with bicarbonate as an intermediate to perform a cycle such as Beller with a [RuCl<sub>2</sub>(benzene)]<sub>2</sub> precatalyst with dppe<sup>[98]</sup> Laurenczy and Joó with a ruthenium catalyst<sup>[99]</sup>, Enthaler with a PCP pincer nickel catalyst<sup>[100]</sup> or Olah with a PNP pincer ruthenium catalyst.<sup>[101]</sup>

Later, in 2016, Himeda using an pH dependent Iridium catalyst reported once again a system able to make the reaction in both ways under mild conditions.<sup>[102]</sup> The hydrogenation was carried out at 50 °C under 10 bar of gases in a basic aqueous media. The dehydrogenation took place in an acidic media at 60 °C. Very recently, Himeda published an Iridium catalyst with a bidentate ligand with a pyridine and a pyrazole moiety (Figure IV-1-25).<sup>[103]</sup> The catalyst was active in hydrogenation with a TON of 7850 in a basic aqueous solution of NaHCO<sub>3</sub> under 10 bar of gases at 50 °C. On the other hand, the dehydrogenation with a TOF of 6720 h<sup>-1</sup> took place in an aqueous solution of FA at 60 °C. However, once again, the hydrogenation directly followed by the dehydrogenation was not performed.

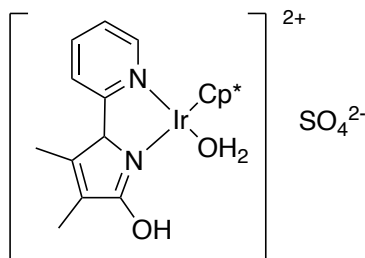
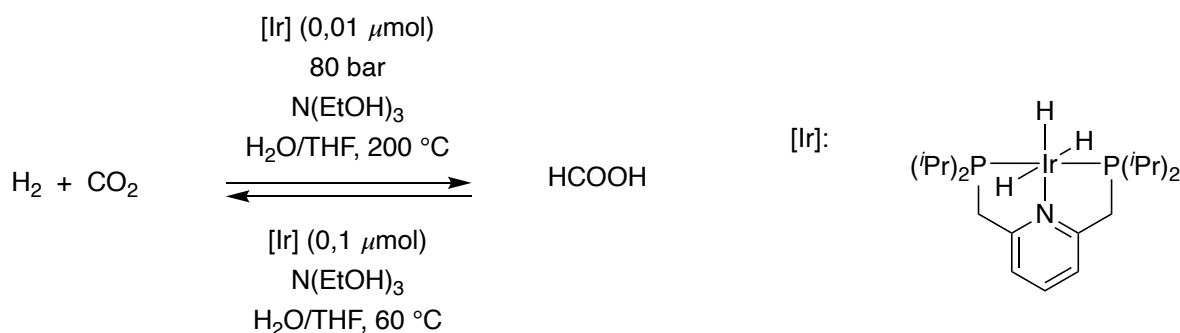


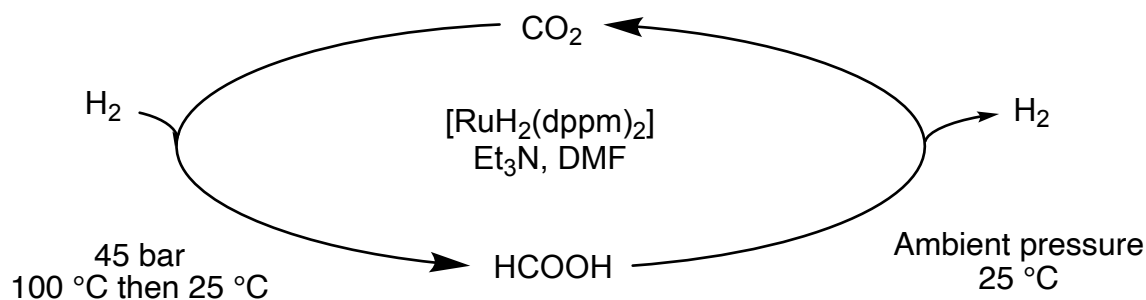
*Figure IV - 1 - 25: Catalyst used by Himeda in 2019.*

The iridium trihydride PNP pincer catalyst used by Nozaki for the hydrogenation of CO<sub>2</sub> into formic acid salt<sup>[28]</sup> was also active for the reverse reaction.<sup>[104]</sup> The reactions proceeded in an aqueous media using triethanolamine (TEOA) as a base. The hydrogenation took place under rather harsh condition of pressure and temperature of 80 bar and 200 °C giving a TON of 29 000. The dehydrogenation was carried out at 60 °C and furnished a TOF of 1 000 h<sup>-1</sup> (Scheme IV-1-22). The performances were lower compared to other catalysts explored by this group but it was the one that worked in both ways. The consecutive reactions were not performed using this catalyst.



Scheme IV - 1 - 22: Reversible hydrogenation of carbon dioxide made by Nozaki.

Beller and Laurency collaborated in 2012 to study and provide a ruthenium catalyst [RuH<sub>2</sub>(dppm)<sub>2</sub>] able to run up to 8 cycles of hydrogenation/dehydrogenation at room temperature (Scheme IV-1-23).<sup>[105]</sup> In a DMF/TEA solution, the CO<sub>2</sub> was converted to FA and formed an adduct with the TEA present. After cooling and gas release, the dehydrogenation of FA took also place at room temperature. After the 8<sup>th</sup> run, the activity decreased compared to the control experiment with a volume of gas of 1620 mL compared to 2105 mL during the first run. The cycles were performed using the same reaction mixture, the system just needed to be refilled with gases and fresh TEA. In this case, we are in the hypothesis 1) of the figure IV-1-23 with no change in condition, only a refill is necessary.



Scheme IV - 1 - 23: Reverse hydrogenation of carbon dioxide with the same reaction mixture by Beller and Laurency.

The same year, Fujita reported a dimeric iridium catalyst with pH sensitive ligands (Figure IV-1-26). Under basic condition CO<sub>2</sub> was hydrogenated to formate and under acidic condition the FA was dehydrogenated.<sup>[106]</sup> To make the reversible reaction, a flow of CO<sub>2</sub> and H<sub>2</sub> was bubbled in an aqueous solution of KHCO<sub>3</sub> with the Iridium catalyst for 136 h to produce 0,48M of formate. The pH was adjusted to 1,7 and the solution was heated to 50 °C resulting in the release of 2,3 MPa of gases with only 0,017M of FA remaining. This system worked despite its long first step (136 h). However, it seems not suitable for multiple cycling as it required a long preparation time to set-up the reaction and it also required to adjust the pH

of the solution to reverse the reactivity. This cycle illustrate hypothesis 2) of figure IV-1-23 with a deep change in the reaction condition to perform a cycle.

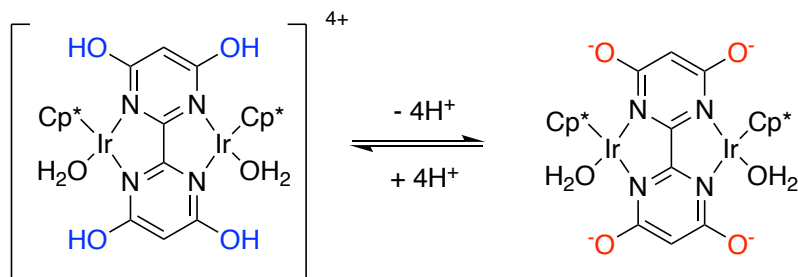
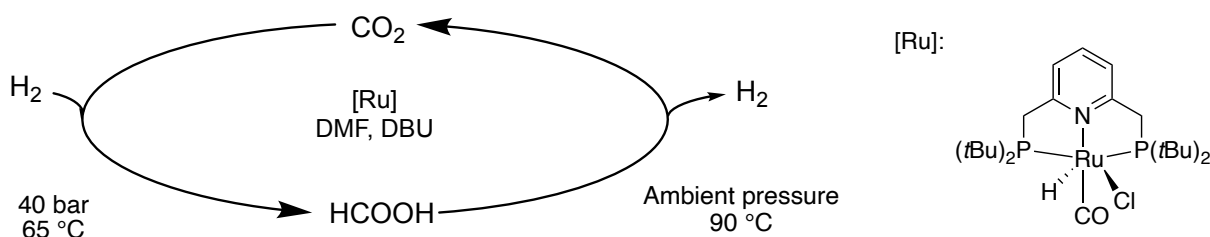


Figure IV - 1 - 26: pH switchable catalyst used by Fujita.

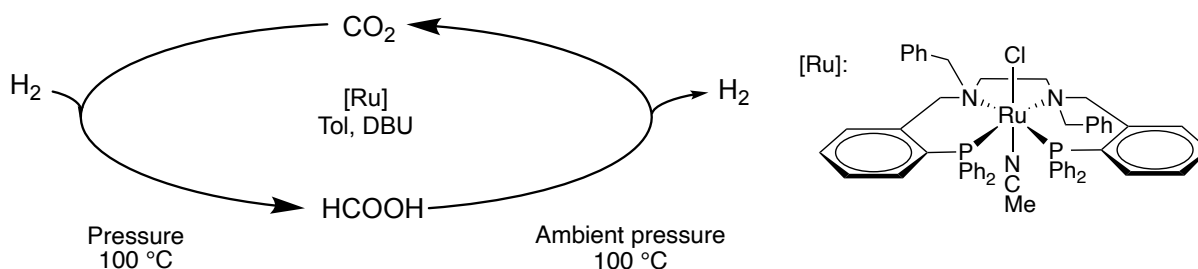
In 2014, Schneider, in a publication on iron pincer catalysts focused on the use of Lewis acid to enhance the reactivity of the dehydrogenation of FA, briefly reported a catalyst able to run the reaction in both ways.<sup>[78]</sup> The TON of the hydrogenation was about 186 in 12h at 80 °C with DBU as a base and a total pressure of 69 bar was reached. In the same condition with LiBF<sub>4</sub>, a TON of 289 in 4 h was obtained. The dehydrogenation gave a TOF of 572 h<sup>-1</sup> at 80 °C with TEA. Here, once again, a full cycle was not reported in this publication.

The same year, Pidko published on a ruthenium pincer catalyst operating in a DMF/DBU solvent mixture that could perform the hydrogen storage into FA under 60 bar at 65 °C and the hydrogen release at 90°C.<sup>[107]</sup> In a first step, both reactions were investigated separately. Finally, a cycle was made (Scheme IV-1-24) and the results obtained were close to the reference reactions with an FA/Amine ratio of 1,6 for the FA synthesis and a TOF around 150 000 h<sup>-1</sup> for the dehydrogenation of FA. Without any extra addition of base, 5 cycles could be made with no decrease in the catalytic activity. The hydrogenation reaction also worked with a low pressure of 5 bar with a FA/Amine ratio of 1,1.



Scheme IV - 1 - 24: Reversible hydrogenation of Carbon dioxide by Pidko.

Still in 2014, Plietker investigated the reversible Hydrogen storage with a PNNP-ruthenium-pincer catalyst and the unusual use of dry ice.<sup>[108]</sup> The charging procedure took place in toluene with DBU. Then, dry ice was added and the reactor was charged with 70 bar of H<sub>2</sub>. The reaction mixture was heated to 100 °C for 1 h. The reaction was degassed and left to cool down prior to the discharging process. The discharging process operated at ambient pressure at 100 °C until the gas flow ceased. After the first run, the charging reaction time was extended to 2,5 h and up to 5 cycles could be made (Scheme IV-1-24). The TON of charging was about 5600 and the TOF concerning the discharging was around 1140 h<sup>-1</sup>.



Scheme IV - 1 - 25: Charging and discharging cycle made by Plietker.

In 2018, Bernskoetter after previous work on the dehydrogenation of FA <sup>[78,109]</sup> with iron catalyst, developed a second generation of catalysts bearing an isonitrile ligand (Figure IV-1-27). <sup>[110]</sup> The results were not improved but the reverse reaction of CO<sub>2</sub> hydrogenation was tested and revealed that these new catalysts were active in dehydrogenation and also in hydrogenation. The hydrogenation was performed in a THF/DBU mixture with LiOTf at 80 °C with a total pressure of 69 bar. The TON obtained ranged from 610 to 5300. The dehydrogenation was made with TEA and dioxane at 80 °C leading to TOFs between 100 and 120 h<sup>-1</sup>. Those catalysts required a change in the reaction condition to perform the 2 reversible reactions which is not practical for energetical applications.

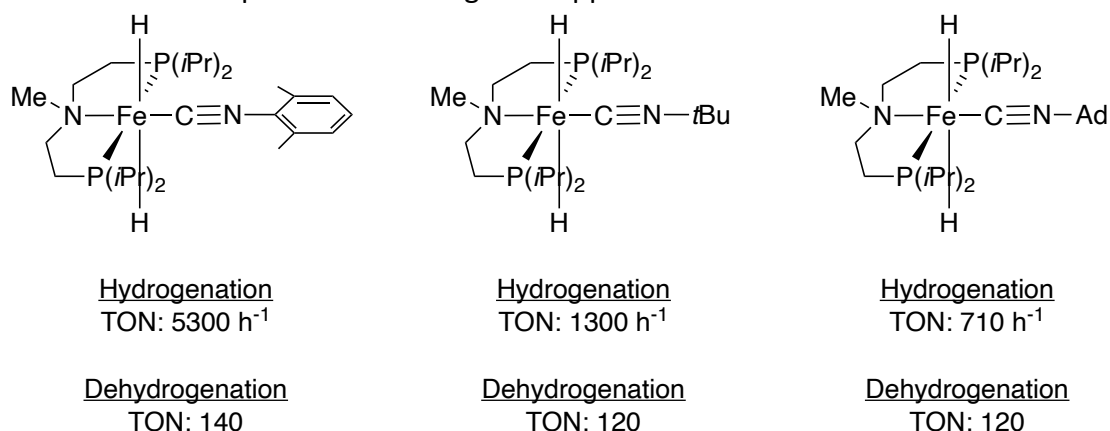
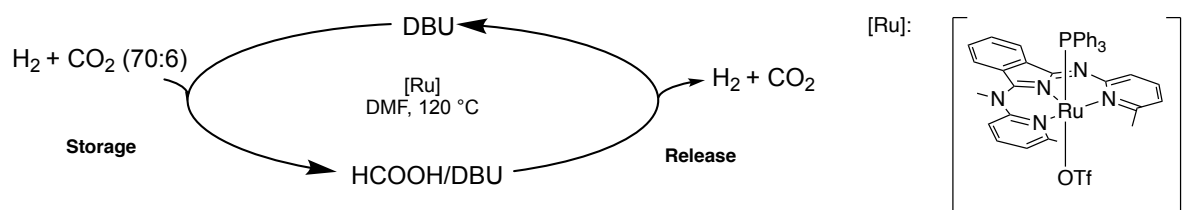


Figure IV - 1 - 27: Catalyst used by Bernskoetter for the hydrogenation of carbon dioxide and the dehydrogenation of FA.

Szymczak in 2018, used a series of NNN-ruthenium-pincer catalysts to perform the hydrogen storage and release with the same reaction mixture without any change in pH, solvent or additive. <sup>[111]</sup> Using the same mixture of DMF and DBU at 120 °C, the hydrogenation was performed with 76 bar of gases (6 CO<sub>2</sub> + 70 H<sub>2</sub>) leading to a TON of 28 000-60 000. The dehydrogenation was run under ambient pressure with a TON of 2 100-17 100. Then, the catalyst with the best performance was used to performed up to 6 cycles of hydrogenation/dehydrogenation (Scheme IV-1-26) with a decrease in the volume of gas released (707 mL to 522 mL).



Scheme IV - 1 - 26: Hydrogenation of Carbon dioxide and dehydrogenation of FA by Szymczak.

Very recently, Yi reported an iridium catalyst (Figure IV-1-28) able to perform the reaction in both ways but under different reaction conditions.<sup>[112]</sup> The Hydrogenation was run in water under 1 bar of gases (CO<sub>2</sub> and H<sub>2</sub>) with CsOH as a base at 25 °C leading to a TOF of 4,5 h<sup>-1</sup>. The dehydrogenation was run under base free conditions in water at 90 °C and a TOF of 19 400 h<sup>-1</sup> was achieved.

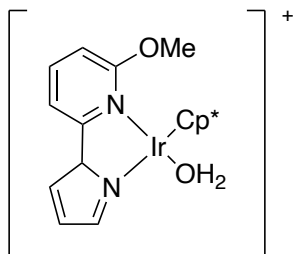


Figure IV - 1 - 28: Catalyst used by Yi.

As presented in this state of the art, a lot of effort has been dedicated to the reversible hydrogen storage and release. However, most of the time it needed different reaction conditions of solvent, additive, pH. Only a few catalysts reported by Beller and Laurenczy, Pidko, Plietker, Szymczak<sup>[105,107,108,111]</sup> were able to perform both of the reaction without any modification of the reaction media. It is important to note that no base-free cycle has been reported.

## 4. General conclusion

Hydrogen storage has attracted a lot of intense researches specially in the last two decades due to environmental issues. A lot of effort has been dedicated to basic system for higher activity in both hydrogenation of CO<sub>2</sub> and dehydrogenation of formic acid. Nevertheless base-free system gained in interest favored by bifunctional catalyst with a metal-ligand cooperation or by hydride catalyst formed in situ or not. Only a few of catalysts have been implemented in a full cycle of H storage. No base-free cycle has been reported yet. Thus, thanks to bifunctional catalyst **1** a full base-free H storage is targeted in this thesis research in the next chapter.

## 5. References:

- [1] “Space applications of hydrogen and fuel cells,” can be found under <https://www.nasa.gov/content/space-applications-of-hydrogen-and-fuel-cells>, **n.d.**
- [2] J. O. Bockris, *Science* **1972**, 176, 1323.
- [3] M. Kayfeci, A. Keçebaş, M. Bayat, in *Sol. Hydrog. Prod.*, Elsevier, **2019**, pp. 45–83.
- [4] A. M. Abdalla, *Energy Convers. Manag.* **2018**, 165, 602–627.
- [5] J. Andersson, S. Grönkvist, *Int. J. Hydrog. Energy* **2019**, 44, 11901–11919.
- [6] H. Barthelemy, M. Weber, F. Barbier, *Int. J. Hydrog. Energy* **2017**, 42, 7254–7262.
- [7] A. F. Dalebrook, W. Gan, M. Grasemann, S. Moret, G. Laurenczy, *Chem. Commun.* **2013**, 49, 8735.
- [8] P. Preuster, C. Papp, P. Wasserscheid, *Acc. Chem. Res.* **2017**, 50, 74–85.
- [9] M. Taube, D. Rippin, D. Cresswell, W. Knecht, *Int. J. Hydrog. Energy* **1983**, 8, 213–225.
- [10] K. Sordakis, C. Tang, L. K. Vogt, H. Junge, P. J. Dyson, M. Beller, G. Laurenczy, *Chem. Rev.* **2018**, 118, 372–433.
- [11] F. Joó, *ChemSusChem* **2008**, 1, 805–808.
- [12] D. A. Bulushev, J. R. H. Ross, *ChemSusChem* **2018**, 11, 821–836.
- [13] B. Loges, A. Boddien, H. Junge, M. Beller, *Angew. Chem. Int. Ed.* **2008**, 47, 3962–3965.
- [14] C. Fellay, P. Dyson, G. Laurenczy, *Angew. Chem. Int. Ed.* **2008**, 47, 3966–3968.
- [15] W.-H. Wang, Y. Himeda, J. T. Muckerman, G. F. Manbeck, E. Fujita, *Chem. Rev.* **2015**, 115, 12936–12973.
- [16] D. Mellmann, P. Sponholz, H. Junge, M. Beller, *Chem. Soc. Rev.* **2016**, 45, 3954–3988.
- [17] N. Onishi, G. Laurenczy, M. Beller, Y. Himeda, *Coord. Chem. Rev.* **2018**, 373, 317–332.
- [18] Inoue, Yoshio, Izumida, Hitoshi, Sasaki, Yoshiyuki, Hashimoto, Harukichi, *Chem. Lett.* **1976**, 5, 863–864.
- [19] W. Leitner, *Angew. Chem. Int. Ed. Engl.* **1995**, 34, 2207–2221.
- [20] E. Graf, W. Leitner, *J. Chem. Soc., Chem. Commun.* **1992**, 623–624.
- [21] F. Gassner, W. Leitner, *J. Chem. Soc., Chem. Commun.* **1993**, 1465–1466.
- [22] W. Leitner, *J. Organomet. Chem.* **1994**, 465, 257–266.
- [23] E. Graf, W. Leitner, *Chem. Ber.* **1996**, 129, 91–96.
- [24] P. G. Jessop, T. Ikariya, R. Noyori, *Chem. Rev.* **1995**, 95, 259.
- [25] R. Noyori, T. Ikariya, P. G. Jessop, *Nature* **1994**, 368, 231–233.
- [26] P. Munshi, A. D. Main, J. C. Linehan, C.-C. Tai, P. G. Jessop, *J. Am. Chem. Soc.* **2002**, 124, 7963–7971.
- [27] C.-C. Tai, T. Chang, B. Roller, P. G. Jessop, *Inorg. Chem.* **2003**, 42, 7340–7341.
- [28] R. Tanaka, M. Yamashita, K. Nozaki, *J. Am. Chem. Soc.* **2009**, 131, 14168–14169.
- [29] G. A. Filonenko, M. P. Conley, C. Copéret, M. Lutz, E. J. M. Hensen, E. A. Pidko, *ACS Catal.* **2013**, 3, 2522–2526.
- [30] G. A. Filonenko, E. Cosimi, L. Lefort, M. P. Conley, C. Copéret, M. Lutz, E. J. M. Hensen, E. A. Pidko, *ACS Catal.* **2014**, 4, 2667–2671.
- [31] G. A. Filonenko, D. Smykowski, B. M. Szyja, G. Li, J. Szczygieł, E. J. M. Hensen, E. A. Pidko, *ACS Catal.* **2015**, 5, 1145–1154.
- [32] C. Ziebart, C. Federsel, P. Anbarasan, R. Jackstell, W. Baumann, A. Spannenberg, M. Beller, *J. Am. Chem. Soc.* **2012**, 134, 20701–20704.
- [33] S. Coufourier, Q. Gaignard Gaillard, J.-F. Lohier, A. Poater, S. Gaillard, J.-L. Renaud, *ACS Catal.* **2020**, 10, 2108–2116.
- [34] M. M. T. Khan, S. B. Halligudi, S. Shukla, *J. Mol. Catal.* **1989**, 57, 47–60.

- [35] J. C. Tsai, K. M. Nicholas, *J. Am. Chem. Soc.* **1992**, *114*, 5117–5124.
- [36] H. S. Chu, C. P. Lau, K. Y. Wong, W. T. Wong, *Organometallics* **1998**, *17*, 2768–2777.
- [37] H. Hayashi, S. Ogo, S. Fukuzumi, *Chem. Commun.* **2004**, 2714.
- [38] S. Ogo, R. Kabe, H. Hayashi, R. Harada, S. Fukuzumi, *Dalton Trans.* **2006**, 4657.
- [39] S. Moret, P. J. Dyson, G. Laurenczy, *Nat. Commun.* **2014**, *5*, 4017.
- [40] K. Rohmann, J. Kothe, M. W. Haenel, U. Englert, M. Hölscher, W. Leitner, *Angew. Chem. Int. Ed.* **2016**, *55*, 8966–8969.
- [41] S.-M. Lu, Z. Wang, J. Li, J. Xiao, C. Li, *Green Chem.* **2016**, *18*, 4553–4558.
- [42] A. R. Sahoo, F. Jiang, C. Bruneau, G. V. M. Sharma, S. Suresh, T. Roisnel, V. Dorcet, M. Achard, *Catal. Sci. Technol.* **2017**, *7*, 3492–3498.
- [43] Z. Zhang, S. Liu, M. Hou, G. Yang, B. Han, *Green Chem.* **2021**, *23*, 1978–1982.
- [44] A. Weilhard, M. I. Qadir, V. Sans, J. Dupont, *ACS Catal.* **2018**, *8*, 1628–1634.
- [45] R. S. Coffey, *Chem. Commun. Lond.* **1967**, 923–924.
- [46] T. Yoshida, Y. Ueda, S. Otsuka, *J. Am. Chem. Soc.* **1978**, *100*, 3941–3942.
- [47] R. B. King, A. D. King, N. K. Bhattacharyya, *Transit. Met. Chem.* **1995**, *20*, 321–326.
- [48] R. M. Laine, R. G. Rinker, P. C. Ford, *J. Am. Chem. Soc.* **1977**, *99*, 252–253.
- [49] S. H. Strauss, K. H. Whitmire, D. F. Shriver, **1979**, *174*, 59–62.
- [50] R. S. Paonessa, W. C. Troglor, *J. Am. Chem. Soc.* **1982**, *104*, 3529–3530.
- [51] C. Po Lau, S. Man Ng, Z. Zhongyuan, M. Man Lok, *Dalton Trans.* **2003**, *19*, 3727–3735.
- [52] Y. Gao, J. Kuncheria, R. J. Puddephatt, G. P. A. Yap, *Chem. Commun.* **1998**, 2365–2366.
- [53] Y. Gao, J. K. Kuncheria, H. A. Jenkins, R. J. Puddephatt, G. P. A. Yap, *J. Chem. Soc. Dalton Trans.* **2000**, 3212–3217.
- [54] C. Fellay, N. Yan, P. J. Dyson, G. Laurenczy, *Chem. - Eur. J.* **2009**, *15*, 3752–3760.
- [55] W. Gan, C. Fellay, P. J. Dyson, G. Laurenczy, *J. Coord. Chem.* **2010**, *63*, 2685–2694.
- [56] W. Gan, D. J. M. Snelders, P. J. Dyson, G. Laurenczy, *ChemCatChem* **2013**, *5*, 1126–1132.
- [57] C. Fink, L. Chen, G. Laurenczy, *Z. Für Anorg. Allg. Chem.* **2018**, *644*, 740–744.
- [58] C. Fink, G. Laurenczy, *Dalton Trans.* **2017**, *46*, 1670–1676.
- [59] C. Fink, G. Laurenczy, *Eur. J. Inorg. Chem.* **2019**, *2019*, 2381–2387.
- [60] S. Gladiali, E. Alberico, *Chem Soc Rev* **2006**, *35*, 226–236.
- [61] A. Boddien, B. Loges, H. Junge, M. Beller, *ChemSusChem* **2008**, *1*, 751–758.
- [62] A. Boddien, B. Loges, H. Junge, F. Gärtner, J. R. Noyes, M. Beller, *Adv. Synth. Catal.* **2009**, *351*, 2517–2520.
- [63] H. Junge, A. Boddien, F. Capitta, B. Loges, J. R. Noyes, S. Gladiali, M. Beller, *Tetrahedron Lett.* **2009**, *50*, 1603–1606.
- [64] P. Sponholz, D. Mellmann, H. Junge, M. Beller, *ChemSusChem* **2013**, *6*, 1172–1176.
- [65] A. Agapova, E. Alberico, A. Kammer, H. Junge, M. Beller, *ChemCatChem* **2019**, *11*, 1910–1914.
- [66] A. Boddien, B. Loges, F. Gärtner, C. Torborg, K. Fumino, H. Junge, R. Ludwig, M. Beller, *J. Am. Chem. Soc.* **2010**, *132*, 8924–8934.
- [67] A. Boddien, D. Mellmann, F. Gärtner, R. Jackstell, H. Junge, P. J. Dyson, G. Laurenczy, R. Ludwig, M. Beller, *Science* **2011**, *333*, 1733–1736.
- [68] A. Léval, H. Junge, M. Beller, *Catal. Sci. Technol.* **2020**, *10*, 3931–3937.
- [69] A. Léval, A. Agapova, C. Steinlechner, E. Alberico, H. Junge, M. Beller, *Green Chem.* **2020**, *22*, 913–920.
- [70] W. Zhou, Z. Wei, A. Spannenberg, H. Jiao, K. Junge, H. Junge, M. Beller, *Chem. – Eur. J.* **2019**, *25*, 8459–8464.
- [71] J. H. Barnard, C. Wang, N. G. Berry, J. Xiao, *Chem. Sci.* **2013**, *4*, 1234.

- [72] I. Mellone, M. Peruzzini, L. Rosi, D. Mellmann, H. Junge, M. Beller, L. Gonsalvi, *Dalton Trans* **2013**, 42, 2495–2501.
- [73] A. Guerriero, H. Bricout, K. Sordakis, M. Peruzzini, E. Monflier, F. Hapiot, G. Laurenczy, L. Gonsalvi, *ACS Catal.* **2014**, 4, 3002–3012.
- [74] I. Mellone, F. Bertini, M. Peruzzini, L. Gonsalvi, *Catal. Sci. Technol.* **2016**, 6, 6504–6512.
- [75] T. Zell, B. Butschke, Y. Ben-David, D. Milstein, *Chem. - Eur. J.* **2013**, 19, 8068–8072.
- [76] T. W. Myers, L. A. Berben, *Chem Sci* **2014**, 5, 2771–2777.
- [77] N. Scotti, R. Psaro, N. Ravasio, F. Zaccheria, *RSC Adv* **2014**, 4, 61514–61517.
- [78] E. A. Bielinski, P. O. Lagaditis, Y. Zhang, B. Q. Mercado, C. Würtele, W. H. Bernskoetter, N. Hazari, S. Schneider, *J. Am. Chem. Soc.* **2014**, 136, 10234–10237.
- [79] G. Papp, G. Ölveti, H. Horváth, Á. Kathó, F. Joó, *Dalton Trans.* **2016**, 45, 14516–14519.
- [80] J. J. A. Celaje, Z. Lu, E. A. Kedzie, N. J. Terrile, J. N. Lo, T. J. Williams, *Nat. Commun.* **2016**, 7, 11308.
- [81] C. Chauvier, A. Tlili, C. Das Neves Gomes, P. Thuéry, T. Cantat, *Chem. Sci.* **2015**, 6, 2938–2942.
- [82] Y. Himeda, *Green Chem.* **2009**, 11, 2018.
- [83] T. P. Rieckborn, E. Huber, E. Karakoc, M. H. Prosenc, *Eur. J. Inorg. Chem.* **2010**, 2010, 4757–4761.
- [84] D. Mellmann, E. Barsch, M. Bauer, K. Grabow, A. Boddien, A. Kammer, P. Sponholz, U. Bentrup, R. Jackstell, H. Junge, G. Laurenczy, R. Ludwig, M. Beller, *Chem. – Eur. J.* **2014**, 20, 13589–13602.
- [85] S. Oldenhof, B. de Bruin, M. Lutz, M. A. Siegler, F. W. Patureau, J. I. van der Vlugt, J. N. H. Reek, *Chem. - Eur. J.* **2013**, 19, 11507–11511.
- [86] M. Vogt, A. Nerush, Y. Diskin-Posner, Y. Ben-David, D. Milstein, *Chem Sci* **2014**, 5, 2043–2051.
- [87] A. Matsunami, Y. Kayaki, T. Ikariya, *Chem. - Eur. J.* **2015**, 21, 13513–13517.
- [88] A. Matsunami, S. Kuwata, Y. Kayaki, *ACS Catal.* **2017**, 7, 4479–4484.
- [89] H. Nakamura, M. Yoshida, A. Matsunami, S. Kuwata, Y. Kayaki, *Chem. Commun.* **2021**, 57, 5534–5537.
- [90] Z. Wang, S.-M. Lu, J. Li, J. Wang, C. Li, *Chem. - Eur. J.* **2015**, 21, 12592–12595.
- [91] L. S. Jongbloed, B. de Bruin, J. N. H. Reek, M. Lutz, J. I. van der Vlugt, *Catal. Sci. Technol.* **2016**, 6, 1320–1327.
- [92] C. Prichatz, M. Trincado, L. Tan, F. Casas, A. Kammer, H. Junge, M. Beller, H. Grützmacher, *ChemSusChem* **2018**, 11, 3092–3095.
- [93] S. Wang, H. Huang, T. Roisnel, C. Bruneau, C. Fischmeister, *ChemSusChem* **2019**, 12, 179–184.
- [94] N. Lentz, A. Aloisi, P. Thuéry, E. Nicolas, T. Cantat, *Organometallics* **2021**, 40, 565–569.
- [95] S. Kar, M. Rauch, G. Leitus, Y. Ben-David, D. Milstein, *Nat. Catal.* **2021**, 4, 193–201.
- [96] Y. Himeda, N. Onozawa-Komatsuzaki, H. Sugihara, K. Kasuga, *Organometallics* **2007**, 26, 702–712.
- [97] Y. Himeda, S. Miyazawa, T. Hirose, *ChemSusChem* **2011**, 4, 487–493.
- [98] A. Boddien, F. Gärtner, C. Federsel, P. Sponholz, D. Mellmann, R. Jackstell, H. Junge, M. Beller, *Angew. Chem. Int. Ed.* **2011**, 50, 6411–6414.
- [99] G. Papp, J. Csorba, G. Laurenczy, F. Joó, *Angew. Chem. Int. Ed.* **2011**, 50, 10433–10435.
- [100] S. Enthaler, A. Brück, A. Kammer, H. Junge, E. Irran, S. Gülak, *ChemCatChem* **2015**, 7, 65–69.
- [101] J. Kothandaraman, M. Czaun, A. Goeppert, R. Haiges, J.-P. Jones, R. B. May, G. K. S.

Prakash, G. A. Olah, *ChemSusChem* **2015**, *8*, 1442–1451.

[102] L. Wang, N. Onishi, K. Murata, T. Hirose, J. T. Muckerman, E. Fujita, Y. Himeda, *ChemSusChem* **2017**, *10*, 1071–1075.

[103] N. Onishi, R. Kanega, E. Fujita, Y. Himeda, *Adv. Synth. Catal.* **2019**, *361*, 289–296.

[104] R. Tanaka, M. Yamashita, L. W. Chung, K. Morokuma, K. Nozaki, *Organometallics* **2011**, *30*, 6742–6750.

[105] A. Boddien, C. Federsel, P. Sponholz, D. Mellmann, R. Jackstell, H. Junge, G. Laurenczy, M. Beller, *Energy Environ. Sci.* **2012**, *5*, 8907.

[106] J. F. Hull, Y. Himeda, W.-H. Wang, B. Hashiguchi, R. Periana, D. J. Szalda, J. T. Muckerman, E. Fujita, *Nat. Chem.* **2012**, *4*, 383–388.

[107] G. A. Filonenko, R. van Putten, E. N. Schulpen, E. J. M. Hensen, E. A. Pidko, *ChemCatChem* **2014**, *6*, 1526–1530.

[108] S.-F. Hsu, S. Rommel, P. Eversfield, K. Muller, E. Klemm, W. R. Thiel, B. Plietker, *Angew. Chem. Int. Ed.* **2014**, *53*, 7074–7078.

[109] Y. Zhang, A. D. MacIntosh, J. L. Wong, E. A. Bielinski, P. G. Williard, B. Q. Mercado, N. Hazari, W. H. Bernskoetter, *Chem. Sci.* **2015**, *6*, 4291–4299.

[110] J. B. Curley, N. E. Smith, W. H. Bernskoetter, N. Hazari, B. Q. Mercado, *Organometallics* **2018**, *37*, 3846–3853.

[111] J. B. Geri, J. L. Ciatti, N. K. Szymczak, *Chem. Commun.* **2018**, *54*, 7790–7793.

[112] X.-F. Mo, C. Liu, Z.-W. Chen, F. Ma, P. He, X.-Y. Yi, *Inorg. Chem.* **2021**, *60*, 16584–16592.

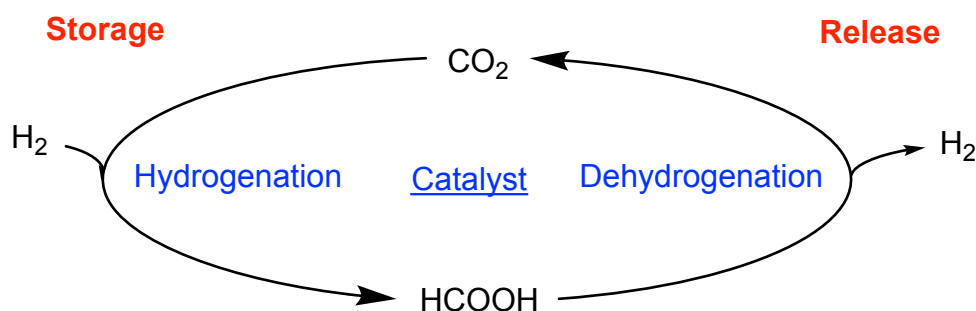


## Part 2: Catalytic application of $\eta^5$ - Oxocyclohexadienyl Ruthenium complex in the Hydrogen Storage



## 1. Introduction

As demonstrated in the state of the art, hydrogen storage is a topic of high importance in the Energy transition domain. LOHCs are among the possibilities of energy storage and as such they are receiving a lot of attention, in particular formic acid. We were interested about applying the  $\eta^5$ -Oxocyclohexadienyl ruthenium complex in this hot field of hydrogen storage (Scheme IV-2-1). Due to the bifunctional properties highlighted earlier in the manuscript, the catalyst **1** was applied to the hydrogen storage without base. Base-free conditions for hydrogen storage is a very challenging topic which is receiving increasing attention. Indeed, the use of base in such process is undesired for economic and environmental reasons. The use of bases is also a problem as it can contaminate the gas flow resulting from formic acid dehydrogenation hence requiring the installation of an intermediate gas purification unit. We have evaluated the potential of catalyst **1** in this very challenging domain. We first studied separately the CO<sub>2</sub> hydrogenation and the formic acid dehydrogenation and at the end we have studied the possibility to make a cycle.



*Scheme IV - 2 - 1: Cycle of Hydrogen storage.*

## 2. CO<sub>2</sub> hydrogenation / Hydrogen storage results and discussion

### 2.1. Preliminary results

To perform preliminary tests, DMSO was selected as a solvent as it was proven to be necessary for base-free CO<sub>2</sub> hydrogenation into FA. The amount of catalyst used was in the same range of what is usually reported in the literature i.e.,  $5,55 \cdot 10^{-6}$  mol ( $1,11 \cdot 10^{-5}$  mol of Ru). The pressure of 40 and 60 bar were chosen for the preliminary tests. The amount of FA synthesized was calculated thanks to an internal standard added at the end of the reaction and analyzed by NMR. A calibration curve was elaborated with commercial FA and DMF as standard (Figure IV-2-1). Hence, the amount of FA produced was determined as well as the productivity of the catalyst with the TON. In general, studies on CO<sub>2</sub> hydrogenation focus on this parameter.

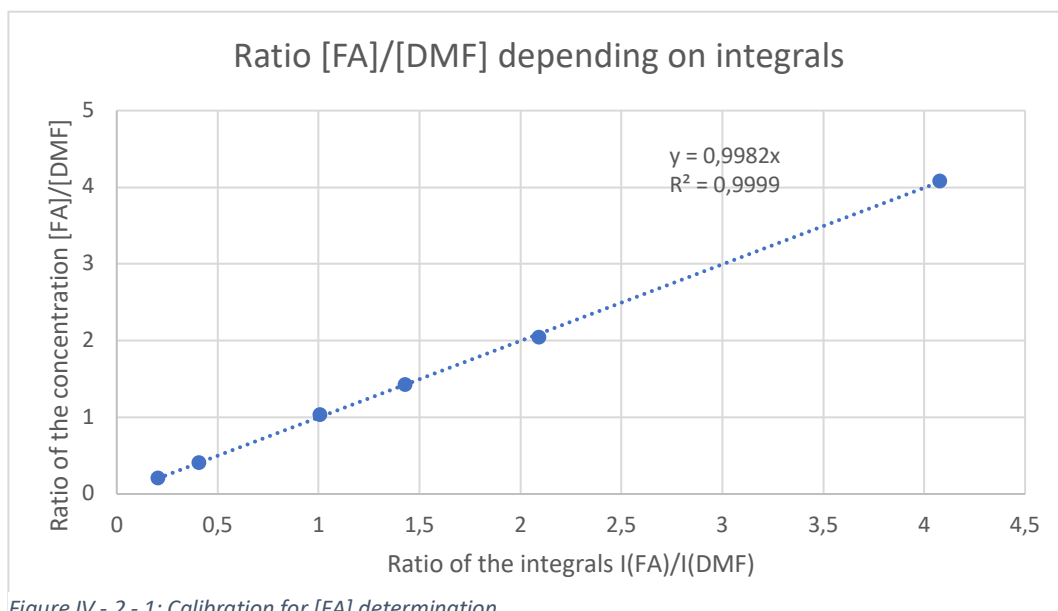
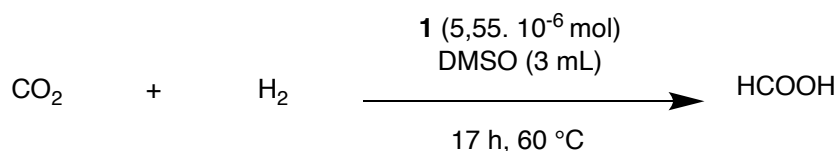


Table IV - 2 - 1: Preliminary results in base-free CO<sub>2</sub> hydrogenation<sup>a</sup>

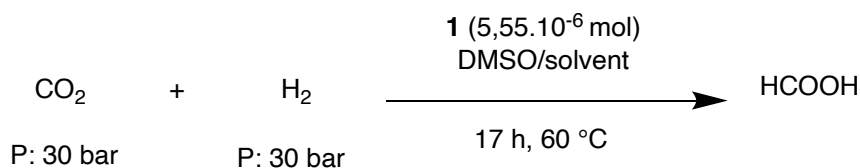


Entry	CO <sub>2</sub>	H <sub>2</sub>	[FA] (mol/L)	TON
1	20	20	$3,18 \cdot 10^{-2}$	9
2	30	30	$4,43 \cdot 10^{-1}$	105

<sup>a</sup> **1** ( $5,55 \cdot 10^{-6}$  mol,  $n(\text{Ru})=1,11 \cdot 10^{-5}$  mol), 60 °C, desired pressure, High pressure reactor, 17 h.

The results in Table IV-2-1 indicates that the reaction took place but with moderate results. The reaction under 60 bar of pressure provided a TON of 105 which is moderate compared to the literature data but encouraging. As a reminder, reported TONs range between 355<sup>[1]</sup> at 70 bar for 72 h and 10 258<sup>[2]</sup> at 76 bar for 8-90 h. However, it should be mentioned that this result is comparable to the ruthenium catalyst [RuCl<sub>2</sub>(PTA)<sub>4</sub>] employed by Laurenczy and reported in a reference article in 2014.<sup>[3]</sup> Indeed, if this catalyst furnished a high TON of 475 at 100 bar the concentration of FA obtained at 60 bar was similar to the one obtained with **1**. Further studies were then conducted in order to improve the performances of the process.

## 2.2. Solvent



*Scheme IV - 2 - 2: Solvent optimization in base-free CO<sub>2</sub> hydrogenation.*

Following preliminary tests, the solvent composition was investigated, more precisely the ratio between DMSO and a co-solvent while maintaining a total volume of 3 mL (Scheme IV-2-2). Various co-solvents were tested (THF, H<sub>2</sub>O, GVL, ACN) but no improvement in the TON was observed (Table IV-2-2). We even noticed a decrease in the catalytic productivity when the co-solvent amount increased. For example, with GVL, the TON was increased to 78 when the GVL ratio increased to 33% (Table IV-2-2, Entry 8) and then with 94% the TON dropped to 16. The same behavior occurred with water (Table IV-2-2, Entry 2 and 3). Considering those results, DMSO was used as solvent for further investigations.

*Table IV - 2 - 2: Solvent influence in base-free CO<sub>2</sub> hydrogenation<sup>a</sup>*

Entry	Solvent	Ratio (%)	[FA] (mol/L)	TON
1	DMSO	100%	4,43.10 <sup>-1</sup>	105
2	DMSO/H <sub>2</sub> O	5%	2,24.10 <sup>-1</sup>	58
3		33%	9,43.10 <sup>-2</sup>	25
4	DMSO/THF	6%	2,80.10 <sup>-1</sup>	68
5		16%	2,79.10 <sup>-1</sup>	71
6	DMSO/ACN	16%	2,94.10 <sup>-1</sup>	53
7	DMSO/GVL	6%	1,79.10 <sup>-1</sup>	71
8		33%	2,94.10 <sup>-1</sup>	78
9		94%	6,32.10 <sup>-2</sup>	16

<sup>a</sup> 1 (5,55.10<sup>-6</sup>, n(Ru)=1,11.10<sup>-5</sup> mol), 60 °C, 30 bar CO<sub>2</sub>, 30 bar H<sub>2</sub>, Solvent Total 3 mL, 17 h.

## 2.3. Pressure

The total pressure of gas and the ratio between CO<sub>2</sub> and H<sub>2</sub> may play a role on the catalytic activity. Therefore, this parameter was studied.

In a first step, the pressure was increased with the same amount of CO<sub>2</sub> and H<sub>2</sub> from 60 bar to 80 bar (Table IV-2-3, entry 1, 2, 3). We noticed a small increase in the catalytic productivity when the total pressure was 70 bar compared to 60 bar. The TON increased from 105 to 116. However, we could not increase the pressure further to 80 bar due to technical limitation during the reaction (Table IV-2-3, entry 3). Indeed, the safety valve of the reactor was limited to a range of 97-110 bar. For this reason, experiments at 80 bar were limited.

In a second step, the pressure ratio between H<sub>2</sub> and CO<sub>2</sub> was studied. Maintaining a total pressure of 60 bar, the amount of CO<sub>2</sub> was reduced to 10 bar (Table IV-2-3, Entry 4) and 20 bar (Table IV-2-3, Entry 5), the TON was around 67 for 10 bar of CO<sub>2</sub> and 73 for 20 bar of CO<sub>2</sub>. At a total pressure of 70 bar, a ratio of 10 bar of CO<sub>2</sub> with 60 bar of H<sub>2</sub> was tested with a TON

of only 62 (Table IV-2-3, Entry 6). With the same pressure of CO<sub>2</sub> associated this time with 70 bar of H<sub>2</sub> for a total pressure of 80 bar, the TON remained the same (Table IV-2-3, Entry 7). At a total pressure of 80 bar, CO<sub>2</sub> was used at a pressure of 20 bar leading to a TON of 71. There was a slight improvement but it was still lower compared to the reference (Table IV-2-3, Entry 1 and 2). A 35 bar CO<sub>2</sub> and 45 bar H<sub>2</sub> ratio was tested providing a TON of 97 (Table IV-2-3, Entry 8) close to the reference run (Table IV-2-3, Entry 1).

By modifying the total pressure and the gases ratio we were not able to make a major breakthrough in the catalytic productivity of the CO<sub>2</sub> hydrogenation into FA.

Table IV - 2 - 3: Pressure study in base free CO<sub>2</sub> hydrogenation<sup>a</sup>

$\text{CO}_2 + \text{H}_2 \xrightarrow[17 \text{ h, } 60^\circ \text{ C}]{\substack{\mathbf{1} (5,55 \cdot 10^{-6} \text{ mol}) \\ \text{DMSO (3 mL)}}} \text{HCOOH}$				
Entry	CO <sub>2</sub> (bar)	H <sub>2</sub> (bar)	[FA] (mol/L)	TON
1	30	30	$4,43 \cdot 10^{-1}$	105 <sup>b</sup>
2	35	35	$4,60 \cdot 10^{-1}$	116 <sup>b</sup>
3	40	40	/ <sup>c</sup>	/ <sup>c</sup>
4	10	50	$2,49 \cdot 10^{-1}$	67
5	20	40	$2,80 \cdot 10^{-1}$	73
6	10	60	$2,57 \cdot 10^{-1}$	62
7	10	70	$2,31 \cdot 10^{-1}$	61
8	20	60	$2,81 \cdot 10^{-1}$	71
9	35	45	$3,58 \cdot 10^{-1}$	97
<sup>a</sup> $\mathbf{1}$ ( $5,55 \cdot 10^{-6}$ mol), $n(\text{Ru})=1,11 \cdot 10^{-5}$ mol, 60 °C, CO <sub>2</sub> , H <sub>2</sub> , DMSO (3 mL), 17 h. <sup>b</sup> average of several run; <sup>c</sup> Breakage of the safety valve				

## 2.4. Temperature

The temperature was increased progressively from 60 °C to 90 °C to study the evolution of the catalytic activity (Table IV-2-4). With the reference reaction using 30 bar of CO<sub>2</sub> and H<sub>2</sub>, the catalytic activity slightly increased when the temperature rose 70 °C and 80 °C leading to a TON of 114 (Table IV-2-4, Entry 2 and 3). Then at 90 °C, the TON decreased to 90 (Table IV-2-4, Entry 4) indicating a lower catalyst stability at this temperature. It could also be due to the exothermic nature of the reaction as well as unfavorable entropic term that influence negatively the Gibbs energy that was already not favored.

The 35/35 ratio of gases showed a small improvement so a run with a temperature of 70 °C was made leading to a TON of 160 that represent the highest TON obtained in the study. Those experimental conditions contributed to a large improvement on the catalytic productivity. However, the pressure reached during the reaction time was too close to the limit of the reactor used that may cause some safety issue.

Table IV - 2 - 4: Influence of the temperature on the base-free hydrogenation of CO<sub>2</sub> into FA<sup>a</sup>

$  \begin{array}{ccc}  \text{CO}_2 & + & \text{H}_2 \\  \text{P: 30 bar} & & \text{P: 30 bar}  \end{array}  \xrightarrow[\text{17 h, T } ^\circ\text{C}]{\begin{array}{c} \text{1 (5,55.10}^{-6}\text{ mol)} \\ \text{DMSO} \end{array}}  \text{HCOOH}  $			
Entry	T. (°C)	[FA] (mol/L)	TON
1	60	4,43.10 <sup>-1</sup>	105 <sup>b</sup>
2	70	4,50.10 <sup>-1</sup>	114
3	80	4,50.10 <sup>-1</sup>	114 <sup>b</sup>
4	90	3,21.10 <sup>-1</sup>	90 <sup>b</sup>
5	70 <sup>c</sup>	6,25.10 <sup>-1</sup>	160

<sup>a</sup> 1 (5,55.10<sup>-6</sup> n(Ru)=1,11.10<sup>-5</sup> mol), T °C, 30 bar CO<sub>2</sub>, 30 bar H<sub>2</sub>, DMSO (3 mL), 17 h. <sup>b</sup> average of several run; <sup>c</sup> 35 bar CO<sub>2</sub>, 35 bar H<sub>2</sub>

## 2.5. Reaction time

An extended reaction time and a shorter one were tested. Three different runs were prepared and stopped at different reaction time. Indeed, as the high-pressure reactors used was not equipped with a sampling valve, we could not collect a small sample for analysis at different time in the same reaction mixture. As we could imagine, a shorter reaction time of 6 h resulted in a poor catalytic productivity (Table IV-2-5, Entry 2). On the opposite, a reaction time of 65h provided a TON of 160 (Table IV-2-5, Entry 3) indicating that a long reaction time was necessary to reach equilibrium.

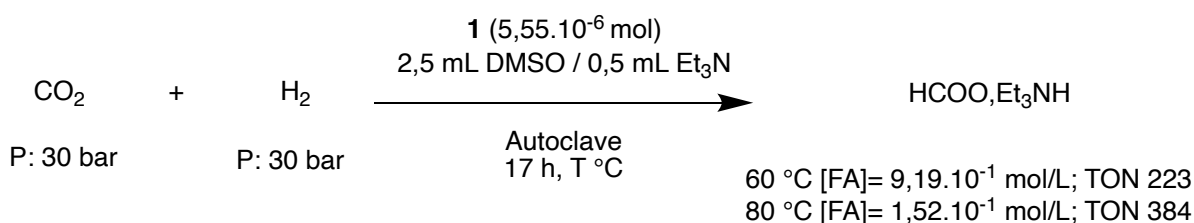
Table IV - 2 - 5: Influence of the reaction time on the base-free hydrogenation of CO<sub>2</sub> into FA<sup>a</sup>

$  \begin{array}{ccc}  \text{CO}_2 & + & \text{H}_2 \\  \text{P: 30 bar} & & \text{P: 30 bar}  \end{array}  \xrightarrow[\text{Time, 60 } ^\circ\text{C}]{\begin{array}{c} \text{1 (5,55.10}^{-6}\text{ mol)} \\ \text{DMSO} \end{array}}  \text{HCOOH}  $			
Entry	Time (h)	[FA] (mol/L)	TON
1	17	4,43.10 <sup>-1</sup>	105 <sup>b</sup>
2	6	4,43.10 <sup>-2</sup>	12
3	65	6,42.10 <sup>-1</sup>	160

<sup>a</sup> 1 (5,55.10<sup>-6</sup>, n(Ru)=1,11.10<sup>-5</sup> mol), 60 °C, 30 bar CO<sub>2</sub>, 30 bar H<sub>2</sub>, DMSO (3 mL), Time. <sup>b</sup> average of several run

## 2.6. CO<sub>2</sub> hydrogenation under basic condition

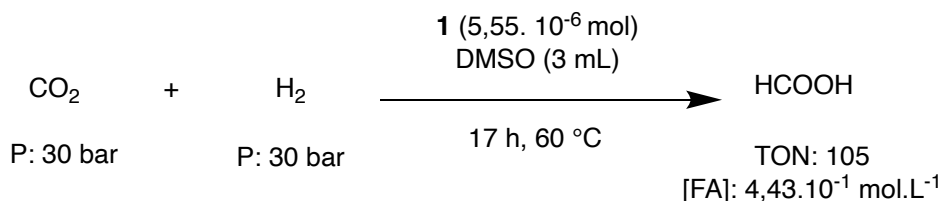
As we were curious about comparing the performances of the catalyst under base-free conditions to base conditions, the reaction was run with TEA (Scheme IV-2-3). The catalytic productivity was doubled. A TON of 223 was obtained with TEA under the standard condition compared to 105. At 80 °C, the TON was about 384 with base compared to 114 without. These results demonstrate once again the improvement achieved under basic condition. However, as discussed in the state of the art, the use of base induces cost increase and possibly purification procedures for TEA removal. It should also be considered that in this case the reaction product is a formate salt and not formic acid.



Scheme IV - 2 - 3: CO<sub>2</sub> hydrogenation in a basic media.

## 2.7. Conclusion

We performed the base-free carbon dioxide hydrogenation into formic acid with catalyst **1**. We were struggled to find experimental conditions able to compete with literature data but we were able to reach some of the early results achieved with ruthenium. Hence, promising results were obtained considering the limitation we had in terms of high-pressure implementation. Indeed, with ruthenium catalysts, the highest performances obtained so far were obtained at pressures higher than 100 bar. Therefore, further improvement may be expected under higher pressure with an appropriate experimental equipment. Beside experimental parameters, the design and synthesis of other catalysts with improved performances will be a challenge. Finally, the experimental conditions tested in the preliminary study was the one selected for the optimized conditions.



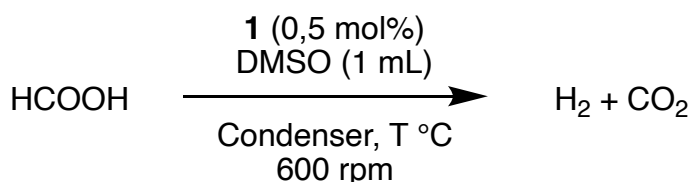
Scheme IV - 2 - 4: Optimized condition for CO<sub>2</sub> hydrogenation into FA.

### 3. Formic acid dehydrogenation / Hydrogen release results and discussion

Having the objective to perform a full cycle for hydrogen storage and release we investigate the dehydrogenation of FA in DMSO. Contrary to CO<sub>2</sub> hydrogenation where productivity (TON) is a key indicator used by researchers, the activity (TOF) of the catalyst is used to evaluate the performance in dehydrogenation. Indeed, for some applications it is necessary to release hydrogen in high rates in order to generate high pressure and flow.

#### 3.1. Preliminary tests

A 2 necked round bottom flask was connected to a condenser and a digital flowmeter calibrated for H<sub>2</sub>/CO<sub>2</sub> (Figure IV-2-2). The solvent used was DMSO and the tests were performed on a 100  $\mu$ L scale of FA with 0,5 mol% of catalyst **1** (Scheme IV-2-5). The reaction was left to run until there was no more gas release. Thanks to the flowmeter, the amount of gas produced can be used to calculate the TOF considering that one mole of a 50/50 mixture of CO<sub>2</sub>/H<sub>2</sub> represents 24,4 L. Hence from the volume of gas monitored, the amount of CO<sub>2</sub> and H<sub>2</sub> were calculated then the TON and the TOF. As mentioned earlier, the reaction was evaluated by the TOF as we want to produce a large amount of H<sub>2</sub> in a short period time to generate a flow and pressure for energetical application.



*Scheme IV - 2 - 5: Formic acid base-free dehydrogenation preliminary test.*



Figure IV - 2 - 2: Experimental set-up for FA dehydrogenation.

The preliminary tests were made at 60 °C and 90 °C. The reaction was faster (25 min) with a better TOF at 90 °C (Table IV-2-6, Entry 2) compared to the reaction run at 60 °C that took more than 6 h (Table IV-2-6, Entry 1). Hence, 90 °C was selected as a reference temperature for the upcoming studies. The reaction at 60 °C required a longer reaction time with still a very high conversion indicating a good stability of the catalyst (Table IV-2-6, Entry 1).

Formic acid having a boiling point of 100 °C, higher temperatures were not attempted to make sure to not evaporate FA.

Table IV - 2 - 6 : Preliminary results in base-free formic acid dehydrogenation<sup>a</sup>

Entry	T (°C)	Time	Conv. (%)	TOF (h <sup>-1</sup> ) <sup>b</sup>
1	60	6 h 30	92%	23
2	90	25 min	92%	186

<sup>a</sup> FA (100 μL, 2,65.10<sup>-3</sup> mol), **1** (0,5 mol%, 1,33.10<sup>-5</sup> mol, n(Ru) 2,66.10<sup>-5</sup>), DMSO (1 mL), 600 rpm; <sup>b</sup> TOF calculated for the 10 first min

### 3.2. Effect of the concentration on the FA dehydrogenation

The ideal temperature was defined to be 90 °C so the influence of the concentration of FA could now be studied by varying the volume of solvent.

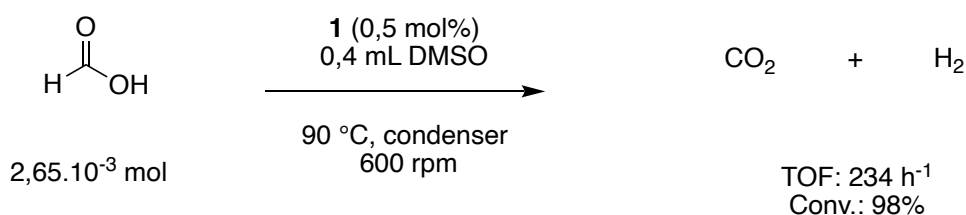
The reaction in pure FA (Table IV-2-7, Entry 1) was not possible, the reaction condition might be too acidic for the catalyst. The reaction at a concentration of 8,8 mol.L<sup>-1</sup> (0,2 mL DMSO) started to be active and presented good results having a TOF of 198 h<sup>-1</sup> and a conversion of 78% (Table IV-2-7, Entry 2). The conversion and the TOF further increased after dilution to 5,3 mol.L<sup>-1</sup> to reach the best results with a conversion of 98% and a TOF of 234 h<sup>-1</sup>. Indeed, with a solution more diluted, the results decreased to a TOF of 184 h<sup>-1</sup> at 2,4 mol.L<sup>-1</sup> (Table IV-2-7, Entry 4) and a TOF of 172 h<sup>-1</sup> at 1,0 mol.L<sup>-1</sup> (Table IV-2-7, Entry 5).

Table IV - 2 - 7: Effect of the concentration on the base-free FA dehydrogenation<sup>a</sup>

Entry	Conc. (mol/L)	H <sub>2</sub> wt%	Conv. (%)	TOF (h <sup>-1</sup> ) <sup>b</sup>
1	26,5 (Pure FA)	4,4%	/	/
2	8,8	1,7%	78%	198
3	5,3	1,1%	98%	<b>234</b>
4	2,65	0,5%	92%	184
5	1,0	0,2%	95%	172

<sup>a</sup> FA (100 μL, 2,65.10<sup>-3</sup> mol), **1** (0,5 mol%, 1,33.10<sup>-5</sup> mol, n(Ru) 2,66.10<sup>-5</sup>), DMSO (0/0,2/0,4/1/2,6 mL), 600 rpm, 90 °C ; <sup>b</sup> TOF calculated for the 10 first min

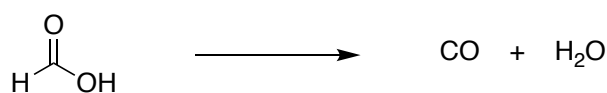
Hence, the optimized condition was obtained in 0,4 mL of DMSO to have a FA concentration of 5,3 mol.L<sup>-1</sup>. Under these conditions, a TOF of 234 h<sup>-1</sup> based on the first 10 minutes was obtained. Moreover, 25 minutes was necessary to reach almost full conversion. This level of performance is somehow moderate compared to the rare examples of base-free dehydrogenation of FA with ruthenium catalyst. For example, Beller obtained the best TOF with a ruthenium catalyst at 60 °C reaching a TOF of 36 000 h<sup>-1</sup> in 1 minute.<sup>[4]</sup> Very recently, Milstein with a pincer ruthenium catalyst obtained a TOF of 3067 h<sup>-1</sup> at 95 °C.<sup>[5]</sup> However, in both cases, it must be noted that studies were conducted with preformed ruthenium-hydride catalysts.



Scheme IV - 2 - 6: Best conditions obtained for base-free FA dehydrogenation.

### 3.3. CO detection

Before thinking about possible energetical application of the process, some parameters including CO detection have to be checked. Indeed, carbon monoxide is a poison for fuel cell electrodes, hence the gas flow generated by formic acid dehydrogenation must be free or containing less than 10 ppm of CO. During the dehydrogenation of FA, CO can be generated by a competitive FA dehydration (Scheme IV-2-7).



*Scheme IV - 2 - 7: Dehydration of FA.*

In order to monitor the CO level during the reaction, the flowmeter was connected to a gas chromatography apparatus equipped with a katharometer detector. With this setup, no CO was detected (below the detection level, < 1 ppm) from the beginning to the end of the reaction (Figure IV-2-3).

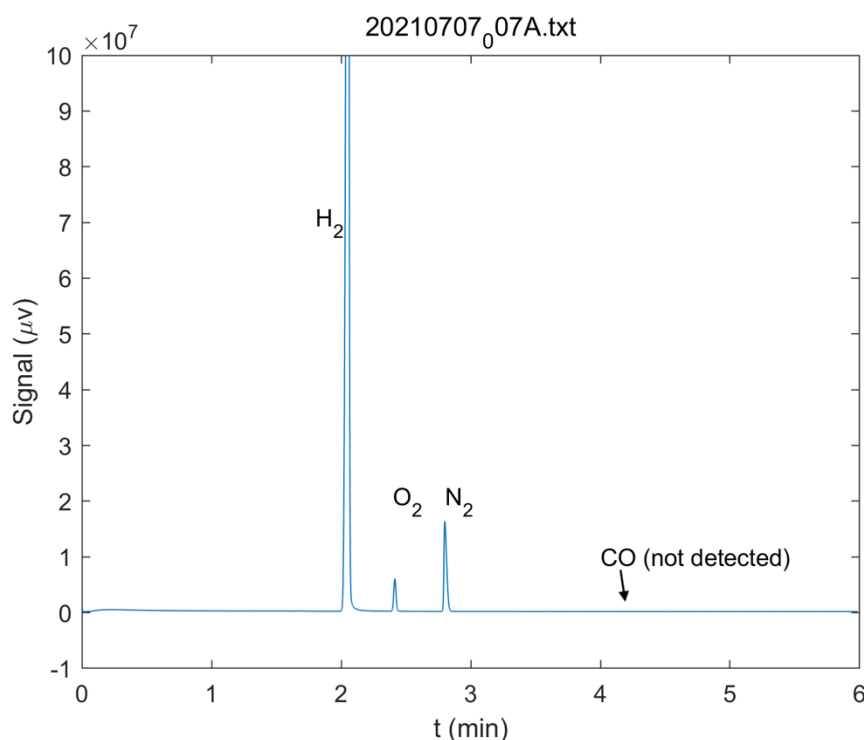
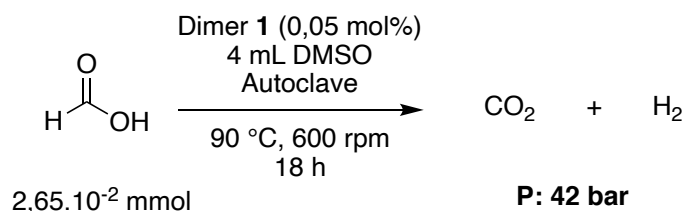


*Figure IV - 2 - 3: GC online analysis of the gas flow generated by FA dehydrogenation.*

### 3.4. Pressure generation

FA dehydrogenation has to be able to generate enough gas and pressure to supply a fuel cell or other devices.<sup>[6]</sup> In this perspective, the reaction was run with 10 times the amount of FA and DMSO compared to the optimized conditions (Scheme IV-2-8). The gas pressure generated reached about 42 bar in 17 h thus indicating that the reaction can be run in a closed system at a larger scale and generating a high pressure at equilibrium. Then, in a second step,

the pressure was release and the reaction let to run for an extra 2 h. The pressure increased to 20 bar confirming that the reaction reached an equilibrium when 42 bar was achieved. Finally, the reaction was stopped and NMR analysis showed the presence of remaining FA. It demonstrated that in a first place, the reaction was at the equilibrium. Then, the consumption of the remaining FA occurred because of the release of gas. It also evidenced the robustness of the catalyst as it was still active.



*Scheme IV - 2 - 8: Base-free FA dehydrogenation in a closed system.*

### 3.5. Continuous addition of FA

An important point for energetical application is to have a catalyst with a long life-time able to transform a large quantity of FA. This characteristic could be useful in a power-plant unit fed with FA. For example, in a batch with a catalyst solution, FA could be added continuously or portionwise to produce hydrogen, hence energy.

In this respect, an experimental setup was used using the optimized conditions for FA dehydrogenation (FA: 100  $\mu\text{L}$ ,  $2,65 \cdot 10^{-3}$  mol; **1**: 0,5 mol%; DMSO: 0,4 mL; 600 rpm; 90  $^{\circ}\text{C}$ ). Then, FA was added portionwise in order to maintain a constant gas flow. By this way, a TON of 1378 could be obtained in 24 h. This result is encouraging but still below the state of the art reported for instance by Beller<sup>[4]</sup> (TON 19000 in 120 days) or Milstein<sup>[5]</sup> (TON 1 700 000 in one month). Further optimizations of the process including appropriate improvement of the experimental setup would be necessary to improve this aspect

### 3.6. Latent behavior of the catalytic system

The latent behavior of the system is its ability to remain stable and inactive for a period of time until the catalytic activity is triggered like we can find in other catalytic field.<sup>[7]</sup> On an experimental and practical point of view, the reaction mixture (solvent, catalyst, FA) produced straight after the FA synthesis should be inactive and stored or transferred until  $\text{H}_2$  production

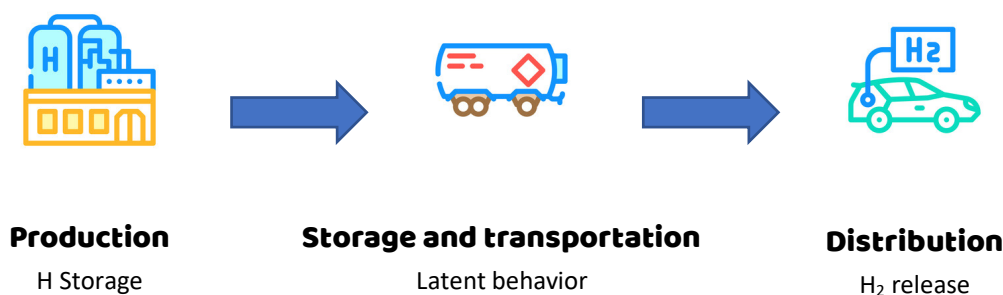


*Figure IV - 2 - 4: Application of the latent behavior in the H cycle storage.*

is required and triggered. This parameter is mandatory if a single catalyst is to be used to proceed to the cycle of H<sub>2</sub> storage and release cycle. By this way, no hydrogen is produced that may cause a safety issue during the storage or the transport of the LOHC. Then, the “ready to use” solution is activated on the hydrogen plant to release hydrogen (Figure IV-2-4).

To evaluate the latent behavior of the system, two reaction mixtures were prepared using the optimized conditions of solvents and catalyst loading (0,4 mL DMSO, 0.5 mol% of **1**). One flask was left on the bench at ambient temperature (Table IV-2-8, entry 1) over the weekend (70 h) and the other left in the fridge ( $\pm 4$  °C) also for 70 h (Table IV-2-8, entry 2). Then, each reaction flask was heated to 90 °C and the gas volume recorded and compared to the reference reaction which provided nearly full conversion in 25 minutes. As depicted in Table IV-2-8 both reactions provided only 21-25% conversion suggesting either catalyst decomposition or FA dehydrogenation during the storage period. In order to clarify this, the reaction mixtures were analyzed by <sup>1</sup>H NMR and no trace of remaining FA was observed. Those results evidenced that the dehydrogenation reaction took place even at low temperature. Therefore, the latent behavior of **1** is not sufficient and it is likely that a similar behavior would be observed in a reaction mixture from the hydrogenation of CO<sub>2</sub> in FA.

Table IV - 2 - 8: Effect of the latent behavior<sup>a</sup>

$$\text{HCOOH} \xrightarrow[\text{DMSO, 90 } ^\circ\text{C}]{\text{1 (0,5 mol\%)}} \text{H}_2 + \text{CO}_2$$

600 rpm

Entry	Latent condition	Conv. (%)	TOF (h <sup>-1</sup> ) <sup>a</sup>	<sup>1</sup> H NMR
<b>1</b>	Ambient temperature	21%	108	No FA
<b>2</b>	Fridge ( $\pm 4$ °C)	25%	126	No FA

<sup>a</sup> FA (100  $\mu$ L,  $2,65 \cdot 10^{-3}$  mol), **1** (0,5 mol%,  $1,33 \cdot 10^{-5}$  mol, n(Ru)  $2,66 \cdot 10^{-5}$ ), DMSO (0,4 mL), 600 rpm, 90 °C ; <sup>b</sup> TOF calculated for the 10 first min

Of note, this result also suggests that some dehydrogenation may occur upon depressurization of the reactors and analysis time following a CO<sub>2</sub> hydrogenation reaction. Hence, the results presented in paragraph 2 may be somehow underestimated.

## 4. Storage and release cycle

### 4.1. Application

The catalyst **1** was active in both hydrogenation of CO<sub>2</sub> into FA and dehydrogenation of FA into CO<sub>2</sub> and H<sub>2</sub> without base. Having demonstrated the activity of **1** in each unitary half-cycle of hydrogen storage and release, we decided to perform a full cycle using the same batch (Scheme IV-2-9). As depicted in the state of the art, this approach was not extensively reported

in literature except by Beller and Laurenczy, Pidko, Plietker, Szymczak and they all used bases.<sup>[8–11]</sup>

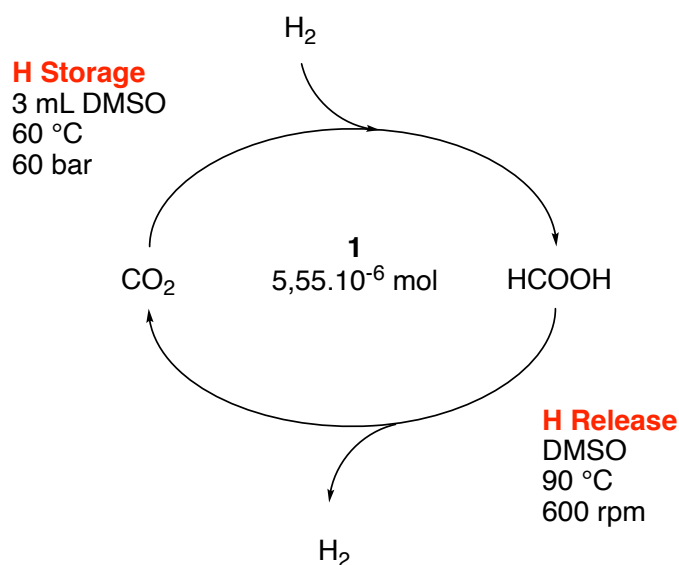
This application was studied by carrying out the hydrogenation of CO<sub>2</sub> into FA followed by FA dehydrogenation without any purification or change in the reaction mixture. Standard conditions for CO<sub>2</sub> hydrogenation were first implemented and a sample was taken for analysis and FA quantification. The crude reaction mixture was then frozen and vacuum applied to remove any residual trace of dissolved gas that could distort the gas volume measured during the FA dehydrogenation. Finally, the crude was transferred and set-up for FA dehydrogenation.

The hydrogenation step gave results in the same range as those previously obtained as TONs of 85 (Table IV-2-9, Entry 1) and 99 (Table IV-2-9, Entry 2) were obtained. Concerning the dehydrogenation, the conversions were very good indicating that a full transformation of the FA was achieved. It was confirmed by <sup>1</sup>H NMR analysis that did not show any trace of remaining FA. Furthermore, the TOF measured (147 and 168 h<sup>-1</sup>) were close to those obtained in the FA dehydrogenation study hence highlighting that the activity of the catalyst in the second step was not altered by the first step. The reactions were slower with a gas flow that stopped after 40 min.

Table IV - 2 - 9: Results of the base-free cycle of H storage and release.

Entry	Hydrogenation <sup>a</sup>		Dehydrogenation <sup>b</sup>	
	[FA] (mol.L <sup>-1</sup> )	TON	Conv. (%)	TOF (h <sup>-1</sup> )
1	3,66.10 <sup>-1</sup>	85	97%	147
2	4,38.10 <sup>-1</sup>	99	88%	168

<sup>a</sup> 1 (5,55. 10<sup>-6</sup> mol, n(Ru) 1,11.10<sup>-5</sup> mol), 60 °C, 30 bar CO<sub>2</sub>, 30 bar H<sub>2</sub>, DMSO (3 mL), 17 h ; <sup>b</sup> 90 °C, 600 rpm.



Scheme IV - 2 - 9: Cycle of base-free H storage and release.

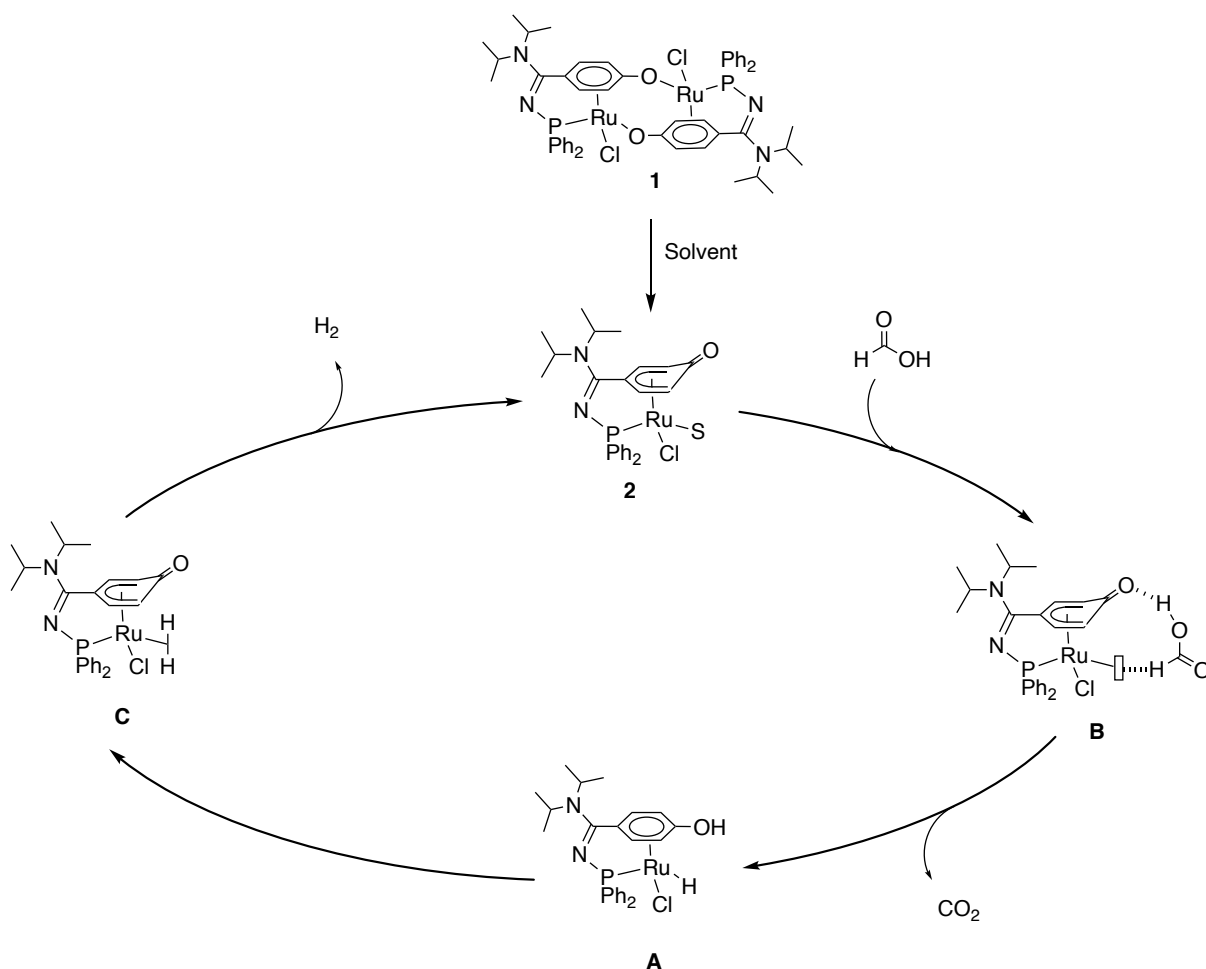
## 5. Mechanism proposal

Although the reaction mechanism has not been studied in details, the available data, in particular concerning the Shvo catalyst combined with the reactivity studies carried out in Toulouse allows to postulate possible mechanisms.

### 5.1. Formic acid dehydrogenation

Dealing with the dehydrogenation of FA into  $\text{CO}_2$  and  $\text{H}_2$ , we may use the observation made on the transfer hydrogenation of ketone with FA.

In solution, the dimeric species dissociates into a monomeric species **2** observed in ACN. Then, formic acid is dehydrogenated hence transferring hydrogen to the catalyst and releasing  $\text{CO}_2$ . This process would involve ligand cooperation via the basic-character of the oxo-dienyl ligand leading to species **A**. Finally, from species **A**, the release of  $\text{H}_2$  occurred.

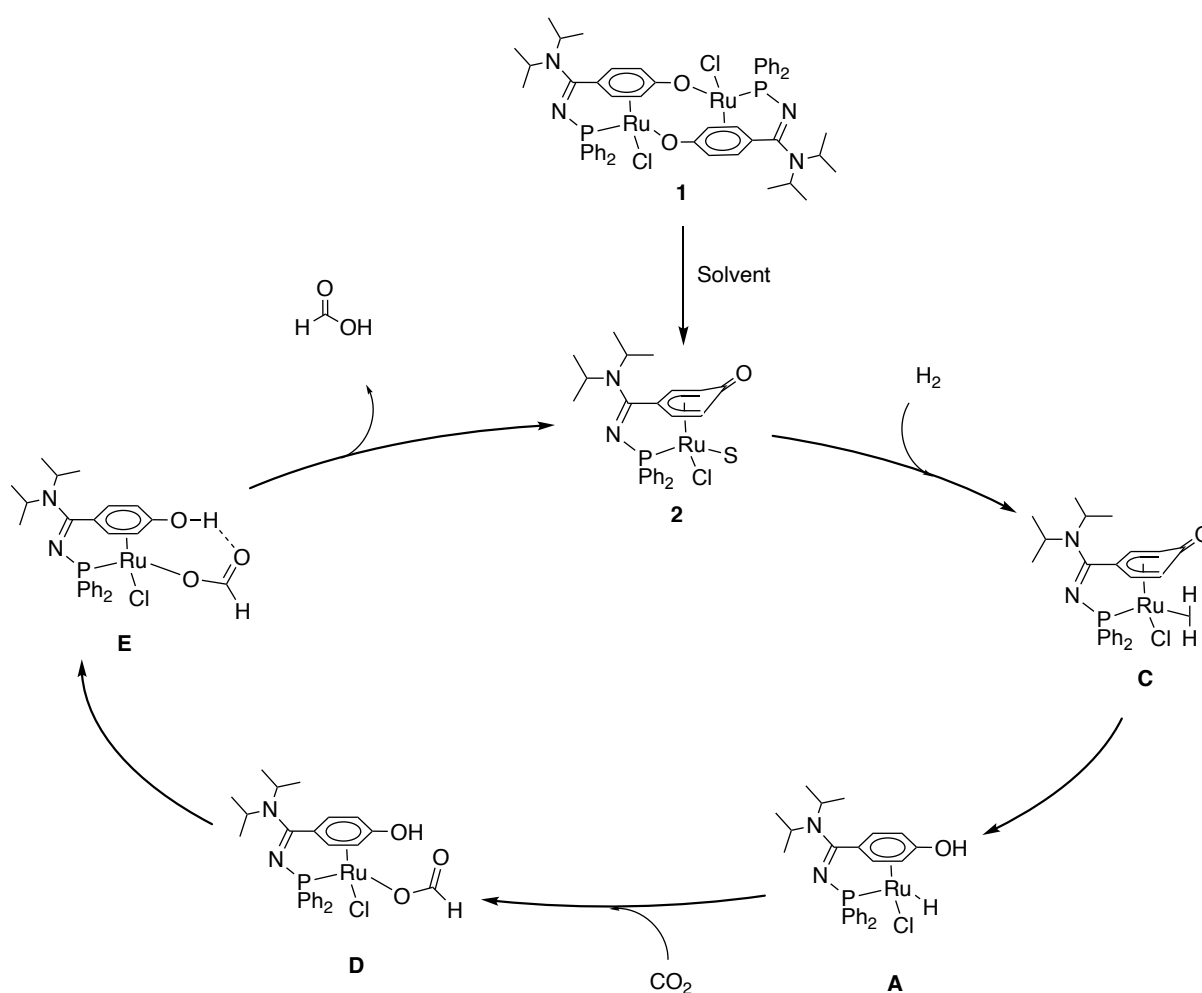


Scheme IV - 2 - 10: Mechanism proposal for the dehydrogenation of FA.

## 5.2. CO<sub>2</sub> hydrogenation into formic acid

As before, the mechanism proposed is based on reported data and studies on the reactivity of **1**. Experimental and theoretical studies are needed to investigate this further.

The hypothesis on the CO<sub>2</sub> hydrogenation starts with the formation of the hydrogenated species **A** via the intermediate  $\eta^2$ -dihydride species **C**. Then, insertion of CO<sub>2</sub> in the Ru-H bond would lead to the formate species **D**. In the last step, the transfer of the proton from the phenol-ligand to the formate (**E**) would release FA and regenerate **2**.



Scheme IV - 2 - 11: Mechanism proposal for the CO<sub>2</sub> hydrogenation.

## 6. Conclusion

The catalyst developed belongs to the group the catalysts active under base-free condition able to perform both the hydrogenation of CO<sub>2</sub> into FA and the reverse reaction. Furthermore, those reaction could be applied one after the other with no change in the reaction mixture. It was the first time that a base-free system was applied to perform an entire cycle of hydrogen storage and release. There is still possible improvement to apply in order to have better performance. Mechanistic insight could also be further studied.

## 7. References:

- [1] A. R. Sahoo, F. Jiang, C. Bruneau, G. V. M. Sharma, S. Suresh, T. Roisnel, V. Dorcet, M. Achard, *Catal. Sci. Technol.* **2017**, *7*, 3492–3498.
- [2] S.-M. Lu, Z. Wang, J. Li, J. Xiao, C. Li, *Green Chem.* **2016**, *18*, 4553–4558.
- [3] S. Moret, P. J. Dyson, G. Laurenczy, *Nat. Commun.* **2014**, *5*, 4017.
- [4] C. Prichatz, M. Trincado, L. Tan, F. Casas, A. Kammer, H. Junge, M. Beller, H. Grützmacher, *ChemSusChem* **2018**, *11*, 3092–3095.
- [5] S. Kar, M. Rauch, G. Leitus, Y. Ben-David, D. Milstein, *Nat. Catal.* **2021**, *4*, 193–201.
- [6] “DOE Technical Targets for Onboard Hydrogen Storage for Light-Duty Vehicles,” can be found under <https://www.energy.gov/eere/fuelcells/doe-technical-targets-onboard-hydrogen-storage-light-duty-vehicles>, **2022**.
- [7] S. Monsaert, A. Lozano Vila, R. Drozdak, P. Van Der Voort, F. Verpoort, *Chem. Soc. Rev.* **2009**, *38*, 3360.
- [8] A. Boddien, C. Federsel, P. Sponholz, D. Mellmann, R. Jackstell, H. Junge, G. Laurenczy, M. Beller, *Energy Environ. Sci.* **2012**, *5*, 8907.
- [9] G. A. Filonenko, R. van Putten, E. N. Schulpen, E. J. M. Hensen, E. A. Pidko, *ChemCatChem* **2014**, *6*, 1526–1530.
- [10] S.-F. Hsu, S. Rommel, P. Eversfield, K. Muller, E. Klemm, W. R. Thiel, B. Plietker, *Angew. Chem. Int. Ed.* **2014**, *53*, 7074–7078.
- [11] J. B. Geri, J. L. Ciatti, N. K. Szymczak, *Chem. Commun.* **2018**, *54*, 7790–7793.

## 8. Experimental part

### 8.1. General information

The solvents were purchased from Aldrich and used as received. DMSO grade was 99,5% NMR spectra were recorded at 300 °K on a Bruker AV III HD 500 MHz spectrometer fitted with a BBFO probe or a Bruker AV III 400 MHz spectrometer fitted with a BBFO probe. For quantitative measurements, the relaxation delay was extended to 45 s (d1=45 s)

Flowmeter used is a EL-FLOW® Prestige with a thermal mass flow sensor from Bronkhorst calibrated for an equimolar gas mixture of CO<sub>2</sub>/H<sub>2</sub>.

Gas analysis were performed on a mGC 3000 SRA equipped with a 5 Å molecular sieves column and a katharometer detector. The CO detection level of the analysis was 1 ppm.

### 8.2. CO<sub>2</sub> hydrogenation

#### 8.2.1. Reaction procedure

In a standard procedure, a Parr high pressure reactor of 22 mL with a security valve ranging between 97 and 107 bar was used. The catalyst **1** ( $\approx 6$  mg,  $5,55 \cdot 10^{-6}$  mol) was weighed in the reactor and DMSO (3 mL) added inside the glovebox. The reactor was flushed with CO<sub>2</sub> then charged with CO<sub>2</sub> (30 bar) and H<sub>2</sub> (30 bar). The reaction was heated at 60 °C for 17 h with stirring at 600 rpm. At the end of the reaction, the reactor was let to cool down to r.t. The gases were gently released and the reactor open. DMF (100  $\mu$ L, 94,4 mg, 1,29 mmol) was added as an internal standard. A small sample of the reaction mixture was taken and analyzed by <sup>1</sup>H NMR. Thanks to the calibration curve, the concentration of FA and so the TON could be obtained.

#### 8.2.2. Analytical procedure

First of all, a calibration curve was set up with 6 different concentrations of formic acid using 10, 20, 50, 70, 100, 200  $\mu$ L in 3 mL of DMSO that correspond to concentrations of  $9,09 \cdot 10^{-2}$  mol.L<sup>-1</sup>,  $1,77 \cdot 10^{-2}$  mol.L<sup>-1</sup>,  $4,49 \cdot 10^{-2}$  mol.L<sup>-1</sup>,  $6,18 \cdot 10^{-1}$  mol.L<sup>-1</sup>,  $8,86 \cdot 10^{-1}$  mol.L<sup>-1</sup>,  $1,77$  mol.L<sup>-1</sup>, respectively. Two different batches were made and the average was used for the data treatment. The equation obtained which correspond to the concentration [FA]/[DMF] over the Integrals was forced to cross 0 to give the equation  $y=0,9982x$  where x represents the integral measurement and y the concentration (Figure IV-2-6).

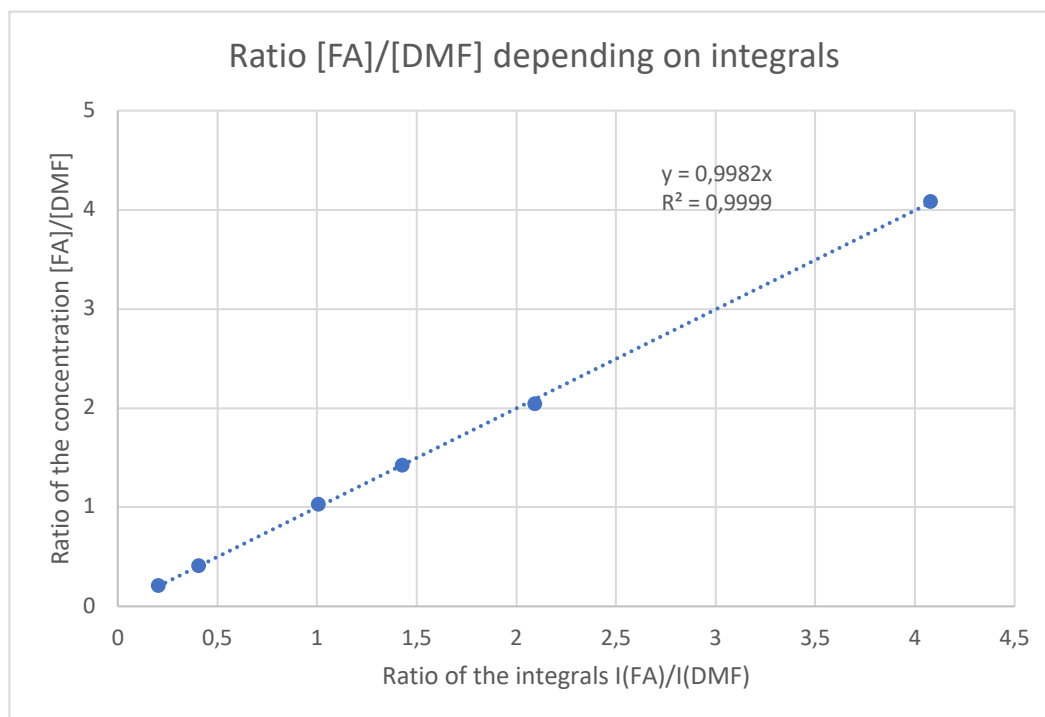


Figure IV - 2 - 5: Calibration curve of FA for CO<sub>2</sub> hydrogenation.

For each experiment, a small sample was taken at the end of the reaction and analyzed by NMR (Figure IV-2-7). The integrals were peaked to determine the concentration in FA of the sample. Then, the TON was calculated with  $n(\text{FA})/n(\text{Ru})$

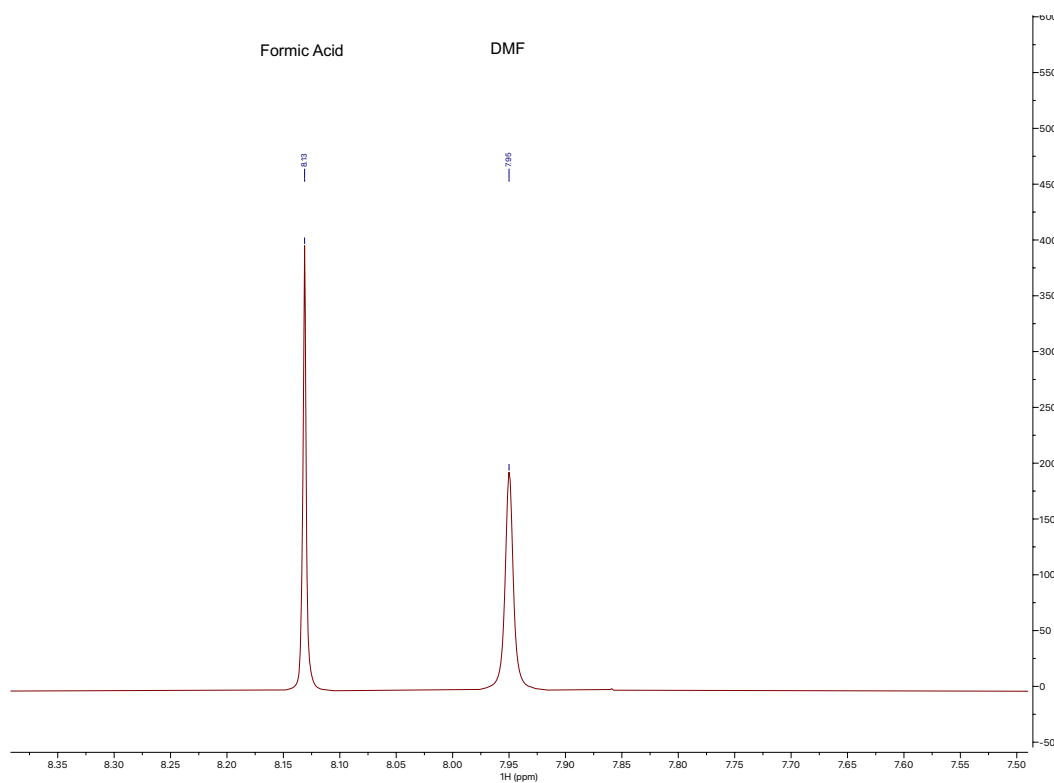


Figure IV - 2 - 6 : <sup>1</sup>H NMR spectra of the FA and standard area.

## 8.3. FA dehydrogenation

### 8.3.1. General reaction procedure

In a standard procedure, the catalyst **1** (14 mg,  $1,33 \cdot 10^{-5}$  mol) was weighed in a 2 neck round bottom flask and dissolved with DMSO (0,4 mL) in a glovebox. Then, the flask was connected to a condenser and a digital flowmeter. Finally, formic acid (100  $\mu$ L,  $2,65 \cdot 10^{-3}$  mol) was added. The reaction was heated at 90 °C with 600 rpm until the end of the reaction (gas flow ended).

TOF was calculated for the 10 first min.

A syringe-pump was used for the continuous experiment to proceed to the addition of FA.

To detect the production of CO, a standard reaction was run with a GC connected after the flowmeter (Figure IV-2-7). The gases were collected in a dried Schlenk and then analyzed. This procedure was repeated until the reaction ceased. The aim was to have an overview from the beginning of the reaction until the end and make sure that no CO was produced throughout the reaction.

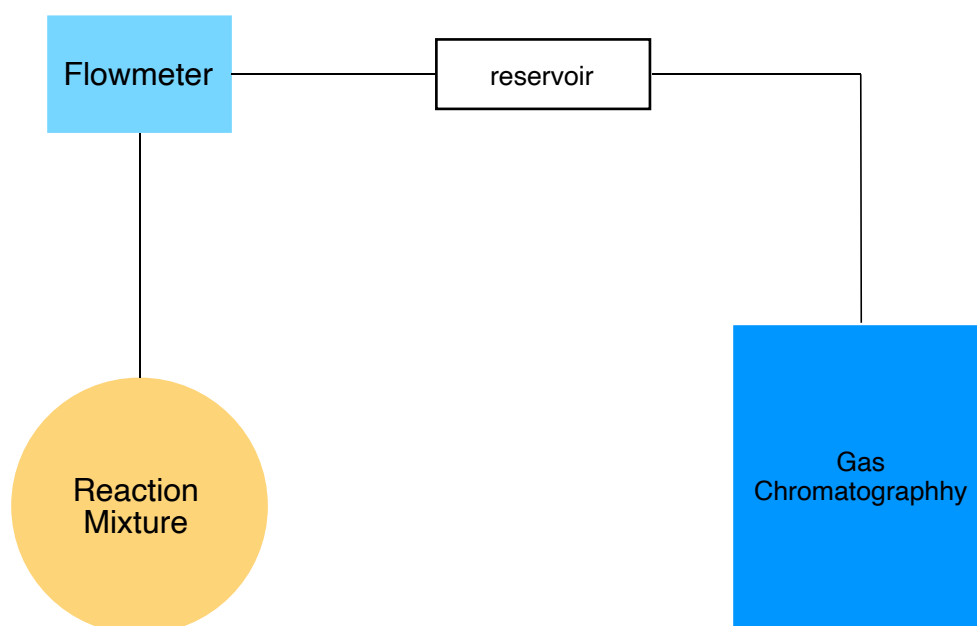


Figure IV - 2 - 7: FA dehydrogenation with CO detected.

### 8.3.2. Analytical Procedure

The flow and the volume of gases produced by the reaction were measured thanks to a digital flowmeter calibrated for CO<sub>2</sub>/H<sub>2</sub>. The volume measured can be used to determine the TOF (based on the first 10 min), the TON and the mole of the product.

- Calculation of the TON
  - $n_{cat} = n(Ru) = 2 \times n(1)$

$$TON = \frac{(\frac{1}{2} V_{tot}) / 24,4}{n_{cat.}}$$

- Calculation of the TOF based on the 10 first min
  - Estimated volume of 1 mol of CO<sub>2</sub>/H<sub>2</sub> is 24,4 L.
  - $V(H_2) = V(CO_2) = \frac{1}{2} V_{total}$
  - All the data are taken at 10 min that correspond to 1/6 h

$$TON_{10min} = \frac{(\frac{1}{2} V_{tot,10min}) / 24,4}{n_{cat.}}$$

$$TOF = \frac{TON_{10min}}{\frac{1}{6}}$$

- Calculation of the conversion

$$Yield = \frac{V_{tot}}{V_{expected}}$$

$$V_{expected} = n(FA) \times 2 \times 24,4$$

### 8.4. Cycle

The general procedure for CO<sub>2</sub> hydrogenation was applied in a first place. Then, the mixture collected was transferred to a round bottom flask to perform the standard procedure for dehydrogenation.

Something that has to be mentioned is that from the mixture transferred, all the new concentration of catalyst and FA were calculated to be able to provide TOF and conversion at the end. Indeed, during the transfer, there was some loss (sample for analysis + transfer)



# Chapter V: Conclusion and Perspectives



## 1. Conclusion and perspectives

The objective of the thesis was to contribute to the domain of energy transition using homogeneous catalysis and particularly using original well-defined ruthenium catalysts. These catalysts with  $\eta^5$ -Oxocyclohexadienyl-ruthenium architecture were studied in three different catalytic transformations aiming to take advantage of their potential bifunctional character. Catalysts were evaluated in base-free processes such as base-free reduction of ketones as well as the more challenging Guerbet reaction and Hydrogen storage process.

First of all, and in the aim to highlight the bifunctional properties of the catalyst through metal-ligand cooperation, catalyst **1** was evaluated in base-free reduction process. Its activity was tested in the base-free hydrogenation and the base-free transfer hydrogenation of ketones. We managed to apply with success the catalyst in hydrogenation with a broad scope of substrate including imine and aldehyde. Best conditions were obtained using 1 mol% of catalyst at 90 °C and 10 bar of H<sub>2</sub> for 17 h. Concerning the transfer hydrogenation, the results varied depending on the hydrogen donor. For example, the activity with *i*PrOH was modest. In contrast, using formic acid, the results were very good and a broad scope of substrates could be used. Here, the best conditions were obtained using 1,5 mol% of catalyst with 5 equivalents of FA at 90 °C for 24 h. Importantly, the use of base sensitive substrate was made possible as no base was required compared to the reported results that extensively used FA associated with TEA as a hydrogen donor. This part of the work was a proof that metal-ligand cooperation is most likely involved in this base-free catalytic process.

As the base-free reduction of ketone was used as a proof of concept, we did not develop some aspects of the reaction. The first aspect dealing with hydrogenation of ketone that should be developed is the enantioselective version of the reaction. Indeed, a lot of catalysts are able to perform enantioselective hydrogenation of ketone. Hence, this aspect has to be tackled as the production of chiral alcohols is of a great interest in fine chemistry. This aspect will require ligand modification. The catalytic activity of the complex was highlighted but the way it works was not deeply investigated. In order to have a better insight of the mechanism involving **1**, some experiments could be run with deuterated formic acid, deuterium or deuterated solvents for example. The hypothesis emitted about the mechanism should also be confronted to theoretical experiment.

Having demonstrated the capabilities of **1** in hydrogenation of ketones, we decided to apply it to a more challenging reaction involving a hydrogen borrowing mechanism to upgrade ethanol into n-butanol, namely the Guerbet reaction. This topic was completely new in the laboratory and the first results obtained were modest compared to the literature. This new research field was confronted to the harsh reaction conditions of the Guerbet reaction. Improvements would come with more robust catalysts as the high temperature and alkaline conditions are certainly very aggressive toward the catalyst. Concerning the duality observed between the conversion of ethanol and the selectivity toward n-butanol, we believe that for biofuel applications, it would be better to focus on the improvement of conversion instead of the selectivity. Indeed, the aim of this reaction is to produce a better fuel than ethanol to increase its energy density while reducing its hydrophilicity. Thus, if a mixture of n-butanol and other C<sub>4+</sub> alcohol is produced, it should still fulfil this property.

Finally, we applied complex **1** to the field of base-free hydrogen storage and release via the couple CO<sub>2</sub>/FA. The hydrogenation of CO<sub>2</sub> to formic acid is not a reaction thermodynamically favoured, bases make the reaction feasible by producing a formate salt. For these reasons the literature on base-free hydrogenation of CO<sub>2</sub> is rather limited. Complex **1** was able to hydrogenate CO<sub>2</sub> into FA in promising yields. Best results were obtained under 60 bar of H<sub>2</sub>/CO<sub>2</sub> (1/1) and 60 °C in 17 h and it could be increased with a longer reaction time of 65h. However, we faced some technical limitations to use very high pressure that other teams employed (> 100 bar). Hence, an improvement is certainly possible.

The reverse reaction of dehydrogenation of FA into CO<sub>2</sub> and H<sub>2</sub> that gained in interest in the last decade and was also largely reported under basic condition was investigated. Once again, the reaction occurred under base-free condition using catalyst **1**. The results obtained are still modest but the catalyst present good properties. Indeed, it was active under pressure and no CO was emitted. Some process such as the continuous addition of FA or the latent property should be improved.

After studying separately each of the reaction involved in the hydrogen storage cycle, they were conducted one after the other in the same batch. Among the fewest catalysts reported to perform a full cycle, all of them were conducted in the presence of a base. We managed to perform the unprecedented base-free hydrogen storage cycle. Following the hydrogenation of CO<sub>2</sub> in DMSO leading to formic acid in a concentration of 3,66.10<sup>-1</sup> mol.L<sup>-1</sup>, the reaction was subjected to the dehydrogenation process that delivered 97% of the hydrogen initially stored.

Regarding the hydrogen storage topic, we believe that more robust catalysts should also improve the performances, just as for the Guerbet reaction. Gaining more experimental and theoretical insights into the mechanism of both hydrogenation and dehydrogenation steps will be necessary to improve the performances of the process.

Beyond the reactions targeted in this thesis, the extension of these catalysts to other reactions should also be considered. In the field of organic synthesis, more complex reduction reactions such as those of amides or esters would be interesting. In the field of energy and LOHC, the extension of the CO<sub>2</sub> hydrogenation reaction to the synthesis of methanol is a subject that would also be interesting to study.





## *Résumé en français*

L'utilisation de l'énergie dans notre vie quotidienne est omniprésente et a toujours joué un rôle dans l'évolution de l'humanité. La révolution industrielle du XIX<sup>ème</sup> siècle basée sur l'utilisation du charbon et du pétrole a profondément changé notre société. Actuellement, les carburants fossiles définissent le modèle énergétique dans lequel nous vivons. Certes, de nouvelles sources non fossiles ont été développées mais l'hégémonie des ressources fossiles est très forte. Cette dépendance entraîne une production de gaz à effet de serre, en particulier le dioxyde de carbone, très forte et en constante augmentation au niveau mondial. Les conséquences sont connues et rapportées par le GIEC dans ses nombreux rapports sur le changement climatique entraînant une détérioration de notre Terre avec une fonte des glaces, une hausse du niveau des mers, une augmentation des événements climatiques extrême, une perte de la biodiversité menant à une augmentation des crises alimentaires, humaines et écologiques.

Une transition énergétique visant à réduire la dépendance aux énergies fossiles et ainsi réduire les émissions de CO<sub>2</sub> s'est engagée. De plus, les ressources en pétrole s'amenuisent avec des gisements de pétrole plus difficile à trouver ou exploiter, parfois situé en zone géopolitiquement instables, avec une consommation et une production à l'équilibre, avec une hausse des prix, etc. Ces observations indiquent que l'ère du pétrole est proche de son maximum. Pour autant, la demande énergétique va rester la même nécessitant le développement de nouvelles sources associées à la démocratisation de leur utilisation. Parmi les ressources développées et utilisées pour réduire les gaz à effet de serre dans le domaine du transport (1<sup>er</sup> producteur de CO<sub>2</sub> en France), les biocarburants ou l'électricité via des batteries ou l'utilisation de « Pile à combustible » sont les plus plébiscités. Pour réduire les rejets de CO<sub>2</sub>, une autre méthode est la capture et la valorisation du CO<sub>2</sub>. Il peut être utilisé tel quel dans certaines industries comme l'agro-alimentaire ou bien utilisé comme « brique élémentaire » pour la synthèse de produits à forte valeur ajoutée.

Dans ce contexte, le projet ANR CatEngy vise à l'implémentation de catalyseurs au ruthénium dans le domaine des énergies renouvelables (production d'alcool et stockage de l'hydrogène). Ce projet rassemble deux équipes aux compétences complémentaires dans la synthèse organométallique et la catalyse homogène que sont l'équipe du Dr. Alain Igau au Laboratoire de Chimie de Coordination de Toulouse et l'équipe du Dr. Cédric Fischmeister à l'Institut des Sciences Chimiques de Rennes.

Le complexe employé et étudié dans ces travaux de thèse appartient à la famille des complexes ruthénium  $\eta^5$ -Oxocyclohexadienyl. Ce complexe a été isolé et caractérisé sous la forme d'une espèce bimétallique dont le design du ligand laisse la possibilité à différentes modifications pour faire varier ses propriétés si nécessaire. Par ailleurs, ce complexe possède les caractéristiques d'un catalyseur bifonctionnel avec un ligand ayant un caractère basique via la fonction carbonyle et un centre métallique acide. Il pourrait ainsi permettre des transformations catalytiques sans base grâce à cette coopération entre le métal et le ligand comme le catalyseur de Shvo l'effectue.

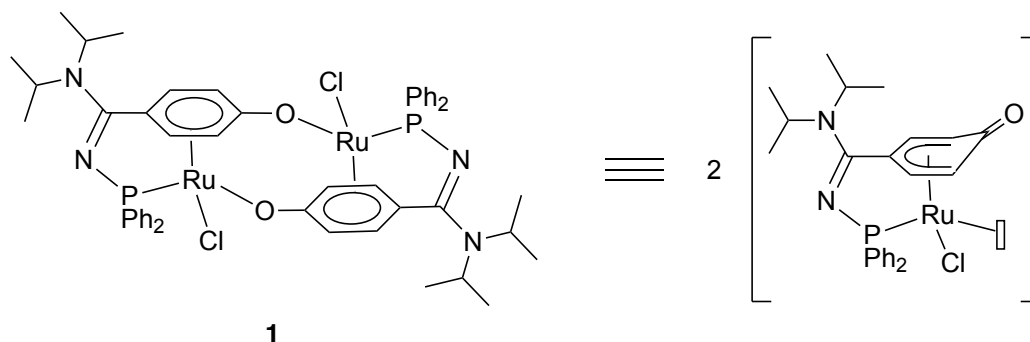


Figure 1: Complexe isolé par Igau.

Dans un premier temps, l'hypothétique caractère bifonctionnel du complexe a été confronté à de simples réactions de réduction de cétones sans base via hydrogénation et hydrogénation par transfert (*iso*-propanol et acide formique).

L'hydrogénation d'un substrat test comme l'acétophénone a pu être effectué sans base avec des conversions totales. Ces résultats ont pu être obtenu par un travail préalable d'optimisation du solvant, de la pression de H<sub>2</sub> utilisée, de la température, etc. Un large éventail de cétones a pu être appliqué notamment des dérivés d'acétophénone portant des groupements sensibles aux bases (hydroxy et acide carboxylique) ainsi que des aldehydes, ou des imines.

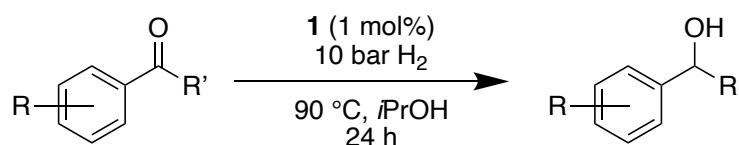


Schéma 1: Hydrogénation de dérivés acétophénone.

L'hydrogénation par transfert en utilisant l'*iso*-propanol comme source d'hydrogène n'a conduit qu'à une conversion modérée de l'acétophénone de 33%. En revanche, l'utilisation de l'acide formique comme source d'hydrogène, a permis, après une optimisation des conditions, d'obtenir une conversion sur le substrat test au-delà de 90%. L'utilisation de l'acide formique sans base n'étant que très rarement rapportée dans la littérature, nous avons appliqué ces conditions à un large scope de cétones notamment des dérivés d'acétophénone portant des groupements sensibles aux bases (hydroxy et acide carboxylique) ainsi que des aldehydes ou des imines.

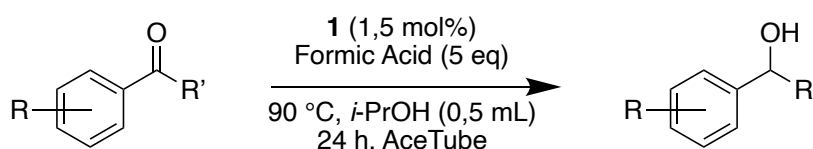


Schéma 2: Hydrogénation par transfert avec de l'acide formique sur des dérivés acétophénonnes.

Une fois les propriétés bifonctionnelles du complexe démontrées grâce à la réduction de cétones effectuée sans base via hydrogénation ou hydrogénation par transfert, nous nous sommes intéressés à l'utilisation du catalyseur dans des réactions du domaine de l'énergie.

Le potentiel du catalyseur a été évalué pour la production d'alcool dans le secteur des biocarburants. Les alcools, plus particulièrement l'éthanol, sont déjà utilisés comme carburant dans les véhicules. En effet, l'éthanol peut être produit en large quantité et de manière simple via, par exemple, une fermentation alcoolique du sucre des produits de récolte. Malgré sa large utilisation, l'éthanol, en tant que carburant, souffre de quelques désavantages. Tout d'abord, sa densité énergétique est moindre face à l'essence entraînant une surconsommation. L'éthanol est également hydrophile ce qui peut endommager les moteurs. Afin de surmonter ces défauts, l'éthanol pourrait servir de bloc de base pour la synthèse

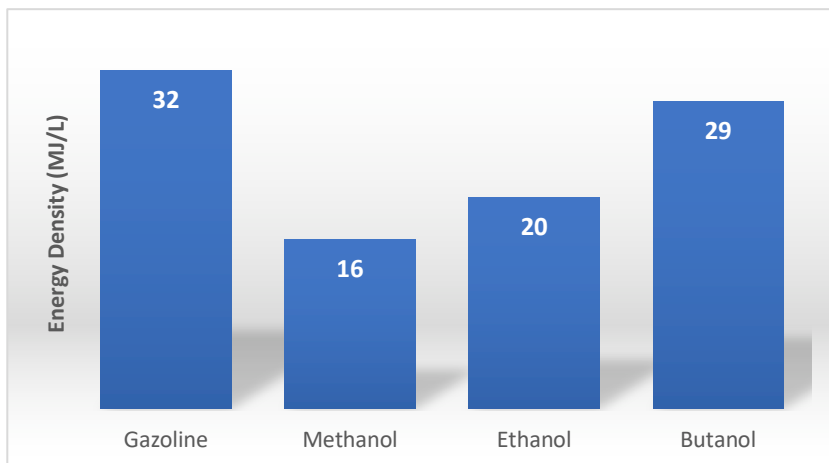
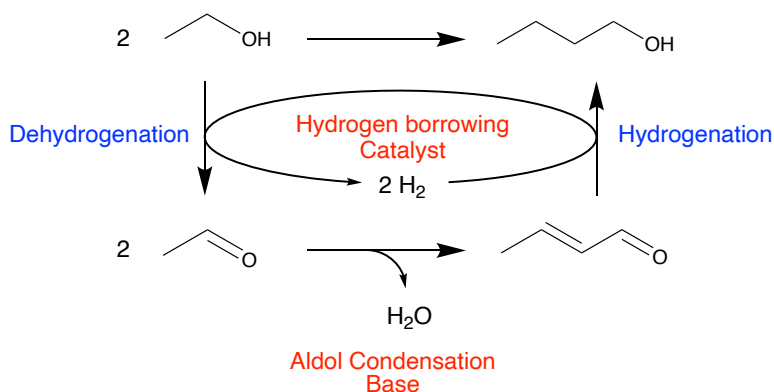


Figure 2: Densité énergétique de l'essence et d'alcools.

d'autres carburants. C'est ainsi que la réaction de Guerbet qui consiste en la transformation d'alcools légers en alcools plus lourds trouve un regain d'intérêt. Grâce à cette réaction, l'éthanol, très facilement et très largement produit, peut être transformé en *n*-butanol qui a l'avantage d'avoir une densité énergétique proche de l'essence conventionnelle et d'être moins hydrophile.



Scheme 1: Réaction de Guerbet appliquée à l'éthanol.

La réaction de Guerbet a été étudiée et nous avons pu remarquer qu'il était difficile d'obtenir à la fois une bonne conversion de l'éthanol en produit de Guerbet (*n*-Butanol et autres alcools) et une haute sélectivité envers le *n*-Butanol. L'étude de la réaction n'a pas permis une avancée majeure dans la conversion ou la sélectivité, nous avons obtenu une conversion de 40% et une sélectivité de 80% dans nos meilleures conditions. Ces résultats

doivent être mis en relief par rapport aux meilleurs résultats actuels qui font état de conversions comprises entre 20% et 70% et des sélectivités allant de 50% à 99%.

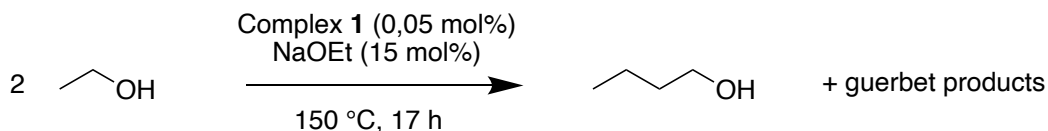


Figure 3: Réaction de Guerbet réalisée

L'autre domaine énergétique étudié avec ce catalyseur fût le stockage de l'hydrogène sous forme chimique en acide formique. L'hydrogène est vu comme une source énergétique pour notre futur puisqu'il possède une densité énergétique supérieure à l'essence et qu'il a l'avantage de pouvoir être produit par électrolyse de l'eau. Cependant, cette source est peu rependue puisqu'elle souffre de problèmes de stockage, transport et production. Concernant la problématique du stockage, actuellement, l'hydrogène est stocké sous pression ou bien sous forme liquide. Ces deux méthodes nécessitent des équipements spéciaux et sont couteuses en énergie, ce qui freine le développement de cette filière énergétique. C'est pourquoi des alternatives de stockage sont développées notamment le concept de « Liquid Organic Hydrogen Carrier » ou liquides organiques comme réservoirs d'hydrogène. Ces LOHCs permettent le stockage sous forme chimique de l'hydrogène dans des molécules organiques stables, non toxique et capables d'absorber et de relâcher de l'hydrogène. Dans ce domaine, l'acide formique est un bon candidat pour cette utilisation comme vecteur énergétique tant par sa densité énergétique que par sa synthèse possible via le recyclage du CO<sub>2</sub>.

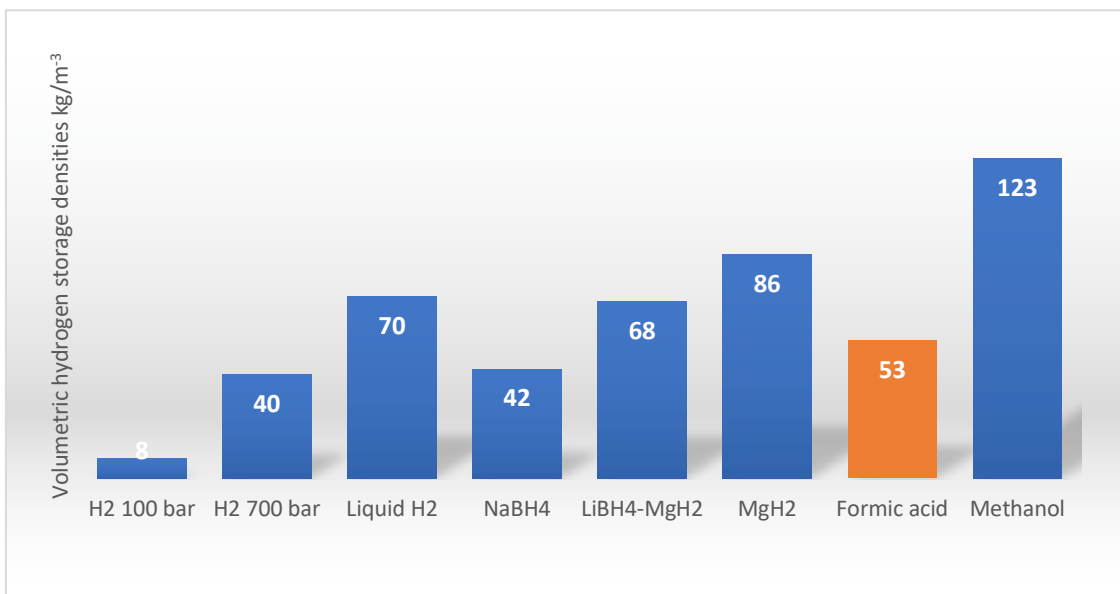


Figure 4: Comparaison des densités en hydrogène de différents composés.

Le cercle vertueux que permet le stockage de l'hydrogène via l'hydrogénation du CO<sub>2</sub> en acide formique puis la production d'hydrogène via la déshydrogénation de l'acide formique a été étudié étape par étape dans un premier temps puis l'un à la suite de l'autre, toujours dans des procédés sans base.

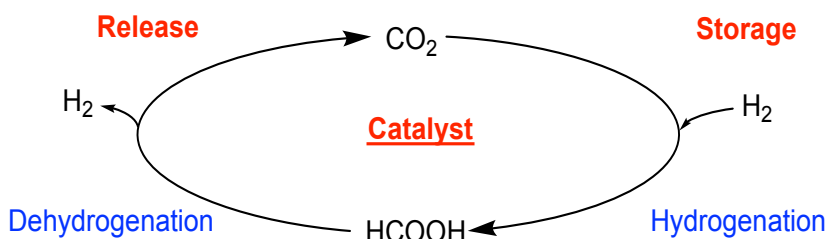


Schéma 3: Cycle du stockage de l'hydrogène.

Le stockage de l'hydrogène par l'hydrogénation du  $\text{CO}_2$  a été réalisé sans base contrairement à la majorité des travaux rapportés dans la littérature. Cette réaction sans base n'étant pas thermodynamiquement favorisée, l'utilisation du DMSO comme solvant s'est avérée essentielle pour la stabilisation de l'acide formique formé. Un TON maximal de 105 en 17 h a pu être obtenu et augmenté à 160 en 65 h.

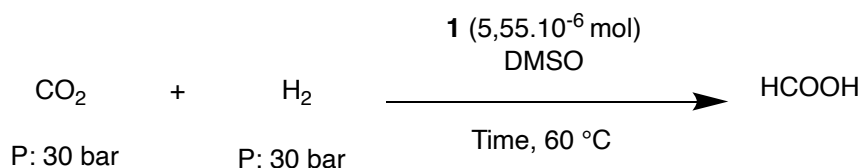


Schéma 4: Hydrogénation du  $\text{CO}_2$  en acide formique.

La production d'hydrogène à partir d'acide formique a abouti au maximum à un TOF de  $234 \text{ h}^{-1}$  dans un procédé n'utilisant pas de base. D'autres caractéristiques importantes pour ce type de réaction ont été étudiées. Par exemple, l'analyse des gaz émis tout au long de la réaction n'a pas révélé la présence de CO qui aurait pu venir d'une réaction parasite qu'est la déshydratation de l'acide formique. La réaction effectuée en système clos produit assez de pression pour pouvoir être reliée à une pile à combustible. Nous avons également pu effectuer la réaction sur 24 h avec l'addition continue d'acide formique.

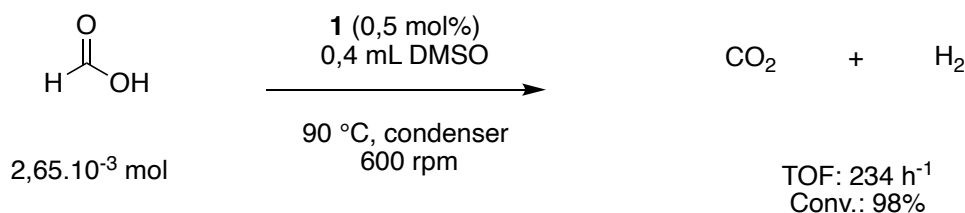


Schéma 5: Déshydrogénation de l'acide formique.

Pour terminer, un cycle complet sans base, qui n'avait jamais été rapporté jusqu'alors, a été réalisé validant l'hypothèse qu'avec le même milieu réactionnel nous pouvions effectuer soit le stockage ou la libération de H<sub>2</sub> en fonction des conditions de pression.

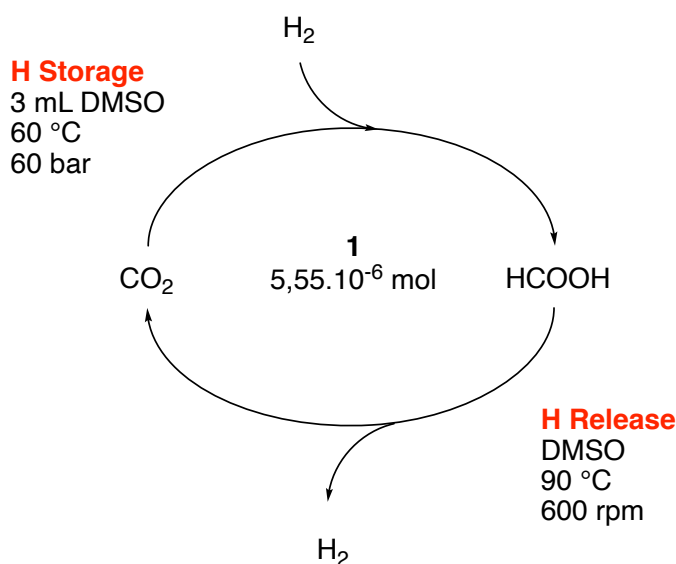


Schéma 6: Cycle du stockage et de libération de H<sub>2</sub> sans base.

Pour conclure, nous avons, au cours de ces travaux de thèse, démontré les propriétés bifonctionnelles du catalyseur développé à Toulouse. En effet, la réduction de cétone a été effectuée sans base par hydrogénation ou hydrogénation par transfert avec l'acide formique. Nous avons pu ainsi réduire des substrats avec des fonctions sensibles aux bases et qui n'étaient pas rapportés dans la littérature. L'utilisation de l'acide formique sans base comme donneur d'hydrogène n'avait été que très peu documentée. Ces travaux ont ainsi pu étoffer ce domaine. Enfin, après avoir utilisé la réduction de cétone comme une preuve de concept, nous pourrions envisager de développer une réduction énantioselective nécessitant une modification du ligand. La partie mécanistique n'a pas pu s'appuyer sur une étude théorique et pourrait donc être étoffée pour avoir une meilleure compréhension de la réaction.

La réaction de Guerbet a pu être effectuée avec succès avec des résultats proche de ceux rapportés avec des catalyseurs au ruthénium. La réaction se déroulant dans des conditions dures (haute température et forte charge en base), seule une amélioration de la robustesse du catalyseur permettra d'obtenir de meilleurs résultats.

Le stockage de l'hydrogène en acide formique a été effectué avec succès ainsi que sa libération. Ces deux réactions ont été menées sans base ce qui est peu décrit dans la littérature puisque ce n'est pas favorisé. En plus de cela, nous avons rapporté le premier cycle effectué sans base. Des améliorations sont possibles notamment par la réalisation de nouvelles expériences expérimentales et d'études théoriques pour avoir une meilleure vision des mécanismes réactionnels.







**Titre :** Complexes  $\eta^5$ -Oxocyclohexadienyl ruthénium pour des transformations catalytiques sans base

**Mots clés :** Hydrogénation sans base / Hydrogénation par transfert sans base / LOHC / Guerbet /  $\text{CO}_2$  / Hydrogène / Ruthénium / Coopération Métal-Ligand

L'utilisation intensive des ressources fossiles, leur épuisement et les problèmes environnementaux causés rendent la recherche de nouvelles sources d'énergie durables essentielle. Dans ce domaine, l'éthanol et l'hydrogène sont des vecteurs énergétiques prometteurs.

L'éthanol, est déjà utilisé comme alternative mais il présente des inconvénients (faible densité énergétique, hydrophilie) pouvant être surmonté en transformant l'éthanol en n-butanol par la réaction de Guerbet.

La seconde solution est l'hydrogène possédant des propriétés énergétiques élevées mais, souffrant de problèmes de sécurité, de transport et de stockage (gaz inflammable). Pour surmonter ces défauts, le stockage chimique de l'hydrogène en acide formique (AF) via l'hydrogénation de  $\text{CO}_2$  est une possibilité créant ainsi un cycle vertueux de stockage énergétique avec le couple AF/ $\text{CO}_2$ .

Le projet implique l'utilisation de complexes  $\eta^5$ -Oxocyclohexadienyl ruthénium, apparentés à celui de Shvo, développé par notre partenaire. Par la catalyse homogène, les propriétés bifonctionnelles et la coopération Métal-Ligand du catalyseur ont été évaluées dans la réduction sans base de cétones soit par hydrogénation ou hydrogénation par transfert avec l'*i*-propanol ou l'AF.

Ensuite, les complexes ont été testés dans des réactions du domaine de l'énergie impliquant des processus d'hydrogénation/déshydrogénation. Ainsi, la réaction de Guerbet, pour transformer de l'éthanol en n-butanol a été étudiée. De même, le stockage sans base d'hydrogène par l'hydrogénation du  $\text{CO}_2$  en AF et la déshydrogénation de l'AF en  $\text{H}_2$  ont été effectués. Enfin, nous avons réalisé un cycle de stockage de l'hydrogène sans base inédit.

**Title:**  $\eta^5$ -Oxocyclohexadienyl ruthenium complexes for base-free catalytic transformations

**Keywords:** Base-free hydrogenation / Base-free Transfer Hydrogenation / LOHC / Guerbet /  $\text{CO}_2$  / Hydrogen / Ruthenium / Metal-Ligand Cooperation

The intensive use of fossil resources, their depletion and the environmental issues it caused makes the research of alternative and sustainable energy sources of great interest. In this field, ethanol and Hydrogen represent energy carriers of a high potential to replace oil.

Ethanol, is already used as an alternative. However, it has some drawbacks (low energy density and high hydrophilicity) that can be overcome with the upgrade of ethanol to n-butanol via the Guerbet reaction.

The second alternative is hydrogen as it has high energetical density. However, due to its gaseous form and flammability it suffers from safety, transportation and storage issues. To overcome these issues, chemical storage in formic acid (FA) via hydrogenation of  $\text{CO}_2$  is a solution that creates a virtuous cycle of energy storage based on FA/ $\text{CO}_2$ .

The project implied the use of innovative  $\eta^5$ -Oxocyclohexadienyl ruthenium complexes, structurally related to the Shvo catalyst, developed by our partner. Using homogeneous catalysis, the bifunctional properties and the Metal-Ligand cooperation of the catalyst have been evaluated in base-free reduction of ketones. The base-free hydrogenation and the base-free transfer hydrogenation with iso-propanol and FA were investigated and a broad scope of ketone applied. Then, the catalysts were studied in more challenging reactions in the domain of sustainable energy involving hydrogenation and dehydrogenation processes. Hence, the Guerbet reaction to upgrade ethanol into n-butanol was studied. The base-free hydrogen storage associated with  $\text{CO}_2$  hydrogenation to FA and the reverse reaction were also studied. We performed the unprecedented base-free hydrogen storage cycle.